uOttawa

L'Université canadienne
Canada's university

FACULTÉ DES ÉTUDES SUPÉRIEURES ET POSTOCTORALES

uOttawa

L'Université canadienne
Canada's university

FACULTY OF GRADUATE AND POSDOCTORAL STUDIES

Xian Wang
AUTEUR DE LA THÈSE / AUTHOR OF THESIS

Ph.D. (Chemistry)
GRADE / DEGREE

Department of Chemistry
FACULTÉ, ÉCOLE, DÉPARTEMENT / FACULTY, SCHOOL, DEPARTMENT

Experimental and Theoretical Studies of Ion-Molecule Complexes and of some Ionized Diketones in the Gas-Phase

TITRE DE LA THÈSE / TITLE OF THESIS

Paul Mayer
DIRECTEUR (DIRECTRICE) DE LA THÈSE / THESIS SUPERVISOR

John Holmes
CO-DIRECTEUR (CO-DIRECTRICE) DE LA THÈSE / THESIS CO-SUPERVISOR

EXAMINATEURS (EXAMINATRICES) DE LA THÈSE / THESIS EXAMINERS

Alexis Bawagan

Diethard Bohme

David Bryce

Javier Giorgi

Gary W. Slater
LE DOYEN DE LA FACULTÉ DES ÉTUDES SUPÉRIEURES ET POSTDOCTORALES /
DEAN OF THE FACULTY OF GRADUATE AND POSTDOCORAL STUDIES

EXPERIMENTAL AND THEORETICAL STUDIES OF ION-MOLECULE COMPLEXES AND OF SOME IONIZED DIKETONES IN THE GAS-PHASE

by

Xian Wang

A thesis submitted to the
Faculty of Graduate and Postdoctoral Studies

In partial fulfillment of the requirements of
the degree of Doctor of Philosophy

In the Ottawa-Carleton Chemistry Institute
Department of Chemistry, University of Ottawa
Ottawa, Ontario, Canada

January 2006

Candidate	Supervisor
Xian Wang	Dr. Paul M. Mayer

© Xian Wang, Ottawa, Ontario, Canada – January 2006

Library and Archives Canada

Published Heritage Branch

395 Wellington Street
Ottawa ON K1A 0N4
Canada

Bibliothèque et Archives Canada

Direction du Patrimoine de l'édition

395, rue Wellington
Ottawa ON K1A 0N4
Canada

Your file Votre référence
ISBN: 978-0-494-15052-8
Our file Notre référence
ISBN: 978-0-494-15052-8

NOTICE:
The author has granted a non-exclusive license allowing Library and Archives Canada to reproduce, publish, archive, preserve, conserve, communicate to the public by telecommunication or on the Internet, loan, distribute and sell theses worldwide, for commercial or non-commercial purposes, in microform, paper, electronic and/or any other formats.

The author retains copyright ownership and moral rights in this thesis. Neither the thesis nor substantial extracts from it may be printed or otherwise reproduced without the author's permission.

AVIS:
L'auteur a accordé une licence non exclusive permettant à la Bibliothèque et Archives Canada de reproduire, publier, archiver, sauvegarder, conserver, transmettre au public par télécommunication ou par l'Internet, prêter, distribuer et vendre des thèses partout dans le monde, à des fins commerciales ou autres, sur support microforme, papier, électronique et/ou autres formats.

L'auteur conserve la propriété du droit d'auteur et des droits moraux qui protège cette thèse. Ni la thèse ni des extraits substantiels de celle-ci ne doivent être imprimés ou autrement reproduits sans son autorisation.

In compliance with the Canadian Privacy Act some supporting forms may have been removed from this thesis.

While these forms may be included in the document page count, their removal does not represent any loss of content from the thesis.

Conformément à la loi canadienne sur la protection de la vie privée, quelques formulaires secondaires ont été enlevés de cette thèse.

Bien que ces formulaires aient inclus dans la pagination, il n'y aura aucun contenu manquant.

Canada

To Mom and Dad

and

Michael

Abstract

This thesis describes some research in gas-phase ion chemistry, using mass spectrometry techniques combined with theoretical calculations. Metastable ion and collision-induced dissociation mass spectra, kinetic energy release and isotopic labelling were used to characterize and identify precursor and fragment ions and to predict reasonable reaction mechanisms which were then further elucidated by calculations. MP2, B3-LYP and G3 levels of theory were employed to obtain the structures corresponding to energy minima and transition states and thus to obtain a complete potential energy surface for each system.

A major focus of this work was to investigate the unimolecular reactions of some ion-molecule complexes, especially the isomerizations that take place within them and then to discover the mechanisms by which such reactions take place. Particular attention was devoted to ion-molecule complexes that comprise ketones (including aldehydes), enols and distonic ions of alcohols.

The first two systems studied were acetaldehyde associated with the distonic methanol cation ($^{\bullet}CH_2OH_2^+$), [$CH_3CHO/H^+O(H)CH_2^{\bullet}$], and with its conventional isomer ($CH_3OH^{+\bullet}$), [$CH_3CHO/^{+\bullet}HOCH_3$]. The isomerization barrier for ionized acetaldehyde to rearrange to its enol isomer, vinyl alcohol $CH_2CHOH^{+\bullet}$, was lowered significantly (by 133 kJ/mol) by its association with $^{\bullet}CH_2OH_2^+$. This reaction resulted from a $H^+/H^{\bullet}$ transfer mechanism, involving a transition state of low energy requirement. In contrast, the $CH_3OH^{+\bullet}$ ion did not facilitate the rearrangement of acetaldehyde to its enol ion. Similar

observations were obtained for ion-molecule complexes of acetone and methanol, $[(CH_3)_2C{=}O/H^+O(H)CH_2^{\bullet}]$ and $[(CH_3)_2C{=}O/^{+\bullet}HOCH_3]$. One metastable ion dissociation of the latter involved the loss of a methyl radical, producing a new $[C_3H_7O_2]^+$ isomer, $[CH_3C^+\cdots(H)OCH_3]$, whose structure was assigned by calculations.

A water molecule is one of the smallest species that have been used as a catalyst within an ion-molecule complex, thus the gas-phase reactions of the ion $[CH_3CHO/H_2O]^{+\bullet}$ were also investigated in this thesis. The metastable ion (MI) mass spectrum revealed that this ion-molecule complex decomposed spontaneously by the losses of H_2O, CO and $^{\bullet}CH_3$. Hydrogen-bridged water complexes were found to be the major products of the losses of CO and $^{\bullet}CH_3$. The CO loss produced the $[^{\bullet}CH_3\cdots H_3O^+]$ ion and involved a backside displacement mechanism. The product ions arising from $^{\bullet}CH_3$ loss (via two different reaction channels) were assigned by theory to be the isomers, $[OC\cdots H_3O^+]$ and $[CO\ldots H_3O^+]$, and their 298 K enthalpy values, calculated at the G3 level of theory are $\Delta_fH[OC\cdots H_3O^+]$ = 420 kJ/mol and $\Delta_fH[CO\cdots H_3O^+]$ = 448 kJ/mol. The interconversions among water-solvated $CH_3CHO^{+\bullet}$, $CH_3COH^{+\bullet}$ and $CH_2CHOH^{+\bullet}$ were revealed by calculations to involve proton-transport catalysis (PTC), a catalyzed-1,2-H transfer and an uncatalyzed H-atom transfer mechanism, respectively.

The second part of the thesis involves a small project that describes the unimolecular dissociations of some ionized diketones, a group of conventional molecular ions that have an unexpectedly rich chemistry. The fragmentation processes of ionized 2,3-pentanedione, 2,3-butanedione and 3,4-hexanedione were investigated. Metastable dissociation of the 2,3-

pentanedione radical cation gave rise to a composite metastable ion peak, m/z 72, resulting from the isobaric losses of CO and C_2H_4. These two fragmentation channels were energetically competitive and they yielded $[CH_3C(O)CH_2CH_3]^{+\bullet}$ and $[CH_3C(OH)=C=O]^{+\bullet}$ respectively. The latter is a new ion, produced by a McLafferty rearrangement, and has Δ_fH^o = 604 kJ/mol, obtained from G3 calculations. The transition states of all dissociation processes for metastable $[CH_3COCOCH_2CH_3]^{+\bullet}$ were placed on a potential energy surface computed at the G3 level of theory. The homologous ionized diketone 2,3-butanedione also displayed the decarbonylation channel yielding $CH_3COCH_3^{+\bullet}$, and 3,4-hexanedione gave rise to a composite metastable ion peak resulting from the losses of both CO and C_2H_4.

Acknowledgements

I would like to express my sincere gratitude to the people who made this PhD. Thesis possible. First of all, my sincere thanks are due to my supervisors, Dr. John L. Holmes and Dr. Paul M. Mayer. I am deeply indebted to Dr. John L. Holmes, for providing me with constant support, encouragement and guidance throughout this journey as well as for reviewing this thesis. He has always been so patient with my questions and concerned about my work. His profound knowledge and enthusiasm for research have made a deep impression on me. I owe him many thanks for introducing me to this field (Mass Spectrometry) and helping me to start my graduate studies. I am grateful to Dr. Paul M. Mayer for accepting me as his PhD. student, for the help extended to me when I approached him and for his great assistance in performing theoretical calculations. Special thanks go to the members in the mass spectrometry centre at the University of Ottawa, who have provided me such a joyful working atmosphere. I thank Sander (Dr. A. A. Mommers) for trouble-shooting the ZAB and for always being so helpful in everything. I thank Clem (Dr. C. Kazakoff) for the analytical instrument discussions. I also thank both past and present students and post-docs that I have worked with: Julie Grabowy, Emma Rennie, Clement Poon, Annick St-Amand, Anne-Marie Boulanger, Abdul Alhazmi, Marie-Soleil Giguere, Lisa Morrison, Danielle Dubien, Richard Ochran, Jie Cao, Weixing Sun and Janeen Casey.

Last but not least, I would like to thank my family for always being there to support me: my husband Michael (whose considerable understanding is especially appreciated), my parents and my brother.

Contents

List of Tables

List of Schemes

List of Figures

Abbreviations

AE	Appearance Energy
amu	atomic mass unit
B3-LYP	Becke Lee-Yang-Parr gradient-corrected correlation functional
BE	Binding Energy
CI	Chemical Ionization
CID	Collision-Induced Dissociation
CIDI	Collision-Induced Dissociative Ionization
DFT	Density Functional Theory
E or ESA	Electrostatic Analyzer
EI	Electron Ionization (also known as Electron Impact)
ESI	Electrospray Ionization
FFR	Field-Free Region
FT-ICR	Fourier-Transform Ion Cyclotron Resonance Mass Spectrometry
HF	Hartree-Fock Theory
HBC	Hydrogen-Bridged Complex
IE	Ionization Energy
IMC	Ion-Molecule Complex
IE_a	Adiabatic Ionization Energy
IE_v	Vertical Ionization Energy
KER	Kinetic Energy Release
MALDI	Matrix Assisted Laser Desorption Ionization

MI	Metastable Ion
MIKES	Mass-analyzed Ion Kinetic Energy Spectroscopy
m/z	mass-to-charge ratio
MO	Molecular Orbital
MP2	Second-Order Møller-Plesset Perturbation Theory
MS/MS or MS^n	Tandem mass spectrometry
NRMS	Neutralization-Reionization Mass Spectrometry
PA	Proton Affinity
PES	Potential Energy Surface
S_N2	Bimolecular nucleophilic substitution
TPEPICO	Threshold Photoelectron Photoion Coincidence
TS	Transition State
ZPE	Zero-Point Energy

CHAPTER 1

INTRODUCTION AND SUMMARY OF THESIS

1.1 Introduction

Since its beginnings about 100 years ago, mass spectrometry (MS) has become a valuable research tool. "Scientific breakthroughs made possible by MS have included the discovery of isotopes, the exact determination of atomic weights, the characterization of new elements, quantitative gas analysis, stable isotope labelling, fast identification of trace pollutants and drugs, and the characterization of molecular structure," writes chemistry Professor F. W. McLafferty of Cornell University. Today, mass spectrometry is not only used for fundamental studies of gas-phase ion chemistry, but is also a powerful technique for environmental, pharmaceutical, agricultural and forensic analyses. A mass spectrometric analysis can provide both identification of the material present and the concentration of each component in a mixture.

In gas-phase ion chemistry studies, mass spectrometry is used to produce gas-phase ions from neutral compounds and to examine the subsequent decomposition of these ions. The elucidation of the ions' structures (which also reflect the structures of neutral molecules) can be revealed, based on the fragmentation patterns together with thermochemical arguments and evidence from isotopic labelling. Ion structure assignment is crucial to determining correct thermochemistry data and to devise

mechanisms for gas-phase ion reactions. As an aid to mass spectrometric experiments, theoretical calculations (especially *ab initio* calculations) are employed to obtain the relative energies of the transition states and other important stable or intermediate ion configurations for a reaction path and to acquire reasonable thermochemistry data (e.g. heats of formation) for all species. With the increasing accuracy of computational methods, their importance has been increasing steadily.

Ionized small organic radicals and molecules have much richer chemistries than their neutral counterparts. The presence of the charge permits the existence of a great number of stable isomers. For example, there are only three C_2H_4O molecules: oxirane (i.e. ethylene oxide), acetaldehyde and vinyl alcohol. However, at least eleven $C_2H_4O^{+\bullet}$ stable isomers have been investigated by theoretical calculation, seven of which have been identified by experiment[1-4]. Four types of ions have been studied in this thesis, as well as their structures, isomerization and dissociation chemistries have been investigated. The four types comprise conventional and distonic ions, ion-molecule complexes and proton-bound pairs.

The discovery of stable odd-electron organic cations having structures that do not correspond to stable molecules has been a significant advance in gas-phase ion chemistry. Some of these odd-electron ions exhibit non-conventional structures in which the charge and the radical are located on separate atoms; they are called distonic ions and they are isomers of an ionized stable molecule. A good example of a conventional ion vs. its distonic form is the methanol ion ($CH_3OH^{+\bullet}$) and its distonic form ($^{\bullet}CH_2OH_2^{+}$). Most of

us are familiar with the conventional ion, $CH_3OH^{+\bullet}$, which is formed by the ionization of a neutral methanol molecule. Its distonic form, $^{\bullet}CH_2OH_2^+$ (the methylene oxonium ion) can be described as a protonated $^{\bullet}CH_2OH$ radical in which the H^+ is not at the radical site but at the adjacent hetero-atom. Distonic ions are now known generally to be thermodynamically more stable than their conventional counterparts and therefore they are often to be found as key intermediates in the unimolecular decomposition of radical cations (e.g. McLafferty rearrangements) or in their bimolecular reactions. For instance, the heat of formation of $^{\bullet}CH_2OH_2^+$ (Δ_fH = 816 kJ/mol) is significantly lower than that of $CH_3OH^{+\bullet}$ (Δ_fH = 845 kJ/mol).[5,6] Depending on the relative position of the charge and of the radical, they are referred to as α, β, γ, δ-distonic ions, e.g. $^{\bullet}CH_2CH_2CH_2OH_2^+$ (the distonic form of ionized n-propanol) is a γ-distonic ion.

Although the ion $^{\bullet}CH_2OH_2^+$ was first found as a stable species by *ab initio* calculations,[6,7] it was quickly generated thereafter and characterized by tandem mass spectrometry experiments. The distonic ions can be produced by ion dissociation reactions, e.g. Equation 1.1[7].

$$HOCH_2CH_2OH^{+\bullet} \rightarrow {}^{\bullet}CH_2OH_2^+ + CH_2O \qquad 1.1$$

They can be also made by the removal of a selected radical from a protonated species under collision conditions[8,9], e.g. Equation 1.2, and this method has been extensively used in this thesis.

$$CH_3CH_2OH_2^+ \rightarrow {}^{\bullet}CH_2OH_2^+ + {}^{\bullet}CH_3 \qquad 1.2$$

It is now well known that some decompositions of ions in the gas-phase take place through ion-molecule complexes and these have been extensively studied during the last three decades or so.[10-15] Ion-molecule complexes (IMCs or ion-neutral complexes INC) are significant because their ion and neutral parts retain the reactivities similar to those expected from the isolated species. IMCs were first used to explain the unusual reactivity of certain metastable ions that will isomerize via IMCs, prior to fragmentation. There is computational and experimental evidence to implicate IMCs in decompositions of singly charged precursor ions.[16-18] A mechanism for fragmentations in gas-phase ions via an IMC is shown in Scheme 1.1.

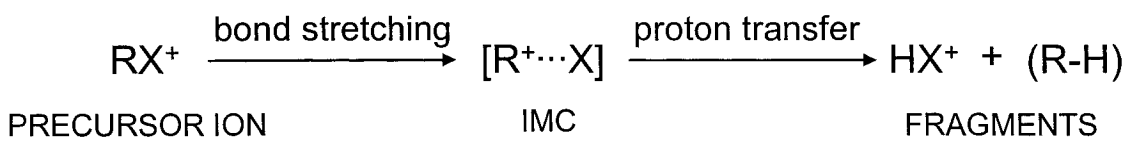

Scheme 1.1 An example of decomposition of gas-phase ions via ion-molecule complexes.

Most of this thesis will describe the role of ion-molecule complexes in unimolecular reactions in the gas-phase. An IMC is formed when an ion is electrostatically bound to a neutral molecule or a radical, e.g. $A^{+\bullet}\cdots N$ or $AH^+\cdots{}^{\bullet}N$. The two components in the complex are connected by an electrostatic bond (ion-dipole or ion-induced dipole interaction) but not by a covalent bond. McAdoo et al.[11] have suggested that a species

will be considered an IMC only if its lifetime from the point of covalent bond breaking to the point of overcoming long-range attractive forces is sufficiently long that a chemical reaction other than dissociation has time to occur.

Computational studies have provided much valuable information about ion-molecule complexes that is not obtainable by experiment. A good example for the existence of an IMC is that in the ion $^{\bullet}CH_2CH_2OH_2^+$, the H_2O molecule is easily exchanged between the carbon atoms via a transition state resembling a complex between ionized ethene and water, $[CH_2CH_2\cdots OH_2]^{+\bullet}$, before it dissociates to $CH_2CH_2^{+\bullet}$ and H_2O. This process, as shown in Equation 1.3, was indicated by calculations by Radom et al.[19] and by Ruttink[20] and was also confirmed by experiments.[21-24]

$$^{\bullet}CH_2CH_2OH_2^+ \rightarrow [CH_2CH_2\cdots OH_2]^{+\bullet} \rightarrow CH_2CH_2^{+\bullet} + H_2O \qquad 1.3$$

Another type of IMC is a bridged ion which comprises two neutral molecules electrostatically bound through a central ion (the bridge). A proton-bound pair (also known as a H^+-bridged ion) belongs in this category and its central ion is a proton, e.g. the proton-bound pair of acetaldehyde and ethanol, $CH_3CHO\cdots H^+\cdots O(H)CH_2CH_3$. Proton-bound pairs are common gas-phase ions and can be readily generated in an electron ionization (EI) ion source, especially a high pressure source (for which the detailed features will be described in Chapter 2), of a sector mass spectrometer. For example, the proton-bound pair, $CH_3CHO\cdots H^+\cdots O(H)CH_2CH_3$, is generated by the following reactions.

$$CH_3CH_2OH + H^+ \rightarrow CH_3CH_2OH_2^+ \qquad 1.4$$

$$CH_3CHO + CH_3CH_2OH_2^+ \rightarrow CH_3CHO\cdots H^+\cdots O(H)CH_2CH_3 \qquad 1.5$$

$CH_3CH_2OH_2^+$ is produced from the self-protonation of CH_3CH_2OH in the EI ion source, as shown in Equation 1.6.

$$CH_3CH_2OH^{+\bullet} + CH_3CH_2OH \rightarrow CH_3CH_2OH_2^+ + CH_3\dot{C}HOH \qquad 1.6$$

In this thesis, proton-bound pairs are used as precursor ions to produce the ion-molecule complexes of interest, see Chapters 4, 5 and 6 for detailed discussions.

In addition to the investigation of stable isomeric ion structures, the energy barriers that separate these isomers need to be determined so that their ease of inverconversion can be established. In many circumstances the energy barrier separating two isomers of the ions, $A^{+\bullet}$ and $B^{+\bullet}$, exceeds that of the lowest energy dissociation channel of one of them and thus they cannot freely interconvert. However, many previous studies and work in this thesis have shown that when an odd-electron ion is attached to a neutral molecule, i.e. forms an ion-molecule complex, it can sometimes undergo completely unexpected reactions. 1) The ion may undergo rearrangements catalyzed either homogeneously (self-catalysis) or heterogeneously by its neutral partner or substrate. 2) Unexpected dissociation channels can be observed because of the great number of stable isomers now accessible due to the increase of the polyatomic ion's size

and the internal reactivity of the ion-molecule complexes. In brief, such ion-molecule complexes often have a very rich chemistry, compared with conventional odd-electron ions. A major focus of this thesis is to explore all the detailed chemistry, including the rearrangements and dissociations and the energy barriers for the ion-molecule complexes of interest. In the present work, tandem mass spectrometry (MS/MS or MS/MS/MS), associated with isotopic-labelling experiments is used to assign structures to all isomers having the same mass-charge ratio. Furthermore, theoretical calculations complement the experimental techniques and are used to explore the potential energy surfaces of the ion-molecule complexes and also to determine the heats of formation of new ions. A brief description of the instrument used for this work is introduced in Chapter 2. Some concepts and techniques (including experimental and computational methods) that are commonly used in the study of gas-phase ion chemistry are discussed in Chapter 3.

1.2 Summary of Thesis

1.2.1 Studies of the Chemistry of Ion-Molecule Complexes

Since the mid-1970's many authors have reported that ion-molecule complexes can be key intermediates in the reactions of organic ions.[10,11,16-18] The chemistry of certain ion-molecule complexes is significant because a critical part of any thermodynamic and kinetic study of a gas-phase reaction is the energies of the reactants, products and intermediates and the chemistry of IMCs provides insight into aspects of the reactions and isomerization. The intrinsic properties of intermediates can only be

explored in the absence of solvation effects; consequently, these studies must be conducted in the gas phase. Many fragmentations of organic ions in the gas phase proceed via an ion-molecule complex mediated process.

Recent studies[25-29] have been carried out on the catalyzed isomerization of a radical cation that is electrostatically bound to (solvated by) a selected neutral molecule. One important catalytic route is called proton-transport catalysis (PTC). This involves the reversible H^+ transport between the ion and the neutral moiety:

$$\underset{\text{I}}{HAB^{+\bullet} + M \rightarrow [HAB^{+\bullet}\cdots M]} \rightarrow \underset{\text{II}}{[AB^{\bullet}\cdots {}^{+}HM]} \rightarrow \underset{\text{III}}{[ABH^{+\bullet}\cdots M]} \rightarrow ABH^{+\bullet} + M \qquad 1.7$$

For the PTC mechanism to operate a necessary criterion must be met, namely that the Proton Affinity (PA) of the catalyst, M, must lie between the PA values for the radical and heteroatom sites in $AB^{\bullet}$, a rule which was established by the calculations of Chalk and Radom.[29] However, proton affinity is not the only criterion for successful catalysis. For example, methanol ions can be catalytically converted into their distonic form by a noble gas[30] (Ar, Kr, Xe), by N_2[30] and by methanol itself.[8] In the former case the PA of the neutral gas is lower than that of the $^{\bullet}CH_2OH$ radical at both the C and O sites and in the latter case the PA of methanol is higher than that of either site. Self-catalysis by methanol involves a reversible intraionic 1,2-hydrogen atom shift.[8] Two more established mechanisms are the $H^{\bullet}$-atom Transfer Mechanism and the Spectator Mechanism, which are described next.

The H$^{\bullet}$-atom Transfer Mechanism (ATM) is also called the "Quid pro Quo" (QpQ) mechanism[31]. In this process, the ion accepts a H atom from the neutral substrate, forming a protonated species which then donates a *different* H atom back to the neutral radical. This ATM model has been described in the $CH_3CHO^{+\bullet}/CH_3OH$ system by van der Rest et al[32] with calculations at the UMP2/6-31G** level of theory, and is shown below:

$$C\mathbf{H}_3CHO^{+\bullet}\cdots O(\underline{H})CH_3 \rightarrow C\mathbf{H}_3CHO\underline{H}^{+}\cdots {}^{\bullet}OCH_3 \rightarrow CH_2CHO\underline{H}^{+\bullet}\cdots O(\mathbf{H})CH_3 \qquad 1.8$$

In the above scheme, the acetaldehyde radical cation is isomerized into the vinyl alcohol ion by exchanging two H$^{\bullet}$ atoms with the methanol molecule. The underlined H$^{\bullet}$ atom shifts from methanol to the aldehydic O atom and then a methyl H$^{\bullet}$ atom of acetaldehyde transfers back to the methoxy radical.

The Spectator Mechanism differs from PTC and ATM in that there is no atom exchange between the ion and the catalyst, i.e. the configuration of the catalyst substrate does not change throughout. For example, computations by Radom and coworkers[25] have described the water-catalyzed inverconversions of the methanol ion to its distonic isomer undergoing the spectator mechanism. The TS for the 1,2-H shift in the methanol ion is lower in energy than the barrier for the isomerization of the isolated methanol ion; the water molecule is electrostatically bound to the shifted H$^{\bullet}$ atom and the water "drags"

the methyl H$^{\bullet}$ of methanol across the C-O bond. This mechanism was first illustrated by experiment by Tu and Holmes[33].

A common method of studying ion-molecule complexes is via bimolecular reactions, e.g. by using a Fourier-transform ion cyclotron resonance (FT-ICR) mass spectrometer[31,32], the odd-electron ion is formed in a FT-ICR cell and allowed to react with a neutral methanol molecule. Such studies were performed as outlined in Figure 1.1.

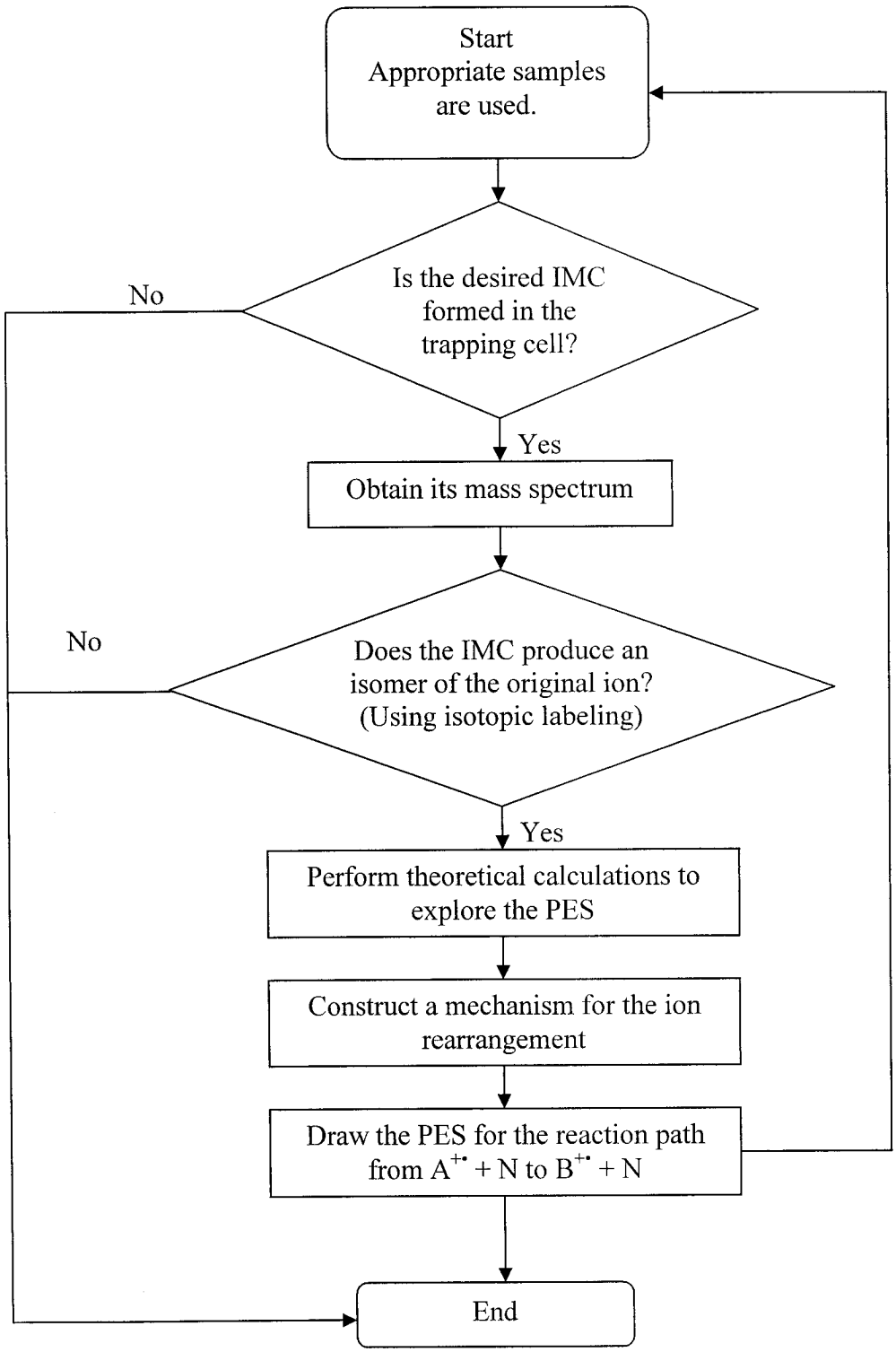

Figure 1.1 Flow-chart of bimolecular studies of ion-molecule complexes.

After the desired ion-molecule complex, $A^{+\bullet}/N$ is successfully generated in the ion source, its CID mass spectrum is obtained. Isotopically labelled ions are often used to provide clear experimental evidence that $B^{+\bullet}$, the isomer of $A^{+\bullet}$ is produced. If $B^{+\bullet}$ is observed from the above mass spectrometric experiments, theoretical calculations will then be performed to establish the mechanism for the rearrangement from $A^{+\bullet}/N$ to $B^{+\bullet}/N$. The resulting potential energy surface will show the reaction path start from the pair $A^{+\bullet}$ and N to the products, $B^{+\bullet}$ and N. The main focus in this approach is whether or not $A^{+\bullet}$ can interconvert to $B^{+\bullet}$ in the presence of N. Other rearrangement or dissociation processes of $A^{+\bullet}/N$ or $B^{+\bullet}/N$ are often ignored.

Instead of using bimolecular reactions to investigate IMCs, this thesis describes the use of unimolecular reactions to study them. We have found that when an ion is electrostatically attached to a molecule, many isomeric structures of an IMC can be obtained via unimolecular rearrangement reactions.[9,34,35] These stable species lie in separate potential wells and can each undergo characteristic dissociations and/or isomerizations and such reactions may involve both catalyzed and uncatalyzed reaction paths. All the processes involved in these accessible IMCs have been investigated, rather than only a single catalyzed isomerization of the ion by the neutral moiety. Recent work in our laboratory has used a collision-induced dissociation (CID) method to generate ion-molecule complexes, a routine that allows us to explore much of the chemistry of the accessible stable and metastable isomeric species.

Because a CID produced ion-molecule complex has sufficient internal energy to undergo further rearrangement and unimolecular decomposition in the field-free regions of the mass spectrometer, it behaves similarly to a regular metastable ion. The description of the field-free regions and metastable ions are discussed in detail in Chapters 2 and 3, respectively. Figure 1.2 illustrates the differences between the unimolecular and bimolecular reaction methods for ion-molecule complex studies. The unimolecular method directly starts from a particular IMC of interest, e.g. $[A^+\cdots N]$ in Figure 1.2, and the IMC will undergo MI and CID dissociations. The internal energy of a metastable IMC lies in a narrow range just above its lowest dissociation threshold. Thus for this IMC, only isomerizations whose energy barriers are lower than this dissociation limit can be observed in the MI time window. For the example shown Figure 1.2, $[A^+\cdots N]$ has two other isomeric configurations, i.e. $[B^+\cdots N]$ or $[C^{+\bullet}\cdots D^\bullet]$. In the MI process, the isomer $[B^+\cdots N]$ is accessible, but $[C^{+\bullet}\cdots D^\bullet]$ is inaccessible because the energy barrier between $[A^+\cdots N]$ and $[C^{+\bullet}\cdots D^\bullet]$ (TS1 in Figure 1.2) lies above the range of the metastable ions' internal energies. Therefore, information about the lower limit for an isomerization barrier can be obtained by experiment. If all the isomers can be generated under appropriate experimental conditions, the MI properties of each of them will be examined and therefore the energy of an isomerization barrier can be approximately estimated. For instance (see Figure 1.2), starting from the isomeric structure $[C^{+\bullet}\cdots D^\bullet]$, both $[A^+\cdots N]$ and $[B^+\cdots N]$ will become accessible and thus TS1 should NOT be greater than the dissociation threshold to $C^{+\bullet}$ and $D^\bullet$. From all the above information, one can draw a conclusion that the energy of TS1 lies between the energies of products B^+ and N to $C^{+\bullet}$ and $D^\bullet$.

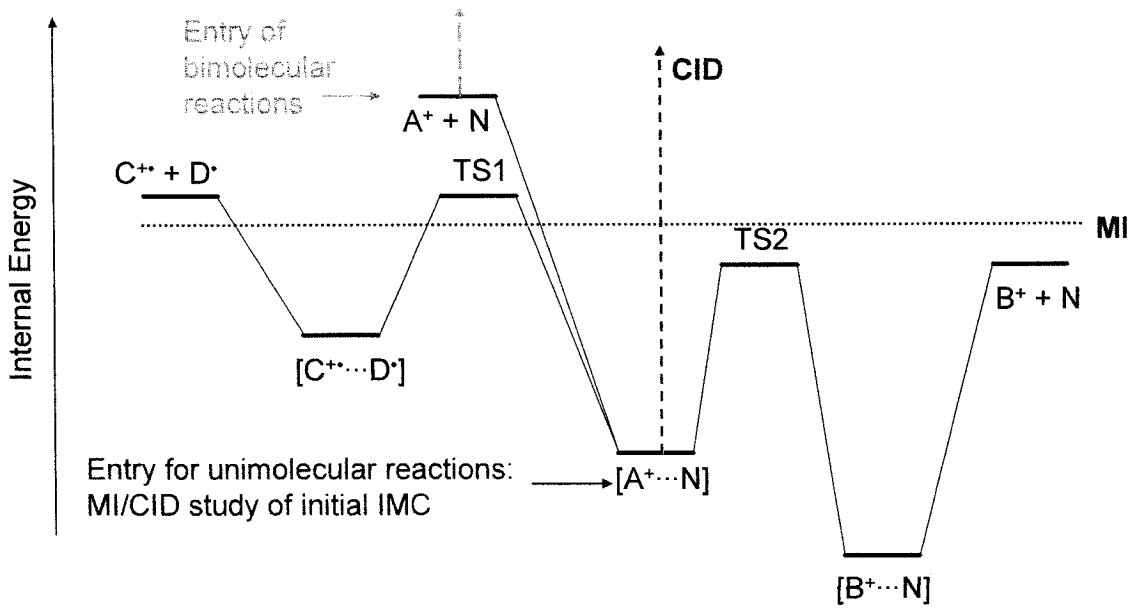

Figure 1.2 Schematic profile illustrating the difference between the unimolecular and bimolecular reaction methods for ion-molecule complex studies.

Collisionally activated IMC have sufficient internal energy to undergo fragmentations requiring higher energy and can provide more structural information about the initial IMC. Computational methods are also used in this study and the calculated energies for the stable and transition states are compared with conclusions from the experiments. In contrast, the bimolecular method starts from the bimolecular species, i.e. collision encounters between the ion and the neutral molecule. These bimolecular encounters carry enough energy to access all reaction channels requiring energy below that of A^+ and N, and therefore under this condition both $[B^+\cdots N]$ and $[C^{+\bullet}\cdots D^\bullet]$ are obtainable. However no information for individual energy barriers is

provided by such experiments; computational chemistry is required to investigate these transition states.

The chemistry of the radical cations of aldehydes, ketones, enols and alcohols constitutes a particularly rich area of research in organic mass spectrometry and recent studies have discovered numerous novel structures and unusual rearrangements of these ions, illustrating the presently recognized important role of distonic ions and ion-molecule complexes for a great number of gas-phase ion reactions.[36-41] It is for example well known that distonic structures and ionized enols are more stable than their conventional isomers resulting from the ionization of the corresponding neutral keto-species. Although the chemistry of these cations has been extensively studied, only limited information is available on the IMCs formed by these species. This thesis investigates structures, thermochemistry, isomerization and dissociation processes of solvated aldehydes, ketones/enols, alcohols, e.g. water-solvated acetaldehyde ion, by experiment and by theory. Such studies are presented in Chapter 4, 5 and 6, which include the IMCs of [acetaldehyde-methanol]$^{+\bullet}$ and [acetaldehyde-distonic methanol]$^{+\bullet}$, [acetone-methanol]$^{+\bullet}$ and [acetone-distonic methanol]$^{+\bullet}$, and [acetaldehyde ion-water]$^{+\bullet}$, respectively.

1.2.2 Gas-Phase Ion Chemistry of Some Ionized Diketones

In addition to IMC studies, Chapter 7 of this thesis concerns some ionized diketones. These two lines of investigation presented in this thesis are both gas-phase ion

chemistry studies. Although the study of diketone ions starts from simple ionized molecules, IMC are also implicated in their dissociations.

Among the most thoroughly studied organic cation dissociations is the very well known "McLafferty Rearrangement".[42-44] This reaction is common to almost all aliphatic aldehydes, ketones, carboxylic acids, esters and amides, and it requires the presence of at least one H-atom attached to the atom at the position -γ to the CO group.[45] Diketone ions have two carbonyl groups that can serve as γ-Hydrogen acceptors and so can be expected to readily undergo a McLafferty rearrangement (Scheme 1.2). The smallest diketone that could display a McLafferty rearrangement is 2,3-pentanedione.

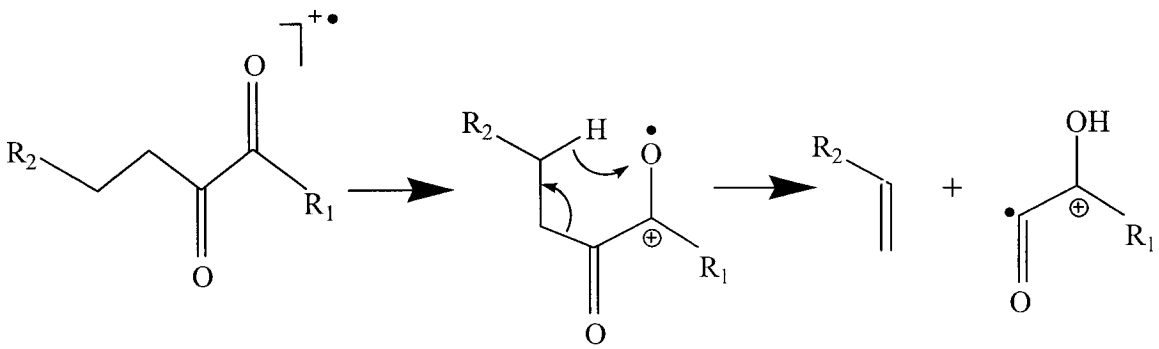

Scheme 1.2. McLafferty rearrangement in diketone ions.

In recent study by Kercher et al.[46] butanone and 2,3-pentanedione were used to determine the heats of formation of acylium fragment ions (R_1CO^+) and their neutral counterparts ($R_2CO^•$) by measuring the dissociative photoionization onsets by the technique of threshold photoelectron photoion coincidence (TPEPICO) spectroscopy.

The simple bond cleavage processes wholly dominated their ion time-of-flight (TOF) mass spectra observations and there was no evidence for the participation of any McLafferty rearrangement in the diketone ion under these experimental conditions. The experiments described in this thesis arose from correspondence with Professor Baer at the University of North Carolina at Chapel-Hill.

In Chapter 7, the MI and CID behaviour of three ionized diketones, 2,3-pentanedione, 2,3-butanedione and 3,4-hexanedione, are described. Gas phase radical cations with low internal energy often dissociate via rearrangement processes in the metastable ion time-frame. The typical flight-time of a metastable ion in a sector mass spectrometer is 10^{-4}-10^{-6} s during which they decompose in a field-free region of the instrument.[47,48] In this study, the 2,3-pentanedione radical cation was observed to undergo a McLafferty rearrangement in the MI time-frame, but unexpectedly giving a composite (two component) peak. As will be described later, this arises because CO loss competes with the ethene loss and therefore it was deemed to be of interest to thoroughly investigate the behaviours of the closest homologues, 2,3-butanedione and 3,4 hexanedione. The mechanism for each reaction was deduced from the combination of mass spectrometry (including MI, CID and isotopic labelling) with theoretical calculations.

References

(1) Bouma, W. J.; MacLeod, J. K.; Radom, L. *J. Am. Chem. Soc.* **1979**, *101*, 5540.

(2) Bouma, W. J.; Poppinger, D.; Saebo, S.; MacLeod, J. K.; Radom, L. *Chem. Phys. Lett.* **1984**, *104*, 198.

(3) Nobes, R. H.; Bouma, W. J.; MacLeod, J. K.; Radom, L. *Chem. Phys. Lett.* **1987**, *135*, 78.

(4) Buschek, J. H.; Holmes, J. L.; Terlouw, J. K. *J. Am. Chem. Soc.* **1987**, *109*, 7321.

(5) Bouma, W. J.; Nobes, R. H.; Radom, L. *J. Am. Chem. Soc.* **1982**, *104*, 2929.

(6) Holmes, J. L.; Lossing, F. P.; Terlouw, J. K.; Burgers, P. C. *J. Am. Chem. Soc.* **1982**, *104*, 2931.

(7) Bouma, W. J.; MacLeod, J. K.; Radom, L. *J. Am. Chem. Soc.* **1982**, *104*, 2930.

(8) Tu, Y.-P.; Holmes, J. L. *J. Am. Chem. Soc.* **2000**, *122*, 3695.

(9) Wang, X.; Holmes, J. L. *Int. J. Mass Spectrom.* **2005**, *242*, 75.

(10) Morton, T. H. *Tetrahedron* **1982**, *38*, 3195.

(11) McAdoo, D. J. *Mass Spectrom. Rev.* **1988**, *7*, 363.

(12) Bowen, R. D. *Mass Spectrom. Rev.* **1991**, *10*, 225.

(13) Longevialle, P. *Mass Spectrom. Rev.* **1992**, *11*, 157.

(14) Bowen, R. D. *Acc. Chem. Res.* **1993**, *24*, 364.

(15) McAdoo, D. J.; Morton, T. H. *Acc. Chem. Res.* **1993**, *26*, 295.

(16) Morton, T. H. *J. Am. Chem. Soc.* **1980**, *105*, 1596.

(17) Longevialle, P.; Botter, R. *J. Chem. Soc., Chem. Commun.* **1980**, *17*, 823.

(18) Hammerum, S. *J. Chem. Soc., Chem. Commun.* **1988**, *13*, 858.

(19) Golding, B. T.; Radom, L. *J. Am. Chem. Soc.* **1976**, *98*, 6331.

(20) Postma, R.; Ruttink, R. J. A.; Terlouw, J. K.; Holmes, J. L. *J. Chem. Soc., Chem. Commun.* **1986**, 683.

(21) Terlouw, J. K.; Heerma, W.; Dijkstra, G. *Org. Mass Spectrom.* **1981**, *16*, 326.

(22) Hammersum, S.; Kuck, D.; Derrick, P. J. *Tetrahedron Lett.* **1984**, *25*, 893.

(23) McAdoo, D. J.; Hudson, C. E. *Org. Mass Spectrom.* **1986**, *21*, 779.

(24) J. K. Terlouw; C. G. de Koster; W. Heerma; J. L. Holmes; Burgers, P. C. *Org. Mass Spectrom.* **1983**, *18*, 222.

(25) Gauld, J. W.; Audier, H.; Fossey, J.; Radom, L. *J. Am. Chem. Soc.* **1996**, *118*, 6299.

(26) Gauld, J. W.; Radom, L. *J. Am. Chem. Soc.* **1997**, *119*, 9831.

(27) Bohme, D. K. *Int. J. Mass Spectrom. Ions Processes* **1992**, *115*, 95 and references therein.

(28) Chalk, A. J.; Radom, L. *J. Am. Chem. Soc.* **1997**, *119*, 7573.

(29) Chalk, A. J.; Radom, L. *J. Am. Chem. Soc.* **1999**, *121*, 1574.

(30) Fridgen, T. D.; Parnis, J. M. *Int. J. Mass Spectrom.* **1999**, *190/191*, 181.

(31) Haranczyk, M.; Burgers, P. C.; Ruttink, P. J. A. *Int. J. Mass Spectrom.* **2002**, *220*, 53.

(32) van der Rest, G.; Nedev, H.; Chamot-Rooke, J.; Mourgues, P.; McMahon, T.B.; Audier, H.E. *Int. J. Mass Spectrom.* **2000**, *202*, 161.

(33) Tu, Y.-P.; Holmes, J. L. *J. Am. Chem. Soc.* **2000**, *122*, 5597.

(34) Wang, X.; Holmes, J. L. *Can. J. Chem.* **2005**, *83*, 1093.

(35) Wang, X.; Sun, W.; Holmes, J. L. *J. Phys. Chem. A.* **2006**, *in Press*.

(36) Bouchoux, G. *Mass Spectrom. Rev.* **1988**, *7*, 1.

(37) Bouchoux, G.; Luna, A.; Tortajada, J. *Int. J. Mass Spectrom. Ion Processes* **1997**, *167/168*, 353.

(38) McAdoo, D. J. *Mass Spectrom. Rev.* **2000**, *19*, 38.

(39) Turecek, F. In *The Chemistry of Enols*; Rappoport, Z., Ed.; Wiley: Chichester, 1990, p 95.

(40) Keeffe, R.; Kresge, A. J. In *The Chemistry of Enols*; Rappoport, Z., Ed.; Wiley: Chichester, 1990, p 399.

(41) Holmes, J. L.; Lossing, F. P.; Terlouw, J. K.; Burgers, P. C. *Can. J. Chem.* **1983**, *61*, 2305.

(42) Nicholson, A. J. C. *Trans. Faraday Soc.* **1954**, *50*, 1067.

(43) McLafferty, F. W. *Anal. Chem.* **1956**, *28*, 306.

(44) McLafferty, F. W.; Hamming, M. C. *Chem. Ind. (London)* **1958**, 1366

(45) Turecek, F. In *Encyclopedia of Mass Spectrometry*; Elsevier: Amsterdam, 2005; Vol. 4, p 396.

(46) Kercher, J. P.; Fogleman, E. A.; Koizumi, H.; Sztaray, B.; Baer, T. *J. Phys. Chem. A* **2005**, *109*, 939.

(47) Holmes, J. L.; Terlouw, J. K. *Org. Mass Spectrom.* **1980**, *15*, 383.

(48) Cooks, R. G.; Beynon, J. H.; Caprioli, R. M.; Lester, G. R. *Metastable Ions*; Elsevier: Amsterdam, 1973.

CHAPTER 2

INSTRUMENTATION

2.1 Introduction

All the experiments described in this thesis have utilized a sector mass spectrometer for the studies of ion-molecule complexes in the gas phase. Mass spectrometry is not only a highly sensitive analytical tool but also one of the most powerful and versatile research techniques in chemistry, physics, and the geological and biological sciences. A great number of mass spectrometers have been developed since W. Wien first analyzed positive ions by magnetic deflection in 1898[1].

The whole field of mass spectrometry was introduced in J. J. Thomson's book "Rays of Positive Electricity and Their Application to Chemical Analysis", published in 1913[2]. Thomson was able to obtain a plot of the ion current as a function of mass-to-charge ratio (m/z), based on the development of the original parabolic method of analysis of positive rays. In 1919[3], F. W. Aston made the first mass spectrometer with velocity focussing and employed its application to isotope identification. Since then a great number of mass spectrometers have been developed broadening the range of their applications in diverse branches in chemistry and physics. Another breakthrough in mass spectrometry resulted from the observation of metastable ions present in a mass spectrum by J. A. Hipple and E. U. Condon[4], leading to the development of tandem mass spectrometry which is often referred to MS/MS or MS/MS/MS or MS^n. In 1972, J.

Beynon described metastable decompositions and proved the utility of high resolution in the determination of the elementary composition of ions[5]. The further development of mass spectrometers focussed on the improvement of high-resolution systems and new ionization methods such as matrix assisted laser desorption ionization (MALDI) and electrospray ionization (ESI). The latter two techniques are often used for biological samples of large molecular weight, for which K. Tanaka and J. B. Fenn shared part of the Nobel Prize in 2002.

2.2 The Modified VG ZAB Mass Spectrometer

In this section, a description will be given for the mass spectrometer that was used to conduct the experiments in this thesis. A mass spectrometer contains the following elements: a device to prepare the ions (ion source), one or more mass analyzers to separate the ions, field free regions wherein the ions may decompose spontaneously or under collisional activation, and finally a detector to "count" the ions.

All experiments described in this thesis were carried out on a modified VG ZAB (VG Analytical, Manchester, UK) triple focussing mass spectrometer[6] with BEE geometry, where B and E refer to magnetic and electrostatic analyzers, respectively. Such a device is often referred to a mass spectrometer of reversed geometry: the ions pass through the magnetic sector (B) before flying through the electric sector (E), in contrast to a MS of conventional geometry comprising an electric sector prior to a magnet. This triple focusing mass spectrometer consists of an ion source, a magnetic sector (B), two

electrostatic analyzers (E or ESA), three field-free regions (FFR) and three detectors as shown in Figure 2.1. All spectra were recorded with the ZABCAT program developed by Mommers Technologies[7].

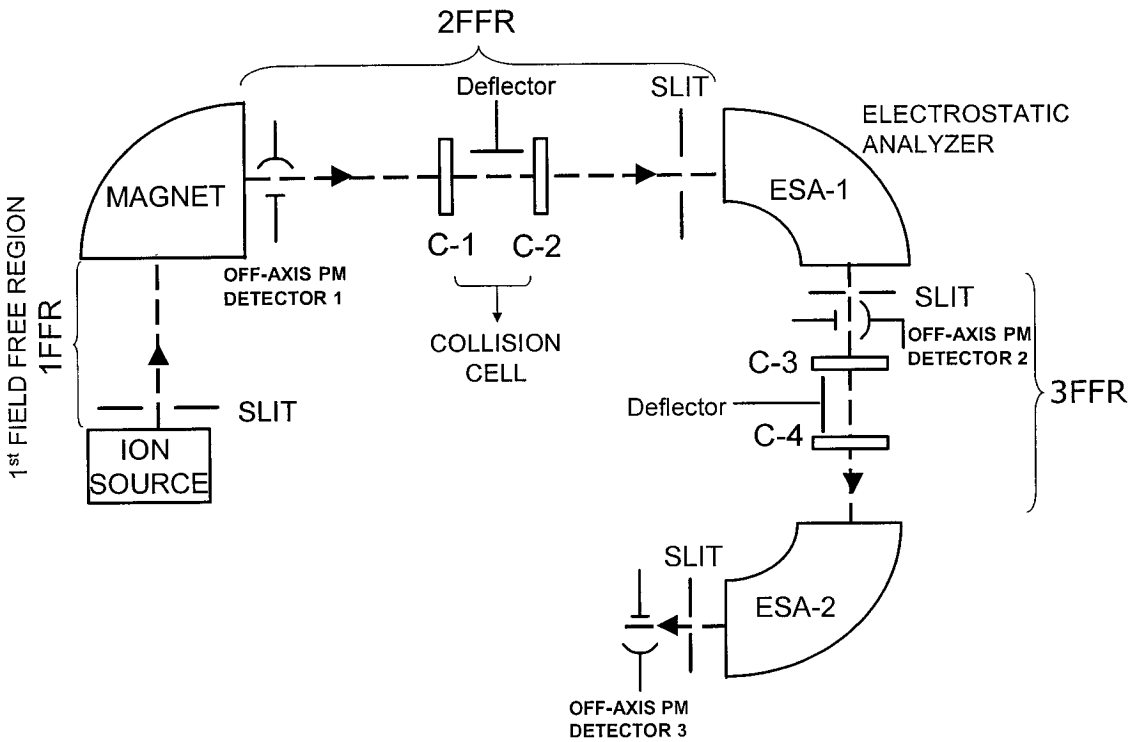

Figure 2.1. Schematic diagram of the VG ZAB triple focusing mass spectrometer.

Using this triple focusing instrument, tandem mass spectrometry experiments can be performed as follows. After introducing samples through a septum or gas inlet into the ion source, molecular ions or other types of ions will be produced in the source. The magnetic analyzer is then used to mass select the ions of interest according to their momentum. The selected precursor ions will travel through the 2nd field free region where they can decompose either spontaneously (metastable ions) or as a result of collisional activation. These fragment ions are then analyzed by the second mass

analyzer ESA1 according to their kinetic energies. Thus a product ion mass spectrum of the original precursor ions can be generated; this process is often referred to as a MS/MS experiment. This experiment can be continued in the 3FFR. Instead of scanning all the ions of different m/z ratios, the first electrostatic analyzer ESA can energy select an fragment ion that has been produced in the 2FFR into the 3FFR. All the fragments produced in the 3FFR will be analyzed by the second electrostatic analyzer ESA, generating a MS/MS/MS spectrum (a tandem mass spectrum). The above experiments allow us to obtain a mass spectrum resulting from the decomposition of an ion selected in the previous analyzer. Generally, this technique requires two or more mass analyzers in series or a single mass analyzer that can be used sequentially to analyze the precursor and product ions; the former instrument is known as tandem-in-space MS and the latter is known as tandem-in-time MS. Tandem MS is used to provide structural information by establishing exact relationships between precursor ions and their fragmentation products.

2.2.1 Ion Source

In the ion source, the sample molecules are ionized prior to analysis in the mass spectrometer. Figure 2.2 represents the ion source of the VG ZAB sector mass spectrometer, attached to a simple magnetic mass analyzer.

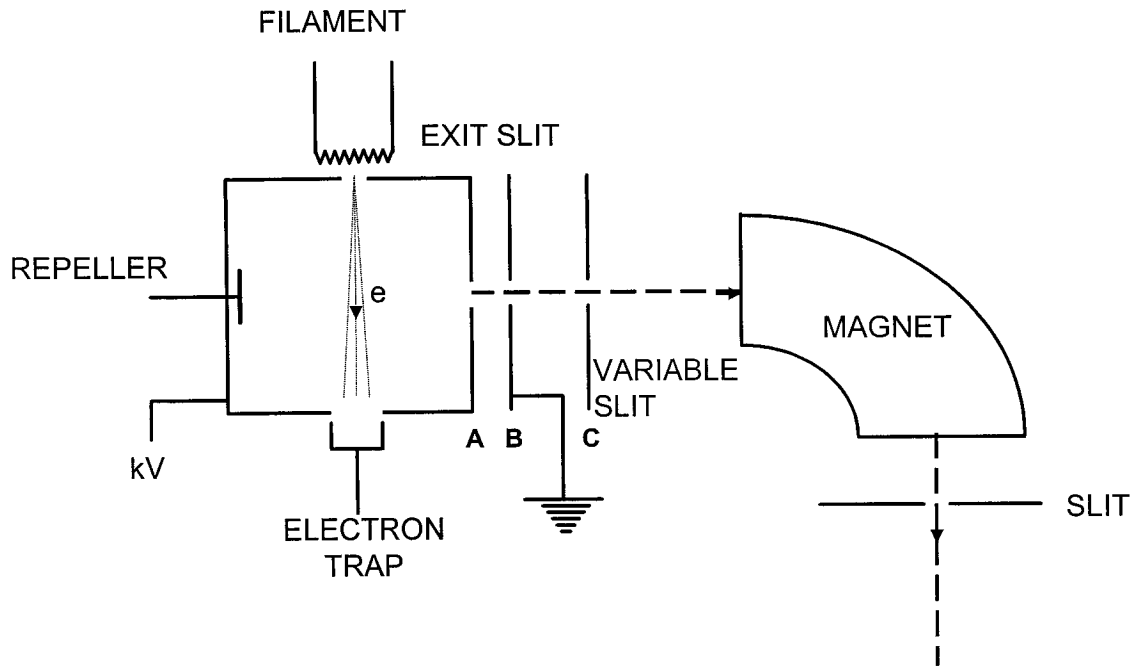

Figure 2.2. Ion source of the VG ZAB sector mass spectrometer.

Samples are introduced into the ion source via an appropriate inlet system. There are four ways to introduce different types of samples into the VG-ZAB sector mass spectrometer: via a liquid septum inlet for volatile liquids, a Granville-Phillips (GP) inlet used for low boiling point liquids, a gas inlet for gas samples or a solids probe for solid samples. Ions are produced in this source by the electron ionization (EI) mode in our experiments. The electrons emitted by the heated filament (>2000 °C) pass through the ionization chamber and are collected by the trap. This electron trap is usually maintained at a positive potential to attract the electrons. Ions are formed by collisions between electrons and molecules along the path of the electron beam, and the ions are forced to move towards the exit of the ionization chamber by the ion repeller plate on which a small positive voltage is applied. The main acceleration of the ions takes place between exit slit A and plate B, because a very high potential up to 8000 kV is applied on the

ionization chamber with respect to the grounded plate B. The narrow slit is used to define the ion beam that will enter the mass analyzer. The numbers and types of ions formed in the ion source depend on the electron energy. At energies just above the ionization potential of the molecule, little fragmentation occurs; but at higher energies ions of all the possible fragments of the molecule are produced. In the case of organic molecules, a constant, optimum yield of ions appears above ca 25 eV of electron energy, but generally the energy is maintained at 70 eV. The ion source is usually kept at a high vacuum of 10^{-4} to 10^{-8} mbar.

In order to produce proton-bound pairs or other cluster ions, a relatively high pressure is required in the ion source to ensure sufficient encounters between ions and molecules. To make protonated acetaldehyde alcohol pairs and protonated acetone alcohol pairs for the studies described in Chapters 4, 5 and 6, a modified high-pressure (HP) ion source was used.[8] In contrast to a regular ion source, the HP source only contains a liquid inlet and a gas inlet, while the GC inlet is sealed. A regular source typically has two exit slits on the ion exit plates, a narrow slit (ca 0.015 mm) for the electron ionization (EI) mode and a wider slit (ca 0.045 mm) for the chemical ionization (CI) mode, while the HP ion source only has an EI slit. These modifications help in maintaining a relatively high pressure in the source, i.e. 1-1.5 orders of magnitude higher than that in a regular source.[8]

The kinetic energy of an ion with mass m, charge ze and velocity v accelerated through the potential drop V_{acc} is determined by the following equation:

$$\frac{1}{2} mv^2 = zeV_{acc} \quad (2.1)$$

Thus all ions of the same charge will acquire the same kinetic energy, irrespective of their mass, when passing through the exit slit.

2.2.2 Magnetic Analyzer

The magnetic analyzer consists of two parallel electromagnets surrounding an iron core. The magnetic field (B) has a direction that is perpendicular to the direction of ion motion. In the field an ion follows a circular trajectory with a radius r described by the following relationship:

$$mv = rBze \quad 2.2$$

For every value of B, ions of the same charge and the same momentum (mv) have a circular trajectory with a characteristic r value. Hence, the magnetic analyzer separates the ions according to their momentum. Indeed, it is a *momentum* selector not a *mass* selector. The velocity of ions with uniform translational kinetic energy (eV) is given by the following equation:

$$v = \left(\frac{2zeV}{m} \right)^{1/2} \quad 2.3$$

Hence equation 2.2 can be written as,

$$m/z = \frac{B^2 r^2 e}{2V} \qquad 2.4$$

Because V is held constant, ions with a particular mass-to-charge ratio, m/z, can be made selectively go through the analyzer for a given value of B. By varying B as a function of time, ions with various values of m/z can be successively observed.

2.2.3 Electrostatic Analyzer (ESA)

The electrostatic analyzer comprises two curved parallel plates and a radial electrostatic field E is produced by applying a potential between them. The trajectory of ion motion is then circular and the velocity is constantly perpendicular to the field. Then the centrifugal force balances the electrostatic force according to the following equation:

$$zE = \frac{mv^2}{R} \qquad 2.5$$

Because the translational kinetic energy of ions is $eV = \frac{1}{2} mv^2$, the above equation can be written as,

$$R = \frac{2V}{E} \qquad 2.6$$

Thus the electrostatic analyzer transmits ions according to their kinetic energy. Ions of greater or smaller energies describe greater or smaller radii so that adjusting the potential applied on the ESA plates allows ions of a particular translational kinetic energy to pass through. The electrostatic analyzer can be used as an energy filter with a slit in place behind it.

2.2.4 Field Free Regions (FFR)

The VG ZAB sector mass spectrometer houses three field free regions as shown in Figure 2.1. They are the regions between the ion source and the magnetic sector (1FFR), between the magnetic sector and the first electrostatic sector (2FFR) and between the first and the second electrostatic sector (3FFR). The FFRs are the regions where observable chemistry occurs in the sector mass spectrometer, as ions can decompose spontaneously or under collisional activation in the FFRs. The 2FFR and 3FFR contain collision cells and ion beam deflection electrodes. The background pressure within the FFRs is ca. 10^{-8} mbar. Each collision cell consists of 2-3 cm long blocks of steel with a 2 mm wide groove to pass the ion beams. A collision gas can be introduced into the groove by a gas line, resulting in ion and target gas collisions. The pressure in the cells is monitored by ionization gauges placed in close proximity. There are two collision cells in each FFR and the deflector plate is placed between the two cells. A potential of +500 V is usually applied to the deflector electrode, deflecting all charged

particles out of the beam path in a neutralization-reionization mass spectrometry (NRMS) experiment.[9-11]

Ions that are able to decompose spontaneously in a FFR are so-called metastable ions (m*). Their fragments give rise to the metastable peaks of which the positions on the mass scale and peak shapes are discussed in Chapter 3. For those ions that decompose in the 2FFR, the kinetic energy of a parent ion M_1^+ (eV_{acc}) will be partitioned between the fragments. If this decomposition takes place without any conversion of internal energy to external energy, each fragment ion M_2^+ will continue to move along the same direction as the parent ion and with the same velocity. According to the law of conservation of energy, the initial kinetic energy of the parent ion $\frac{1}{2} m_1 v^2$ will be equal to the total kinetic energy ($\frac{1}{2} m_2 v^2 + \frac{1}{2} m_3 v^2$) of the products. Thus the kinetic energy is shared between the fragments in the ratio of their masses, as shown in the following equations:

$$\frac{1}{2} m_2 v^2 = m_2/m_1 \, eV_{acc} \qquad 2.7$$

$$\frac{1}{2} m_3 v^2 = m_3/m_1 \, eV_{acc} \qquad 2.8$$

The mass of a fragment ion, generated from a mass selected parent ion, can be calculated from its kinetic energy measured by the electrostatic sector. This results in the ESA functioning as a "mass" analyzer for the fragment ions. In addition, the electrostatic sector can be used to focus or select a fragment ion M_2^+ by fixing the potential on the ESA, only allowing the transmission of ions with the kinetic energy $m_2/m_1 \, eV_{acc}$.

2.2.5 Detector

The detectors installed on the VG ZAB mass spectrometer are off-axis photomultipliers, which are made up of a conversion dynode, a CaF_2 scintillator and a photomultiplier, as shown in Figure 2.3. The device allows the detection of positive ions.[12] In the positive mode, the conversion dynode, on which a high negative potential (-20 kV) is applied, attracts ions coming from the exit slit of the mass analyzer. The high energy positive ions impinge on the central portion of the conversion dynode and secondary electrons are emitted. These electrons are accelerated by the electric field towards a CaF_2 scintillator and the scintillations produced are detected by an optically coupled photomultiplier. A restriction on the maximum possible potential applied to the dynode may result in mass discrimination.

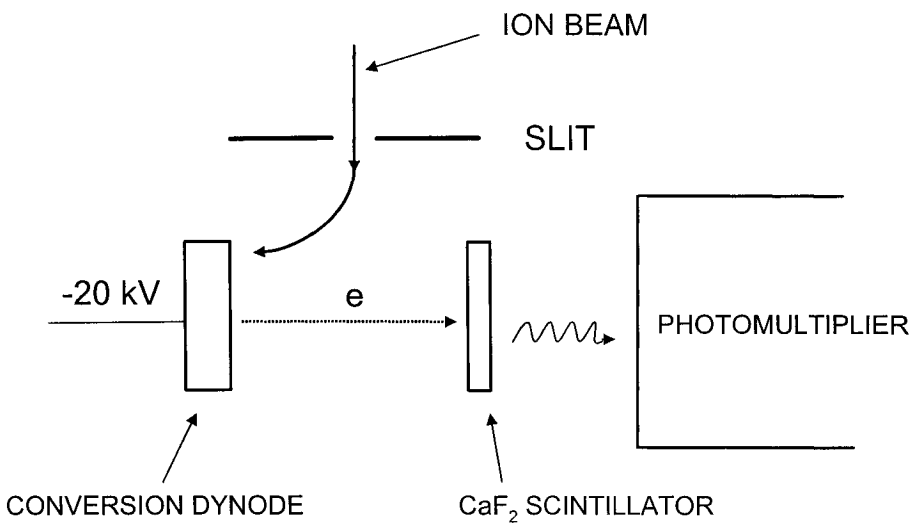

Figure 2.3. Schematic diagram of the ion detector: a photon multiplier.

References

(1) Wien, W. *Verhanal. Phys. Ges.* **1898**, *17*.

(2) Thomson, J. J. *Rays of Positive Electricity and Their Application to Chemical Analysis*; Green & Co. Ltd.: London, 1913.

(3) Aston, F. W. *Phil. Mag.* **1919**, *38*, 709.

(4) Hipple, J. A.; Condon, E. U. *Phys. Rev.* **1945**, *68*, 54.

(5) R. G. Cooks; J. H. Beynon; Capriol, R. M.; Lester, G. R. *Metastable Ions*; Elsevier: Amsterdam, 1973.

(6) Holmes, J. L.; Mayer, P. M. *J. Phys. Chem.* **1995**, *99*, 1366.

(7) Traeger, J. C.; Mommers, A. A. *Org. Mass Spectrom.* **1987**, *22*, 592.

(8) Rennie, E.; Mayer, P. M. *J. Chem. Phys.* **2004**, *120*, 10561.

(9) G. I. Gellene; Porter, R. F. *Acc. Chem. Res.* **1983**, *16*, 200.

(10) Wesdemiotis, C.; McLafferty, F. W. *Chem. Rev.* **1987**, *87*, 485.

(11) Holmes, J. L. *Mass Spec. Rev.* **1989**, *8*, 513.

(12) Hoffmann, E. D.; Charette, J.; Stroobant, V. *Mass Spectrometry Principles and Applications*; Masson, John Wiley & Sons: Paris, 1996.

CHAPTER 3

CONCEPTS AND METHODS USED IN THE STUDY OF GAS-PHASE ION CHEMISTRY

3.1 Introduction

This chapter will introduce some basic concepts of gas-phase ion chemistry including the types of ions generated in a mass spectrometer, ion thermochemistry, ion structure assignment and ion reaction mechanisms (for ion dissociations and rearrangements); it also will describe the experimental and computational techniques employed in the studies of gas-phase ion chemistry. Experimental methods that have been used for this thesis involve Mass-analyzed Ion Kinetic Energy Spectrometry (MIKES, also known as Metastable Ion dissociation spectrometry), Collision-Induced Dissociation (CID) mass spectrometry and Kinetic Energy Release (KER) measurements. The last part of this chapter will briefly review some of the computational methods employed for the investigation of ground state and transition state configurations of gas-phase ions, providing a complete potential energy profile for the mechanisms of their reactions.

3.2 Types of Ions Generated in a Mass Spectrometer

Many different types of ions are formed in a mass spectrometer. This section will describe some common ions found in the mass spectra of organic compounds and also

explain how they are generated in the ion source or other regions in the mass spectrometer.

3.2.1 Source-Generated Ions

Positively charged ions and *negatively charged ions* are the two major categories of source-generated ions. Positive ions, namely molecules or radicals from which one or more electrons have been removed so that they carry net positive charges, form the basis of mass spectrometry in their great variety and abundance. All of the ionic species discussed in this thesis are positive ions. A negative ion can be produced by the attachment of one or more electrons to a molecule or a free radical, although their abundance in a typical ion source is low compared with positive ions.

Molecular ions belong in the category of positive ions. A molecular ion ($M^{+\bullet}$) can be directly formed by the ionization of a neutral molecule (M) by removal of one electron from it. The process of the formation of a singly-charged molecular ion in an electron ionization source (EI) is shown by the following equation[1]:

$$M + e \rightarrow M^{+\bullet} + 2\,e \qquad 3.1$$

The encounter between a molecule and an electron beam, released from the heated filament of the EI source, results in removal of an electron from the neutral species. Thus the amount of energy transferred to the molecule is equal to or greater than the ionization energy of the molecule. Because most organic molecules contain an even number of

electrons, their molecular ions typically carry an odd number of electrons and so are called "odd-electron ions". In comparison, those ions that contain an even number of electrons are "even-electron ions", e.g. NO^+, and correspond to ionized free radicals. The ionization of a molecule takes place by an almost "vertical" process, as the interaction between a molecule and a high speed bombarding electron (the electron energy is usually about 70 eV) is very rapid. Figure 3.1 shows a typical electron ionization (EI) source used for the ionization of molecules or radicals, attached to a simple magnetic mass analyzer.

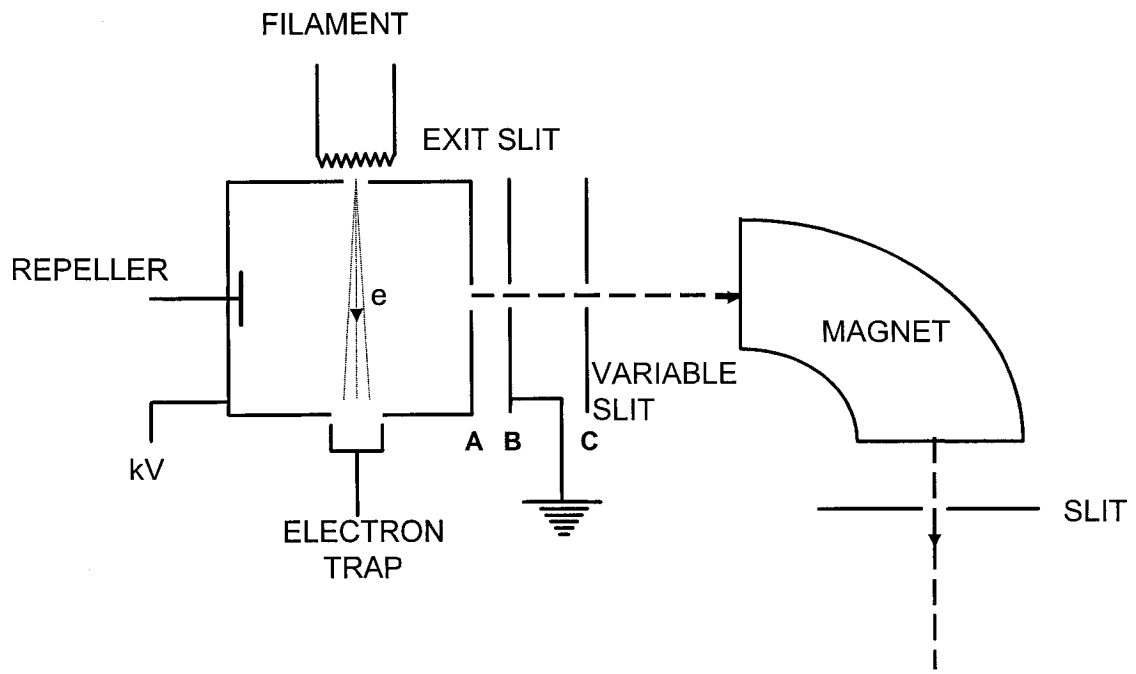

Figure 3.1 Diagram of a typical electron ionization source and a magnetic sector.

This ionization process nearly follows the Franck-Condon principle: the total time taken for ionization to occur is similar in magnitude to the period of the vibration of the molecule and so the internuclear separation can change somewhat during this process.

Therefore, the molecular ion's geometry can relax somewhat from that of the neutral's ground state.

If the energy that has been transferred from the bombarding electron to the molecule is sufficient to break one or more chemical bonds in the ion, *fragment ions* can be generated. The process can be represented as:

$$M^{+\bullet} \rightarrow m_1^{+} + N^{\bullet} \qquad 3.2$$

or

$$M^{+\bullet} \rightarrow m_2^{+\bullet} + N \qquad 3.3$$

In reaction 3.2, m_1^{+} represents an even-electron fragment ion and $N^{\bullet}$ the neutral (radical) fragment. Reaction 3.3 shows the formation of an odd-electron fragment ion $m_2^{+\bullet}$. It was first noted by Stevenson that for hydrocarbons, the positive charge remained on the fragment with the lower ionization energy[2].

A molecular ion may decompose by a series of competing unimolecular reactions, resulting in the production of many different fragment ions. In addition, the fragment ions (m_1^{+} or $m_2^{+\bullet}$) can undergo further decomposition, if these ions still carry sufficient excess internal energy. The quasi-equilibrium theory (QET) of mass spectra explains the production and relative intensities of those fragments.[3,4] The theory states that after ionization the excess internal energy above the ground state of a molecular ion is converted into vibrational energy in a series of radiationless transitions between crossing potential energy surfaces. In one state, if the internal energy transferred from another state is above the state's dissociation energy the ion will fragment.

3.2.2 Stable Ions

Stable ions are those ions that are formed in the ionization source and travel from the source to the detector without decomposition. They comprise all the major peaks in a mass spectrum. The flight time of a stable ion in a mass spectrometer depends on their translational kinetic energy, which results from the acceleration energy applied to the ion (*zeV*). On our VG ZAB mass spectrometer, an accelerating voltage of 8 kV is used so that it will take an ion of m/z = 100 amu approximately 10^{-4} s to reach the second detector after the first EAS, as shown in Figure 2.1, after it leaves the ion source, having traversed a distance of ca 200 cm.

For clarification, the expression "stable ion" is different from that of "stable ion structure". Stable structures or ground state structures of an ion mentioned in this thesis refer to those configurations for isomeric ion structures that lie in potential wells on its Potential Energy Surface (PES).

3.2.3 Unstable Ions

Unstable ions are those ions that are formed with sufficient internal energy so that they will decompose before they exit the ionization chamber of the source. The life-time of an unstable ion is typically of the order of $<10^{-6}$ s;[5] the ion source residence time is ca 1×10^{-6} s. As mentioned in section 3.2.1, ions that are generated in the source will

continue decomposing until the fragments carry little excess internal energy and so they will leave the source as stable ions or as metastable ions; the latter will be introduced next.

3.2.4 Metastable Ions (MI)

3.2.4.1 Definition of Metastable Ions

Metastable ions are those ions that undergo decomposition after they leave the ionization chamber but before they reach the detector. Ions that are metastable have acquired the internal energy (necessary for their dissociation) within the ion source and not from any event in a field free region (FFR)[6]; compare with collision-induced dissociation; see section 3.2.5. The development of double-focusing mass spectrometers and particularly reverse-geometry instruments in which the magnet precedes the electric sector, greatly motivated the study of metastable ions.[7]

Compared with stable ions and unstable ions, metastable ions have intermediate internal energies and so they dissociate with intermediate rate constants. For sector mass spectrometers, metastable ions have a range of lifetimes of ca 1-50 μs[8,9], flying through the 1st and 2nd FFR (see Figure 2.1, 50 cm and 100 cm in length, respectively) after they exit the source (1-2 μs). Therefore, the amount of internal energy of a metastable ion corresponds to its dissociation rate constants that lie between ca. $10^4 - 10^6$ s^{-1}, depending on the accelerating energy V_{acc} and the dimensions of the mass spectrometer. The life-time intervals thus define the "metastable ion (observation) window" and establish the range of rate constants and ion internal energies that can be sampled in metastable ion

observation (see Figure 3.2). Figure 3.2 shows the rate constant and internal energy distribution for stable, metastable, unstable ions accelerated by a V_{acc} of 4 - 10 kV in a typical sector mass spectrometer.

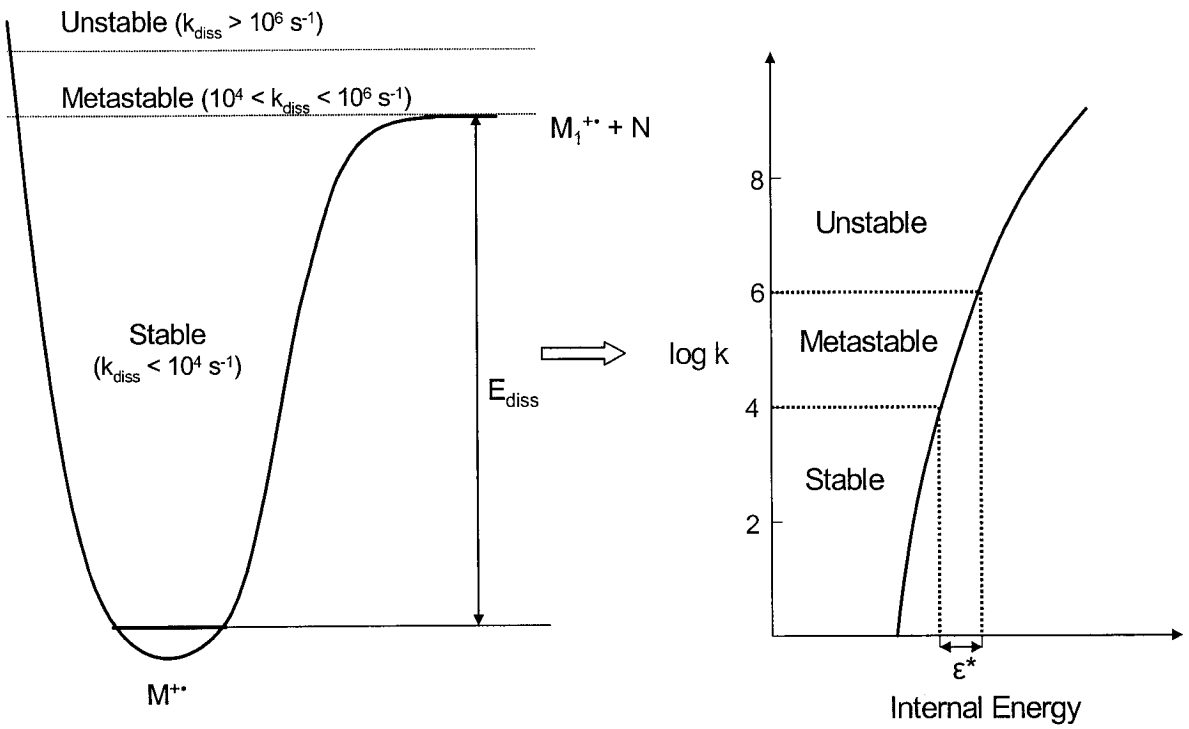

Figure 3.2. The PES, rate constant and internal energy distribution for stable, metastable and unstable ions.

The internal energies of metastable ions fall into a narrow range close above the dissociation threshold. If the barrier for their rearrangement is close to or less than the critical energy for dissociations, then the ions can rearrange into another configuration. Because of the limit of the maximum internal energy that a metastable ion contains, only

a few metastable decompositions are usually displayed in the mass spectra of organic ions, rarely exceeding four metastable ion peaks[10].

3.2.4.2 Apparent Mass of Metastable Ions

As mentioned in Chapter 2, for an ion M_1^+ that decomposes in the FFRs, its translational kinetic energy ($\frac{1}{2} m_1 v^2$) is distributed between the product ion M_2^+ ($\frac{1}{2} m_2 v^2$) and the neutral fragment M_3 ($\frac{1}{2} m_3 v^2$). The dissociation fragments have, to a very close approximation, the same velocity as the precursor ion. If this fragmentation happens in the 1FFR (see Figure 2.1), the magnetic sector will not transmit M_2^+ at the m/z value given by the regular magnet selection equation, $m/z = B^2r^2e/2V$, because the product ion M_2^+ only has $(m_2/m_1)\bullet(eV_{acc})$ translational kinetic energy. Therefore, the magnet will select M_2^+ at an *apparent mass*, m*. From equations of 2.3 and 2.4 in Chapter 2, the fragment ion, resulting from the dissociation of the metastable ion M_1^+, will have an apparent mass of M_2^2/M_1.

3.2.5 Collisionally Activated Ions

Collisionally activated ions are those high internal energy ions arising from energetic collisions between metastable or stable ions and a neutral target gas, in the collision cells within a field free region in a tandem mass spectrometer. In collisional activation the high translational kinetic energy ions interact with (relatively stationary) neutral atoms or molecules (target gas) and as a result a fraction of their translational energy is converted into internal energy of the ions. It has been found that as much as 10

eV of energy can be added to ion internal energy during this collision process. Thus an activated ion with sufficient energy can undergo subsequential decompositions to give many more fragment peaks in its mass spectrum than those in a metastable ion mass spectrum. These fragmentation processes are independent of the original internal energy of the precursor ion and the details will be addressed in Section 3.3.3.

3.3 Experiments on Mass-Selected Ions with the VG ZAB Mass Spectrometer

3.3.1 Mass-Analyzed Ion Kinetic Energy Spectrometry (MIKES)

The dissociation products of a metastable mass-selected ion can be observed by a mass-analyzed ion kinetic energy (acronym MIKE) mass spectrum. The magnetic analyzer can transmit M_1^+ ions by fixing its field strength at an appropriate value and some of these ions can undergo metastable dissociation in the 2FFR between the magnet and the electric sector. As discussed in Section 3.2.4.2, the fragments produced from the metastable ions will carry a fraction of the kinetic energy of their precursor ion. The kinetic energy (E_{K2}) of a fragment ion M_2^+ and E_{K1} of the precursor ion M_1^+ are:

$$E_{K2} = \tfrac{1}{2} m_2 v^2 \qquad E_{K1} = \tfrac{1}{2} m_1 v^2 = eV_{acc} \tag{3.4}$$

Thus we deduce that

$$\frac{E_{K2}}{E_{K1}} = \frac{m_2}{m_1} \tag{3.5}$$

where v is the velocity of ions, V_{acc} is the source acceleration potential and m_2 and m_1 are mass of the fragment ion and the precursor ion, respectively.

The electric sector separates ions according to their kinetic energy and the ions passing through the analyzer must satisfy the condition that

$$\frac{1}{2} mv^2 = \frac{1}{2} zER \qquad 3.6$$

where E is the electric strength, R is the radius of the ion's circular trajectory. The value of E is the same for all the primary ions generated in the source, because the kinetic energies of these ions are the same. For ions that are produced during metastable dissociation in the 2FFR, the value of E has to be adjusted to transmit the fragment ions with their various kinetic energies to the detector. If E_1 is the electric field strength required to transmit mass-selected ion M_1^+, then lower potentials $((m_2/m_1)x(E_1)$, $(m_3/m_1)x(E_2)$, etc.) will be needed to select fragment ions (M_2^+, M_3^+, etc.) Therefore, by scanning the ESA, all fragment ions produced by a metastable M_1^+ ion will be sequentially passed through the ESA onward to the detector. The mass of a product ion can then be calculated from its kinetic energy measured by the ESA. Thus the output of ion abundance versus kinetic energy spectrum can be converted to an ion abundance versus fragment ion m/z spectrum. The resulting spectrum is known as a mass-analyzed ion kinetic energy mass spectrum.

3.3.2 Kinetic Energy Release (KER) and Metastable Ion Peak Shapes

3.3.2.1 Kinetic Energy Release Measurements

Suppose that a mass-selected ion, M_1^+, undergoes dissociation in a FFR of a mass spectrometer, $M_1^+ \rightarrow M_2^+ + M_3$. The excess internal energy of the precursor ion (electronic, vibrational and rotational energy) is distributed among all the degrees of freedom of the products. It follows that part of this energy is released into translational kinetic energy of the departing fragments. This phenomenon is known as kinetic energy release (KER). The KER is isotropic and consequent, the KER along the x-axial (the beam path) results in the observation of fragment ion peaks which show a wider kinetic energy distribution than that of the precursor ions. If u_2 and u_3 are the vector velocities of the fragment ion and the neutral counterpart, respectively, the corresponding velocities in the laboratory frame are $(v_1 + u_1)$ for the product ion and $(v_1 + u_2)$ for the neutral fragment[11]. This will then induce an increase or decrease in the fragments' velocities along the beam path, depending on the direction of the vector velocities (forward or backward on the x-axis). Therefore, the above approximation (see section 3.3.1) that the fragments have retained the same velocity of the precursor ion is no longer quite true when KER occurs during the fragmentation. Since the KER is isotropic, the peak centre will coincide with the calculated value, but the signal will be greatly broadened relative to the main, non-dissociating ion beam.

The kinetic energy released in a unimolecular reaction is typically expressed as the value at half-height of the fragment ion peak, $T_{0.5}$, measured in electric sector or ion acceleration volts. KER is calculated by the following equation:

$$T_{0.5,m_2}\,(\text{meV}) = \frac{m_1^{\,2}\left(W^{\,2}_{0.5,m_2} - W^{\,2}_{0.5,m_1}\right)}{16 m_2 m_3 V_{acc}} \qquad 3.7$$

where m stands for the mass of the respective species, $W_{0.5}$ is the full width energy spread of precursor and fragment ion peaks at half height. V_{acc} is the acceleration energy of the precursor ion and conventionally set at the value at 8000 eV. $T_{0.5}$ is typically reported in meV units.

3.3.2.2 Metastable Ion Peak Shapes and Dissociation Processes

Early measurements of KERs were used to characterize isomeric ion structures and the scope of metastable peak observations has been reviewed by Holmes and Terlouw.[6] The kinetic energy release distributions (KERD) are obtained experimentally. The mass-selected M_1^+ ions usually have a narrow range of translational kinetic energies when they exit the ion source, e.g. ca. 2 eV in 8000 eV. Energy resolution can be obtained by narrowing the variable slits mounted on the mass spectrometer (see Figure 2.1), until the peak width of the main ion beam no longer changes. The shape of the very narrow main ion beam, i.e. the mass-selected ion beam, is Maxwell-Boltzmann like and the ion peak presents a "Gaussian" profile, as shown in Figure 3.3.a. Fragment ions also produce Gaussian-shaped peaks when they are produced by a single dissociation process

and KER ($T_{0.5}$) values are typically in the range of 10 – 40 meV. These values correspond to signals that are typically an order of magnitude wider than the main ion beam.

Energy resolved metastable ion peaks usually have a Gaussian or flat-topped or even dish-topped peak, Figure 3.3. The dish-topped peak is derived from z-axial discrimination in the instrument. The entrance ports of the variable slits or mass analyzers (B or ESA) have a finite height in the z-axis (vertical to the ion beam). The isotropic KER results in some fragment ions moving along the z-axis direction and these ions will fail to pass through the entrances. This will result in fewer ions being detected near the peak centroid. In the absence of z-axial discrimination, these metastable ion peaks would have flat-topped profiles.

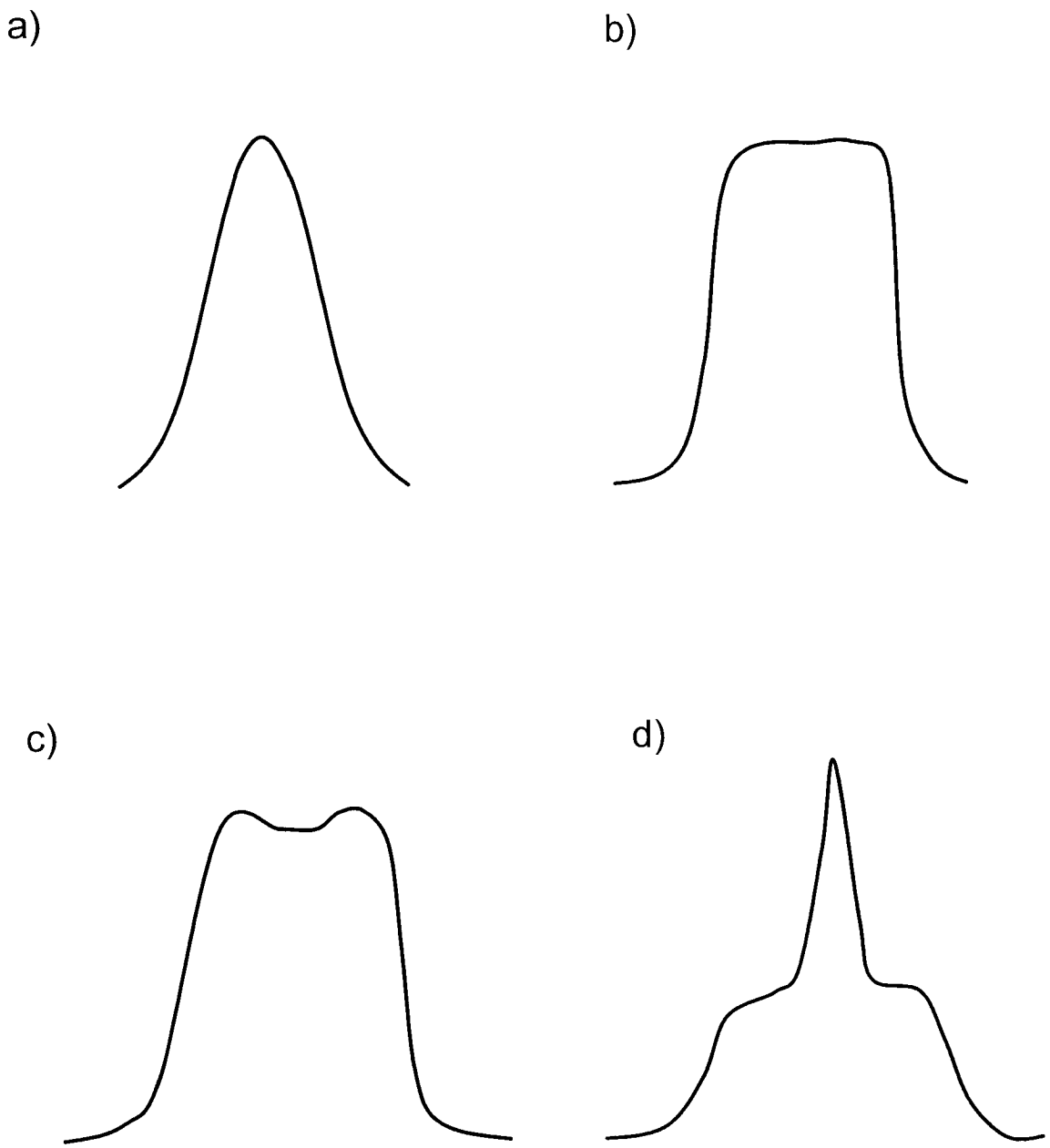

Figure 3.3. Basic metastable ion peak shapes, a) Gaussian, b) flat-topped, c) dish-topped, d) composite.

The shapes of metastable ion peaks in energy resolved MIKE spectra can provide information about the ion dissociations. Figure 3.4 represents the potential energy curves for two different ion dissociation processes, corresponding to the Gaussian or flat-topped peaks observed in the mass spectra, respectively. The former are usually associated with reactions that take place at the thermochemical threshold and the latter are for dissociations that must have a reverse energy barrier. E is the internal energy of a metastable ion; E_0 is the activation energy required for the reaction; $\varepsilon^{\neq}$ is the difference between the E and E_0, also known as the non-fixed energy; E_{rev} is activation energy of the reverse reaction, also called as the fixed energy. Non-fixed and fixed energies both contribute to the energy available for dissociation.

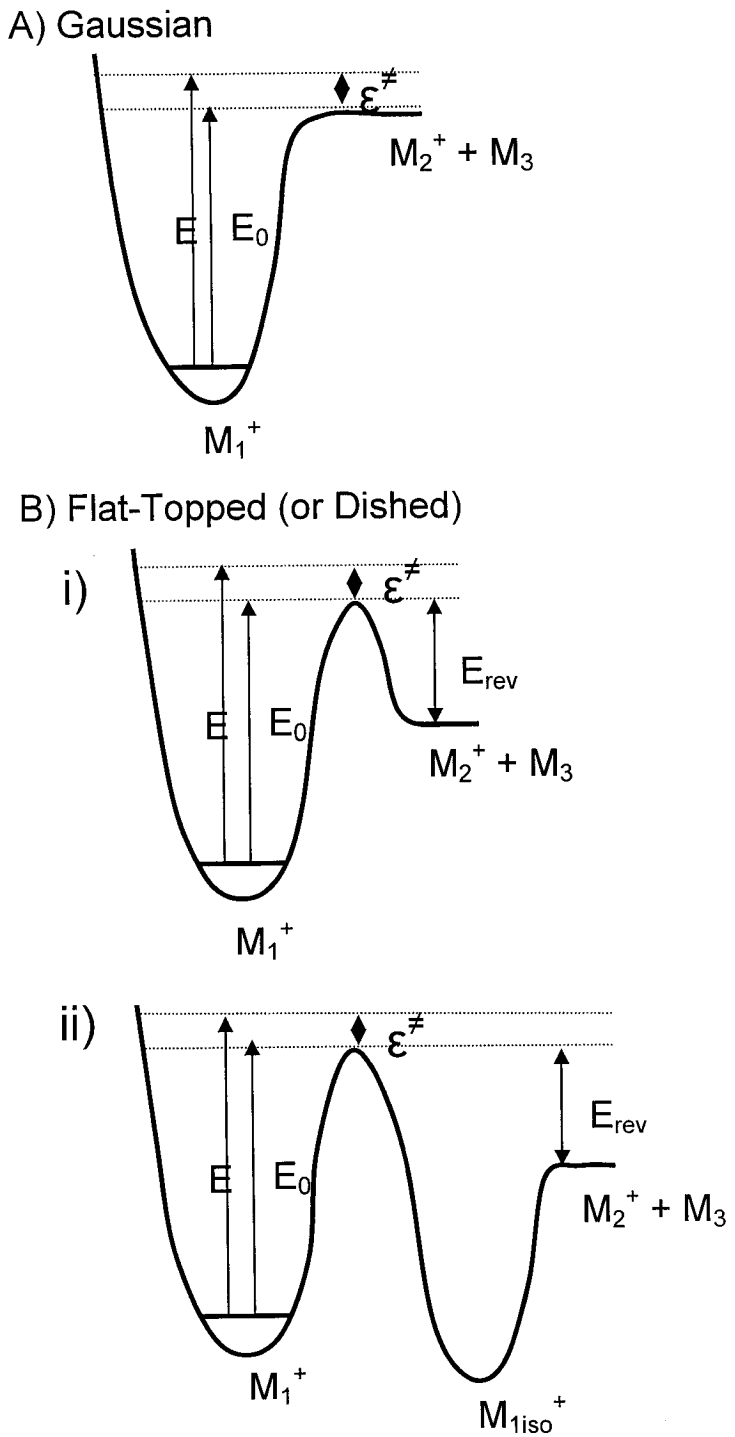

Figure 3.4 Potential energy surfaces for an ion dissociation A) without a reverse energy barrier (Gaussian peak), B) with a reverse energy barrier (flat- or dished-topped peak).

A Gaussian-type fragment ion peak arises from reactions having little or no reverse energy of activation. These reactions normally proceed via a very loose transition state, e.g. a simple bond cleavage. The values of KER (in $T_{0.5}$) are normally in the range of 10 – 25 meV. For such cases, the excess internal energy that is distributed among the translational degrees of freedom of the fragments is very small (Figure 3.4.A). Note that dissociations resulting from a cleavage of an electrostatic bond (non-covalent bond) typically have very small $T_{0.5}$ values ca. < 2 meV, e.g. the metastable fragment of water loss from an ethylene ion attached to water molecule, $[CH_2CH_2 \cdots OH_2]^{+\bullet}$.

A flat-topped or dish-topped peak indicates that the dissociation reaction has a significant reverse activation energy. This can arise from the following two circumstances: 1) An ion dissociation requires a substantial rearrangement in the transition state (a tight transition state), as shown in Figure 3.4.B.i. 2) The reaction (Figure 3.4.B.ii) involves an isomerization of the precursor ion, M_1^+, to its stable isomer, M_{1iso}^+ via a high energy transition state lying above the dissociation limit. Thus the excess internal energy in ions is sufficient and will contribute a larger translational kinetic energy release to the products, resulting in a broad ion peak.

Characteristic properties of potential surfaces for the above two types of metastable ion peaks are summarized in Table 3.1

Table 3.1 Characteristic properties of potential energy surfaces for metastable ions

	Potential energy surface	
	A	B
Metastable ion peak	Narrow (Gaussian)	Wide (Flat-topped)
Kinetic energy release	Small	Large
Type of reaction	Simple bond cleavage	Isomerization
Reverse energy barrier (E_{rev})	Zero or small	Large
Transition State	Loose	Tight

In addition, composite ion peaks (Figure 3.3.d) are also observed in MIKE spectra and they can result from the following scenarios: 1) A metastable ion undergoes two competing dissociations and gives two fragment ions of different structures. For example, ionized 2,3-pentanedione produces a composite $(M-28)^{+\bullet}$ peak due to the losses of CO and C_2H_4, and the details are discussed in Chapter 7. 2) A mass-selected ion has two stable isomers both of which can undergo metastable dissociations either to produce product ions of different structures or to give a single product ion structure, with the two barriers having closely similar energies. A good example of the production of a composite metastable ion peak, shown in Figure 3.5, is the dissociation of the $C_3H_5^+$ ion by loss of H_2.[9] The two metastable dissociation processes are represented as the following reactions:

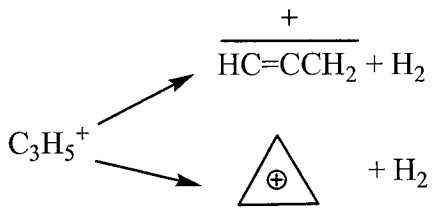

Two isomeric $C_3H_3^+$ ions are produced: cyclopropenium (the broad component) and the propargyl cation, $HCCCH_2^+$ (the narrow component). As will be described later (Chapter 7), narrow sections of such peaks can be transmitted from the 2FFR to the 3FFR in order that the ion structures may be investigated further.

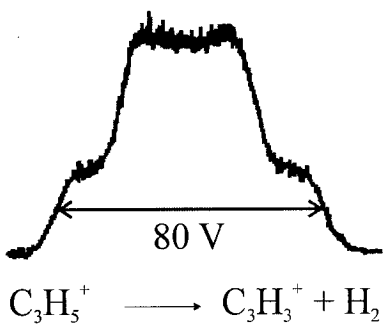

Figure 3.5. A composite metastable ion peak resulting from the dissociation of $C_3H_5^+$ ion.[9]

3.3.3 Collision-Induced Dissociation (CID) Experiments

Ion fragmentation resulting from collisional excitation was observed in the early days of mass spectrometry. This process is based on the principle that ions are activated via collisions with a neutral target gas and it is an easy experiment to implement on tandem mass spectrometers. The type of experiment is referred to collision-induced dissociation (CID) or collision activated dissociation (CAD); both terms are used

extensively in the literature and are not distinguishable. In 1913, J. J. Thomson recorded a parabola ion image showing "beads" which was the first evidence for the process of collision-induced dissociation.[12] Since the early 1970s, the collision-induced dissociation method has been very widely applied on various instruments for revealing the structure of polyatomic ions.[13-17]

When the mass selected ion interacts with a target gas, some of the ion's translational kinetic energy is converted into internal energy. A CID process involves two steps: ion activation resulting from one or multiple collisions, followed by unimolecular dissociations (see Figure 3.6). The CID mass spectrum of a mass selected ion provides abundant structure information for the (non-isomerizing) ions that are produced originally in the ion source, whereas the metastable ion dissociation (MI or MIKE) mass spectrum often produces peaks resulting from the dissociation of a rearranged ion and thus contains structure information for an isomer(s) of the original species. When the latter ions are sufficiently excited in a CID process, they tend to fragment quickly via structurally diagnostic cleavage reactions before rearrangements occur. Many examples have clearly shown that the CID mass spectra of isomeric ions are strikingly different, while the MI spectra are much less distinguishable. Also, there are more fragmentation channels available to the collision activated ions, the CID mass spectrum typically contain as many peaks as are generated in a full, normal electron impact mass spectrum. Structure features can be identified by fragment ion peaks that show the atom connectivity of the ion.

Collision Induced Dissociation

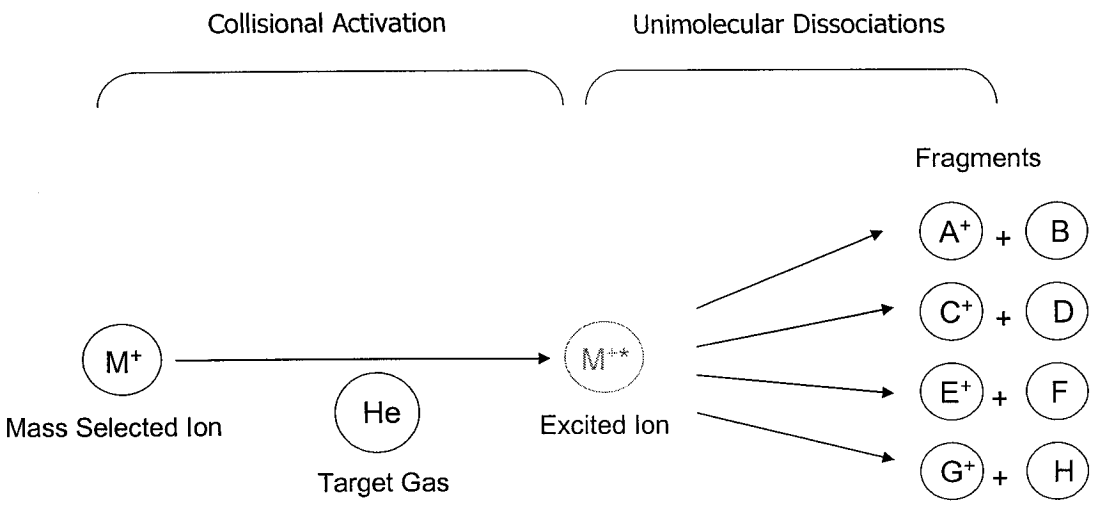

Figure 3.6. A two-step collision-induced dissociation process.

Collision-induced dissociation studies involve both low and the high ion translational kinetic energy collisions. The former process is observed in ion trap and quadrupole instruments[18]; the latter work is normally performed on magnetic and electric sector mass spectrometers where the ions carry high kinetic energies (up to 10 keV). In this thesis, the collision events observed on the VG ZAB mass spectrometer are all at high ion kinetic energies, 8 keV. To obtain the CID mass spectra, the target gas is introduced to the collision cell in the 2FFR or 3FFR. The ion excitation results from non-momentum transfer collisions between the ion and target gas molecule. The ions move at least 100 times faster than the target gas, e.g. an ion of m/z = 100 amu travels at ca. 4.5 x 10^4 m/s, such activated ions do not deviate from their flight path after the collision. The mass spectrum of the resulting fragment ions is obtained by scanning the electrostatic

analyzer voltage. In a CID mass spectrum, the ion peaks are poorly resolved because of the large KER accompanying the fragmentation. In our experiments, helium was chosen as the target gas mainly due to the following three reasons: 1) It is a chemically inert gas. 2) It is light so that it can be quickly pumped away after one CID experiment by the diffusion or turbo-molecular pump mounted below the collision cell. 3) The ionization energy of He is high, 24.6 eV, hence there is no or little charge exchange between the target gas and the ions. Note that that summit of a CID ion peak, e.g. M_2^+ produced from the CID reaction $M_1 \rightarrow M_2^+ + N$, is not exactly at $(m_2/m_1)\bullet(eV_{acc})$, but at a slightly lower energy. This results from the very small translational energy conversion into ion internal energy.

The product ion distribution in a CID mass spectrum is dependent on the competing fragmentation channels available to the precursor ion, the laboratory timescale for the reactions and the internal energy distribution of the precursor ion. The relative abundances of the product ions and internal energy distribution of the precursor ion are greatly affected by the collision condition. When the beam intensity of the mass-selected ion is reduced by ca. 10% by the collision with the target gas at a certain pressure, the ions predominantly suffer a single interaction with the target gas.[19] Such cases are called *single-collision conditions*, under which the processes of collisional activation and unimolecular dissociation are distinct in time and the CID mass spectra are reproducible. Under multiple-collision conditions, the two processes can occur in overlapping time windows. Under such conditions, the fragment ion yield increases, particularly in low mass ions, but no new fragment ions are produced.

3.3.4 Generating Ion-Molecule Complexes and Acquiring Their Mass Spectra

As mentioned in Chapter 1, we are interested in the chemistry of ion-molecule complexes (IMC). An IMC is produced from an appropriate proton-bound pair by the loss of a selected free radical initiated by collision.[20,21] Figure 3.7 represents a general scheme for generating the IMC of interest.

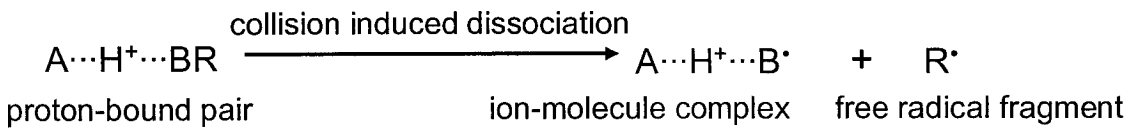

Figure 3.7 A general scheme for the formation of an ion-molecule complex.

Ion-molecule complexes are generated and analyzed using the modified VG ZAB tandem mass spectrometer[22] that has BEE geometry. The detailed experimental procedure is as follows (also see Figure 3.8). An appropriate proton-bound pair is chosen to make the IMC of interest. For example, if we want to make the methanol and water IMC, $[CH_3OH/H_2O]^{+\bullet}$, a proton-bound dimer of methanol, $CH_3O(H)\cdots H^+\cdots O(H)CH_3$ can be used as the precursor ion. Note that the two methanol molecules are bound through an $O\cdots H^+\cdots O$ bridge. This proton-bound methanol pair (or dimer) can be generated in the ion source. The "high-pressure" ion source (which is described in detail in Section 2.2.1) is beneficial to produce cluster ions and so was used in our experiments to make a relatively large flux of the proton-bound pair in the source. The pressure in the ion source is read by an ionization gauge mounted above the ion source diffusion pump. The

"high-pressure" source pressure is about three or four orders of magnitude higher than the gauge indicated pressure, e.g. an observed pressure of 8×10^{-5} mbar for an ion with m/z = 100 indicates an ion source pressure of ca. 0.3 mbar[23]. The vapour of liquid samples, e.g. CH_3OH, is admitted to the source via the septum inlet. All ions produced in the source chamber are accelerated by a potential of 8 kV when they exit the source. The magnet is set to mass select (actually momentum select) the proton-bound pair, e.g. $CH_3O(H)\cdots H^+\cdots O(H)CH_3$ m/z = 65, into the 2FFR. Helium is introduced into one of the collision cells in the 2FFR, and the proton-bound pair undergoes collision-induced dissociation after the encounters with the target gas. The fragment ion for the selected free radical loss peak can be then observed on the oscilloscope screen of the mass spectrometer. For the above example, in order to make the $[CH_3OH/H_2O]^{+\bullet}$ complex ion, a $CH_3^\bullet$ radical is lost from the proton-bound dimer, $CH_3O(H)\cdots H^+\cdots O(H)CH_3$, the reaction is shown in the following equation:

$$\underset{m/z = 65}{CH_3O(H)\cdots H^+\cdots O(H)CH_3} \rightarrow \underset{m/z = 50 \text{ (ion-molecule complex)}}{[CH_3O(H)/HOH]^{+\bullet}} + CH_3^\bullet \text{ (CID)} \qquad 3.8$$

Because the fragmentation involving such a free radical loss requires a relatively high energy compared with reactions involving the losses of neutral molecules (e.g. H_2O, CO, C_2H_4 etc.), the fragment ion peak is not visible in the metastable ion (MI) mass spectrum of the precursor ion, the proton-bound pair. However, a minor peak for the ion-molecule complex, corresponding to this $CH_3^\bullet$ loss, appears in the CID mass spectrum of the parent ion. With an increase of the target gas pressure, the peak intensity of this ion grows. Thus the yield of the ion-molecule complexes can be improved by increasing collision

gas pressure by which the main beam (the precursor ion beam) is reduced by the target gas by ca. 20%. The desired ion-molecule complex will be energy-selected by the first electric sector and transmitted into the 3FFR for the observation of their further dissociation or isomerization.

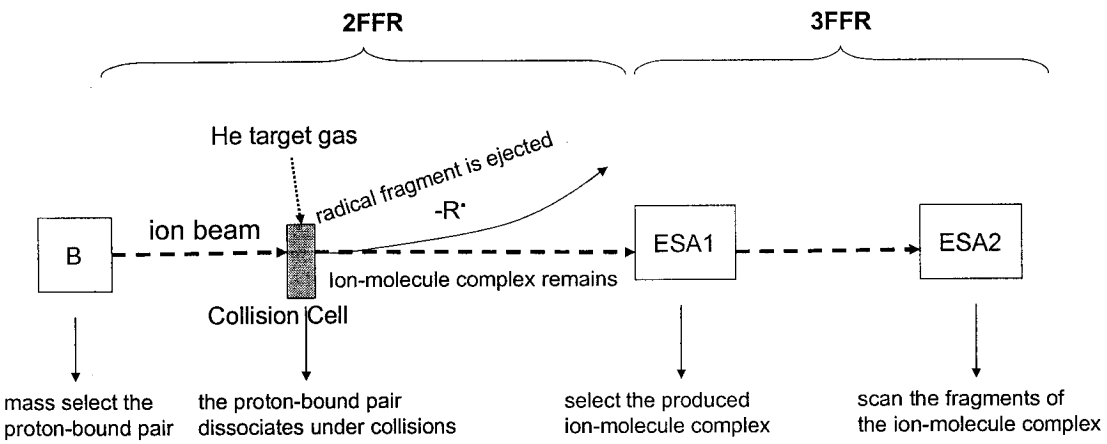

Figure 3.8. Experimental procedure for the formation of the desired ion-molecule complex.

Because the IMC is formed by a high energy dissociation process induced by collisions, such an ion still has sufficient energy to decompose during its flight through the 3FFR prior to the second ESA. Such a process is similar to a typical metastable ion dissociation (MI) observed in the 2FFR. When a target gas is admitted to the 3FFR, the ion-molecule complex can also undergo collision-induced dissociations (CID). The fragment ions generated either by MI or CID process will be analyzed by the second electrostatic analyzer (ESA) according to their kinetic energies. If we call the IMC the first-generation fragment of the parent ion (i.e. the proton-bound pair), the product ions

from the IMC, formed in the 3FFR, are called second-generation fragment ions. Suppose that the kinetic energy of the parent ion (mass of m_1) is E_{k1} (corresponding to the instrument acceleration's voltage), the first-generation fragment (mass of m_2) has kinetic energy of $E_{k2} = m_2/m_1 \times E_{k1}$. Similarly, the second-generation fragment's energy (mass of m_3) can be calculated by the following equation:

$$E_{K3} = \frac{m_3}{m_2} E_{K2} = \frac{m_3}{m_2} \times \frac{m_2}{m_1} E_{K1} = \frac{m_3}{m_1} E_{K1} \qquad 3.9$$

Therefore, by scanning ESA2, the fragment ions generated from the IMC will appear at a sector voltage value very close to that appropriate to their masses, e.g. $E_3 = (m_3/m_1)x(E_1)$. All metastable ion (MI) and collision-induced dissociation (CID) mass spectra of the desired ion-molecule complex were recorded with the ZABCAT program[22]. Understanding its MI and CID characteristics is necessary to discover the ion structures of stable states and fragment ions.

3.4 Experimental Approaches to Ion Structure and Reaction Mechanism Determinations

The unimolecular dissociation of a gas phase ion can be characterized by interpretation of its mass spectra produced by a variety of experimental techniques. Like solving a puzzle, a mass spectrum is generally analyzed by noting the correlations of the fragments, the relative peak abundances and peak shapes etc., giving an appropriate elucidation for ion structures and the mechanisms of reactions to produce the ion and fragmentation pathways. Thus a complete fragmentation profile of a given ion will

illustrate all important isomerizations and dissociation processes, including the transition state energy barriers for rearrangements, the accessible stable isomeric structures, the resulting fragment ion structures and their neutral counterparts. Common experimental methods to illustrate ion structures and reaction mechanisms involve metastable ion (MI) and collision-induced dissociation (CID) mass spectrometry, isotopic labelling ion, thermochemistry (e.g. ion heats of formation, ionization energy, ion appearance energy, ion stability etc.) determinations, and some other methods such as Collision-Induced Dissociative Ionization (CIDI) mass spectrometry and Neutralization-Reionization Mass Spectrometry (NRMS)[9]. The first three are the main methods used in this thesis and so they are described in detail below.

3.4.1 The Significance of Metastable Ion (MI) and Collision-Induced Dissociation (CID) Mass Spectrometry

Depending on the internal energy of an ion, isomerization reactions can occur as well as dissociations. Therefore a variety of isomeric ion structures may contribute to the fragment ion peaks in a mass spectrum, making the assignment of ion structures challenging. The conventional method for distinguishing ion structures was the interpretation of the electron ionization mass spectrum (normal mass spectrum) of neutral molecules on a single mass analyzer instrument. The disadvantage of this method is that fragment peaks may be contaminated by other compounds in the source and the relationship between the given mass precursor ion and the fragment ion is often unclear. However, this obstacle can be overcome by measuring the metastable ion dissociation (MI or MIKE) mass spectra on a sector instrument (i.e. double focussing or triple

focussing mass spectrometer). The relative energy barriers for dissociation (E_{diss}) and isomerization (E_{iso}) are the predominant factors that determine whether or to what extent an ion structure A^+ rearranges to an isomer B^+ at a given internal energy. The different potential energy curves, as shown in Figure 3.9, illustrate some of the commonly encountered circumstances of ion isomerizations.

In Figure 3.9-a, the barrier for isomerization is much larger than the dissociation thresholds (the critical energy for the lowest energy dissociation), i.e. $E_{iso} >> E_{diss}$. In this case, no ion isomerization can be observed because the decomposition reaction rate is much larger than isomerization due to the large activation energy required for the rearrangement. Thus the fragment ions will reflect the original structure of the precursor ion, A^+.

Figure 3.9-b shows that a rearrangement of the ion can occur at internal energies lower than the dissociation threshold, $E_{iso} << E_{diss}$. In this case, isomerizations will result in the partial or full loss of the initial ion structure before any decomposition proceeds. A metastable ion has an internal energy falling in a narrow band above its dissociation barrier and so in 3.9-b the ion can freely interconvert between the isomeric forms prior to dissociation. Therefore, the fragmentation of such a metastable ion is not necessarily characteristic of the initial structure of the precursor ion. Note that depending on the relative magnitudes of E_{diss} (A^+ or B^+), one or two MI peaks may be observed.

Figure 3.9-c shows the situation where an ion has to undergo a rate-determining isomerization, e.g. from A^+ to B^+, prior to dissociation. In this example, A^+ and B^+ ions

will generate the same metastable ion dissociation (MI) mass spectrum. The fragment ion peaks in such MI mass spectra may not be characteristic of the initial ion structure. In this case, how and to what extent the rearrangements that occur can be identified by isotopic labelling experiments, will be discussed in the following section 3.4.2.

The first semi-quantitative relationship between metastable ion dissociation and ion structure, which was named the "metastable ion peak abundance-ratio rule" was first proposed by Shannon and McLafferty[24] in 1966. It was based on the assumption that if two metastable ions of the same molecular formula display the same fragment peaks and with the same relative peak abundances in their MI mass spectra, then they must have the same structure. However, as discussed above, the product ions may result from a mixture of fragmenting species and thus the measured relative peak abundances would depend on the composition of the ion beam. Thereafter the MI peak shapes were taken into account as an aid to ion structure identification. The kinetic energy release value ($T_{0.5}$) was first used as a characteristic feature of ion structure by Jones et al. in 1973[25]. $W_{0.5}$ is another term to describe the KER in some of the earlier literature and is expressed as the width of the energy spread at half peak height. The KER method was particularly useful when isomeric metastable ions dissociated via only one significant fragmentation channel. For example, Holmes and Terlouw[26] have measured $W_{0.5}$ values of the MI peaks for the $H^{\bullet}$ loss from three $[C_2H_4O]^{+\bullet}$ isomers (i.e. acetaldehyde radical cation, ethylene oxide and vinyl alcohol) as 11V, 35V, 41V, respectively. Because these three peaks are also significantly different in shape (narrow Gaussian, broad and dish-topped respectively), they can be used to identify the isomeric ions.

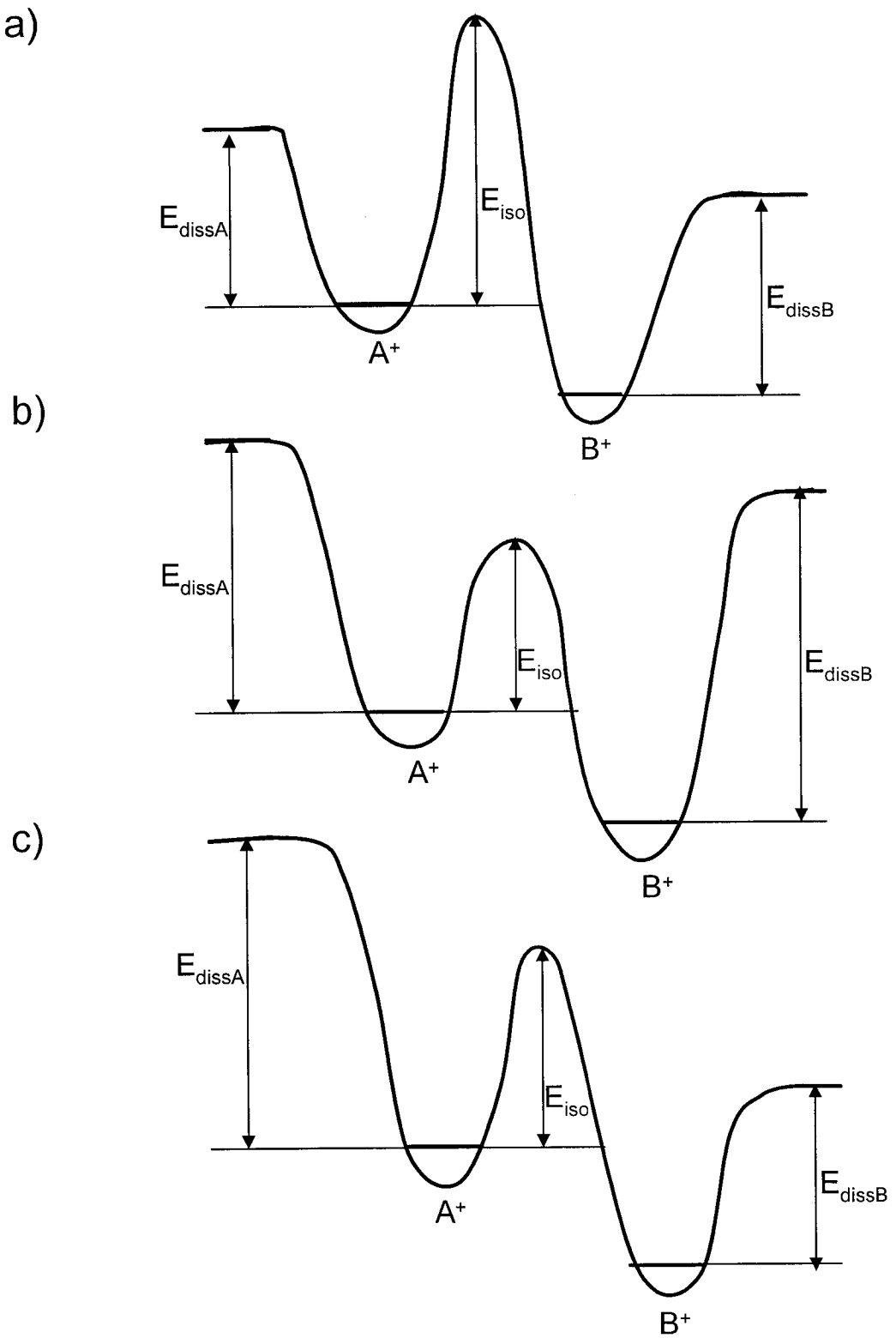

Figure 3.9. Potential energy curves featuring ion isomerizations (see text for explanation).

In a collision-induced dissociation process, the ion has gained sufficient energy from the collision so that it can overcome relatively high dissociation barriers. Fragment peaks observed in CID mass spectra correspond to rapid dissociations rather than those resulting from rearrangements. Collision-induced dissociations commonly involve a simple bond cleavage and so they are more readily interpretable for ion structure elucidations.[27] Moreover, if one compares an MI mass spectrum of a given ion with its CID mass spectrum, he or she can usually tell which fragment ions observed are result of simple bond cleavage reactions or ion rearrangements. After an MI mass spectrum has been recorded, the effect of collision gas on it therefore should be carefully examined. If an MI peak is unaffected by collision gas, known as *collision insensitive*, then the process giving rise to the peak must involve an ion rearrangement. If an MI peak results from a simple bond cleavage then the peak will be *collision sensitive.* This is illustrated by the following example. The MI and CID mass spectra of the proton-bound methanol dimer, $(CH_3OH)_2H^+$ m/z = 65, both show two major fragmentation peaks (Figure 3.10): one at m/z 33 from the loss of a methanol molecule due to a simple bond cleavage and the other at m/z 47 corresponding to a water molecule lost following an ion rearrangement. In the MI mass spectrum, the ion rearrangement reaction (producing the m/z 47 ion) dominates the simple bond cleavage reaction (producing m/z 33 ion) by a factor of ca. 3:1. In the CID mass spectrum, m/z 47 peak abundance is unaffected by the presence of collision gas; whereas the m/z 33 peak has increased about twelve-fold in abundance, making m/z 33 the dominant peak. Thus, in this example, the m/z 33 peak is collision sensitive, while m/z 47, the product of a rearranged $(CH_3OH)_2H^+$ is collision insensitive.

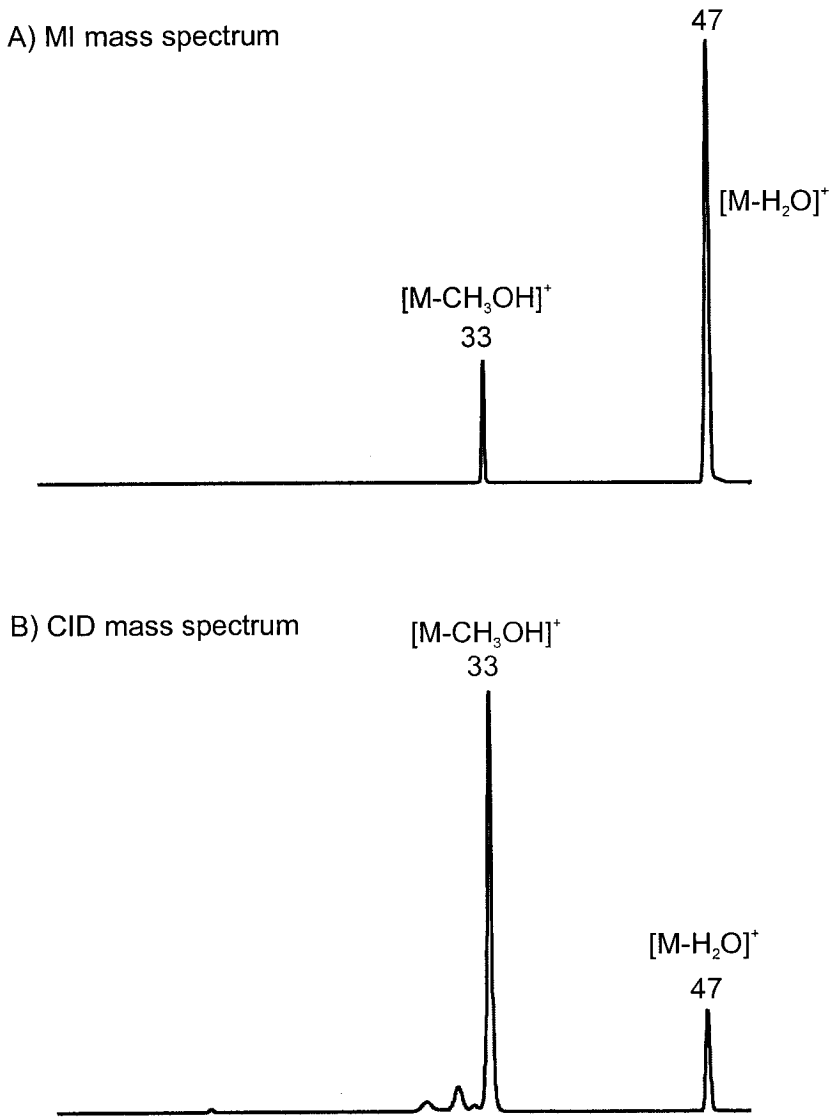

Figure 3.10. MI and CID mass spectra of the proton-bound methanol dimer, $(CH_3OH)_2H^+$ m/z = 65.

At relatively low internal energies (in an MI process), the fragment from the most energetically favourable channel predominates. For other dissociations to be able to compete as observable MI processes, their activation energies must lie in a narrow range of ca. 0-30 kJ/mol above the energy barrier for the most energetically favourable process.

At higher internal energies (in CID reactions), the prevailing processes are fast dissociations, which may crucially depend on dynamic phenomena. In order to appreciate these differences, let us consider a hypothetical graph of log k(E) vs. E, as shown in Figure 3.11.

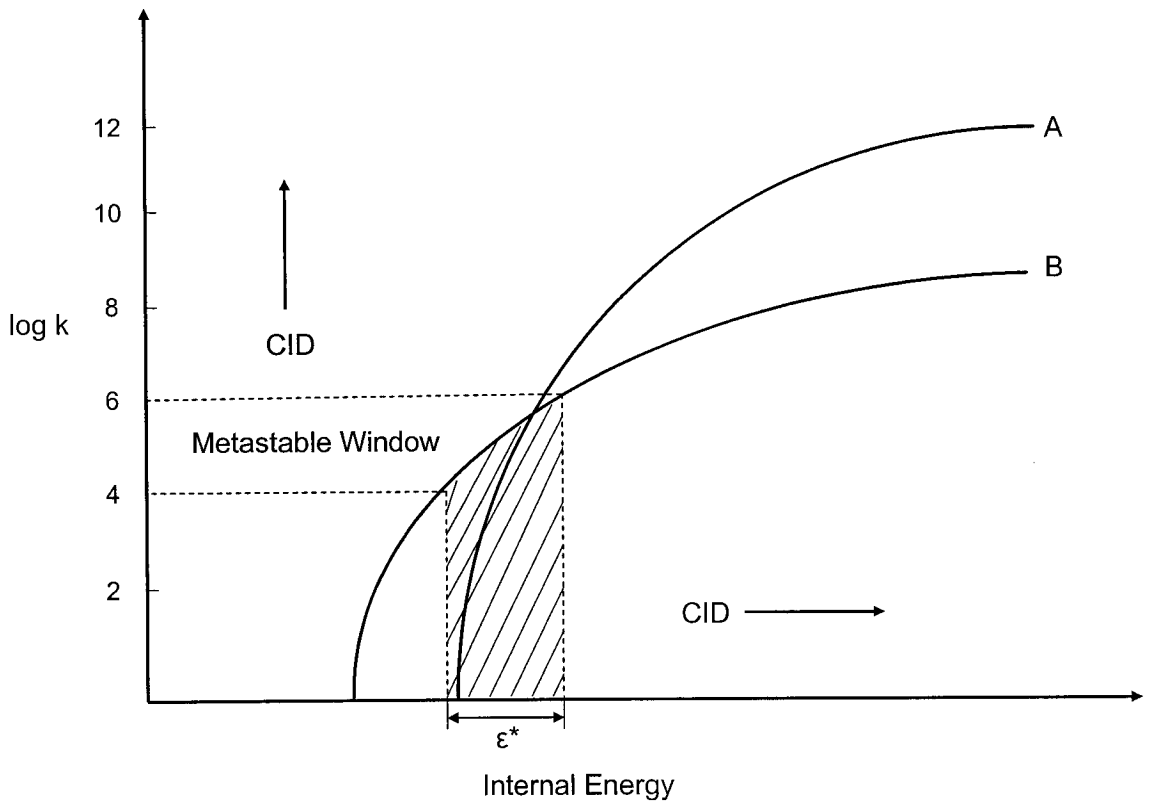

Figure 3.11. Curves of log k(E) vs. E for competing rearrangement and dissociation reactions.

In general, rearrangement reactions have a low activation energy and a negative activation entropy ($\Delta S^{\neq} < 0$), due to the unfavourable entropy change necessary to reach the transition state; while simple bond cleavage reactions usually have a higher activation

energy and a positive activation entropy ($\Delta S^{\neq} > 0$). In Figure 3.11, curve A represents a simple bond cleavage reaction and curve B refers to an ion isomerization. In the metastable ion window of the VG ZAB mass spectrometer, i.e. where the rate constants fall into the range of 10^4-10^6 s^{-1}, curve B (the isomerization path) occupies a larger area under the curve than does A (the simple bond cleavage path). As one approaches the higher internal energies (in CID), the simple bond dissociation has a higher reaction rate and becomes the dominant process. Thus in metastable ion dissociations (MI reactions), a lower activation energy dissociation dictates the ion chemistry, while in CID reactions, the simple bond cleavage reactions tend to predominate due to their greater reaction rate.

3.4.2 Isotopic Labelling

Isotopic labelling combined with metastable ion studies has been used as a powerful technique for unravelling ion fragmentation mechanisms, as well as discovering unexpected rearrangement reactions. Isotopic labels, such as a deuterium atom (in H/D exchange), ^{13}C and ^{18}O etc, are used for identifying the positions of labelled and/or unlabelled atoms in both the reactant and the ion product and for establishing which atoms are involved in a particular ion's dissociation or rearrangement processes.[28]

Note that gas phase ions can undergo surprisingly great rearrangement prior to fragmentation and the hidden isomerization of a given ion can only be discovered by isotopic labelling. A good example is that of the MI mass spectrum of deuterated benzoic acid, C_6H_5COOD, which shows the losses of both $^{\bullet}OD$ and $^{\bullet}OH$, in a ratio of 1:2, indicating that an unexpected H/D exchange has taken place between the carboxyl group

and hydrogens on the ring.[29] Substitution of D at the two ortho-positions gave the loss of $^{\bullet}$OD and $^{\bullet}$OH but now in the ratio of 2:1. The conclusion that only the ortho-H atoms are equilibrated with the hydroxyl group has been further confirmed by another isotopic labelling experiment that when the meta- and para- hydrogen atoms of benzoic acid were replaced by deuterium, no $^{\bullet}$OD loss was observed.[30]

Although isotopic labelling can provide vital mechanistic information for many reactions, one observation in mass spectrometry is the complete loss of positional identity of the labelled and unlabelled atoms in the product. This phenomenon is called "*atom scrambling*". Such cases are common for hydrocarbon cations, and they provide no mechanistic information but only indicate that many isomeric ion structures are accessible below the ion's first dissociation limit.

3.4.3 Ion Thermochemistry

The role of ion thermochemistry in organic ion structure assignment has been reviewed by Holmes.[19] The measurement of the heats of formation ($\Delta_f H$) of ions can be used as a key feature to identify or confirm ion structures, because an ionized molecule of given molecular formula likely has a large number of isomers. For example, there are eleven isomers of $C_2H_4O^{+\bullet}$ that have been shown by *ab initio* calculations to be stable, seven of which have identified by experiments.[31-34] Thermochemistry and ion energetics data include enthalpies, free energies, entropies, ionization energies, proton affinities, electron affinities, binding energies, and heat capacities etc., and the knowledge of them is a significant aid to understanding the physicochemical properties and dissociations of

ions, and also the relationships of ion energies and structures for homologous series[35-37]. Because heats of formation of ions and neutrals are often used to establish the relative stabilities of isomeric species and ion dissociation energies, this section mainly focuses on how to acquire $\Delta_f H$ values. A stable ion structure refers to any ground state isomer that lies in an independent potential well. "Ion Stability" is a relative term: if $\Delta_f H$ of an ion A^+ is less than that of its isomeric ion B^+, then we say A^+ is more stable than B^+. It is well known, for example, that an enol ion is more stable than its keto isomer, which is the opposite of the thermochemical stabilities of neutrals (keto molecules are more stable than their enols.)

The thermochemical properties of neutral molecules, especially homologous series, can be easily estimated by using Benson's schemes[38], which are based on the principle of additivity. However, simple additivity does not work for cations because the ionization energies (IE) of molecules and free radicals are not directly proportional to the number of repeated functional groups therein.[37] The heat of formation of a molecular ion can be calculated from the known IE and $\Delta_f H$ of the molecule and the equation is written as,

$$\Delta_f H^\circ \text{ (ion)} = \text{IE (molecule)} + \Delta_f H^\circ \text{ (molecule)} \qquad 3.10$$

where the ionization energy (IE) of a molecule (M) is the minimum energy required to remove an electron from the molecule to form the molecular ion ($M^{+\bullet}$), $M \rightarrow M^{+\bullet} + e$. Two types of IE values that are referred to are the *adiabatic* and *vertical* ionization energies (IE_a and IE_v), shown in Figure 3.12. IE_a, the *adiabatic ionization energy*, is

defined as the energy difference between the electronic and vibrational ground states of the neutral and ionized molecules. IE_a is the appropriate thermochemical datum that should be used in equation 3.10 for an accurate $\Delta_f H^\circ$ calculation. The ground state geometry of an ion is however not necessarily identical to that of the neutral molecule. IE_v, *vertical ionization energy*, is the energy difference between the ground state of the neutral molecule and the level on the potential energy curve of the ion, corresponding to the ion configuration that is the same as the geometry of the neutral molecule. The excitation during the vertical ionization is a "Franck-Condon" process, in which there is no displacement of nuclei. IE_v can be obtained experimentally by photo-ionization. If the configuration of the ion and neutral species are identical or quite closely similar, the assumption that $IE_a = (\text{or} \approx) IE_v$ can be made and so IE_a can be estimated from electron impact ionization. On the other hand, if the geometry of the ion is greatly different from that of the neutral species, the above assumption is not valid and thus the precise measurement of IE_a values become challenging. Note that electron ionization is only a quasi-vertical process, there being time during the electrons approach for some relaxations of the molecule's ground-state geometry.[39] Therefore it is important to distinguish between the adiabatic ionization energy and the vertical ionization energy before an IE value is applied to Equation 3.10 for an enthalpy calculation.

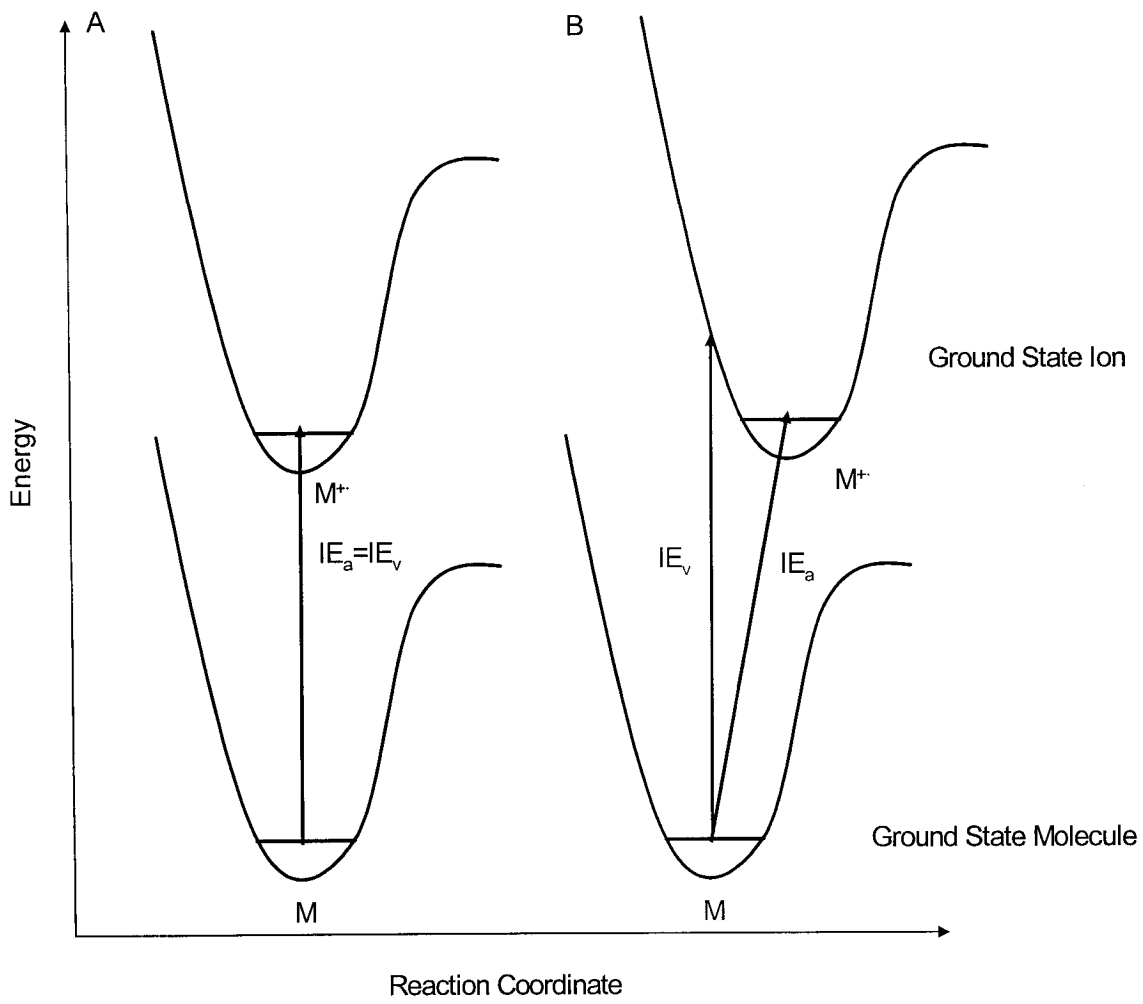

Figure 3.12. Potential energy diagrams illustrating ionization energies, IE_a and IE_v.

A large number of even-electron ions in the gas phase are fragments commonly observed in electron ionization mass spectra. These species correspond to ionized free radicals which can sometimes be generated pyrolytically[40,41,42] For example, some aliphatic radicals ($R^{\bullet}$) were generated from RCH_2ONO pyrolysis by F. P. Lossing.[43,44]

$$RCH_2ONO \xrightarrow{\Delta} R^{\bullet} + CH_2O + NO^{\bullet}$$

Due to the difficulty of making such radical species, the use of the relationship between IE(molecule) and $\Delta_f H$(ion), as indicated in equation 3.10, is not practical. Instead, heats of formation of even-electron ions are often determined from the measurement of the *appearance energy* (AE) of the ion. AE refers to the minimum energy required for the appearance of a given fragment ion from a precursor molecule which is ionized by electron collision or photon absorption. In such a process, a fragment ion A^+ is produced directly from the ionized molecule $M^{+\bullet}$ via a simple bond cleavage, as shown in the equation below:

$$M \rightarrow M^{+\bullet} \rightarrow A^+ + B^\bullet + e \qquad 3.11$$

$$\Delta_r H^\circ = AE = \Delta_f H^\circ (A^+) + \Delta_f H^\circ (B^\bullet) - \Delta_f H^\circ (M) \qquad 3.12$$

The above equation can be also written as,

$$\Delta_f H^\circ (A^+) = AE (A^+) + \Delta_f H^\circ (M) - \Delta_f H^\circ (B^\bullet) \qquad 3.13$$

Therefore, $\Delta_f H^\circ (A^+)$ can be obtained from the measurement of AE (A^+). The heats of formation of M and B can for example be found from the NIST Chemistry Webbook[45] and the data in Lias et al.[46]. To acquire an accurate $\Delta_f H$ from the AE measurement, some necessary conditions have to be met: the fragmentation of the parent ion, $M^{+\bullet}$, must have no significant kinetic shift or reverse energy barrier. Kinetic shift is defined as the excess energy required to produce detectable dissociation of a ion during a certain experimental time frame (typically in ca. 10^{-5} second).[47,48] It may introduce some errors in AE determinations because an ion may require a significant excess energy above the

thermochemical minimum to dissociate on the time-scale of the experiment. Kinetic shifts then show the energy difference between the measured AE and the absolute AE_0, depending upon the time-scale of the experiment. For example in Figure 3.13, three AE values determined by experiment are indicated in a log k (dissociation rate constant) vs E (internal energy) curve, in which $k_3 > k_2 > k_1$ and therefore experiment III has the largest kinetic shift and experiment I the least.

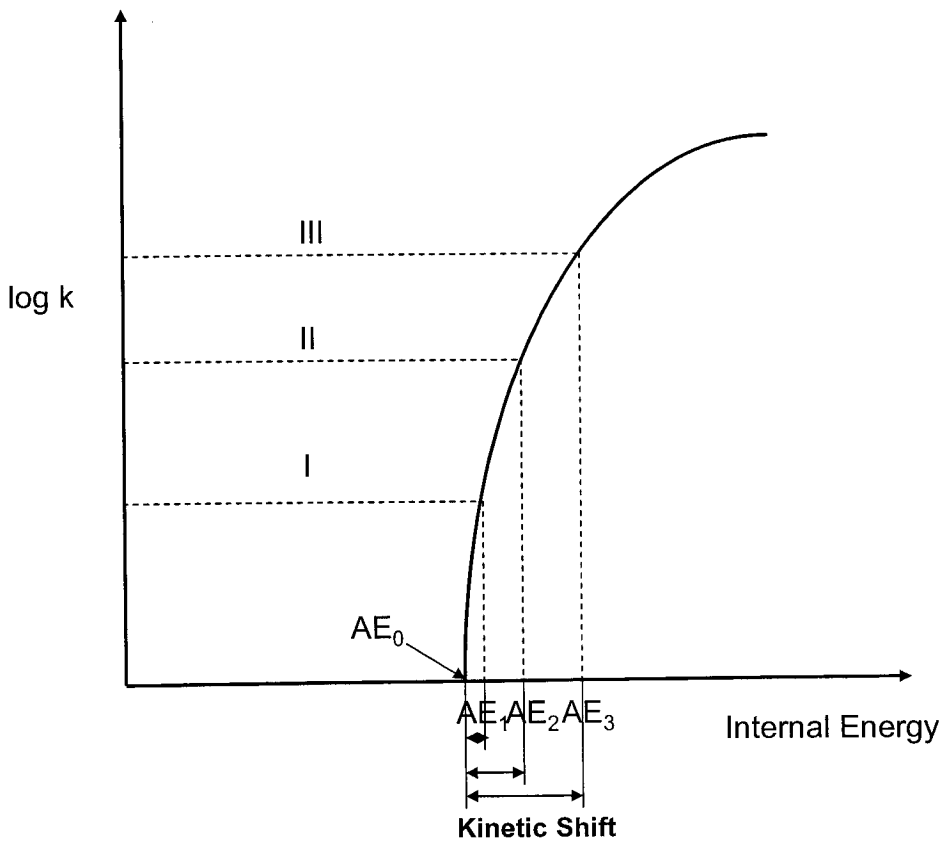

Figure 3.13. Kinetic shift diagram.

Protonated molecules (MH^+) often play important roles in gas phase ionic reactions. To determine the heats of formations of such protonated species, it is necessary to define another thermochemical property, proton affinity (PA), which is

defined as the negative of the heat of reaction for the protonation reaction of a molecule, M:

$$M + H^+ \rightarrow MH^+ \qquad 3.14$$

$$PA\ (M) = -\Delta_r H = \Delta_f H\ (M) + \Delta_f H\ (H^+) - \Delta_f H\ (MH^+) \qquad 3.15$$

Equation 3.15 can be rearranged as,

$$\Delta_f H\ (MH^+) = \Delta_f H\ (M) + \Delta_f H\ (H^+) - PA\ (M) \qquad 3.16$$

The heat of formation of the protonated molecule MH^+ can be calculated by the above equation with reliable PA values. Experimental methods of the measurement of proton affinities involve equilibrium, bracketing and kinetic studies. The equilibrium study is the best method for PA measurement, based on the measurement of the temperature-dependent equilibrium constants of a gas phase proton transfer reaction between two bases A (a reference) and B (an unknown base), as shown in Equation 3.17.

$$AH^+ + B \leftrightarrow A + BH^+ \qquad 3.17$$

The experiments require the establishment of chemical equilibrium in order to measure K_{eq} values for gas phase proton transfer reactions. This is achieved by using a number of collisions to thermalize all the species involved in the reactions, with a high pressure ion source with a sector instrument[49] or ion-cyclotron resonance mass spectrometer[50].

The bracketing method[51] is applied to systems in which equilibrium is difficult to achieve. This method is used to determine relative proton affinities via a series of proton transfer reaction between an unknown base (B) and a few selected bases (A_1,A_2,…,A_n) which are standards of known PA. The results of bracketing studies provide an upper and lower limit for PA of unknown species.

The kinetic method, reviewed in many papers[52-56], measures the product ion peak ratios of $[AH^+]$ and $[BH^+]$ for the following competing MI or CID dissociations of a proton bound pair, AH^+B:

$$AH^+B \xrightarrow{k_1} AH^+ + B \qquad 3.18$$

$$AH^+B \xrightarrow{k_2} BH^+ + A \qquad 3.19$$

In the kinetic method, the rate constant ratio for the above two reactions, k_1/k_2, is considered to be equal to $[AH^+]/[BH^+]$.[57] The difference in PAs between molecule A and B can be determined by the following relationship:

$$\ln [AH^+]/[BH^+] = \ln k_1/k_2 = [PA(A) - PA(B)]/RT_{eff} \qquad 3.20$$

where T_{eff} is the effective temperature term for describing the internal energy distribution of the proton-bound pair. Again, a series of reliable PA(A) values are used as standards, and PA(B) is unknown. Thus, Equation 3.20 allows one to plot the logarithm of the peak ratios against the known PA(A) values, and PA(B) can be obtained from the graph. Although entropy effects and reverse energy barriers are major sources of uncertainties

for this measurement, the kinetic method is particularly capable of providing fairly accurate results for homologous series of molecules where entropy effects are largely cancelled out.[58] In addition to the above methods, PA values can be obtained from high-level computational chemistry,[59] which is discussed below.

3.5 Computational Methods

With the rapid development of computer technologies, computational methods have become a powerful tool for assigning ion structures and discovering reaction mechanisms. The main strengths of such theoretical methods are to provide detailed ion structures (such as bond lengths, bond angles, electron distribution) for stable isomers and transition states and to provide ion thermochemistry data, thus a complete potential energy surface for an ion's dissociation and isomerization pathways can be determined. In this thesis, theoretical calculations were used to supplement the mass spectrometric methods in order to fully elucidate the chemistry of the gas phase ions investigated. To do so, calculations performed in this thesis are mainly interested in the following three pieces of information: 1) equilibrium and transition state geometries that are involved in the reaction pathways, 2) vibrational frequencies and 3) reliable thermochemical values for the species (e.g. heats of formation of gas phase ions). This section here will not give a detailed discussion on computational chemistry, but rather to briefly describe the various methods and how to perform a calculation for the above purposes.

When we have a task requiring computational chemistry, the first step is to choose an appropriate computational "level of theory". The method consists of two main

components: a method which is used for treating electron correlation and a basis set to describe molecular orbitals. The fundamental molecular orbital (MO) computational methods include *ab initio* and semiempirical methods. The former are derived directly from theoretical principles with no inclusion of experimental data, whereas the latter are parameterized by curve fitting a few parameters (or numbers) to give the best agreement with experimental data. The two methods apply quantum mechanics and implicitly consider the electron distribution in a chemical system as a function of nuclear position. Quantum mechanics relates the behaviour of electrons to those of waves and gives a mathematical description of atomic and by extension, molecular characteristics. It is worth emphasizing that *ab initio* and density functional theory (DFT) methods have been applied to the great majority of cases and been proven to give very good results. These two methods have been used on all the jobs performed in this thesis and they will be further described below.

3.5.1. *Ab initio* Methods and Density Functional Theory

The Latin term *ab initio* means "from the beginning". These calculations are derived from the Hartree-Fock assumptions/approximations and involve a near complete mathematical treatment of the theoretical model underlying the Hartree-Fock theory. The most common *ab initio* method is the Hartree-Fock calculation (HF),[60] which is very helpful in giving initial, first level predictions for many systems. The primary approximation in HF method is the central field approximation, which means the Coulombic electron-electron repulsion is taken into account by integrating the repulsion term. One of the limitations of HF calculation is that no explicit repulsion electron-

electron interaction is given by such calculations, other than the average effect of the repulsion. Because of the neglect of electron correlation, the energies provided from HF are generally larger than the exact energy and tend to a limiting value known as the Hartree-Fock limit as the basis set is improved.[61] However, HF calculations are reasonably good at computing the structures and vibrational frequencies of some equilibrium and transition states.

A number of methods begin with a HF calculation and then correct it for electron correlation. One approach to the correlation problem is the Møller-Plesset perturbation theory (MPn, where n is the order of correction) by adding a perturbation to the Hartree-Fock wave function and therefore including the effect of electron correlation.[62] By substituting the HF wave function into a perturbation theory formulation, the solution of the new equation to zero or first order (n=1) gives the unperturbed HF wavefunction and energy.[63] Thus a minimal amount of correlation is the use of the second order, MP2, method. MP2, MP3 and MP4 are standard levels used in calculating small systems and are implemented in many computational chemical systems. At the MP4 level, additional single, double, triple (MP4 SDT) and quadruple (MP4 SDTQ) are included.[64] Higher level MP calculations are rarely used because of the high computational cost. Due to the good cost (CPU time) to accuracy ratio, the MP2 level has been extensively used for this thesis work. MP2 is able to recover a large fraction of the correlation energy when the Hartree-Fock method is used as a good starting point. A great practical advantage is that MP2 is fast (of the same order of magnitude as Self-Consistent Field, i.e. SCF) and is quite reliable in its behaviour. However, at the MP2 level, convergence may become

poor if there is a serious spin contamination or if the Hartree-Fock is not a good starting point.

An alternative *ab initio* method is density functional theory (DFT), which is similar to, yet still different from, other HF molecular orbital techniques.[65,66] Because current DFT calculations contain empirical or adjustable parameters, they are thereby not acknowledged to be "*ab initio*" methods (however whether DFT belongs to *ab initio* method is still debated). DFT methods are less expensive in terms of computing time and disk space than other *ab initio* methods with similar accuracy and so have recently become very popular, being especially used for complex systems such as peptides and proteins. Whereas Hartree-Fock theory is based on the many-electron wavefunction, density functional theory uses the electronic density as the basic quantity. DFT originated with the Hohenburg-Kohn (HK) theorem[67] and a practical application of the theory was developed by Kohn and Sham[68] who proposed a method similar in structure to the Hartree-Fock method. In a DFT formulation, the electron density is expressed as a linear combination of basis functions similar in mathematical form to Hartree-Fock orbitals. A determinant is then formed from these functions, called Kohn-Sham orbitals from which the electron density is used to compute the energy.[61] While the original theorem applied to finding the ground state properties, practical applications of DFT are based on approximations for the so-called exchange-correlation potential which describes the Pauli principle and the Coulomb potential beyond a purely electrostatic interaction of electrons. The most popular DFT method, B-LYP, uses the gradient-corrected exchange functional developed by Becke[69] and the gradient-corrected correlation functional proposed by Lee, Yang and Parr[70]. Hybrid functionals are also used to define the

exchange functional as a linear combination of Hartree-Fock, local, and gradient-corrected exchange terms. The most widely used DFT methods are B3-LYP and B3-PW91, both of which used the Becke's three-parameter formulation[71] which is a hybrid between HF and DFT.

The B3-LYP method has been extensively applied to the geometry optimization of the equilibrium and transition states in this thesis, because it provides significantly greater accuracy than the HF method and has just as good a treatment for electron correlation as MP2. Because B3-LYP has the great advantage of speed and computational resources over HF and MP2, DFT calculations have become the norm in ion structure determination. We have also found good relative energy values (i.e. they have a satisfactory agreement with experimental data) can be obtained when single point energy calculations at a high basis set or G3 (see the following section) level of theory are applied to B3-LYP optimized geometries.

3.5.2 Basis Sets

To start a calculation, it is very important to choose an appropriate basis set for the chemical system at hand in order to obtain a good description of the molecule or ion structure and energies. A basis set is a set of functions used to describe the shape of the orbitals for each atom within a chemical system, so as to approximate the total electronic wavefunctions. Molecular orbitals and entire wavefunctions are created by a linear combination of basis functions and angular functions. The basis functions are referred to as contracted functions. Larger basis sets more accurately approximate the orbitals by

imposing fewer restrictions on the spatial locations of the electrons. Standard basis sets for electronic structure calculations use linear combinations of Gaussian functions (referred to as primitives) to form the orbitals. A full description of the basis sets available can be found in the manual for the corresponding software package. GAUSSIAN offers a wide range of pre-defined basis sets, which are classified by the number and types of basis functions that they contain.

A common type of basis sets, often referred to as the Pople basis sets, are expressed by the notation 6-31G, which are available for H(4s) through Ar(16s10p) and are very popular for quantitative results for organic molecules. Most calculations performed in this thesis used the 6-31+G(d) basis set, in which diffuse functions (+) and polarization (in the form of d-orbitals) functions were added to non-H atoms to increase flexibility. It is a split valence basis set in which each valence atomic orbital of the constituent atoms comprises two parts described by (31). Figure 3.14 illustrates the composition of a basis set for the modular Pople basis sets.

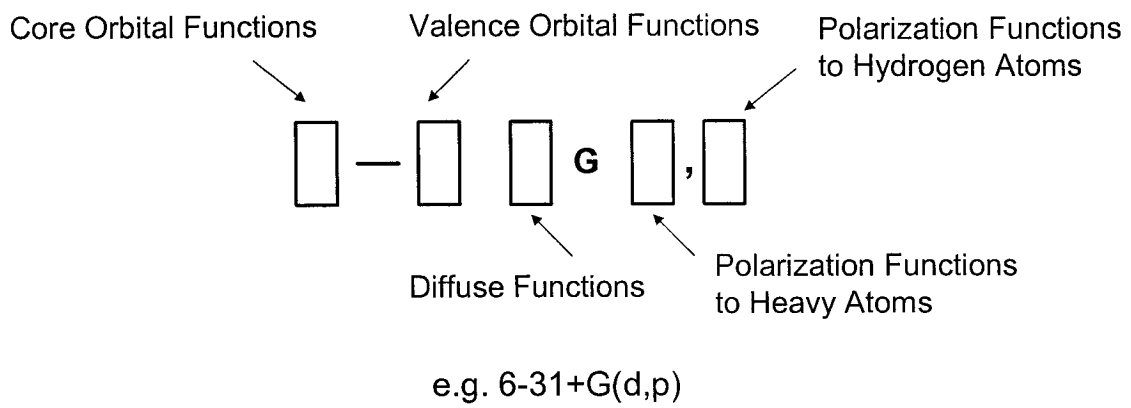

Figure 3.14. Composition of a Pople basis set.

3.5.3 Gaussian Theory

The Gaussian methods Gaussian-1, Gaussian-2 and Gaussian-3, abbreviated as G1, G2 and G3, are complex energy computations. These methods arose from the observation that certain levels of *ab initio* methods with certain basis sets always tended to give results with systematic errors for predicting the energies of ground states of organic species. Gaussian methods are used to extrapolate a very accurate result from a correction equation that uses the energies from a series of *ab initio* calculations with different basis sets and levels of theory. The extrapolation to complete correlation is an semi-empirically defined equation that is parameterized to reproduce results from a test set of molecules as accurately as possible and is based on the number of electrons times an empirically determined constant. Therefore, Gaussian methods belong to the semiempirical family. The accuracy of these methods can be extremely good for systems similar to those for which they were parameterized, whereas for other systems, they are often less accurate than some *ab initio* methods.

The G1 method is seldom used nowadays, because G2 has been proved to yield an improved accuracy of results. The G2 procedure was introduced by Pople and his co-workers, based on *ab initio* molecular orbital theory, for the computations of total energies of molecules at their equilibrium geometries.[72,73] This method uses the 6-311G(d,p) basis set and corrections for several basis set extensions. G2 approximates final total energies at the quadratic configuration interaction single point calculation [QCISD(T)] at the 6-311+G(3df,2p) basis set and involves a series of additive corrections by Møller-Plesset perturbation theory. Three more economical variants of G2 theory,

referred to G2(MP2), G2(MP3)[74] and G2(MP2,SVP)[75,76], are found to consistently predict accurate results and provide substantial savings in computational time and disk space. In G2(MP2) theory, the basis-set-extension corrections are obtained at the MP2 level, while in G2(MP3) theory, they are obtained at the MP3 level. In G2(MP2,SVP) theory, an alternative additivity approximation has been established to achieve the same effective level of calculation as the G2 methods (the details are discussed in Radom's paper[75]) and the split-valence plus polarization (SVP) 6-31G(d) basis set is used for the QCISD(T) single point calculation.

The G3 theory, recently developed by Curtiss et. al.[77], has shown some improvement in accuracy by elimination many of the deficiencies of the G2 theory. Significant improvement is also observed by them for ionization potentials and electron affinities. In the G3 procedure, MP4 and QCISD(T) single point calculation are based on 6-31G(d) basis set instead of the 6-311G(d,p) basis set. The MP2 calculation uses the G3large basis set which is a modification of the standard 6-311+G(3df,2p) basis set in G2 theory. With the use of G3large basis set, more polarization functions are added to first-row elements (3d2f), fewer on second-row elements (2df), and core polarization functions are incorporated. In addition, a spin-orbit correction for atoms and a core-correlation correction by the used of the MP2(full)/G3large component are added in G3 method. Finally, an empirical higher-level correction (HLC) is applied to residual basis set errors.

The typical G3 theory uses geometries optimized at MP2(full)/6-31G(d) level and scaled zero-point energies from Hartree-Fock theory, HF/6-31G(d). A modified G3

procedure, referred to G3//B3-LYP[78], is also extensively used in this thesis. Density functional (DFT) theory for the calculations of geometries has been examined in several studies[65,79] and has shown a slight improvement over MP2 theory at the 6-31G(d) level for a set of 53 molecules[79]. G3//B3-LYP calculations use the B3-LYP density functional method for geometries and zero-point energies instead of MP2/6-31G(d) geometries and scaled HF/6-31G(d) zero-point energies. Overall, the G3//B3-LYP results are slightly better than the typical G3 as the average absolute deviation (from experiment) decreases from 1.01 to 0.99 kcal/mol in terms of enthalpy, ionization energy, electron affinity and proton affinity calculations.[78]

All the calculations that go into these Gaussian methods are *ab initio* calculations and all of the distinct steps are performed automatically once the level of theory and the basis set are specified for each job. As they are single point energy calculation jobs, no keyword is needed in the job card. The final computed energies are displayed in the output archives. Here is given an example of a G3 input file (known as filename.com file):

```
%mem=250MB
%chk=min_coloss3.chk
%rwf=a,240Mw,b,240Mw,c,240Mw,d,240Mw,e,240Mw,f,240Mw,g,240Mw,h,240Mw
#QCISD(T,e4T)/6-31g(d) geom=check

Minimum structure for CO loss from 2,3 pentanedione

1,2

--link1--
%mem=250MB
%chk=min_coloss3.chk
%rwf=a,240Mw,b,240Mw,c,240Mw,d,240Mw,e,240Mw,f,240Mw,g,240Mw,h,240Mw
#mp4/6-31+g(d) geom=check

Minimum structure for CO loss from 2,3 pentanedione
```

```
1,2

--link1--
%mem=250MB
%chk=min_coloss3.chk
%rwf=a,240Mw,b,240Mw,c,240Mw,d,240Mw,e,240Mw,f,240Mw,g,240Mw,h,240Mw
#mp4/6-31g(2df,p) geom=check

Minimum structure for CO loss from 2,3 pentanedione

1,2

--link1--
%mem=250MB
%chk=min_coloss3.chk
%rwf=a,240Mw,b,240Mw,c,240Mw,d,240Mw,e,240Mw,f,240Mw,g,240Mw,h,240Mw
#mp2(full)/GTlarge geom=check

Minimum structure for CO loss from 2,3 pentanedione

1 2
```

In the above file, the geometry of the species will be directly read from the checkpoint file (filename.chk) provided by the previous geometry optimization with a selected method such as MP2 or B3-LYP.

In this thesis, we have utilized G3 theory for predicting heats of formation of gas phase cations and molecules/radicals at 0 K and at 298 K, with the use of the approaches illustrated by Radom and his co-workers[80]. The calculation of a heat of formation at 0 K is based on atomization and formation reaction procedures. The difference between the enthalpy at a certain temperature (usually at 298 K) and 0 K is evaluated according to standard thermodynamic formulas[81]. The contributions of translation (*3/2 RT*) and rotation (*3/2 RT* for nonlinear molecules, *RT* for linear molecules) partition functions have been taken in to account and an additional *RT* is added for converting energy to

enthalpy (the *PV* term). For the vibrational component, the harmonic oscillator approximation is generally invoked and uses an analytical expression.

3.5.4 Performing a Theoretical Calculation

The GAUSSIAN 98 program[82] has been used to perform all the calculations presented in this thesis. The first step is certainly to decide the calculation method, i.e. the level of theory + the basis set. The computation programs are controlled by specific key words, which are used to request a certain type of calculation. These keywords are then converted into parameters which control the execution of the calculation. An example of the input file for a GAUSSIAN calculation is shown as below:

```
%mem=150mb                                              -memory line
%chk=ch3oh.chk                                          -checkpoint line
# b3lyp/6-31+g(d) opt freq                              -route line/job card
                                                        -blank line
methanol molecular ion                                  -job title
                                                        -blank line
1,2                                                     -charge and multiplicity (1,2 for odd-electron cation)
C                                                       -beginning of Z-matrix
H     1     R2
H     1     R3    2     A3
H     1     R4    2     A4    3     D4
O     1     R5    2     A5    3     D5
H     5     R6    1     A6    2     D6
                                                        -blank line
R2    1.127974                                          -variable specification
R3    1.127879
R4    1.089372
R5    1.366819
R6    0.993003
A3    96.187566
A4    115.015694
A5    105.983339
A6    114.838377
D4    121.377486
D5    -108.624322
D6    -129.184153                                       -end of Z-matrix
                                                        -blank line
```

This input file uses a list of bond lengths, angles and dihedral angles to define the position of each atom in the ion, which is called a Z-matrix. Z-matrix is conventionally built manually by using the chemist's intuition regarding what this ion or molecular should look like. Many *ab initio* and semiempirical programs, including GAUSSIAN, also do geometry optimization in Cartesian coordinates in which the geometry of a species is defined as a set of Cartesian coordinates for each atom, as shown in Figure 3.15.

	Coordinates (Angstroms)		
	X	Y	Z
C	-0.64259	0.064629	-0.00012
H	-1.04817	-0.56914	0.840221
H	-1.04853	-0.57109	-0.83867
H	-0.98095	1.100121	-0.00081
O	0.710146	-0.13109	-3.1E-05
H	1.252005	0.701044	0.000204

Figure 3.15. Cartesian coordinate representation of the methanol molecular ion ($CH_3OH^{+\bullet}$).

A Cartesian coordinate optimization may be more efficient than a poorly constructed Z-matrix but usually less efficient than a well constructed Z-matrix.[61] It is often generated by a graphical user interface.

Nowadays it is becoming more popular to use programs to draw the ion/molecule structure to be calculated. One of such programs is frequently used for this thesis work is GaussView. It is a straightforward method for a used to build a structure in a Windows-like interface and then to set up and submit GAUSSIAN jobs directly from this program.

We also use GaussView to monitor the progress as a calculation job runs and to visualize the motion of each degree of freedom in a structure provided by a frequency analysis job.

3.5.5 Geometry Optimizations to Find a Minimum or a Transition State.

A most basic function of a computational chemistry program in the context of this thesis is to determine an ion structure corresponding to a stationary point on its potential energy surface. The stationary point represents either an equilibrium state (i.e. a minimum lying in a potential energy well) or a transition state (i.e. a first-order saddle point on the potential energy surface), both of which are shown in Figure 3.16. When conducting a geometry calculation, an initial geometry of a molecule or an ion must be first specified, by a Z-matrix or a set of Cartesian coordinates. Then the program computes the energies and gradients of the energy in order to find the geometry corresponding to the lowest energy. This process involves the optimization of bond lengths, angles and dihedral angles of the molecular or ion structure to minimize its energy.

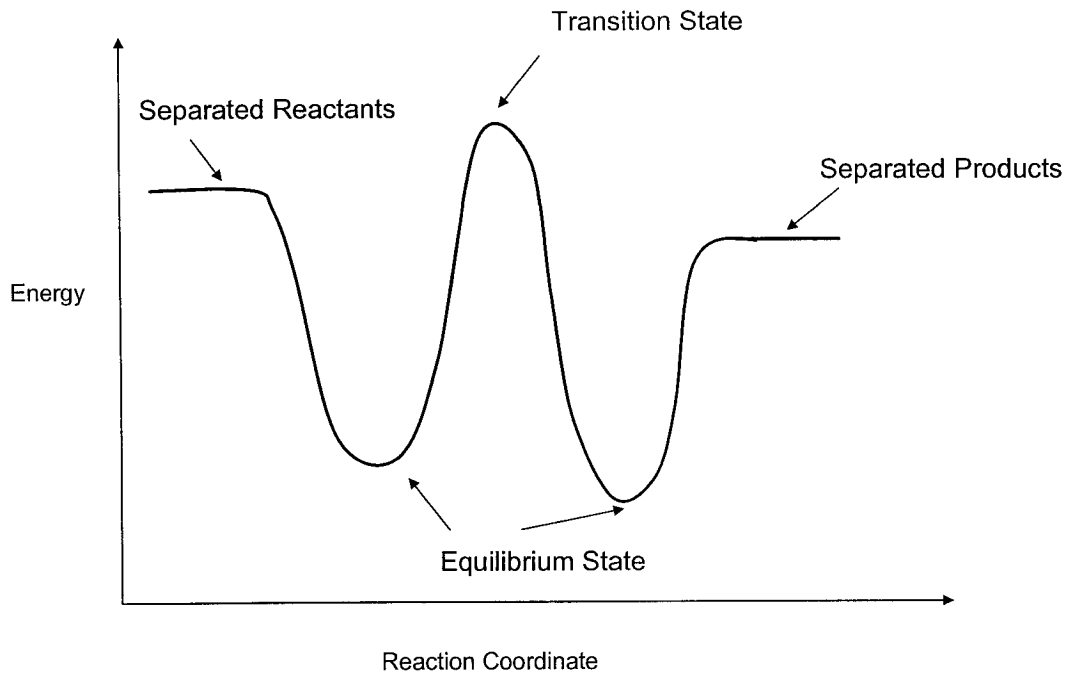

Figure 3.16. Schematic diagram illustrating different points on a simple reaction coordinate.

The calculation of a minimum structure on a potential energy surface is conducted by using the "opt" keyword in job card line. Geometry optimizations converge to a structure on the potential energy surface where the forces on the system are essentially zero. The computed structure given by a geometry optimization job should have all positive vibrational frequencies. This can be verified by a frequency job, in which the "freq" keyword is needed. A frequency job must use the same theoretical level of theory and basis set as produced in the optimized geometry.

By definition, a first order saddle point (transition state) is a maximum in one degree of freedom and a minimum in all other orthogonal degrees of freedom. Thus, in the optimization of transition states, all degrees of freedom are optimized except for one

imaginary frequency which should go with a negative eigenvalue. This degree of freedom is responsible for motion over the barrier that connects two equilibrium states. An Intrinsic Reaction Coordinate (IRC) calculation is invoked to confirm whether the correct transition state has been determined for the two given minima. This method actually involves two calculation jobs by using the keyword "forward" and "reverse", respectively. It starts at the saddle point and follows the path in both directions from the transition state, optimizing the geometry of the chemical system at each point along the reaction path towards the two minima that it connects. Because for most cases, an IRC job does not go all the way to the minimum on either side of the path (i.e. the output structure is not necessary a equilibrium state), an optimization job will be required following the IRC calculation.

What should one do if the level of theory chosen for the geometry optimization fails? There are several things one can do. First, try to build a well defined geometry listed in the input file as good as possible. Because many *ab initio* and semiempirical programs optimize the geometry of the species by changing the parameters in the Z-matrix, a poorly constructed Z-matrix can result in a very inefficient geometry optimization or even a failure. For *ab initio* calculations, one can try either to change the basis set or to increase the method slightly, e.g. if MP2 fails, try MP3 or QCISD. In terms of DFT methods, the options are a little bit more limited and so one can simply try to change the basis set. As the final geometry obtained will be used to compute the energy, the accuracy, as well as the computation cost, is the key factor for choosing a level of theory.

3.5.6 Calculated Energies and Ion Thermochemistry

In addition to the determination of ionic/molecular geometries, the energy calculation is another important objective of computational chemistry. The analysis of energetics can predict what reaction processes are likely to occur or what are the significant peaks that may be seen in the mass spectrum. By defining the energies of all the conformers and their accessible isomers and transition structures, a complete potential energy surface (PES) can be established for a system and by extension to the study of ion thermochemistry and reaction dynamics.

The total energy computed by a calculation is an absolute energy of a species but this absolute energy is often very inaccurate, resulting from systematic errors in the theoretical model. *Ab initio* and DFT calculations give the total computed energies in units called Hartrees (1 Hartree = 27.2116 eV = 627.5 kcal = 2625.5 kJ). However, the relative energy, which is the difference between the calculated absolute energies of two isomers, will be satisfactory because the systematic errors cancel out.

The energy computed by a geometry optimization corresponds to the minimum of a potential energy well. However, in reality, a molecule cannot have this energy because it must always have some vibrational motions. To take the vibrations into account, zero-point energies (ZPEs) must be added to the total energies of the species, prior to the determination of relative energies. ZPEs are obtained by performing frequency calculations on the optimized geometries. For an accurate result, the ZPE value is scaled by an empirical factor to improve agreement with experiment. For example, the scaling

factor for the ZPE predicted at the Hartree-Fock level is 0.9135[83] in order to eliminate known systemetic errors resulting from the neglect of electron correlation. Table 3.2 lists the recommended scaling factors for zero-point energies and for frequencies of the some common methods/levels of theories[78,83]. Although the scaling factor of zero-point energies is slightly different from that of frequencies for a given level of theory, it is common to use the same factor to both of them (e.g. 0.96 for the B3-LYP/6-31G(d) level of theory) and the calculated energies differ by less than 1.0 kJ/mol between the two scaling methods.

Table 3.2. Recommended scaling factors for zero-point energies and frequencies.

Level of Theory	Zero-Point Energy Scaling Factors	Frequency Scaling Factors
HF/6-31G(d)	0.9135	0.8953
HF/6-31G+(d)	0.9153	0.8970
HF/6-31G(d,p)	0.9181	0.8992
HF/6-311G(d,p)	0.9248	0.9051
MP2/6-31G(d)	0.9670	0.9434
B-LYP/6-31G(d)	1.0126	0.9945
B3-LYP/6-31G(d)	0.9806	0.9614
QCISD/6-31G(d)	0.9776	0.9537

To obtain a PES, the level of theory employed will produce a unique set of relative energies. The achievement of reliable relative energies (to subsequently determine ion thermochemistry data) generally requires higher levels of theory than do geometry optimizations or vibrational frequency calculations, which need very intensive

computations that may be impossible for large ions/molecules. Thus a single point energy calculation by composite methods (e.g. G3) is invoked to solve the above problem. A composite method uses several low level calculations to additively produce a result as accurate as that given by a high level of theory, for more details see Section 3.5.3. The accuracy of this result also depends on the accuracy of the optimized geometry that is employed for the single point energy calculation. An assessment of the performance of a variety of levels of theory may be essential for acquiring reliable computed results.

The G3 method (the regular G3 and G3//B3-LYP) was therefore used in this thesis for obtaining reliable relative energies and theoretical thermochemical predictions (e.g. $\Delta_f H$). The procedure for calculating $\Delta_f H$ of an ion or a molecule/radical is best illustrated by example, which the case of $^{\bullet}CH_3$ radical is shown here. The G3//B3-LYP method is described here, as other G3 theories (G3, G3(MP2), G3(MP2)//B3LYP) have very similar steps and the differences between them have been discussed in detail in the publication by Baboul et al[78]. First, the geometry of $^{\bullet}CH_3$ radical is optimized at the B3-LYP/6-31+G(d) level. Second, the zero-point energy is obtained at the same level of theory and scaled by 0.96. These two steps can be done by including both the "opt" and "freq" keywords in the job card of a single calculation. It is very important to examine the calculated minimum structure (or stationary point) before performing the further single-point energy calculations at G3 level. Therefore, the optimized geometry of $^{\bullet}CH_3$ is visualized by the Gauss View program and it should be represented as a planar structure. In addition, the frequencies in this structure also need to be checked: a minimum structure should have all positive frequencies and an ordinary transition structure should have only one imaginary frequency which is corresponding to the

transition state mode. Third, a series of single-point energy calculations are carried out at a series of higher levels of theory: QCISD(4,e4T)/6-31G(d), MP4/6-31+G(d), MP4/6-31G(2df,p) and MP2(full)/G3large. The higher-level correction (HLC) is added to take into account remaining deficiencies in the energy calculations, and is $-An_\beta-B(n_\alpha-n_\beta)$ for molecules and $-Cn_\beta-D(n_\alpha-n_\beta)$ for atoms and atomic ions. For G3//B3-LYP method, the A = 6.760 mhartrees, B = 3.233 mhartrees, C = 6.787 mhartrees and D = 1.269 mhartrees. And the total G3 energy at 0 K is obtained by adding the scaled zero-point energy, acquired from the second step. Then, this $G3_0$ energy is used to calculated the 0 K heat of formation ($\Delta_fH_0[^\bullet CH_3]$) of $^\bullet CH_3$ based on the atomization approach[80]. The atomization reaction of $^\bullet CH_3$ is shown in Equation 3.21.

$$^\bullet CH_{3(g)} \rightarrow C_{(g)} + 3H_{(g)} \qquad 3.21$$

Thus $\Delta_fH_0[^\bullet CH_3]$ can be calculated from the heat of reaction ($\Delta_rH^\circ_a$) of the atomization reaction together with the experimental heats of formation of $C_{(g)}$ and $H_{(g)}$, giving

$$\Delta_fH_0[^\bullet CH_3] = -\Delta_rH^\circ_a + \Delta_fH_0^{exp}[C_{(g)}] + 3\Delta_fH_0^{exp}[H_{(g)}] \qquad 3.22$$

The relation between $\Delta_rH^\circ_a$ and $G3_0$ energies of the reactant and products is shown as:

$$-\Delta_rH^\circ_a[^\bullet CH_3] = G3_0[^\bullet CH_3] - G3_0[C_{(g)}] - 3G3_0[H_{(g)}] \qquad 3.23$$

where $G3_0$ is the G3 total energy at 0 K obtained from G3//B3-LYP calculations. Therefore the combination of Equation 3.22 and 3.23 gives

$$\Delta_f H_0[^{\bullet}CH_3] = G3_0[^{\bullet}CH_3] - G3_0[C_{(g)}] - 3G3_0[H_{(g)}] + \Delta_f H_0^{exp}[C_{(g)}] + 3\Delta_f H_0^{exp}[H_{(g)}] \quad 3.24$$

The G3//B3-LYP atomic energies are given in reference 76 and experimental $\Delta_f H_0$ values for gas-phase atoms are given in reference 46. For this example, $G3_0[C_{(g)}]$ = -37.82845 hartrees = -99317.12 kJ/mol, $G3_0[H_{(g)}]$ = -0.50109 hartrees = -1315.59 kJ/mol, $\Delta_f H_0^{exp}[C_{(g)}]$ = 711.20 kJ/mol and $\Delta_f H_0^{exp}[H_{(g)}]$ = 216.035 kJ/mol are used in the above equation, and so 0 K $\Delta_f H$ [$^{\bullet}CH_3$] is calculated to be 146.6 kJ/mol. Finally, the 298 K $\Delta_f H[^{\bullet}CH_3]$ is determined by

$$\Delta_f H_{298}[^{\bullet}CH_3] = \Delta_f H_0[^{\bullet}CH_3] + \Delta H_{298}[^{\bullet}CH_3] - \Delta H_{298}[C_{(g)}] - 3\Delta H_{298}[H_{(g)}] \quad 3.25$$

$\Delta H_T[X]$ (in equation 3.25, X = $^{\bullet}CH_3$, $C_{(g)}$ or $H_{(g)}$, T = 298 K) is the thermal enthalpy of a species, which is the difference between the enthalpy at temperature T and 0 K, and ΔH_T for elements refer to their standard states, ($H_{298} - H_0$). The $\Delta H_T[X]$ value can be evaluated according to standard thermodynamic formulas[81]. The partition function consists of contributions of translational (*3/2 RT*), rotational (*3/2 RT* for non-linear molecules and *RT* for linear molecules), vibrational, electronic and nuclear component. The electronic and nuclear terms are usually ignored, i.e. their corresponding partition functions are set to unity. The relations between different energies are

$$E_{therm} = E_{tran} + E_{rot} + E_{vib} = 3/2\ RT + 3/2\ RT + E_{vib} \quad \text{for non-linear molecules} \quad 3.26$$

$$= 3/2\ RT + RT + E_{vib} \quad \text{for linear molecules}$$

$$\Delta H_T = E_{therm} + RT \quad 3.27$$

The harmonic oscillator approximation is invoked for the vibrational energy which can be calculated by the following equation:

$$E_{vib} = \sum_{n=1}^{3n-6} \frac{v}{(e^{\frac{v}{k_b T}} - 1)} \times hcN \qquad 3.28$$

where v is the frequency (cm^{-1}) and is scaled by 0.9614, h is the Planck's constant (6.626069×10^{-34} J s)[84], N is Avogadro's constant (6.022142×10^{23})[84], k_b is Boltzmann's constant (1.380650×10^{-23} J K^{-1}= 0.69509 cm^{-1} K^{-1})[84], c is speed of light (2.997925×10^{10} cm s^{-1}) and T is the desired temperature (K).

Experimental ΔH_T values for elements in their standard states are given in reference 85.[85] For the $^{\bullet}CH_3$ case, $\Delta H_T[C_{(s)}]$ = 1.050 kJ/mol and $\Delta H_T[H_{(g)}]$ = 4.234 kJ/mol are applied to Equation 3.25 and so 298 K heat of formation ($\Delta_f H_{298}[^{\bullet}CH_3]$) of $^{\bullet}CH_3$ is calculated to be 144 kJ/mol. This theoretical enthalpy value has a very good agreement with the experimental data, $\Delta_f H_{298}^{exp}[^{\bullet}CH_3] = 147 \pm 1$ kJ/mol.[45]

References

(1) Cooks, R. G.; Beynon, J. H.; Caprioli, R. M.; Lester, G. R. *Metastable Ions*; Elsevier: Amsterdam, 1973.

(2) Stevenson, D. P. *Discuss. Faraday Soc.* **1951**, *10*, 35.

(3) Howe, I.; Williams, D. H. *J. Am. Chem. Soc.* **1969**, *91*, 7137.

(4) Yeo, A. N. H.; Williams, D. H. *J. Am. Chem. Soc.* **1970**, *92*, 3984.

(5) Busch, K. L.; Glish, G. L.; McLuckey, S. A. *Mass Spectrometry/Mass Spectrometry Techniques and Applications of Tandem Mass Spectrometry*; VCH Publishers: New York, 1988.

(6) Holmes, J. L.; Terlouw, J. K. *Org. Mass Spectrom.* **1980**, *15*, 383.

(7) Beynon, J. H.; Cooks, R. G.; Amy, J. W.; Baitinger, W. E.; Ridley, T. Y. *Anal. Chem.* **1973**, *45*, 1023A.

(8) Holmes, J. L. In *The Encyclopedia of Mass Spectrometry*; Armentrout, P. B., Ed.; Elsevier: Amsterdam, 2003; Vol. 1, p 91.

(9) Holmes, J. L.; Terlouw, J. K. In *Encyclopedia of Mass Spectrometry*; Elsevier: Amsterdam, 2005; Vol. 4, p 287.

(10) Holmes, J. L.; Benoit, F. In *MTP International Review of Science*; Maccoll, A., Ed.; Butterworths: London, 1972; Vol. 5, p 259.

(11) Laskin, J.; Lifshitz, C. *J. Mass Spectrom.* **2001**, *36*, 459.

(12) Thomson, J. J. *Rays of Positive Electricity and Their Application to Chemical Analysis*; Longmans, Green: London, 1913.

(13) McLafferty, F. W.; Bente, R. F.; Kornfeld, R.; Tsai, S.-C.; Howe, I. J. *J. Am. Chem. Soc.* **1973**, *95*, 2120.

(14) McLafferty, F. W.; Kornfeld, R.; Haddon, W. F.; Levsen, K.; Sakai, I.; Bente, P. F.; Tsai, S.-C.; Schuddemage, H. D. R. *J. Am. Chem. Soc.* **1973**, *95*, 3886.

(15) Cooks, R. G. *J. Mass Spectrom.* **1995**, *30*, 1215.

(16) McLuckey, S. A.; Georinger, D. E. *J. Mass Spectrom.* **1997**, *32*, 461.

(17) Marzluff, E. M.; Campbell, S.; Rodgers, M. T.; Beauchamp, J. L. *J. Am. Chem. Soc.* **1994**, *116*, 6947.

(18) Douglas, D. J. *J. Phys. Chem.* **1982**, *86*, 185.

(19) Holmes, J. L. *Org. Mass Spectrom.* **1985**, *20*, 169.

(20) Tu, Y.-P.; Holmes, J. L. *J. Am. Chem. Soc.* **2000**, *122*, 3695.

(21) Tu, Y.-P.; Holmes, J. L. *J. Am. Chem. Soc.* **2000**, *122*, 5597.

(22) Holmes, J. L.; Mayer, P. M. *J. Phys. Chem.* **1995**, *99*, 1366.

(23) Rennie, E.; Mayer, P. M. *J. Chem. Phys.* **2004**, *120*, 10561.

(24) Shannon, T. S.; McLafferty, F. W. *J. Am. Chem. Soc.* **1966**, *88*, 5021.

(25) Jones, E. G.; Baumann, L. E.; Beynon, J. H.; Cooks, R. G. *Org. Mass Spectrom.* **1973**, *7*, 185.

(26) Holmes, J. L.; Terlouw, J. K. *Can. J. Chem.* **1975**, *53*, 1076.

(27) McLafferty, F. W.; P. F. Bente, I.; Kornfeld, R.; Tsai, S.-C.; Howe, I. *J. Am. Chem. Soc.* **1973**, *95*, 2120.

(28) Holmes, J. L.; Terlouw, J. K. In *Encyclopedia of Mass Spectrometry*; Armentrout, P. B., Ed.; Elsevier: Amsterdam, 2004; Vol. 4, p 287.

(29) Beynon, J. H.; E., J. B.; Williams, A. E. Z. *Naturforsch* **1965**, *20a*, 883.

(30) Meyerson, S.; Corbin, J. L. *J. Am. Chem. Soc.* **1965**, *87*, 3045.

(31) Bouma, W. J.; MacLeod, J. K.; Radom, L. *J. Am. Chem. Soc.* **1979**, *101*, 5540.

(32) Bouma, W. J.; Poppinger, D.; Saebo, S.; MacLeod, J. K.; Radom, L. *Chem. Phys. Lett.* **1984**, *104*, 198.

(33) Nobes, R. H.; Bouma, W. J.; MacLeod, J. K.; Radom, L. *Chem. Phys. Lett.* **1987**, *135*, 78.

(34) Buschek, J. M.; Holmes, J. L.; Terlouw, J. K. *J. Am. Chem. Soc.* **1987**, *109*, 7321.

(35) Holmes, J. L.; Fingas, M.; Lossing, F. P. *Can. J. Chem.* **1981**, *59*, 80.

(36) Aue, D. H.; Webb, H. M.; Bowers, M. T. *J. Am. Chem. Soc.* **1972**, *94*, 4726.

(37) Aubry, C.; Holmes, J. L. *Int. J. Mass Spectrom.* **2000**, *200*, 277.

(38) Benson, S. W. *Chemical Kinetics*; John Wiley and Sons: New York, 1976.

(39) Morrison, J. D. In *Mass Spectrometry (MTP International Review of Science)*; Maccoll, A., Ed.; The Butterworth Group: London, 1972; Vol. 5, p 25.

(40) Topchiev, A. V. *Radiolysis of Hydrocarbons*; Elsevier Publishing Co.: London, 1964.

(41) Bansal, K. M.; Freeman, G. R. *J. Am. Chem. Soc.* **1966**, *88*, 4326.

(42) Bansal, K. M.; Freeman, G. R. *J. Am. Chem. Soc.* **1968**, *90*, 7190.

(43) Homer, J. B.; Lossing, F. P. *Can. J. Chem.* **1966**, *44*.

(44) Lossing, F. P. *Can. J. Chem.* **1972**, *50*, 3973.

(45) *NIST Chemistry Webbook; NIST Standard Reference Database Number*; National Institute of Standards and Technology: Gaithersburg MD, 1998.

(46) Lias, S. G.; Bartmess, J. E.; Liebman, J. G.; Holmes, J. L.; Levin, R. D.; Mallard, W. G. *J. Phys. Chem. Ref. Data* **1988**, *17, Suppl. 1.*, 1.

(47) Lifshitz, C.; Malinovich, Y. *Int. J. Mass Spectrom. Ion Processes* **1984**, *60*, 99.

(48) Lifshitz, C. *Eur. J. Mass Spectrom.* **2002**, *8*, 85.

(49) Szulejko, J. E.; McMahon, T. B. *J. Am. Chem. Soc.* **1993**, *115*, 7839.

(50) Meot-Ner, M.; Sieck, L. W. *J. Am. Chem. Soc.* **1991**, *113*, 4448.

(51) Munson, M. S. B.; Field, F. H. *J. Am. Chem. Soc.* **1966**, *87*, 3294.

(52) Cooks, R. G.; Patrick, J. S.; Kotaho, T.; McLuckey, S. A. *Mass Spectrom. Rev.*, *13*, 287.

(53) Armentrout, P. B. *J. Mass Spectrom.* **1999**, *34*, 74.

(54) Cooks, R. G.; Koskinen, J. T.; Thomas, P. D. *J. Mass Spectrom.* **1999**, *34*, 85.

(55) Cooks, R. G.; Wong, P. S. H. *Acc. Chem. Res.* **1998**, *31*, 379.

(56) Vekey, K. *J. Mass Spectrom.* **1996**, *31*, 445.

(57) Harrison, A. G. *Mass Spectrom. Rev.* **1997**, *16*, 201.

(58) Cao, J.; Aubry, C.; Holmes, J. L. *J. Phys. Chem. A.* **2000**, *104*, 10045.

(59) Smith, B.; Radom, L. *J. Am. Chem. Soc.* **1993**, *115*, 4885.

(60) Scott, A. P.; Radom, L. *J. Phys. Chem.* **1996**, *100*, 16502.

(61) Young, D. C. *Computational Chemistry: A practical guide for applying techniques to real-world problems*; Wiley-Interscience: New York, 2001.

(62) Moller, C.; Plesset, M. S. *Phys. Rev.* **1934**, *46*, 618.

(63) Leininger, M. L.; Allen, W. D.; Schaefer, H. F.; Sherrill, C. D. *J. Chem. Phys.* **2000**, *112*, 9213.

(64) Bartlett, R. J.; Shavitt, I. *Chem. Phys. Lett.* **1977**, *50*, 190.

(65) Johnson, B. G.; Gill, P. M. W.; Pople, J. A. *J. Chem. Phys.* **1993**, *98*, 5612.

(66) Koch, W.; Holthausen, M. C. *A Chemist's Guide to Density Functional Theory*; Viley-VCH: New York, 2000.

(67) Hohenberg, P.; Kohn, W. *Phys. Rev.* **1964**, *136*, B864.

(68) Kohn, W.; Sham, L. J. *Phys. Rev.* **1965**, *140*, A1133.

(69) Becke, A. D. *Phys. Rev. A* **1988**, *38*, 3098.

(70) Lee, C.; Yang, W.; Parr, R. G. *Phys. Rev. B* **1988**, *37*, 785.

(71) Becke, A. D. *J. Chem. Phys.* **1993**, *98*, 5648.

(72) Curtiss, L. A.; Raghavachari, K.; Trucks, G. W.; Pople, J. A. *J. Chem. Phys.* **1991**, *94*, 7221.

(73) Curtiss, L. A.; Carpenter, J. E.; Ragavachari, K.; Pople, J. A. *J. Chem. Phys.* **1992**, *96*, 9030.

(74) Curtiss, L. A.; Raghavachari, K.; Pople, J. A. *J. Chem. Phys.* **1993**, *98*, 1293.

(75) Smith, B. J.; Radom, L. *J. Phys. Chem.* **1995**, *99*, 6468.

(76) Curtiss, L. A.; Redfern, P. C.; Smith, B. J.; Radom, L. *J. Chem. Phys.* **1996**, *104*, 5148.

(77) Curtiss, L. A.; Raghavachari, K.; Redfern, P. C.; Rassolov, V.; Pople, J. A. *J. Chem. Phys.* **1998**, *109*, 7764.

(78) Baboul, A. G.; Curtiss, L. A.; Redfern, P. C.; Raghavachari, K. *J. Chem. Phys.* **1999**, *110*, 7650.

(79) Bauschlicher, C. W.; Partridge, H. *Chem. Phys. Lett.* **1995**, *246*, 40.

(80) Nicolaides, A.; Rauk, A.; Gluckhovtsev, M. N.; Radom, L. *J. Phys. Chem.* **1996**, *100*, 17460.

(81) McQuarrie, D. A. *Statistical Mechanics*; Harper & Row: New York, 1976.

(82) Frisch, M. J.; Trucks, G. W.; Schlegel, H. B.; Scuseria, G. E.; Robb, M. A.; Cheeseman, J. R.; Zakrzewski, V. G.; Montgomery, J. A.; Stratmann, R. E.; Burant, J. C.; Dapprich, S.; Millam, J. M.; Daniels, A. D.; Kudin, K. N.; Strain, M. C.; Farkas, O.; Tomasi, J.; Barone, V.; Cossi, M.; Cammi, R.; Mennucci, B.; Pomelli, C.; Adamo, C.; Clifford, S.; Ochterski, J.; Petersson, G. A.; Ayala, P. Y.; Cui, Q.; Morokuma, K.; Malick, D. K.; Rabuck, A. D.; Raghavachari, K.; Foresman, J. B.; Cioslowski, J.; Ortiz, J. V.; Stefanov, B. B.; Liu, G.; Al-Laham, A.; Peng, C. Y.; Nanayakkara, A.; Gonzalez, C.; Challacombe, M.; Gill, P. M. W.; Johnson, B.; Chen, W.; Wong, W. W.; Andres, J. L.; Gonzalez, C.; Head-Gordon, M.; Replogle, E. S.; Pople, J. A. *"GAUSSIAN 98 Rev. A. 7"*; Gaussian Inc.: Pittsburgh, PA, 1998.

(83) Scott, A. P.; Radom, L. *J. Phys. Chem.* **1996**, *100*, 16502.

(84) CODATA, values of the constants in 1998.

(85) Wagman, D. D.; Evans, W. H.; Parker, V. B.; Schumm, R. H.; Halows, I.; Bailey, S. M.; Churney, K. L.; Nuttall, R. N. *J. Phys. and Chem. Ref. Data* **1982**, *11*, Suppl. 2.

CHAPTER 4

EXPLORING THE POTENTIAL ENERGY SURFACE OF ION-MOLECULE COMPLEXES OF ACETALDEHYDE AND METHANOL

4.1 Introduction

For many years it has been known that the keto-enol isomerization of an ionized aldehyde or ketone in the gas phase involves a large energy barrier[1-5]. These barriers generally lie at an energy above the lowest dissociation threshold for the carbonyl compound and therefore the isomerization is never directly observed for the isolated ion without decomposition. For example, a theoretical study at the G2 molecular orbital level was devoted to the keto-enol isomerization of $[C_2H_4O]^{+\bullet}$ radical cations and the critical energies separating $CH_3CHO^{+\bullet}$ and $CH_2CHOH^{+\bullet}$ was calculated to be 112 kJ/mol higher than the dissociation threshold of $CH_3CHO^{+\bullet}$ to CH_3CO^+ and $H^{\bullet}$.[2] However, within an ion-molecule complex in the gas-phase, the catalyzed isomerization of the ion by the neutral moiety is now becoming a rather common phenomenon (i.e. such barriers can be reduced inside an IMC, compared with isolated species).[6-12] Much of this work has involved the identification of the mechanisms for the ion isomerizations.

In a previous study[13,14], the enol or keto cations of acetaldehyde were formed in an FT-ICR cell and allowed to react with a neutral methanol molecule. Under these conditions,

the methanol molecule was found to catalyze the isomerization of the acetaldehyde ion to its isomeric form. The generation of keto ions can be achieved by direct electron impact ionization of the molecule, while enol ions were made in an ion source by the fragmentation of an appropriate ionized cyclic alcohol (e.g. by loss of an olefin)[15] or by a McLafferty rearrangement of a selected carbonyl compound.[15,16]

In this chapter, we have investigated the keto-enol isomerization of acetaldehyde when associated with ionized methanol and its distonic isomer in a stable or metastable ion-molecule pair. The method for making such stable ion-molecule pairs is as follows. Proton-bound dimers are easily obtained from a high pressure ion source and they can be made to lose a radical under collision-induced dissociation (CID) conditions.[17,18] These CID fragmentations can produce the ion-molecule complexes of interest, namely solvated conventional or distonic odd electron ions. The advantage of this method is that the majority of the ions are stable, but with some having sufficient internal energy to undergo competing metastable dissociations. Appropriate isotopic labelling and collision-induced dissociation mass spectra of the above stable ions allow one to explore the rearrangement processes that they can undergo.

This work presents an experimental study of the aldehyde/$CH_4O^{+\bullet}$ ion-molecule complexes, formally represented as $CH_3CHO/^{+}H_2OCH_2^{\bullet}$ ion **1** and $CH_3CHO/^{+\bullet}HOCH_3$ ion **2.** They were generated in the mass spectrometer by selecting the appropriate fragment ions in the CID mass spectra of proton-bound molecular pairs. To aid the explanation of the

experimental results, potential energy surfaces (PES) for the species were obtained by theoretical calculations. Thus the PES constructed should be compatible with the experimental observations in terms of the observed competing metastable ion fragmentations, the relative abundances of the product ions, the collision sensitivity of the metastable ion peaks and the detailed appearance of the CID mass spectra. Furthermore they should be also compatible with the fate of isotopic labels among the dissociation products. In addition, the PES identifies the possible presence of high isomerization barriers that effectively eliminate some plausible rearrangement pathways.

4.2 Experimental and Theoretical Procedures

All experiments were carried out on a modified ZAB-3F tandem mass spectrometer[19] with BEE geometry (VG Analytical, Manchester, U.K.). Metastable ion (MI) and collision-induced dissociation (CID) mass spectra of the proton-bound dimer and the ion-molecule pairs were acquired in the second field-free region (2FFR) and third field-free region (3FFR) of the mass spectrometer, respectively. The ion accelerating voltage was 8 kV. In the 2FFR and 3FFR helium was used as the collision gas for the CID experiments. All spectra were recorded with the ZABCAT program developed by Mommers Technologies[19] (Ottawa, ON, Canada).

The proton-bound dimer of acetaldehyde and propanol was generated by admitting the mixed reagents $CH_3CH_2CH_2OH$ and CH_3CHO into a high pressure ion source (see Chapter 2 for detailed description) at a total observed pressure of ca. 8×10^{-5} mbar, indicating

an ion source pressure of 0.3 mbar[20]. The proton-bound dimer $CH_3CHO\cdots H^+\cdots O(H)CH_2CH_2CH_3$ (m/z = 105) was mass-selected by the magnet and collisionally activated in the second field-free region. The fragment ion [$CH_3CHO/{}^{\bullet}CH_2OH_2^+$] (m/z 76) was produced by loss of $CH_3CH_2^{\bullet}$ from the precursor ion (m/z 105) and it was transmitted into the third field-free region to study its MI and CID characteristics.

A similar experiment was used for the acetaldehyde/dimethyl ether proton-bound pair, $CH_3CHO\cdots H^+\cdots O(CH_3)_2$ (m/z 91), in order to collisionally generate labelled [$CH_3CHO/CH_3OH^{+\bullet}$] (m/z 76) by specific loss of $CH_3^{\bullet}$ from the ether. An experiment using $CD_3CHO\cdots H^+\cdots O(CH_3)_2$ (m/z 94) showed that it was an ether methyl group that was lost in the CID. Dimethyl ether was introduced through the gas inlet at an observed pressure of 5 x 10^{-5} mbar producing 0.3 mbar in the high pressure ion source.

CH_3CHO, $CH_3CH_2CH_2OH$, $(CH_3)_2O$, and the isotopically labelled compounds, CD_3CHO, CD_3CDO, $CH_3CH_2CD_2OH$, $CH_3CH_2{}^{13}CH_2OH$ were used to generate various isotopomeric ion-molecule pairs. All chemicals were commercially available and were used without further purification. Labelled compounds were purchased from CDN Isotopes (Montreal, QC, Canada).

GAUSSIAN 98 programs were used to perform standard ab initio molecular orbital calculations to investigate the potential energy surface. Optimized geometries and the energies of all minima and transition states were calculated at the MP2/6-31+G(d) level of

theory. Zero-point energies obtained from vibrational frequencies at the same level of theory were scaled by a factor of 0.9434[21]. A potential energy profile was also obtained from density functional theory B3-LYP/6-31+G(d) to compare with the PES acquired by the MP2/6-31+G(d) calculations. Zero-point energies obtained at B3-LYP/6-31+G(d) level are scaled by 0.9616[21]. The differences between the two levels of theory are discussed later. Finally, a single point energy calculation at the G3 level of theory was applied to obtain accurate relative energies of the optimized ion structures at MP2/6-31+G(d) and B3-LYP/6-31+G(d), respectively.

4.3 Results and Discussion

4.3.1 Experimental Observations

4.3.1.1 $[CH_3CHO/^{\bullet}CH_2OH_2^{+}]$ (ion **1**)

An ion of formal structure **1**, was obtained by the collision-induced loss of a $CH_3CH_2^{\bullet}$ radical from the proton-bound dimer $CH_3CHO\cdots H^{+}\cdots O(H)CH_2CH_2CH_3$ (m/z 105). The PA of propanol, 786.5 kJ/mol, is higher than that of acetaldehyde, 768.5 kJ/mol, and so the proton is preferentially attached to the alcohol to give protonated propanol electrostatically bound to an acetaldehyde molecule, i.e. $CH_3CHO/\ ^{+}H_2OCH_2CH_2CH_3$. In the CID mass spectrum of this proton-bound dimer, m/z 105, the major peaks are protonated propanol (m/z 61, 100%), protonated acetaldehyde (m/z 45, 23%), and the peak for $CH_3CH_2^{\bullet}$ loss (m/z 76).

The first two reactions are the only MI processes, showing that rearrangement of the proton bound dimer does not take place at internal energies up to those for MI dissociations; m/z 76 appears only when collision gas is admitted.

$$\underset{\text{m/z 105}}{CH_3CHO\cdots H^+O(H)CH_2CH_2CH_3} \rightarrow \underset{\text{m/z 76}}{[CH_3CHO/{}^{\bullet}CH_2O(H)H^+]} + CH_3CH_2^{\bullet} \quad \text{(CID)} \qquad 4.1$$

The MI spectrum of ion **1** (Figure 4.1-a) indicates that there are six competing dissociation reactions of m/z 76: the losses of $CH_3^{\bullet}$ (m/z 61), H_2O (m/z 58), and the formation of CH_3CHOH^+ (m/z 45), CH_3CO^+ (m/z 43), $CH_3OH_2^+$ (m/z 33); the base peak, m/z 44, has been determined to be the vinyl alcohol ion (see the discussion below).

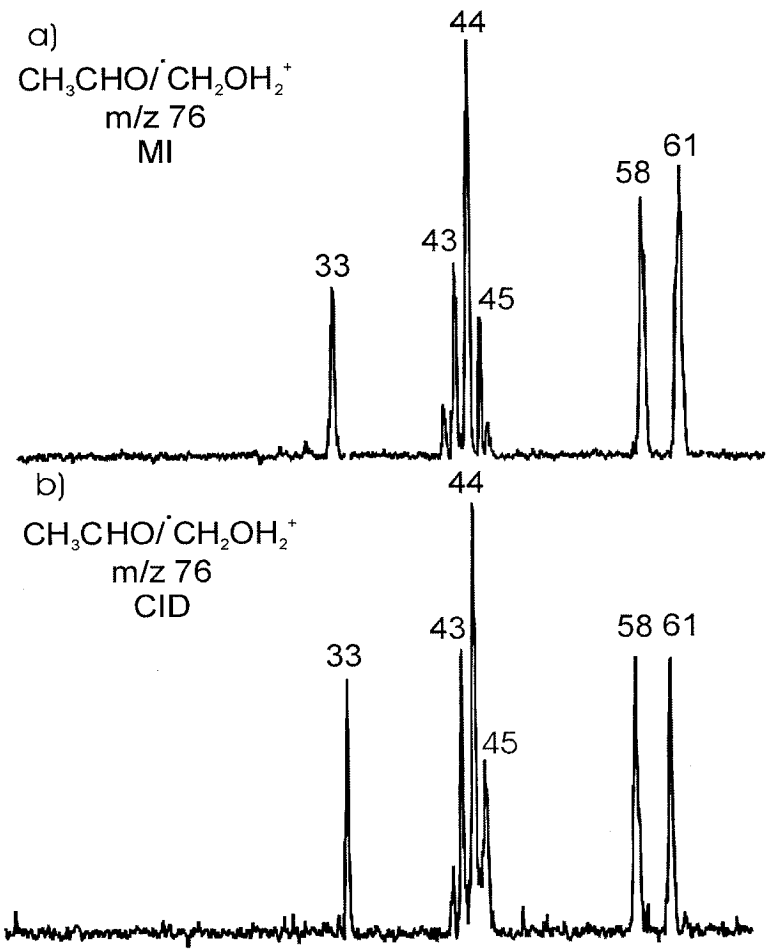

Figure 4.1. MI and CID mass spectra of $CH_3CHO/^{\bullet}CH_2OH_2^+$.

In the CID mass spectrum of ion **1** (Figure 4.1-b) the intensity of the metastable ion peak at m/z 45, CH_3CHOH^+, is increased, i.e. the formation of CH_3CHOH^+ is collision sensitive, being a simple bond cleavage in ion **1**. The PA of CH_3CHO at O is 768.5 kJ/mol, which is much higher than the PA of $^{\bullet}CH_2OH$ at O, 695 kJ/mol, so that the structure of the stable ion **1** is better represented as $CH_3CHOH^+\cdots O(H)CH_2^{\bullet}$. However, the peak corresponding to the formation of the m/z 44 ion is not collision sensitive, indicating that ion **1** rearranges before it fragments.

The dissociation channel leading to the enol form of ionized acetaldehyde, the vinyl alcohol ion, is energetically the most favourable process. If the ion m/z 44 has the enol structure, the dissociation threshold energy is at 569 kJ/mol (from $\Delta_fH[CH_2CHOH^{+\bullet}]$ = 771 kJ/mol, $\Delta_fH[CH_3OH]$ = -202 kJ/mol)[22]. This is lower than the dissociation limit, 576 kJ/mol, for the formation of the protonated acetaldehyde ion m/z 45, (from $\Delta_fH[CH_3CHOH^+]$ = 595 kJ/mol, $\Delta_fH[^\bullet CH_2OH]$ = -19 kJ/mol)[22]. If the m/z 44 ion had the keto structure, the threshold energy for this dissociation would be much higher, at 619 kJ/mol (from $\Delta_fH[CH_3CHO^{+\bullet}]$ = 821 kJ/mol, $\Delta_fH[CH_3OH]$ = -202 kJ/mol)[22]. Thus in the MI mass spectrum of ion **1**, the base peak would be peak m/z 45 if the $CH_3CHO^{+\bullet}$ ion had not isomerized. That the enol ion is produced is also supported by the results of isotopic labelling.

The isotopically labelled ion-molecule pairs, $[CD_3CHO/^\bullet CH_2OH_2^+]$, **1**-$d_3$ (m/z 79), $[CD_3CHO/^\bullet CD_2OH_2^+]$, **1**-$d_5$ (m/z 81), $[CH_3CHO/^\bullet CD_2OH_2^+]$, **1**-$d_2$ (m/z 78), $[CH_3CHO/^\bullet CD_2OHD^+]$, **1**-$d_3$ (m/z 79), $[CH_3CHO/^\bullet CD_2OD_2^+]$, **1**-$d_4$ (m/z 80) were examined to assign the structure of the above m/z 44 ion as that of vinyl alcohol. The MI mass spectrum of $[CH_3CHO/^\bullet CD_2OD_2^+]$, **1**-$d_4$ (m/z 80) (Figure 4.2-a) shows the most intense peak at m/z 45, to which the structure $CH_2CHOD^{+\bullet}$ is assigned; if the keto ion were the major product, it would have resulted in m/z 44, $CH_3CHO^{+\bullet}$, being observed instead. Similar observations were found for the other labelled pairs. For example, Figure 4.2-b shows the MI mass spectrum of $[CD_3CHO/^\bullet CH_2OH_2^+]$, **1**-$d_3$ (m/z 79), with the base peak at m/z 46, i.e. $CD_2CHOH^{+\bullet}$, not $CD_3CHO^{+\bullet}$ (m/z 47).

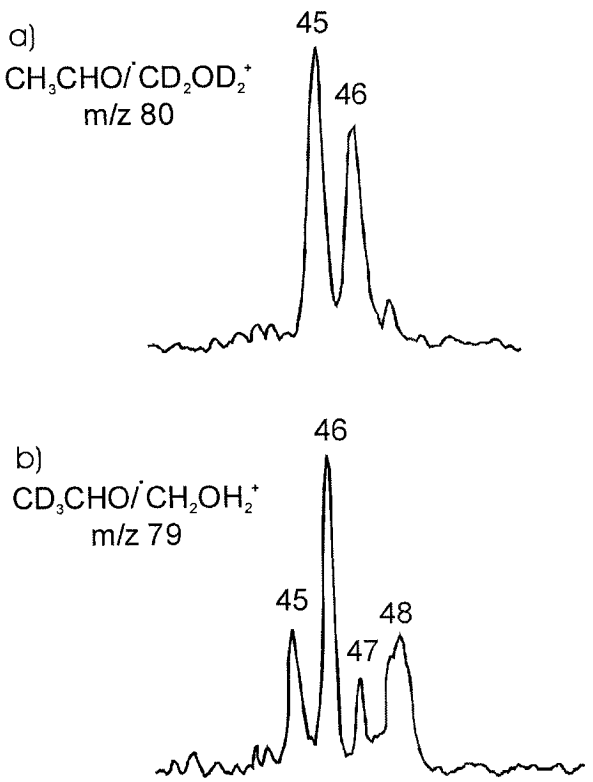

Figure 4.2. a) The major fragment ion of $CH_3CHO/^{\cdot}CD_2OD_2^+$ gives m/z 45, CH_2CHOD^+, b) the major fragment ion of $CD_3CHO/^{\cdot}CH_2OH_2^+$ gives m/z 46, CD_2CHOH^+.

The experimental data for all labelled ion-molecule pairs are shown in Table 4.1. The results are explained as follows. Before the ion-molecule pair **1**, $[CH_3CHO\cdots H^+\cdots OHCH_2^{\cdot}]$, dissociates to the vinyl alcohol ion and methanol, a $H^{\cdot}$ atom from $C\underline{H}_3CHO$ moves to the $^{\cdot}C\underline{H}_2OH$ radical via a 1,6-H shift. This process involves TS3 on the PES, see Figure 4.7 and the discussion of the computations. Furthermore, two $H^{\cdot}$ atoms of $C\underline{H}_3CHOH^+$ in ion **1**-d_2, exchange with D atoms at the radical site of $^{\cdot}C\underline{D}_2OH$ during such a rearrangement.

Table 4.1. Fragmentations of labelled acetaldehyde/distonic methanol ion-molecule complexes in their MI spectra.

precursor ion m/z	ion-molecule pair m/z	fragments of ion-molecule pair m/z				
		protonated methanol	vinyl alcohol	protonated acetaldehyde	$-H_2O$	- methyl
$(CH_3CHO)H^+$ $(HOCH_2CH_2CH_3)$ 105	$[CH_3CHO/ {}^{\bullet}CH_2OH_2^+]$ 76	33	44	45	58	61
$(CH_3CHO)H^+$ $(HOCD_2CH_2CH_3)$ 107	$[CH_3CHO/ {}^{\bullet}CD_2OH_2^+]$ 78	33 34 35	44	45 46	59 60	61 62 63
$(CD_3CHO)H^+$ $(HOCH_2CH_2CH_3)$ 108	$[CD_3CHO/ {}^{\bullet}CH_2OH_2^+]$ 79	33 34	45 46 47	48	60 61	62 63 64
$(CH_3CHO)D^+$ $(DOCD_2CH_2CH_3)$ 109	$[CH_3CHO/ {}^{\bullet}CD_2OD_2^+]$ 80	35 36 37	44 45	46 47	60 61 62	63 64 65
$(CD_3CHO)H^+$ $(HOCD_2CH_2CH_3)$ 110	$[CD_3CHO/ {}^{\bullet}CD_2OH_2^+]$ 81	35 36 37	45 46 47	48	61 62 63[a]	63[a] 64 65
$(CH_3CHO)H^+$ $(HO^{13}CH_2CH_2CH_3)$ 106	$[CH_3CHO/ {}^{13}{}^{\bullet}CH_2OH_2^+]$ 77	34	44	45	59	61(major) 62(minor)
$(CH_3CHO)D^+$ $(DO^{13}CH_2CH_2CH_3)$ 108	$[CH_3CHO/ {}^{13}{}^{\bullet}CH_2OD_2^+]$ 79	35 36	45	46	59 60	62 63 64
$(CD_3CHO)H^+$ $(HO^{13}CH_2CH_2CH_3)$ 109	$[CD_3CHO/ {}^{13}{}^{\bullet}CH_2OH_2^+]$ 80	34 35 36	45 46	48	62[b]	62[b] 63 64
$(CD_3CHO)H^+$ $(DO^{13}CH_2CH_2CH_3)$ 110	$[CD_3CHO/ {}^{13}{}^{\bullet}CH_2ODH^+]$ 81	35 36 37	45 46 47	48	62	63 64 65
$(CD_3CHO)D^+$ $(DO^{13}CH_2CH_2CH_3)$ 111	$[CD_3CHO/ {}^{13}{}^{\bullet}CH_2OD_2^+]$ 82	36 37 38	47	49	63	64 65 66

[a] m/z 63 ions are a mixture of the losses of H_2O and $^{\bullet}CD_3$ in the MI mass spectrum of $[CD_3CHO/ {}^{\bullet}CD_2OH_2^+]$ (m/z 81).

[b]m/z 62 ion results from the losses of H_2O and $^{\bullet 13}CD_2H$ in the MI mass spectrum of $[CD_3CHO/^{13\bullet}CH_2OH_2^+]$ (m/z 80).

One question remains: could m/z 44 possibly be the carbene ion $CH_3COH^{+\bullet}$, even though it is unlikely to be produced on energetic grounds ($\Delta_fH[CH_3COH^{+\bullet}]$=865kJ/mol[22])? To test this, the ion $CH_3COH^{+\bullet}/CH_3OH$, ion **3**, was made by CID loss of an ethyl radical from the proton-bound dimer, $CH_3CH_2C(CH_3)=O\cdots H^+\cdots O(H)CH_3$. Its MI mass spectrum, Figure 4.3, shows four major products: protonated methanol (m/z 33), the acetyl ion (m/z 43), water loss (m/z 58) and methyl loss (m/z 61). However, it does not produce any m/z 44, $CH_3COH^{+\bullet}$, whose generation cannot compete energetically with the other dissociation channels. Therefore, the carbene ion can be ruled out.

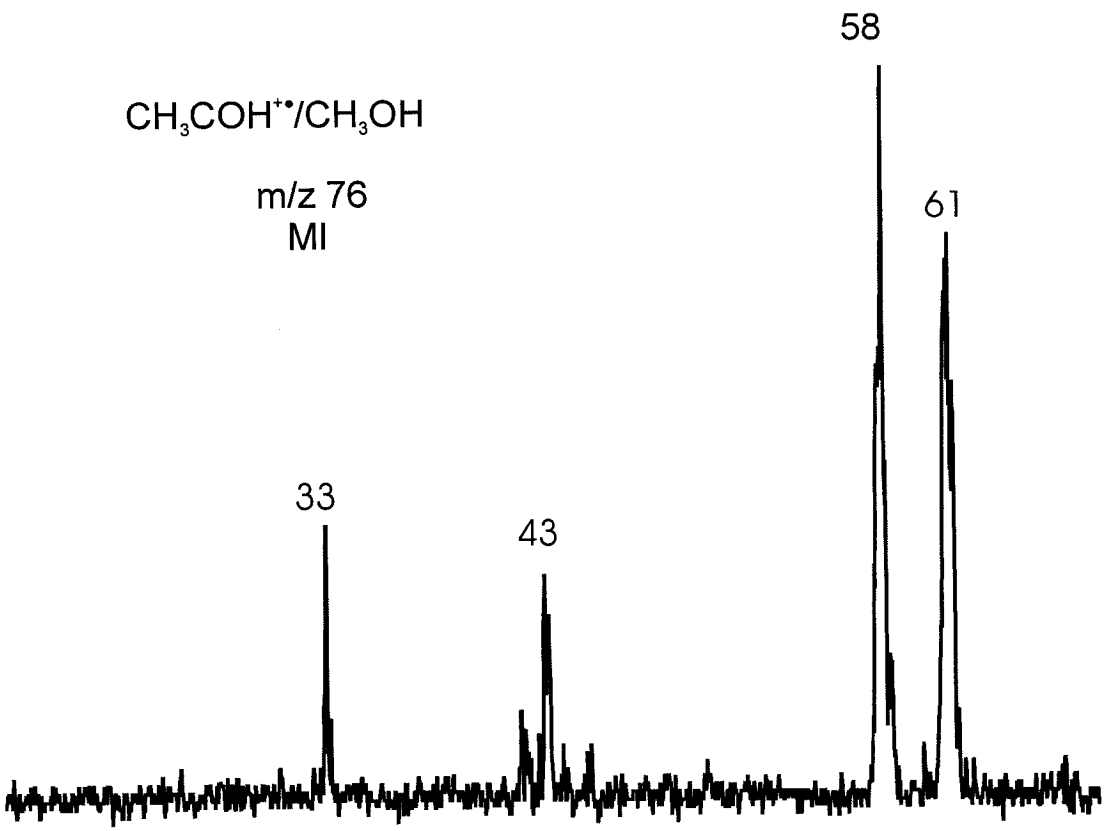

Figure 4.3. MI mass spectrum of the $CH_3COH^{+\bullet}/OHCH_3$ ion.

An experiment using the ^{13}C labelled ion $CD_3CHO/^{13\bullet}CH_2O(D)H^+$, m/z = 81 Figure 4.4, proved that the lost methyl is from the methanol portion of the ion. The kinetic energy release (obtained from the width of the peak at half-height, $T_{0.5}$) associated with the $CH_3^\bullet$ radical loss has been measured as 67 meV, indicative of a reverse energy barrier. The structure assigned to the fragment ion for $CH_3^\bullet$ loss from ion **1** is $CH_3C^+(OH)_2$, protonated acetic acid, Δ_fH = 313 kJ/mol. This low energy species is indeed the likely product, as will be discussed later. The production of $CH_3OH_2^+$ and isotopomers involves formal H/D exchange between the acetaldehyde and methanol species.

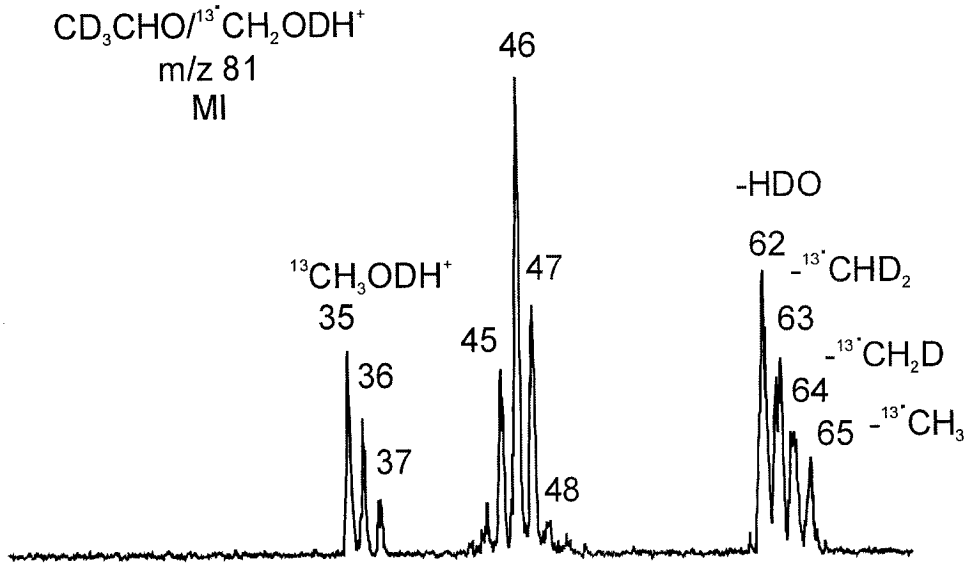

Figure 4.4. MI mass spectrum of labelled $CD_3CHO/^{13\bullet}CH_2ODH^+$.

4.3.1.2 $[CH_3CHO/CH_3OH^{+\bullet}]$ (ion **2**)

The CID mass spectrum of the proton bound acetaldehyde-dimethyl ether dimer $CH_3CHO\cdots H^+\cdots O(CH_3)_2$ (m/z 91) ion showed two major peaks, namely protonated dimethyl ether (m/z 47), protonated acetaldehyde (m/z 45), and the minor $CH_3^\bullet$ loss peak (m/z 76). The relevant reaction is shown below.

$$CH_3CHO\cdots H^+O(CH_3)_2 \rightarrow [CH_3CHO/CH_3OH^{+\bullet}] + CH_3^\bullet \quad \text{(CID)} \qquad 4.2$$

m/z 91 m/z 76

The methyl radical lost could come from either molecule and so deuterium labelling was used to identify the methyl group, e.g. $CD_3CHO\cdots H^+\cdots O(CH_3)_2$, **2-d$_3$**, $CD_3CDO\cdots H^+\cdots O(CH_3)_2$, **2-d$_4$**, and $CD_3CDO\cdots D^+\cdots O(CH_3)_2$, **2-d$_5$**, only lost $^{\bullet}CH_3$ in their CID mass spectra, showing that only an ether methyl group is involved.

Compared with its isomer **1,** the MI mass spectrum of ion **2** (and its isotopomers) is simpler. There are four competing dissociation channels, giving protonated acetaldehyde (m/z 45), the acetaldehyde ion (m/z 44), protonated methanol (m/z 33), and $CH_3^{\bullet}$ loss (m/z 61). In contrast with the mass spectra of its isomer, ion **1,** the MI and CID mass spectra of ion **2** show that hydrogen and deuterium atoms do not mix (see Figure 4.5), the MI mass spectrum of $CD_3CHO/CH_3OH^{+\bullet}$, **2-d$_3$** m/z 79. The base peak is protonated acetaldehyde, CD_3CHOH^+ (m/z 48), and the smaller peak m/z 47 has to be the acetaldehyde radical cation, not the vinyl alcohol ion even though it is more energetically favoured than protonated acetaldehyde, see the discussion of ion **1** above. The H/D atoms in m/z 47, $CD_3CHO^{+\bullet}$, have retained their original positions, indicating no rearrangement of ion **2** to the enol form. There is an exclusive peak at m/z 33, $CH_3OH_2^+$, and only one methyl loss peak, M-18, corresponding to the $CD_3^{\bullet}$ group. The CID mass spectrum of the **2-d$_3$** ion showed that the M-18 peak is collision sensitive and very likely arises from a simple C-C bond cleavage. The M-18 peak cannot arise from loss of H_2O because the MI mass spectrum of the ion $CD_3CDO/CH_3OD^{+\bullet}$ (m/z 81), **2-d$_5$**, gave an intense peak M-18 (m/z 63), but no M-20 ($-D_2O$) peak or M-19 (-HDO).

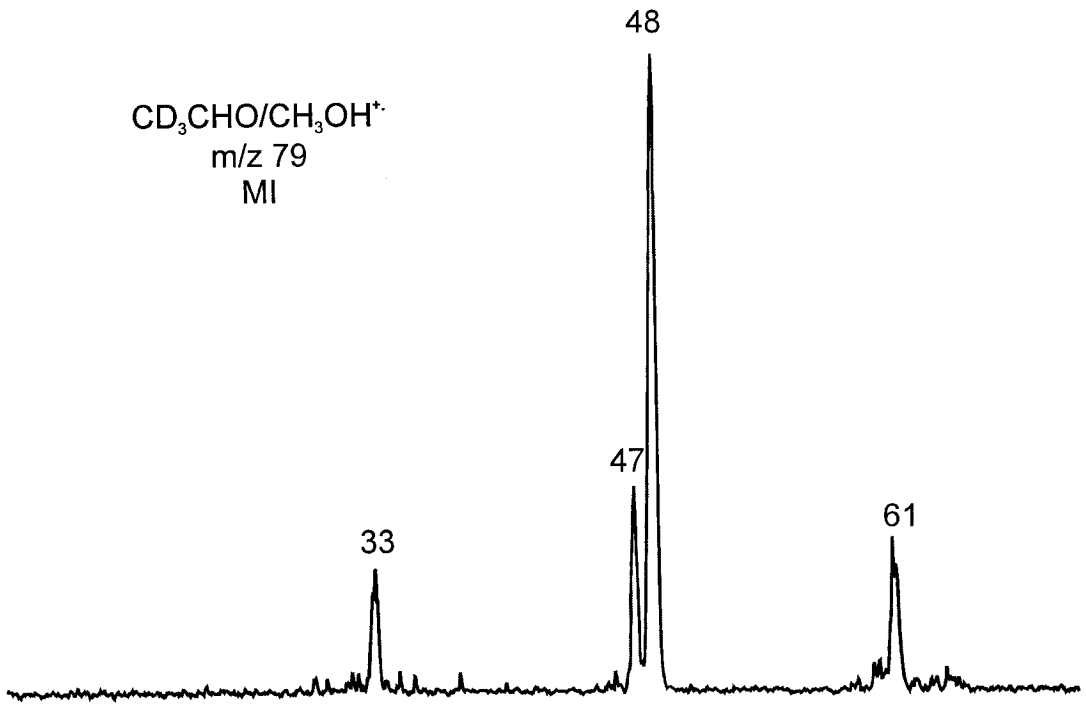

Figure 4.5. MI mass spectrum of the ion $CD_3CHO/CH_3OH^{+\bullet}$.

4.3.2 Theoretical Calculations

The two ions, $[CH_3CHO/^{\bullet}CH_2OH_2^{+}]$ and $[CH_3CHO/CH_3OH^{+\bullet}]$, display different chemistries in their mass spectra. Thus these two systems do not communicate with each other, presumably because there is a high energy barrier to their interconversion. Theoretical calculations were performed to investigate this and to produce a PES for each ion and its fragmentations.

4.3.2.1 The [$CH_3CHO/^{\bullet}CH_2OH_2^+$] System

The theoretical energy profile is shown schematically in Figure 4.7. The optimized structure of ion **1** is $CH_3CHO\cdots H^+\cdots O(H)CH_2^{\bullet}$, Stable State IV, in which the proton is close to the aldehydic oxygen, rather than to the methanol oxygen; the former bond length $(CH_3CH)O$-H is 1.057 Å, the latter O-H length is 1.487 Å, see Figure 4.6-a. This is in keeping with the PA of CH_3CHO being greater than that for $^{\bullet}CH_2OH$ at oxygen (see also Section 4.3.1). Ion IV rearranges to the vinyl alcohol-methanol ion, $CH_2CHOH^{+\bullet}\cdots O(H)CH_3$, complex V, via a cyclic transition state (TS3). This requires only about 115 kJ/mol and lies below the dissociation threshold of IV to form protonated acetaldehyde and the hydroxyl methyl radical, 136 kJ/mol. The relative energies given above are obtained at the MP2/6-31+G(d) level of theory, see Figure 4.7. The energy for the isolated acetaldehyde ion to vinyl alcohol isomerization is at 215 kJ/mol[2] and lies above the dissociation limit of the keto ions (103 kJ/mol)[2]. Note that TS3, the seven-membered ring structure, would be favoured by entropy considerations. Complex V then dissociates to produce the vinyl alcohol ion and a methanol molecule, the dissociation limit for which is ~130 kJ/mol; this process involves the low energy barrier TS3 and is the competing dissociation channel of lowest energy, giving rise to the most intense peak in the MI mass spectrum of ion **1**. Thus the initial aldehyde has been isomerized to its enol-form by transferring a proton and a $H^{\bullet}$ atom. We believe that the free radical site functions as a good $H^{\bullet}$ or H^+ accepter and facilitates the enolization of acetaldehyde.

The formation of the protonated methanol ion can be via two pathways. In the first, ion V rearranges to complex VI, $CH_3CO^{\bullet}\cdots H^+OHCH_3$, via a 1,2-H shift in the vinyl alcohol to generate the acetyl radical and protonated methanol. This process requires a large energy barrier TS5, ~193kJ/mol, for the internal 1,2-H shift. There is another more facile pathway, namely the isomerization of complex IV to VI via a 1,5-H shift, transition state TS4, at 145 kJ/mol and so is more accessible than TS5. This explains why the protonated methanol in the MI mass spectrum of $CD_3CHO/^{13\bullet}CH_2OHD$ (Figure 4.4) is chiefly $^{13}CH_3OHD^+$, but with some evidence of H, D exchanges.

We also observed an intense water loss peak in the above experiments, in the complex IV, a species that when initially made in the mass spectrometer does not contain a H_2O species. An S_N2 mechanism has been considered for this water loss process. It has long been recognized that an S_N2-type rearrangement can occur among a variety of gas-phase unimolecular reactions, e.g. the water molecule loss from proton-bound alcohol pairs or proton-bound acetonitrile and alcohols.[23-26] After complex IV converts to V, the rotation of $CH_3OH_2^+$ along the O-C bond, TS6a, allows the protonated methanol to turn around, ready to be back-attacked by $CH_2CHOH^{\bullet}$, the intermediate complex (INT, in Figure 4.7) contains three species, and TS6b leads to dissociation to H_2O and $CH_2CHOCH_3^{+\bullet}$.

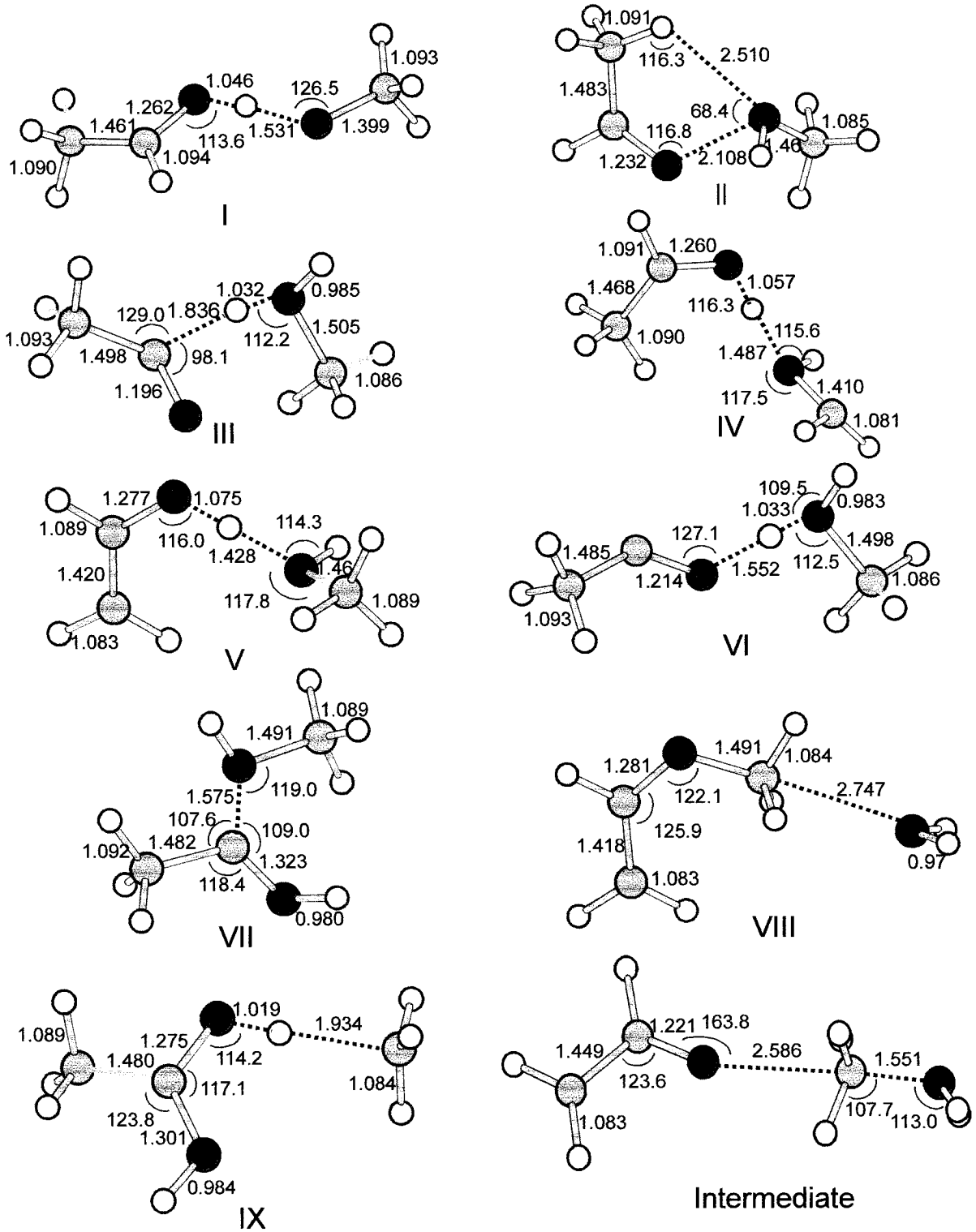

Figure 4.6-a. Optimized geometries of the stable states at the MP2/6-31+G(d) level of theory (Carbon in pink, Oxygen in red and Hydrogen in white).

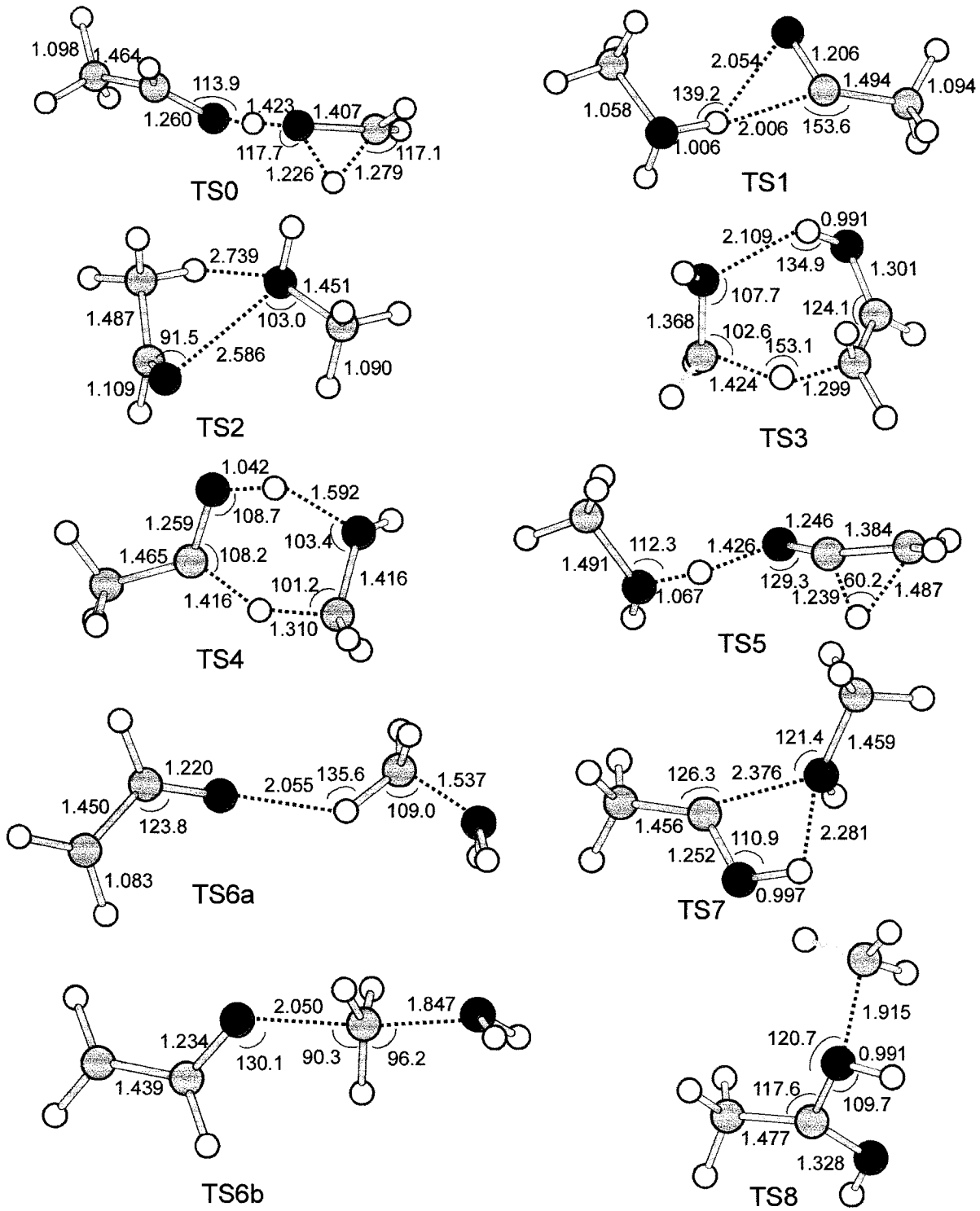

Figure 4.6-b. Optimized geometries of the transition states at the MP2/6-31+G(d) level of theory (Carbon in pink, Oxygen in red and Hydrogen in white).

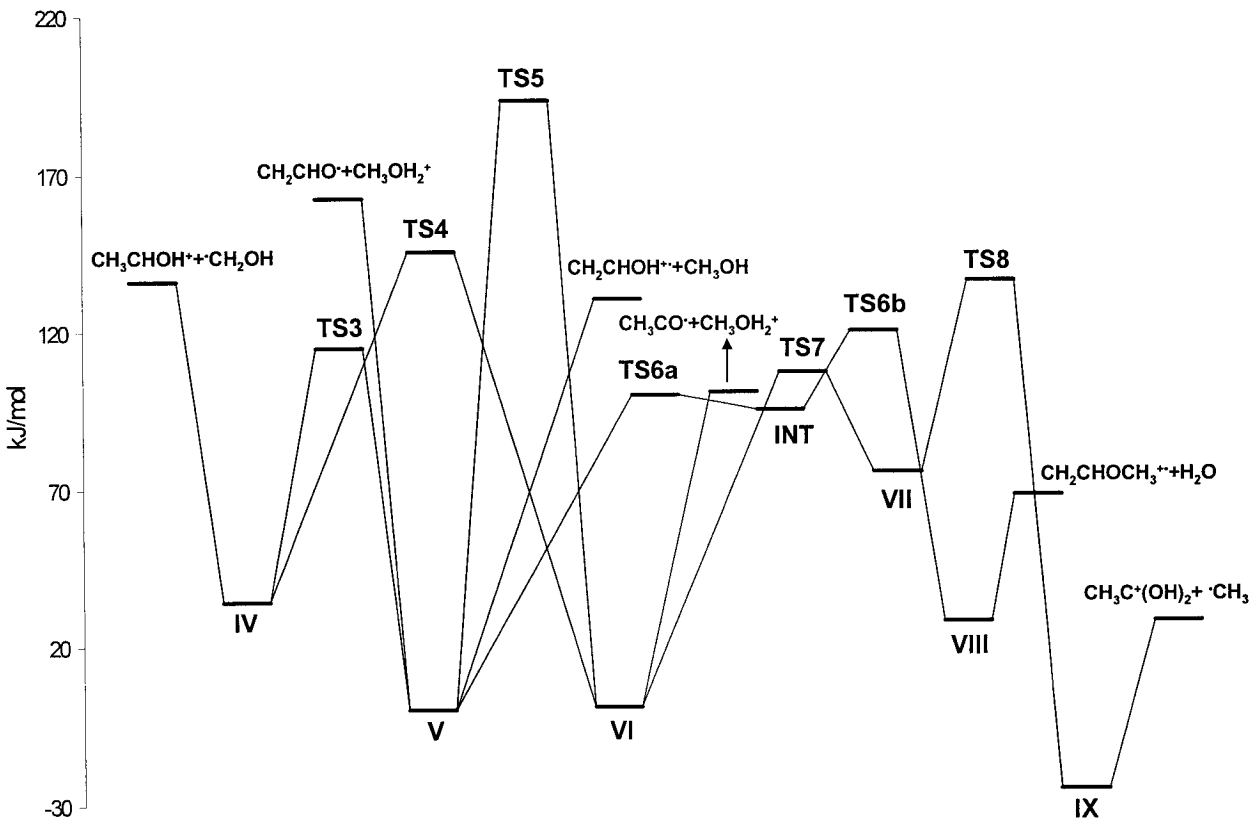

Figure 4.7. Potential Energy Surface (at 0 K) of the $CH_3CHO/CH_2OH_2^{+\bullet}$ system at the MP2/6-31+G(d) level of theory.

The experimental results indicate that the production of the $(M-15)^+$ ion is due to the methanol methyl radical loss, and the mechanism explored by the calculations is as follows. Interconversion between complex VI and the carbene ion with methanol $CH_3C^{+\bullet}(OH)\cdots OHCH_3$, complex VII, takes place via transition state TS7 (~107 kJ/mol). In TS8, the extension of the C-O bond in methanol leads to the OH moving towards the

carbonyl C of $CH_3COH^{+\bullet}$. VII then converts to complex IX, protonated acetic acid electrostatically bound to the methyl radical, which is a very stable species lying at about -25 kJ/mol on PES **1**, (even 25 kJ lower than the Stable State V). Structure IX fragments readily to the products, protonated acetic acid and methanol (~28 kJ/mol.), see Fig. 4.7.

Kinetic energy release (KER) measurement experiments[27] were made on all the MI ion peaks and KER values ($T_{0.5}$) are consistent with the TS heights on the PES **1**, Figure 4.7. The $CH_3^{\bullet}$ loss ion had the largest KER, 67 meV, in keeping with it having the largest reverse energy barrier on the PES **1**, the energy difference between TS4 (the highest transition state in its pathway) and the dissociation limit, 117 kJ/mol. This is compatible with the smaller KER for the H_2O loss ion, 48 meV, corresponding to a reverse energy barrier of 52 kJ/mol, the difference between the products' energy and that of TS6b. However, it was surprising to find that the generation of the protonated methanol ion (m/z 33) had the lowest KER, 8 meV, although it is not a simple bond cleavage process. This may be due to the tight cyclic transition state TS4. In order to form the complex VI from TS4, a heavy methyl group must rotate to reform the proton bound pair, and thus a large rotational energy component is involved, resulting in a smaller translational energy release in the products. Alternatively, at the energy corresponding to TS4, there may be little coupling between the degrees of freedom in the ion and neutral moieties, i.e. the radical may be free to move around the $CH_3OH_2^+$ ion, leading to a relatively small KER.

4.3.2.2 The [$CH_3CHO/CH_3OH^{+\bullet}$] System

The major dissociation thresholds on the PES of ion **2**, shown as Figure 4.8, are the formation of CH_3CHOH^+ and a methoxyl radical (~171 kJ/mol), $CH_3CHO^{+\bullet}$ and methanol (~180 kJ/mol). The stable complex I, $CH_3CHOH^+\cdots{}^{\bullet}OCH_3$, is able to rearrange to complex II, $CH_3CHO^{+\bullet}\cdots HOCH_3$. However no transition state structure has been found to connect these two minima; other workers have encountered the same problem.[13,14] In the complex II, the O atom of CH_3OH is associated with the carbonyl O and methyl H of $CH_3CHO^{+\bullet}$ in the form of a five-membered ring structure. The computational difficulty arises when I converts to II, the charge centre migrates from the proton to the aldehydic C atom and at the same time a $H^{\bullet}$ radical moves to $CH_3O^{\bullet}$. Because protonated methanol is observed in the MI mass spectrum, this transition state, TS1/2, should be below the dissociation limits of the precursor ion-molecule complex I. Haranczyk et al.[13] found a minimum energy crossing point (MECP) at RHF/DZP level which works as the transition state for the interconversion of I and II.

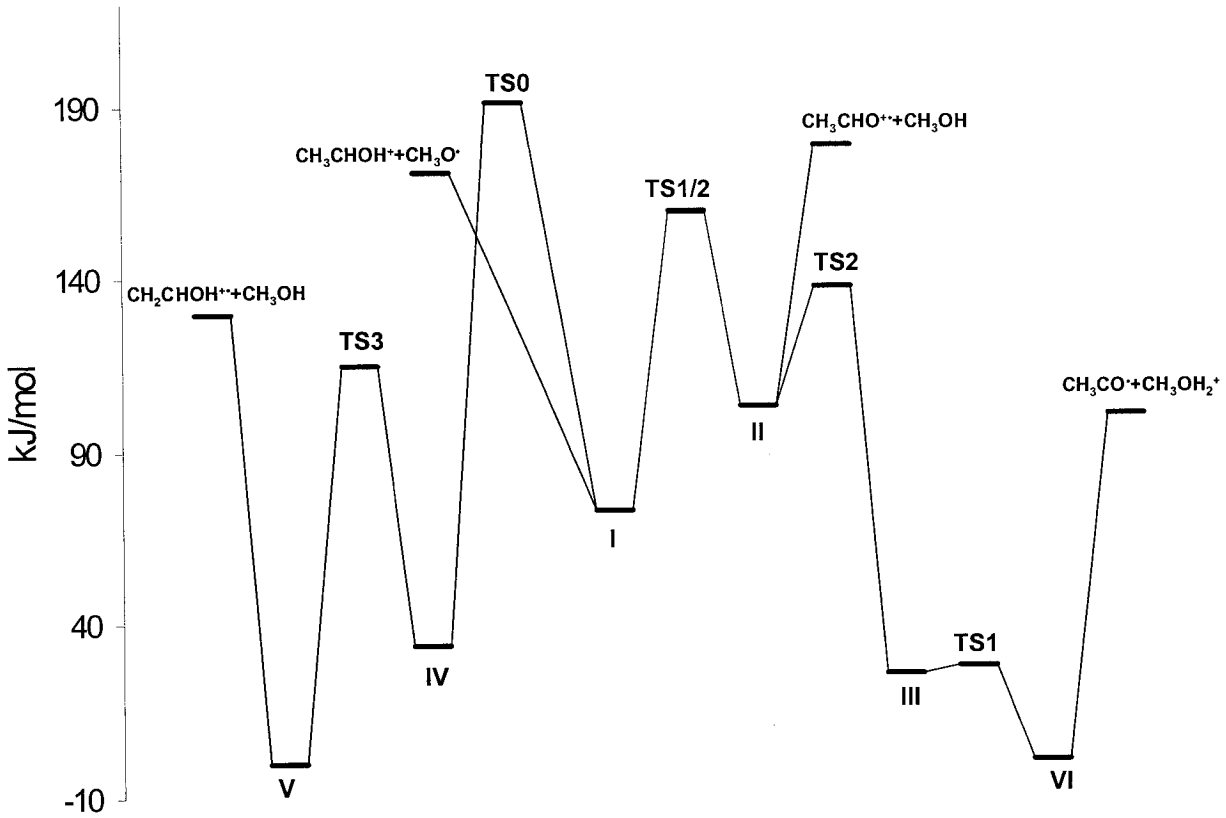

Figure 4.8. Potential Energy Surface (at 0 K) of $CH_3CHO/CH_3OH^{+\bullet}$ system at the MP2/6-31+G(d) level of theory.

The common dissociation channel on PES **1** and **2** is to form $CH_3OH_2^+$ and $CH_3CO^\bullet$, but it involves different pathways on the two surfaces. Rotation in the transition state TS2 results in the isomerization of II to III, $CH_3C(O)^{\bullet}\cdots{}^{+}HOHCH_3$, and further, III converts to its isomer VI by a very flat transition state TS1 that is only about 2 kJ/mol higher than III. The difference between the structures III and VI is that in III, the $CH_3CO^\bullet$ is electrostatically bound to $CH_3OH_2^+$ by a C···H···O bridge, but via a O···H···O bridge in VI. Then from VI, the

complex quickly dissociates to the products. As was mentioned in Section 4.3.2.1 above, VI can rearrange to IV, $CH_3CHO\cdots H^+\cdots O(H)CH_2^{\bullet}$, but it should be noted that the transition state TS4 (~145 kJ/mol) for this isomerization is at a higher energy than the dissociation limit of VI, (~101 kJ/mol). Hence PES 1 and PES 2 do not communicate with each other, although they have a common Stable State VI.

Another transition state energy, TS0, has been calculated, by which complex I, ion **2**, converts to IV, ion **1**. TS0 lies at a rather high energy, about 191 kJ/mol. In the metastable time frame of the mass spectrometer, a reaction requiring such a high relative internal energy is usually not observable. Again it reflects the experimental observations that the ions **1** and **2** do not have a common chemistry or share the same PES.

4.3.2.3 Comparison of Energy Results Obtained at Different Level of Theories with Experimental Data

The relative energies calculated at MP2/6-31+G(d), B3-LYP/6-31+G(d) and G3 level of theories are listed in Table 4.2. Note that the single point energies obtained at the G3 level of theory and based on the optimized MP2/6-31+G(d) geometries are close to the MP2/6-31+G(d) results, shown in Table 4.2, and so further G3 calculations were not performed.

Table 4.2. Calculated electronic energies (in Hartrees), incorporating a scaled zero-point energy correction, and relative energies (in kJ mol^{-1}) at 0 K for the different structures.

Structures	B3-LYP/ 6-31+G(d)		G3//B3-LYP[a]		MP2/6-31+G(d)		G3//MP2[b]	
	E_{cal}	E_{rel}	E_{cal}	E_{rel}	E_{cal}	E_{rel}	E_{cal}	E_{rel}
I	-269.13500	39	-269.01071	65	-268.27967	73		
II	-269.12809	57	-269.00430	82	-268.26842	103		
III	-269.13662	34	-269.02578	25	-268.29778	26	-269.03189	33
IV	-269.13330	43	-269.02846	18	-268.29465	34	-269.03029	37
V	-269.14967	0	-269.03547	0	-268.30751	0	-269.04450	0
VI	-269.14401	15	-269.03367	5	-268.30703	1		
VII	-269.11586	89	-269.00801	72	-268.27899	75		
INT	-269.11605	88	-269.00603	77	-268.27122	95		
VIII	-269.13616	35	-269.02754	21	-268.29688	28		
IX	-269.13749	32	-269.03522	1	-268.31686	-25		
TS0	-269.08149	179	-268.96971	173	-268.23477	191		
TS1	-269.13122	48	-269.02369	31	-268.29704	28		
TS2	-269.13594	91	-268.98352	136	-268.25488	138	-268.99909	119
TS3	-269.12010	78	-269.00121	90	-268.26357	115	-269.00540	103
TS4	-269.10259	124	-268.98845	123	-268.25221	145		
TS5	-269.08189	178	-268.97078	170	-268.23398	193		
TS6a	-269.11497	91	-269.00450	81	-268.26937	100		
TS6b	-269.11112	101	-268.99710	101	-268.26202	120		
TS7	-269.10754	111	-268.99476	107	-268.26676	107		
TS8	-269.10268	123	-268.98750	126	-268.25568	136		

[a]G3//B3-LYP: A single point energy calculation at G3 based on the optimized B3-LYP/6-31+G(d) geometries.

[b]G3//MP2: A single point energy calculation at G3 based on the optimized MP2/6-31+G(d) geometries.

In order to compare these calculated values with experimental data, reference values of $\Delta_f H$ for all the products[22] are used and shown in Table 4.3. In column 5, the values are the heats of formation of the products relative to the sum of the heats of formation of the vinyl alcohol ion and methanol, in row 8. Column 4 lists the calculated relative energies at the MP2/6-31+G(d) level with row 8, column 3 are the G3//B3-LYP results, column 2 gives the B3-LYP/6-31+G(d) values. Note that the G3 energies are very close to the current best experimental data, the differences being no more than 5 kJ/mol. Moreover, the MP2 results are very similar to the G3 energies, with differences of only a few kJ/mol except for the relative energy of the pair, $CH_3CO^{\bullet}$ + $CH_3OH_2^+$: this may be caused by spin contamination for the double bonded radical structure.

Table 4.3. Comparison of calculated relative energies (in kJ/mol) with experimental values[22].

Products	B3-LYP/ 6-31+G(d)	G3//B3-LYP	MP2/ 6-31+G(d)	Experimental Data
$CH_3O^{\cdot}+CH_3CHOH^+$	17	40	41	42
$CH_2OH^{\cdot}+CH_3CHOH^+$	9	3	6	7
$CH_3CO^{\cdot}+CH_3OH_2^+$	-4	-9	-29	-7
$CH_3C^+(OH)_2+CH_3^{\cdot}$	-83	-102	-102	-109
$CH_2CHOCH_3^{+\cdot}+H_2O$	-55	-62	-62	-68
$CH_3CHO^{+\cdot}+CH_3OH$	36	45	49	50
$CH_2CHOH^{+\cdot}+CH_3OH$	0	0	0	0

In summary, the distonic methanol ion facilitates the isomerization of acetaldehyde into its enol ion, but the conventional ion does not.

$$CH_3CHO/^{+}H_2OCH_2^{\bullet} \longrightarrow CH_2CHOH^{+\bullet}/OHCH_3 \qquad 4.3$$

$$CH_3CHO/^{+\bullet}HOCH_3 \not\longrightarrow CH_2CHOH^{+\bullet}/OHCH_3 \qquad 4.4$$

A distonic ion is a good proton donor and hydrogen atom acceptor. In reaction 4.3, a proton is given to a keto group and the radical moiety takes a H$^{\bullet}$ atom back. Thus the ketone is readily converted to its enol-ion form. The key transition state, TS3 shown below, transfers a H$^{\bullet}$ atom back to the methyl hydroxyl radical undergoing a *$H^{+}/H^{\bullet}$ transfer mechanism.*

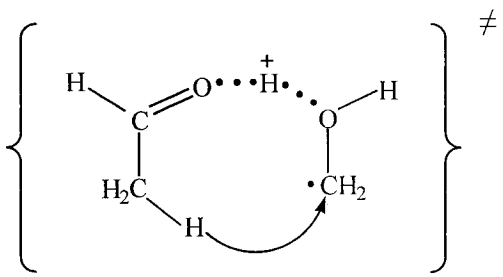

Figure 4.9. 1,6-Hydrogen shift for TS3 on the PES of $CH_3CHO/CH_2OH_2^{+\bullet}$.

4.4. Conclusions

It has been shown that the stable or metastable ions [$CH_3CHO/^{\bullet}CH_2OH_2^+$], **1**, and [$CH_3CHO/CH_3OH^{+\bullet}$], **2**, have distinct chemistries, i.e., they do not share a common potential energy surface because the transition state connecting them is very high in energy. The two ion-molecule complexes were produced collisionally from appropriate proton-bound pairs and the complex ions have sufficient internal energy to dissociate in the metastable time-frame. The important result in the [$CH_3CHO/^{\bullet}CH_2OH_2^+$] ion study is that the acetaldehyde rearranges to its enol ion. The isomerization is considered to be a new mechanism, a $H^+/H^{\bullet}$ *transfer mechanism*: after acetaldehyde has accepted a proton from the distonic methanol, the protonated acetaldehyde gives a $H^{\bullet}$ atom back to the $^{\bullet}CH_2OH$ radical by a 1,6-H transfer, producing the vinyl alcohol cation attached to a methanol molecule. In contrast, if the acetaldehyde is formally attached to a methanol ion, ion **2**, it cannot access the adjacent [$CH_3CHO/^{\bullet}CH_2OH_2^+$] surface. In the former complex, the enol-form ion is not produced, as shown by the isotopic labelling experiments (see Section 4.3.1). This may be due to a higher barrier preventing ion **2** from rearranging to vinyl alcohol ion and methanol, complex V (see Figure 4.8). Bimolecular encounters involve higher energies and are able to overcome this high barrier[14]; however, the stable or metastable ion-molecule pairs which were made in this study cannot surmount this barrier. Instead, ion **2** rearranges to a very stable complex VI and then dissociates to a stable protonated methanol ion and acetyl radical. The theoretical calculations support all the experimental observations. Calculated product energies at the MP2/6-31+G(d) level of theory and single point energy G3 calculations on optimized

geometries at the B3-LYP/6-31+G(d) level of theory are in good agreement with experimental data.

References

(1) Turecek, F. In *The Chemistry of Enols*; Rappoport, Z., Ed.; Wiley: Chichester, 1990, p 95.

(2) Bertrand, W.; Bouchoux, G. *Rapid Commun. Mass Spectrom.* **1998**, *22*, 1697.

(3) Bouchoux, G.; Flament, J. P.; Hoppilliard, Y. *Int. J. Mass Spectrom. Ion Processes* **1984**, *57*, 179.

(4) Apeloig, Y.; Karni, M.; Ciommer, B.; Depke, G.; Frenking, G.; Meyn, S.; Schmidt, J.; Schwarz, H. *Int. J. Mass Spectrom. Ion Processes* **1984**, *59*, 21.

(5) Apeloig, Y. In *The Chemistry of Enols*; Rappoport, Z., Ed.; Wiley: Chichester, 1990, p 48.

(6) Petrie, S.; Freeman, C. G.; Mautner, M.; McEvans, M. J.; Ferguson, E. E. *J. Am. Chem. Soc.* **1990**, *112*, 7121.

(7) Freeman, C. G.; Knight, J. S.; Love, J. G.; McEvans, M. J. *Int. J. Mass Spectrom. Ion Processes* **1987**, *80*, 255.

(8) Gauld, J. W.; Audier, H.; Fossey, J.; Radom, L. *J. Am. Chem. Soc.* **1996**, *118*, 6299.

(9) Gauld, J. W.; Radom, L. *J. Am. Chem. Soc.* **1997**, *119*, 9831.

(10) Bohme, D. K. *Int. J. Mass Spectrom. Ions Processes* **1992**, *115*, 95 and references therein.

(11) Chalk, A. J.; Radom, L. *J. Am. Chem. Soc.* **1997**, *119*, 7573.

(12) Chalk, A. J.; Radom, L. *J. Am. Chem. Soc.* **1999**, *121*, 1574.

(13) Haranczyk, M.; Burgers, P. C.; Ruttink, P. J. A. *Int. J. Mass Spectrom.* **2002**, *220*, 53.

(14) van der Rest, G.; Nedev, H.; Chamot-Rooke, J.; Mourgues, P.; McMahon, T. B.; Audier, H. E. *Int. J. Mass Spectrom.* **2000**, *202*, 161.

(15) van der Rest, G.; Mourgues, P.; Nedev, H.; Audier, H. E. *J. Am. Soc. Mass Spectrom.* **2000**, *11*, 705.

(16) McLafferty, F. W. *Anal. Chem.* **1959**, *31*, 477.

(17) Tu, Y.-P.; Holmes, J. L. *J. Am. Chem. Soc.* **2000**, *122*, 5597.

(18) Tu, Y.-P.; Holmes, J. L. *J. Am. Chem. Soc.* **2000**, *122*, 3695.

(19) Holmes, J. L.; Mayer, P. M. *J. Phys. Chem.* **1995**, *99*, 1366.

(20) Rennie, E.; Mayer, P. M. *J. Chem. Phys.* **2004**, *120*, 10561.

(21) Scott, A. P.; Radom, L. *J. Phys. Chem.* **1996**, *100*, 16502.

(22) Lias, S. G.; Bartmess, J. E.; Liebman, J. G.; Holmes, J. L.; Levin, R. D.; Mallard, W. G. *J. Phys. Chem. Ref. Data* **1988**, *17, Suppl. 1.*, 1.

(23) Ochran, R. A.; Annamalai, A.; Mayer, P. M. *J. Phys. Chem. A* **2000**, *104*, 8505.

(24) Ochran, R. A.; Mayer, P. M. *Eur. Mass Spectrom.* **2001**, *7*, 267.

(25) Fridgen, T. D.; Keller, J. D.; McMahon, T. B. *J. Phys. Chem. A* **2001**, *105*, 3816.

(26) McCormack, J. A. D.; Mayer, P. M. *Int. J. Mass Spectrom.* **2001**, *207*, 183.

(27) Holmes, J. L.; Terlouw, J. K. *Org. Mass Spectrom.* **1980**, *15*, 383.

CHAPTER 5

A STUDY OF THE ISOMERIZATIONS AND DISSOCIATIONS OF FORMAL [ACETONE-METHANOL]$^{+\bullet}$ ION-MOLECULE COMPLEXES

5.1. Introduction

Acetone and its proton bound clusters have been detected in the upper troposphere and lower stratosphere.[1-4] The investigation of solvated ions, i.e. ion-molecule complexes, is of interest from the point of view of bridging the gap between the gas phase and solution phase chemistry. The structures and thermodynamics of IMCs have therefore applicative significance. Recent studies have discovered many novel structures and unusual rearrangements for aldehydes, ketones and enols, and illustrated the presently recognized important role of these IMCs during the unimolecular behaviour of numerous ionic systems.[5-10]

It has been well established that the enol form of the acetone ion is more stable than its keto form, i.e. ionized acetone. A great number of studies have discovered the relative stabilities of ionized and neutral enol and ketone species.[5,6] Keto-enol isomerization is a well-known process in solution, in which the keto species is readily isomerized by acid or base catalysis into the corresponding enol.[8] In the gas phase, isolated ketone or aldehyde radical cations do not enolize spontaneously. High-energy barriers that exceed the ions' first dissociation threshold effectively prevent this reaction.[7]

For example, experiments and theoretical calculations show that the acetone radical cation in the gas-phase is 58 kJ/mol[11,12] less stable than its enol isomer, and the energy barrier for the required intra-ionic 1,3-H shift lies 74 kJ/mol higher than the dissociation threshold of the lowest energy reaction (it is ca 81 kJ/mol higher than the energy of acetone ion.)[13,14]:

$$(CH_3)_2C{=}O^{+\bullet} \rightarrow CH_3CO^{+} + CH_3^{\bullet} \qquad 5.1$$

Therefore, acetone cations undergo dissociation rather than enolization.

Recent studies have been focused on the catalyzed isomerizations of a cation in the gas-phase, i.e. the isomerization barrier of the ion may be greatly reduced when an ion is electrostatically bound to a neutral molecule.[15] The keto-enol isomerization of the acetone cation is a good subject for such catalyzed isomerizations and has been investigated by many groups. Trikoupis et al.[16-18] have reported that benzonitrile and acetone itself convert ionized acetone into its enol isomer in a chemical ionization (CI) source of a sector mass spectrometer. Mourgues et. al.[19] have studied the isomerization using a variety of substrates having a wide range of PA values, using FT-ICR experimental conditions in which only bimolecular reactions are observed. A disadvantage of this latter method is that the initially formed ion/substrate complex has a high internal energy, equal to or greater than its dissociation energy. It therefore investigates only those processes (e.g. H^+-transport) that can take place at such an

elevated energy. The method cannot therefore study the many stable equilibrium structures that lie in potential wells far below the energy of the bimolecular adduct.

We have employed an alternative strategy, in which we explicitly make ions of structure(s) corresponding to adduct isomers that occupy deep potential wells. In such an experiment, a variety of stable or metastable isomeric species are made in which a formal H^+ or $H^\bullet$ transfer may already be in place. Detailed studies of the complete potential energy surface (PES) for acetaldehyde and methanol ion-molecule pairs have been described.[20,21] On the PES of the $[CH_3CHO/^\bullet CH_2OH_2^+]$ system (Chapter 4), the adduct ion structure, $[CH_3CHO\cdots H^+\cdots O(H)CH_2^\bullet]$ corresponds to the ground state of the ion-molecule complex made by a unimolecular reaction process. Calculations show that in this proton-bridged stable structure, the proton is attached to the acetaldehyde, rather than to $^\bullet CH_2OH$, in keeping with the PA of CH_3CHO (at O) being greater than that for the $^\bullet CH_2OH$ radical at oxygen. This complex ion, $CH_3CHO\cdots H^+\cdots O(H)CH_2^\bullet$ lies in a well on the PES and its metastable dissociation produces an unexpected product, the vinyl alcohol ion $CH_2CHOH^{+\bullet}$. This shows that there is a rearrangement, prior to the loss of CH_3OH. Because it is a metastable ion (MI) process, the isomerization must involve a low internal energy. Isotopic labelling experiments and *ab initio* calculations were then employed for mechanistic studies and ion structure assignments. In Chapter 4, the chemistry of$[CH_3CHO/^\bullet CH_2OH_2^+]$ proceeded via protonated acetaldehyde attached to a $^\bullet CH_2OH$ radical, and yielded ionized vinyl alcohol and a methanol molecule, $[CH_2CHOH^{+\bullet}\cdots OHCH_3]$, via a $H^+/H^\bullet$ transfer mechanism.[20] In contrast, if the protonated acetaldehyde is instead attached to a methoxyl radical, $[CH_3CHOH^+\cdots{}^\bullet OCH_3]$, the enol

ion is not produced and the precursor ion directly dissociates to the keto ion and methanol. The stable ion-molecule complexes of desired structure were generated in the mass spectrometer by selecting the appropriate fragment ions in the CID mass spectra of proton-bound molecular pairs.[22]

As described in Chapter 4, the unimolecular chemistry for a methanol ion associated with the simpler keto-molecule, acetaldehyde was established. The work presented in this chapter was to investigate whether the above mechanism was a general one that could apply to larger polyatomic keto species and so we here describe the behaviour of [acetone/methanol]$^{+\bullet}$ ion-molecule complexes, having structures $[(CH_3)_2C{=}O\cdots H^+\cdots O(H)CH_2^{\bullet}]$, ion **1** and $[(CH_3)_2C{=}O\cdots H^+\cdots {}^{\bullet}OCH_3]$, ion **2.** The mechanisms of rearrangements and dissociations of ions **1** and **2** have been explored by experiment and by computation and the PESs for these two systems will be discussed in Section 5.3.

5.2 Experimental and Theoretical Procedures

All experiments were performed on a modified ZAB-3F tandem mass spectrometer[23] with BEE geometry (VG Analytical, Manchester, U.K.). MI and CID mass spectra of selected proton-bound pairs were acquired and the desired ion-molecule complex was produced by CID of the proton-bound ion in the second field-free region (2FFR) of the mass spectrometer. MI and CID dissociations of the ion-molecule complex were observed in the third field-free region (3FFR). The ion accelerating voltage on the

proton-bound pairs was 8 kV. In the 2FFR and 3FFR helium was used as the collision gas for the CID experiments. All spectra were recorded with the ZABCAT program developed by Mommers Technologies (Ottawa, Ontario,Canada)[23].

The proton-bound dimer of acetone and propanol was generated by admitting the mixed reagents $CH_3CH_2CH_2OH$ and $(CH_3)_2C{=}O$ into a high pressure ion source at a total observed pressure of ca. 8 x 10^{-5} mbar (1 bar = 100 kPa), indicating an ion pressure of 0.28 mbar[24]. The proton-bound dimer $(CH_3)_2C{=}O\cdots H^+\cdots O(H)CH_2CH_2CH_3$ (m/z = 119) was mass-selected by the magnet and dissociated by collision in the second field-free region. The fragment ion $[(CH_3)_2C{=}OH^+\cdots O(H)CH_2^{\bullet}]$ (m/z 90) resulted from the loss of $CH_3CH_2^{\bullet}$ from the precursor ion (m/z 119) and it was transmitted into the third field-free region in order to observe its MI and CID characteristics.

A similar experiment was used for the acetone/dimethyl ether proton-bound dimer, $(CH_3)_2C{=}O\cdots H^+\cdots O(CH_3)_2$ (m/z 105), in order to collisionally generate the ion $[(CH_3)_2C{=}OH^+\cdots{}^{\bullet}OCH_3]$ (m/z 90) by the specific loss of $CH_3^{\bullet}$ from the ether moiety. An experiment with $(CD_3)_2C{=}O\cdots H^+\cdots O(CH_3)_2$ (m/z 111) showed that it was an ether methyl-group that was specifically lost following collisional activation. Dimethyl ether was introduced through the gas inlet at an observed pressure of 5 x 10^{-5} mbar producing ca. 0.18 mbar in the high pressure ion source.

The molecules $(CH_3)_2C{=}O$, $CH_3CH_2CH_2OH$, $(CH_3)_2O$, and the isotopically labelled compounds, $(CD_3)_2C{=}O$, $CH_3CH_2CD_2OH$, $CH_3CH_2{}^{13}CH_2OH$ were used to

generate various isotopomeric ion-molecule pairs. The unlabelled chemicals were purchased from Aldrich and all the labelled samples, of 99.5%-99.9% isotopic purity, were obtained from CDN Isotopes (Montreal, QC) and were used without further purification.

The GAUSSIAN 98 programs were used to perform standard *ab initio* molecular orbital calculations to investigate the potential energy surface. Optimized geometries and the energies of all minima and transition states were calculated at the MP2/6-31+G(d) level of theory. Zero-point energies obtained from calculations of vibrational frequencies at the same level of theory were scaled by a factor of 0.9434.[25]

5.3 Results and Discussion

5.3.1 Experimental observations

5.3.1.1 $[(CH_3)_2C{=}O\cdots H^+\cdots O(H)CH_2^{\bullet}]$ (Ion **1**)

An ion of structure **1**, was obtained by the collision-induced loss of a $CH_3CH_2^{\bullet}$ radical from the proton-bound dimer $(CH_3)_2C{=}O\cdots H^+\cdots O(H)CH_2CH_2CH_3$ (m/z 119), ion **P1**. The PA of acetone, 812.0 kJ/mol,[26] is greater than that of propanol, 786.5 kJ/mol,[26] and so the proton is preferentially attached to the ketone thus resembling protonated acetone electrostatically bound to a propanol molecule, i.e. $(CH_3)_2C{=}OH^+\cdots O(H)CH_2CH_2CH_3$. Its MI mass spectrum has m/z 59 (100%),

$(CH_3)_2C{=}OH^+$, as the most intense peak and a small signal for protonated propanol (m/z 61, 5%) as shown in Figure 5.1.

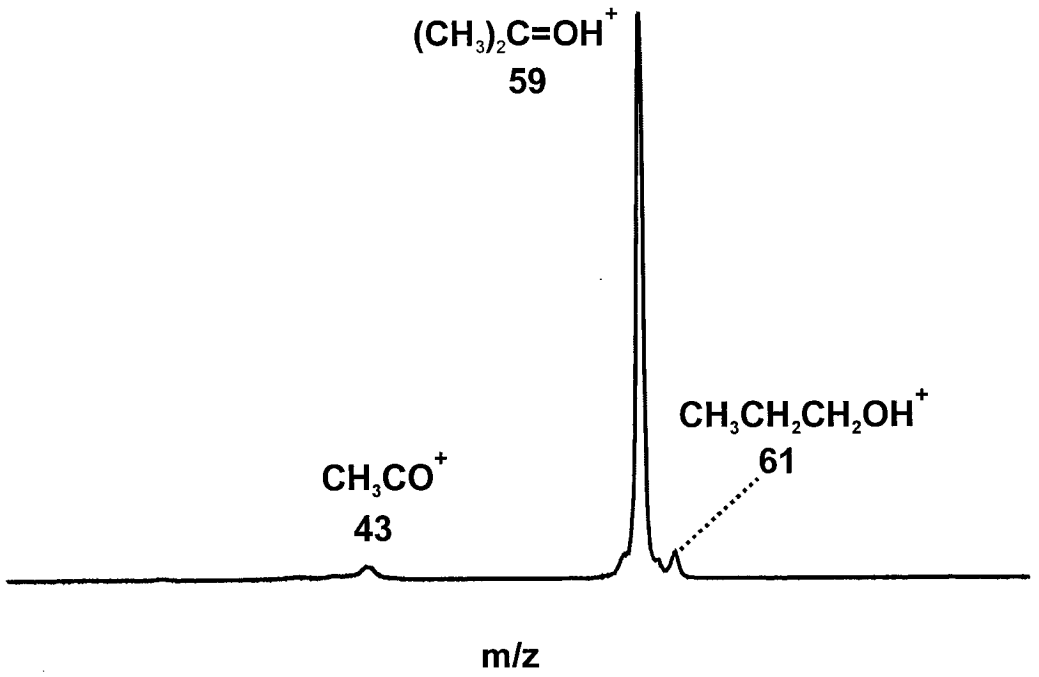

Figure 5.1. MI mass spectrum of the proton-bound pair $(CH_3)_2C{=}O\cdots H^+\cdots O(H)CH_2CH_2CH_3$ (m/z = 119).

These are the only MI processes, showing that no rearrangement of the proton bound dimer can likely take place at internal energies up to those for MI dissociations. In its CID mass spectrum, in addition to the above major peaks there is now a small signal for $CH_3CH_2^{\bullet}$ loss (m/z 90, <1%).

$$(CH_3)_2C{=}OH^+\cdots O(H)CH_2CH_2CH_3 \rightarrow [(CH_3)_2C{=}OH^+\cdots O(H)CH_2^{\bullet}] + CH_3CH_2^{\bullet} \quad \text{(CID)} \quad 5.2$$

m/z 119 m/z 90, (Ion **1**)

The MI spectrum of ion **1,** Figure 5.2-a, contains two peaks: protonated acetone $(CH_3)_2C{=}OH^+$ (m/z 59, 53%) and as base peak, m/z 58, which was shown to be the distonic acetone ion $^{\bullet}CH_2C(CH_3){=}OH^+$ (see the following discussion).

In the CID mass spectrum of ion **1,** Figure 5.2-b, the intensity of the peak at m/z 59, $(CH_3)_2C{=}OH^+$, is increased, and is now the base peak. The formation of $(CH_3)_2C{=}OH^+$ is thus collision sensitive, being a simple bond cleavage in ion **1**. The observation that a metastable ion peak is insensitive to collision gas signifies that the mass selected ion has undergone a rearrangement to an isomeric species over an energy barrier close to the lowest energy fragmentation for that ion. In cases where this energy barrier is lower or non-existent, the collision sensitivity of the peak is correspondingly greater. If the MI peak is for a simple bond cleavage in the mass selected ion, the collision sensitivity is greatest and often produces the base peak in a CID mass spectrum.[27] Ion **1** keeps the proton bridged form of the precursor proton-bound pair, m/z 119, and so it is represented as $[(CH_3)_2C{=}OH^+\cdots O(H)CH_2^{\bullet}]$. This is also in keeping with the PA of $(CH_3)_2C{=}O$ at O, 812.0 kJ/mol, being higher than the PA of $^{\bullet}CH_2OH$, 695.0 kJ/mol. However, note that the peak at m/z 58 ion is *not* collision sensitive, indicating that ion **1** rearranges before it fragments by this route.

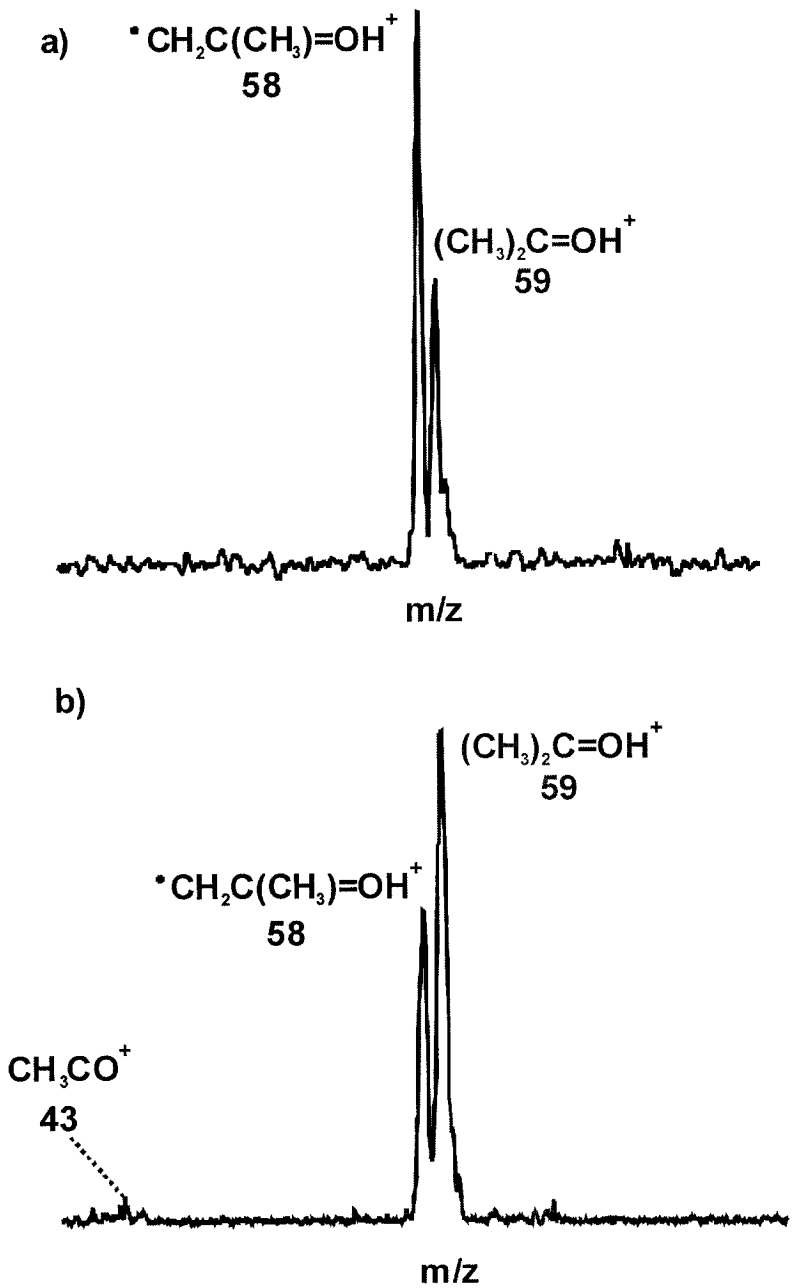

Figure 5.2 a) MI mass spectrum of $[(CH_3)_2C{=}OH^+\cdots O(H)CH_2^\bullet]$ (m/z = 90). b) CID mass spectrum of $[(CH_3)_2C{=}OH^+\cdots O(H)CH_2^\bullet]$ (m/z = 90).

The dissociation channel that leads to the enol form of ionized acetone is energetically the most favourable process. If the ion m/z = 58 has the enol structure, the

dissociation threshold energy is at 459 kJ/mol (from $\Delta_fH[^{\bullet}CH_2C(CH_3)=OH^+]$ = 661kJ/mol, $\Delta_fH[CH_3OH]$ = -202 kJ/mol)[28]. This is lower than the dissociation limit, 470 kJ/mol, for the formation of protonated acetone m/z 59, (from $\Delta_fH[(CH_3)_2C=OH^+]$ = 489 kJ/mol, $\Delta_fH[^{\bullet}CH_2OH]$ = -19 kJ/mol)[28]. If the m/z 58 ion had the keto structure, the threshold energy for this dissociation would be much higher, at 517 kJ/mol (from $\Delta_fH[(CH_3)_2C=O^{+\bullet}]$ = 719 kJ/mol, $\Delta_fH[CH_3OH]$ = -202 kJ/mol)[28], and would be unable kinetically to compete with the simple bond cleavage to m/z 59. That the enol ion is produced is fully supported by the results of isotopic labelling.

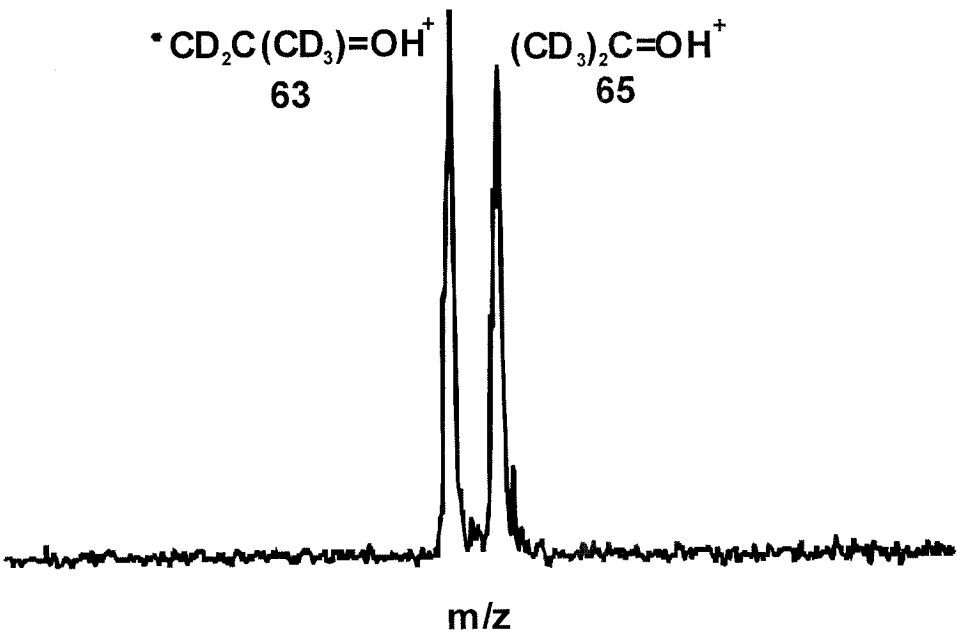

Figure 5.3. MI mass spectrum of $[(CD_3)_2C=OH^+\cdots O(H)CD_2^{\bullet}]$, **1**-$d_8$ (m/z 98).

The deuterium labelled ion-molecule pairs, $[(CH_3)_2C=OH^+\cdots O(H)CD_2^{\bullet}]$, **1**-$d_2$ (m/z 92), $[(CD_3)_2C=OH^+\cdots O(H)CD_2^{\bullet}]$, **1**-$d_8$ (m/z 98) and $[(CD_3)_2C=OD^+\cdots O(H)CD_2^{\bullet}]$, **1**-$d_9$ (m/z 99), were examined to help assign the structure of the m/z 58 ion to that of the enol

of acetone. The MI mass spectrum of **1**-d_8 (m/z 98) (Figure 5.3), shows intense peaks at m/z 63 and m/z 65, corresponding to the ions $^{\bullet}CD_2C(CD_3)=OH^+$ and $(CD_3)_2C=OH^+$, respectively. No peak at m/z 64 was observed; had the keto ion been the product, it would have resulted in m/z 64, $(CD_3)_2C=O^{+\bullet}$, being observed instead. The relative abundance of the two product ions for the labelled complexes differs from that for the unlabelled ion **1**, due to an isotope effect in the H transport in the isomerization process. In general the rate constant for k_{isom} (H) has been found to be greater than k_{isom} (D), resulting in smaller distonic acetone peaks in the mass spectra of labelled ions. The MI mass spectra of **1**-d_2 (m/z 92), and **1**-d_9 (m/z 99), showed only two dissociation reactions, again resulting from the explicit formation of distonic acetone and protonated acetone. These two ions carry different labels for the hydroxyl or methyl H atoms of the radical site, indicating that the H atoms from $^{\bullet}CH_2OH$ were not found in the product ions. Thus there was no H, D mixing involved in the ion dissociations. The rearrangement process is described as follows. Before the ion-molecule complex **1**, $[(CH_3)_2C=OH^+\cdots O(H)CH_2^{\bullet}]$ dissociates to the distonic acetone ion and methanol, a $H^{\bullet}$ atom from $C\underline{H}_3C(CH_3)=OH^+$ is transferred to the $^{\bullet}\underline{C}H_2OH$ radical via a 1,6-H shift. This process involves a low energy barrier, shown as TS1 on the PES of ion **1** (see Figure 5.5. and the discussion of the computations).

5.3.1.2 $[(CH_3)_2C=O\cdots H^+\cdots{}^{\bullet}OCH_3]$ (Ion **2**)

The MI mass spectrum of the proton-bound acetone-dimethyl ether ion pair $(CH_3)_2C=O\cdots H^+\cdots O(CH_3)_2$ (m/z 105), **P2**, showed two major peaks, namely protonated

acetone (m/z 59) and protonated dimethyl ether (m/z 47), indicating that the ion keeps its original structure prior to dissociations. A minor $CH_3^{\bullet}$ loss peak (m/z 90) is produced by collision induced dissociation; this reaction is shown in Equation 5.3.

$$(CH_3)_2C{=}O\cdots H^+\cdots O(CH_3)_2 \rightarrow [(CH_3)_2C{=}OH^+\cdots {}^{\bullet}OCH_3] + CH_3^{\bullet} \quad \text{(CID)} \qquad 5.3$$

m/z 105 m/z 90 (Ion **2**)

The lost methyl radical could come from either molecule and so deuterium labelling was used to identify the methyl groups, e.g. $(CD_3)_2C{=}O\cdots H^+\cdots O(CH_3)_2$, **P2-d$_6$** and $(CD_3)_2C{=}O\cdots D^+\cdots O(CH_3)_2$, **P2-d$_7$**, which lost only $^{\bullet}CH_3$ in their CID mass spectra, showing that only an ether methyl group is involved.

Compared with its isomer **1** where the radical is located on the carbon atom, ion **2** carries the radical on methoxyl group, due to a removal of a radical from the oxygen atom. Their MI dissociation profiles are different. For example, the MI mass spectrum of $[(CD_3)_2C{=}OH^+\cdots OCH_3]$, **2-d$_6$** (m/z 96), showed that there are three competing dissociation channels, giving protonated acetone (m/z 65), the acetone ion (m/z 64), and $CD_3^{\bullet}$ loss (m/z 78), see Figure 5.4.

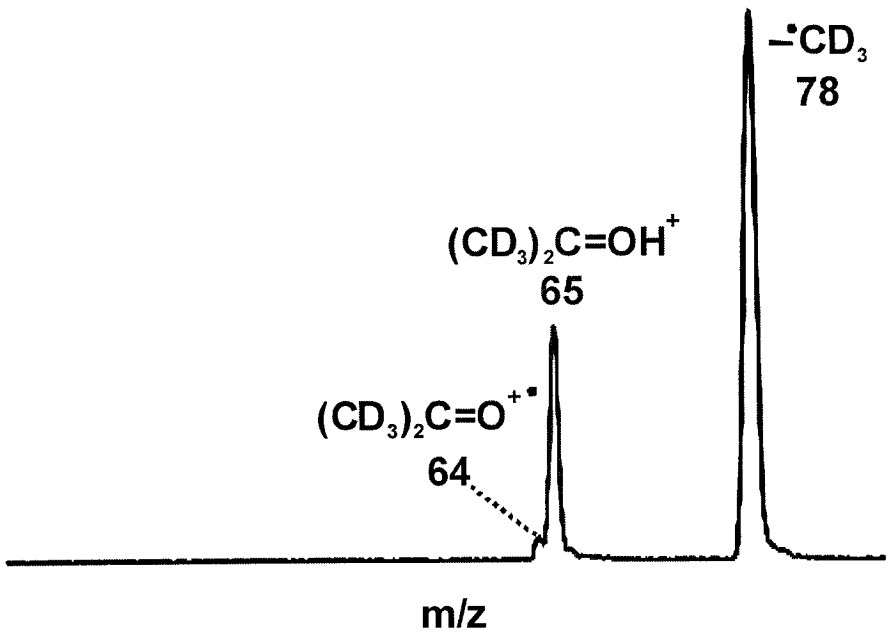

Figure 5.4. MI mass spectrum of $[(CD_3)_2C{=}OH^+\cdots OCH_3]$, **2-d$_6$** (m/z 96).

The smaller peak m/z 58 in the MI mass spectrum of unlabelled ion **2** must be the acetone cation, not the enol ion, even though the latter is more energetically favoured than protonated acetone (see the Discussion for ion **1**), showing no rearrangement of ion **2** to its enol form. The deuterium labelling results indicate that the lost methyl group comes exclusively from the acetone moiety, and that H and D atoms in ion **2** have retained their original positions before it fragments, i.e. no H/D mixing between the two moieties in the complex. Surprisingly, the methyl loss peak is collision insensitive, indicating that it does not arise from a simple C-C bond cleavage. It was concluded from the computations that the product ion from the methyl lost from ion **2** is an ion-molecule complex of the acetyl ion and methanol, $[CH_3C^+(O)\cdots O(H)CH_3]$, an ion that comprises a new member of the $[C_3H_7O_2]^+$ isomers. The detailed path for the generation of the ion $[CH_3C^+(O)\cdots O(H)CH_3]$ is discussed in Section 5.3.2.2. To date, the other three identified

ion $[C_3H_7O_2]^+$ structures that have been characterized are $[CH_3OCH{=}OCH_3]^+$ and the proton-bound complex of acetaldehyde and formaldehyde, $CH_3CHO\cdots H^+\cdots OCH_2$, by McLafferty and Proctor[29], and protonated ethyl formate, $CH_3CH_2OC^+(H)OH$, by Larson and McMahon[30].

5.3.2 Theoretical Calculations

The two ion-molecule complexes, $[(CH_3)_2C{=}OH^+\cdots O(H)CH_2^{\bullet}]$ and $[(CH_3)_2C{=}OH^+\cdots {}^{\bullet}OCH_3]$ display different chemistries in their mass spectra. Thus these two systems do not communicate with each other, presumably because a high energy barrier prevents them from freely interconverting in the metastable ion dissociation time-frame. Calculations were performed to produce a PES for each ion and to investigate the mechanisms of the isomerizations and fragmentations. The energies (in kJ/mol) shown on the PES are relative to the calculated energy of the stable complex IV of distonic acetone and methanol, $[{}^{\bullet}CH_2C(CH_3){=}OH^+\cdots O(H)CH_3]$, obtained at the MP2/6-31+G(d) level of theory, and are given in Table 5.1. Intrinsic Reaction Coordinate (IRC) calculations have been used to follow the reaction paths from all transition states in order to identify intermediates. IRCs were also used to test whether a transition state is the correct structure that connects two minimum wells.

5.3.2.1 The $[(CH_3)_2C{=}O\cdots H^+\cdots O(H)CH_2^{\bullet}]$ System

The 0 K potential energy profile is shown in Figure 5.5. The optimized structure of ion **1** is indeed $[(CH_3)_2C{=}O\cdots H^+\cdots O(H)CH_2^{\bullet}]$. In the stable species III, the proton is closer to the keto oxygen than to the hydroxyl oxygen of the radical, the two bond lengths being 1.031 Å for $(CH_3)_2C{=}O$-H and 1.565 Å for $^{\bullet}CH_2O(H)$-H, (see Figure 5.6-a). This is in keeping with the PA of $(CH_3)_2C{=}O$ being greater than that for $^{\bullet}CH_2OH$ at oxygen. Ion III rearranges to the stable complex IV, distonic acetone ion and methanol, $[^{\bullet}CH_2C(CH_3){=}OH^+\cdots O(H)CH_3]$, via a cyclic transition state, TS 1. This rearrangement requires only ca 113 kJ/mol and the TS 1 lies below the dissociation threshold of III to protonated acetone and the hydroxymethyl radical, 120 kJ/mol. The energy for the isolated ionized acetone ion to isomerize to its enol form is at 213 kJ/mol[14,31], above the heat of formation of the latter and lies well above the dissociation limit for the keto ion's loss of $CH_3^{\bullet}$ (139 kJ/mol)[31]. Note that TS1, the seven-membered ring intermediate structure, would be favoured by entropy considerations. Complex IV then dissociates to produce the enol ion and a methanol molecule, the dissociation limit for which is 117 kJ/mol. This process involves the low energy-barrier TS1 and is the competing dissociation channel with an energy lower than that for the production of protonated acetone (m/z 59), and thus distonic acetone (m/z 58) gives rise to the most intense peak in the MI mass spectrum of ion **1**. Thus the initial acetone molecule has been ionized and isomerized to its enol ion-form by the transferring of H^+ and $H^{\bullet}$ from the substrate, in which the free-radical site functions as a good $H^{\bullet}$ or H^+ acceptor, facilitating the enolization of acetone.

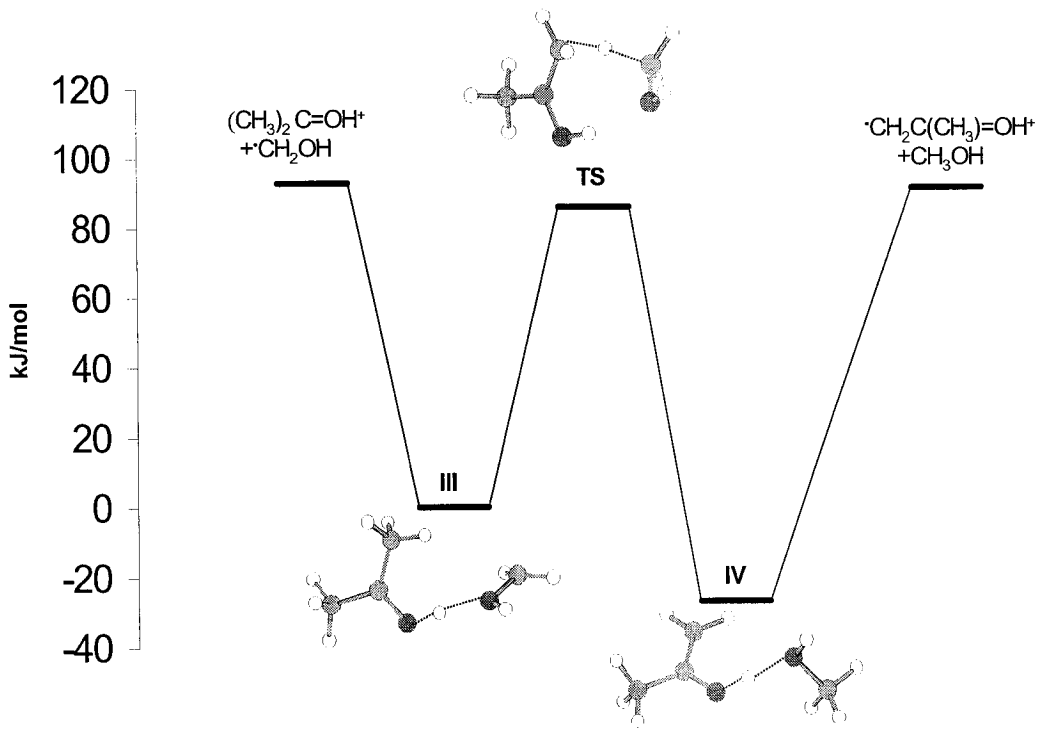

Figure 5.5. The 0 K potential energy surface of $[(CH_3)_2C{=}OH^+\cdots O(H)CH_2^{\bullet}]$ system at the MP2/6-31+G(d) level of theory.

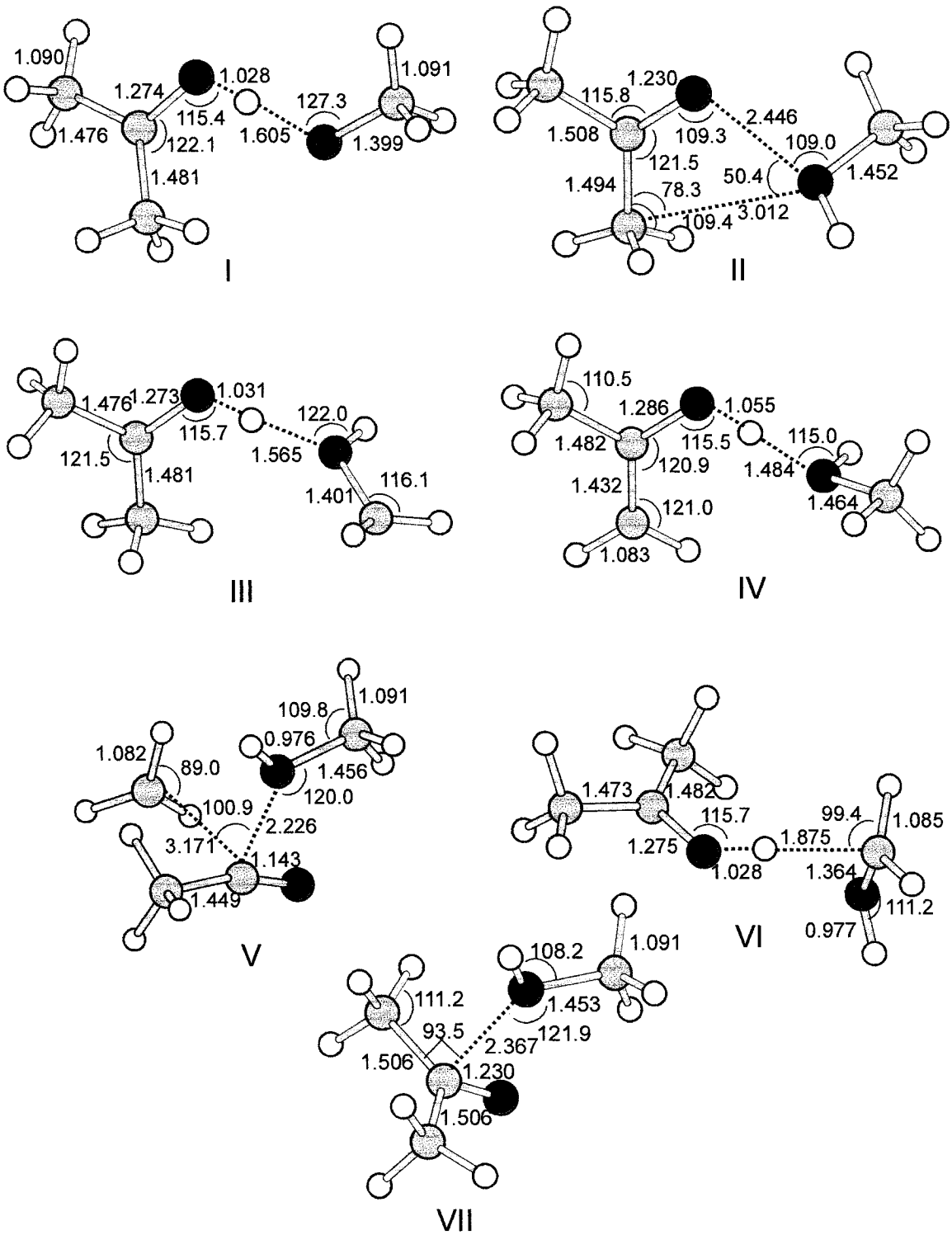

Figure 5.6. a) Optimized geometries of the stable complexes at the MP2/6-31+G(d) level of theory.

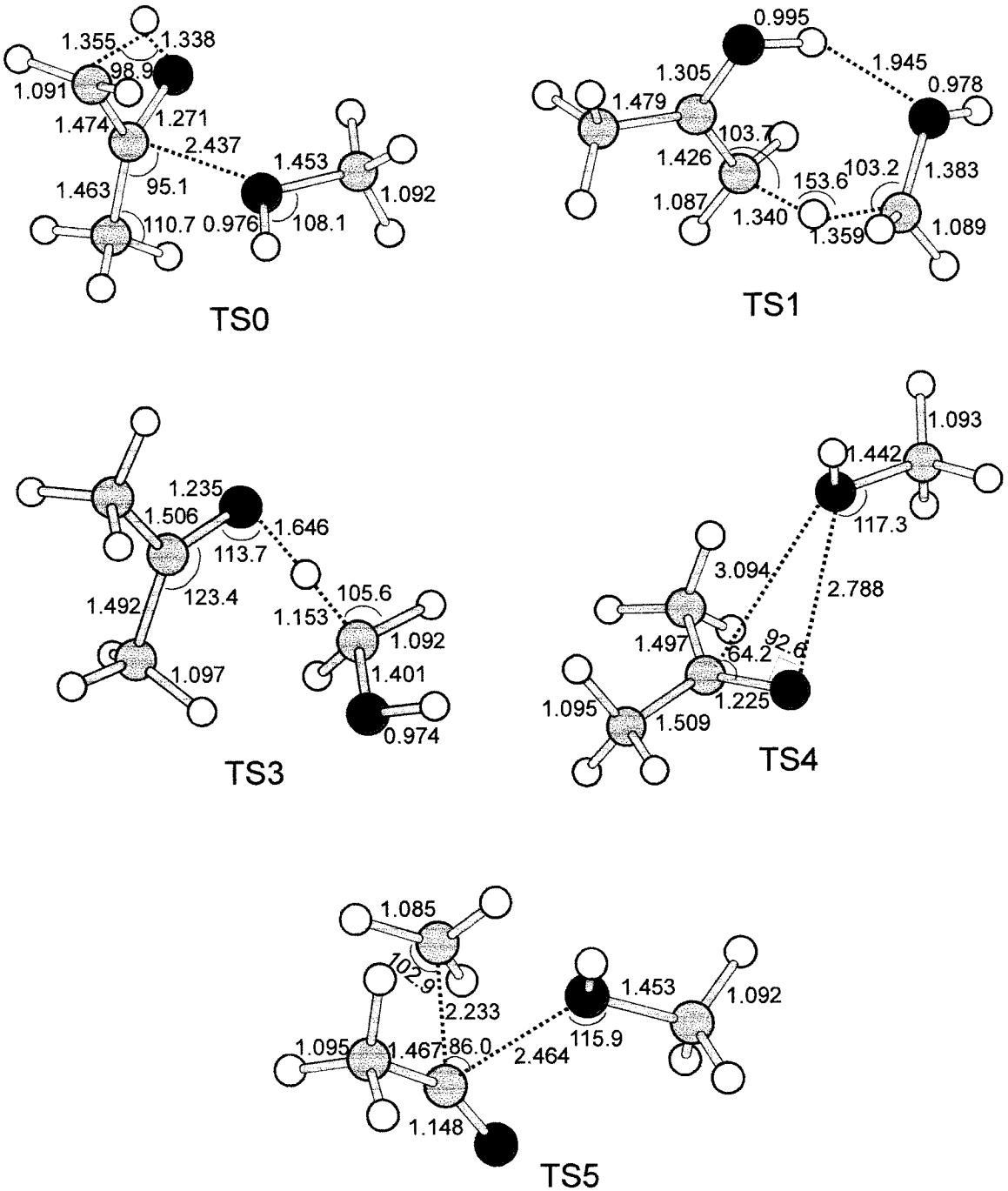

Figure 5.6. b) Optimized geometries of the transition states at the MP2/6-31+G(d) level of theory.

5.3.2.2 The $[(CH_3)_2C{=}O\cdots H^+\cdots {}^{\bullet}OCH_3]$ System

Ion **2** is shown as the stable complex I on the 0 K PES (Figure 5.7). In this proton-bound complex, acetone is more strongly associated with the proton because the PA of acetone, 812 kJ/mol, is significantly higher than that of $CH_3O^{\bullet}$, 658 kJ/mol. A simple bond cleavage produces $(CH_3)_2C{=}OH^+$ (m/z 59) and $CH_3O^{\bullet}$ at a dissociation threshold of 155 kJ/mol. The ion I, $[(CH_3)_2C{=}OH^+\cdots {}^{\bullet}OCH_3]$, is able to rearrange to a complex of the acetone ion and methanol, stable complex II $[(CH_3)_2C{=}O^{+\bullet}\cdots HOCH_3]$. However no transition state structure has been found to connect these two minima. The same problem has been encountered when calculating the transition state between the stable $[CH_3CHOH^+\cdots {}^{\bullet}OCH_3]$ complex and of CH_3CHOH^+ with CH_3OH on the PES for the acetaldehyde/methanol ion complex.[20,21,32] Similarly, here, with the complex II, $[(CH_3)_2C{=}O^{+\bullet}\cdots HOCH_3]$, the O atom of CH_3OH is associated with the carbonyl O and methyl C of $(CH_3)_2C{=}O^{+\bullet}$ in the form of a four-membered ring structure. The computational difficulty arises when I converts to II, the charge centre migrates from the proton to the acetone C atom and a $H^{\bullet}$ atom moves to $CH_3O^{\bullet}$. A minimum energy crossing point (MECP) has been suggested by Ruttink[16] and by Haranczyk[21], which is defined as the geometry corresponding to minimum energy complex for the intersection of the two discontinuous PES. Because the acetone ion (m/z 58) is observed in the MI mass spectrum of ion **2**, this transition state, TS2, should be below the dissociation limits of the precursor ion-molecule complex I, at 155 kJ/mol. Complex II can also fragment to the acetone ion (m/z 58) and methanol.

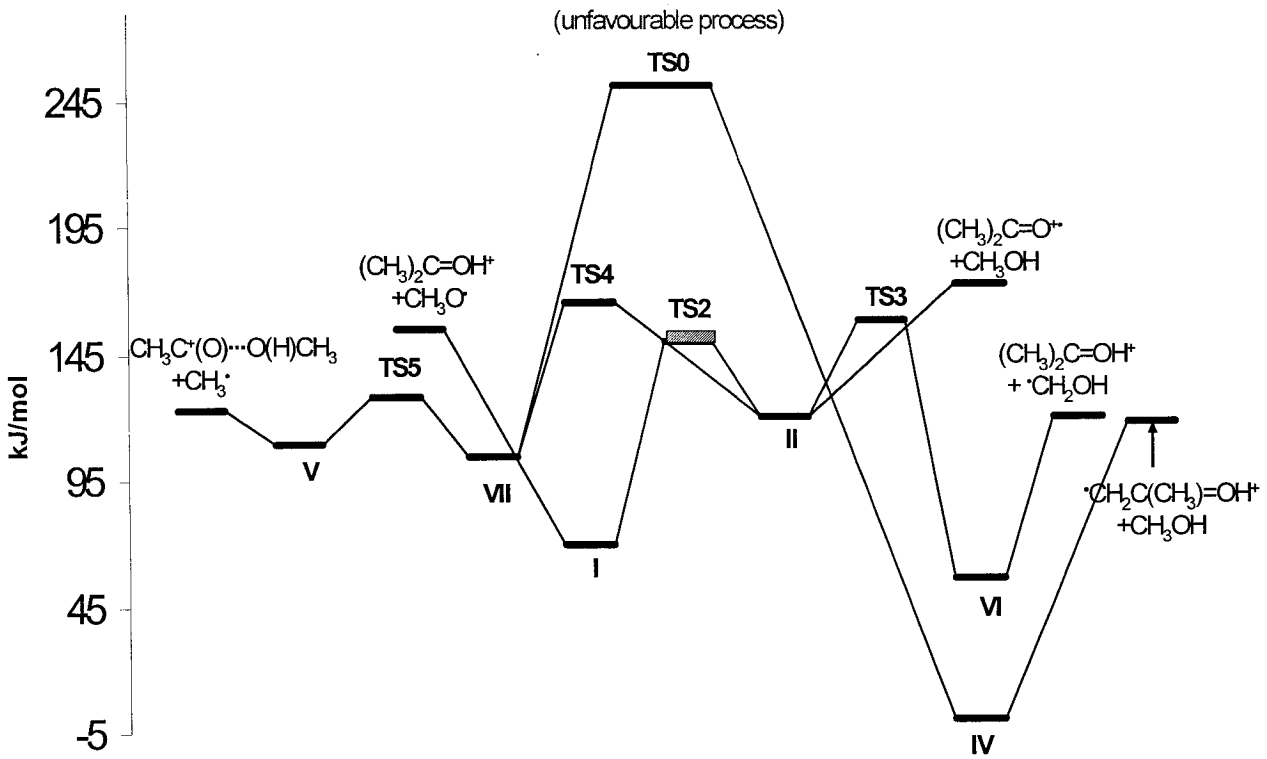

Figure 5.7. The 0 K potential energy surface of $[(CH_3)_2C{=}OH^+\cdots{}^\bullet OCH_3]$ system at MP2/6-31+G(d).

Another competing dissociation channel of ion **2** is the generation of $(CH_3)_2C{=}OH^+$ (m/z 59) and a $^\bullet CH_2OH$ radical, a reaction that is energetically more favourable than the simple bond dissociation to $(CH_3)_2C{=}OH^+$ and $CH_3O^\bullet$, because the heat of formation of $^\bullet CH_2OH$, -19 kJ/mol[28], is lower than that of $CH_3O^\bullet$, 16 kJ/mol.[28] This reaction involves an ion rearrangement from complex II to ion VI, $[(CH_3)_2C^+(=OH)\cdots O(H)CH_2{}^\bullet]$. The latter is an isomer of complex III, $[(CH_3)_2C{=}OH^+\cdots O(H)CH_2{}^\bullet]$. In structure VI, $CH_2OH^\bullet$ is bound to $(CH_3)_2C{=}OH^+$ through a C(of $^\bullet CH_2OH$)···H···O(of acetone) bridge, different from the O···H···O proton bridge in complex III. In TS3, the H

atom moves from the methyl group of methanol to carbonyl O. TS3 between complex II and VI lies at 158 kJ/mol, close to the dissociation threshold of complex I, 155 kJ/mol. Thus, the two reactions can compete in terms of their energy requirements.

The MI mass spectrum of ion **2** shows a base peak the loss of methyl from the acetone moiety and the mechanism explored by the calculations is as follows. Interconversion between complex II and its isomer, i.e. complex VII, takes place via transition state TS4 (165 kJ/mol). In complex VII, the methanol is perpendicular to the acetone plane and separated by an elongated C···O bond of 2.367Å between the two species. Note that in ion VII the rearrangement of the methanol molecule leads to stabilization of the charge on the carbonyl C-atom, facilitating the ensuing methyl loss. In TS5, the extension of the C-C bond in acetone leads to the elimination of a methyl radical, leaving a new complex of an acetyl ion and methanol, $[CH_3C^+(O)\cdots(H)OCH_3]$. The geometry of this ion is shown in Figure 5.8.

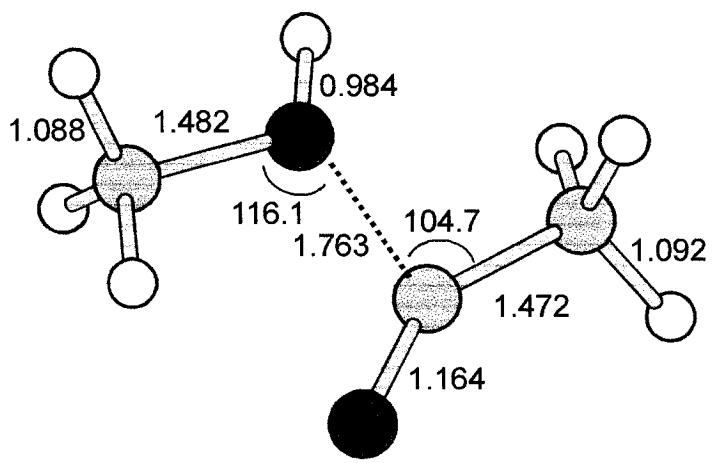

Figure 5.8. Geometry of $[CH_3C^+(O)\cdots O(H)CH_3]$, the methyl radical loss product from $[(CH_3)_2C{=}OH^+\cdots{}^{\bullet}OCH_3]$.

The dissociation limit for **2** to produce $[CH_3C^+(O)\cdots(H)OCH_3]$ and $CH_3^\bullet$ is 128 kJ/mol at 298 K (Table 1). Heats of formation of new products can be calculated by normalizing the computed relative energies (at 298 K) using the well established experimental energies of a selected product pair, e.g. $\Delta_fH[^\bullet CH_2C(CH_3)=OH^+]$ + $\Delta_fH[CH_3OH]$ = 459kJ/mol[28]; adding 341 kJ/mol to all relative energies achieves this (see Table 1). The heat of formation of the product ion $[CH_3C^+(O)\cdots(H)OCH_3]$, 322 kJ/mol, is obtained by subtracting $\Delta_fH[^\bullet CH_3]$=147 kJ/mol from the dissociation limit for the ion, 469 kJ/mol (=128 kJ/mol + 341 kJ/mol). Thus the binding energy in this ion to the products CH_3CO^+ + CH_3OH is 129 kJ/mol, using $\Delta_fH[CH_3C^+O]$ = 653 kJ/mol[26], $\Delta_fH[CH_3OH]$ = -202 kJ/mol[26]. The relatively high energy of the electrostatic bond in this ion is similar to that of $-O\cdots H^+\cdots O-$ (~130 kJ/mol) in proton-bound pairs[33] although this ion does not contain a proton bridge. It follows therefore that the attachment of methanol to ionized acetone (shown as complex VII) results in a remarkable weakening of the H_3C-C bond from 81 kJ/mol in the isolated ion ($\Delta_fH[(CH_3)_2CO^{+\bullet}]$ = 719 kJ/mol)[28], to only 26 kJ/mol (the 298 K energy difference between TS5 and ion VII) in the complex, and this results from the high stability of the $[CH_3C^+(O)\cdots(H)OCH_3]$ product ion.

The flat transition state of this reaction, TS5, lies at 128 kJ/mol in Figure 5.7, but the overall energy-determining barrier for this process is TS4 at 165 kJ/mol. As previously mentioned, these three reactions for the production of protonated acetone (m/z 59), the acetone ion (m/z 58) and the methyl loss product at m/z 75, are all MI processes and so they have closely similar energy requirements. The PES of ion **2** shows that the major energy barriers for these three reactions lie within a small energy range of 18 kJ,

(the highest energy limit 173 kJ/mol – the lowest energy limit 155 kJ/mol) which ensures the observation of all three products in the MI time frame.

Another transition state energy has been calculated, that for TS0, by which complex VII, the acetone ion and methanol, converts to ion IV, the distonic acetone ion and methanol. TS0 lies at a rather high energy, 251 kJ/mol. In the metastable time frame of the mass spectrometer, a reaction requiring such a high relative internal energy is usually not competitive and therefore is not observed. This is confirmed by the experimental observation that ion **2** does not isomerize to an enol form.

Table 5.1. Calculated electronic energies (in Hartrees), incorporating a scaled zero-point energies, and relative energies, E_{rel} (in kJ mol^{-1}) at 0 K and at 298 K for the different structures.

Structures	MP2/6-31+G(d) 0 K	E_{rel}	MP2/6-31+G(d) 298K	E_{rel}[a]
I	-307.442602	69	-307.432051	69
II	-307.423063	120	-307.411855	122
III	-307.458494	27	-307.447603	29
IV	-307.468849	0	-307.458509	0
V	-307.427055	110	-307.413557	118
VI	-307.447685	56	-307.437100	56
VII	-307.429401	104	-307.418488	105
TS0	-307.373164	251	-307.363053	251
TS1	-307.425812	113	-307.416873	109
TS3	-307.408672	158	-307.398900	157
TS4	-307.406161	165	-307.395807	165
TS5	-307.419918	128	-307.408595	131
$(CH_3)_2C{=}OH^+ + {}^{\bullet}CH_2OH$	-307.423212	120	-307.412746	120
${}^{\bullet}CH_2C(CH_3){=}OH^+ + CH_3OH$	-307.423780	118	-307.413405	118
$(CH_3)_2C{=}OH^+ + CH_3O^{\bullet}$	-307.409759	155	-307.399554	155
$(CH_3)_2C{=}O^{+\bullet} + CH_3OH$	-307.402802	173	-307.392064	174
$[CH_3C^+(O)\cdots O(H)CH_3] + CH_3^{\bullet}$	-307.421890	123	-307.409611	128

[a]The relative energies (at 298 K) can be *also* normalized using the established energies of a selected product pair, e.g. $\Delta_fH[{}^{\bullet}CH_2C(CH_3){=}OH^+] + \Delta_fH[CH_3OH]$ = 459 kJ/mol, and so adding 341 kJ/mol (= 459 kJ/mol - 118kJ/mol) to all values achieves this (see text).

5.4 Conclusions

In summary, the proton-bound complex of acetone and $CH_2OH^{\bullet}$, ion **1**, isomerizes into the enol ion, i.e. distonic acetone, attached to a methanol molecule. In contrast, ion **2** does not produce the enol ion. It simply dissociates into the keto ion, i.e. ionized acetone, and the methanol neutral counterpart.

$$[(CH_3)_2C{=}O\cdots H^+\cdots O(H)CH_2^{\bullet}] \longrightarrow [^{\bullet}CH_2C(CH_3){=}OH^+\cdots O(H)CH_3] \qquad 5.4$$

$$[(CH_3)_2C{=}O\cdots H^+\cdots {}^{\bullet}OCH_3] \longrightarrow [(CH_3)_2C{=}O^{+\bullet}\cdots HOCH_3] \qquad 5.5$$

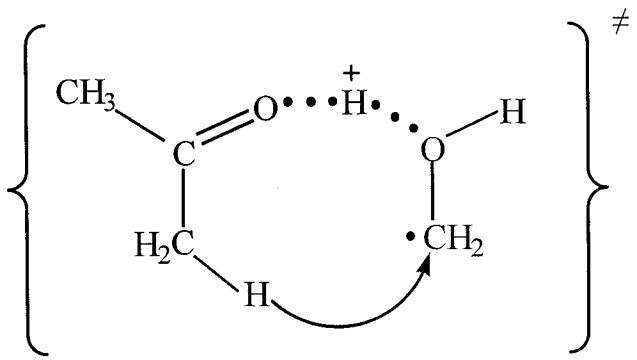

Figure 5.9. 1,6-Hydrogen shift for TS1 on the PES of $[(CH_3)_2C{=}OH^+\cdots {}^{\bullet}OCH_3]$.

These observations are in keeping with the chemistries of $[CH_3CHO\cdots H^+\cdots O(H)CH_2^{\bullet}]$ and $[CH_3CHO\cdots H^+\cdots {}^{\bullet}OCH_3]$. We believe that the first reaction proceeds because the charge and radical sites are on separate groups in ion **1**. In reaction 5.4, a proton shifts to the keto group and the radical moiety takes back an $H^{\bullet}$ atom. The ketone is thus readily converted to its enol-ion form. The key transition state,

TS1 shown in Figure 5.9, transfers an H$^{\bullet}$ atom back to the methyl hydroxyl radical by an H$^{\bullet}$ atom transfer mechanism. The important result from ion **1** is that the enol ion results from proton transfer to acetone which then gives an H$^{\bullet}$ atom back to the $^{\bullet}CH_2OH$ radical by a 1,6-H transfer, producing the enol ion. In contrast, when the protonated acetone is attached to the radical $CH_3O^{\bullet}$, ion **2**, the above rearrangement does not take place. Ion **2** cannot communicate with ion **1** on their PES. A high barrier prevents the complex of the acetone ion with methanol, complex VII, from rearranging to distonic acetone and methanol, complex IV, see Figure 5.7. Radom's rule predicts that PTC cannot facilitate the isomerization either, because the PA of methanol, 755 kJ/mol, is lower than PA values of $^{\bullet}CH_2(CH_3)C{=}O$ at the O atom, 811 kJ/mol and the C site, 769 kJ/mol. Instead, ion **2** dissociates to a stable complex of an acetyl ion with methanol. The energy barriers calculated at the MP2/6-31+G(d) level of theory for all the MI processes fully support the experimental observations.

References

(1) Hauck, G.; Arnold, F. *Nature* **1984**, *311*, 547.

(2) Arnold, F.; Hauck, G. *Nature* **1985**, *315*, 307.

(3) Arnold, F.; Knop, G.; Ziereis, H. *Nature* **1986**, *321*, 505.

(4) Arnold, F.; Knop, G. *Int. J. Mass Spectrom. Ion Processes* **1987**, *81*, 33.

(5) Bouchoux, G.; Luna, A.; Tortajada, J. *Int. J. Mass Spectrom. Ion Processes* **1997**, *167/168*, 353.

(6) McAdoo, D. J. *Mass Spectrom. Rev.* **2000**, *19*, 38.

(7) Turecek, F. In *The Chemistry of Enols*; Rappoport, Z., Ed.; Wiley: Chichester, 1990, p 95.

(8) Keeffe, R.; Kresge, A. J. In *The Chemistry of Enols*; Rappoport, Z., Ed.; Wiley: Chichester, 1990, p 399.

(9) Holmes, J. L.; Lossing, F. P.; Terlouw, J. K.; Burgers, P. C. *Can. J. Chem.* **1983**, *61*, 2305.

(10) Bouchoux, G. *Mass Spectrom. Rev.* **1988**, *7*, 1.

(11) Turecek, F.; Cramer, C. *J. Am. Chem. Soc.* **1995**, *117*, 12243.

(12) Lee, D.; Kim, C. K.; Lee, B. S.; Lee, I.; Lee, B. C. *J. Comput. Chem.* **1997**, *18*, 56.

(13) Williams, D. H. *Acc. Chem. Res.* **1977**, *10*, 280.

(14) Burgers, P. C.; Holmes, J. L. *Org. Mass Spectrom.* **1982**, *17*, 123.

(15) Chalk, A. J.; Radom, L. *J. Am. Chem. Soc.* **1999**, *121*, 1574.

(16) Trikoupis, M. A.; Burgers, P. C.; Ruttink, P. J. A.; Terlouw, J. K. *Int. J. Mass Spectrom.* **2002**, *217*, 97.

(17) Trikoupis, M. A.; Burgers, P. C.; Ruttink, P. J. A.; Terlouw, J. K. *Int. J. Mass Spectrom.* **2001**, *210/211*, 489.

(18) Trikoupis, M. A.; Terlouw, J. K. *J. Am. Chem. Soc.* **1998**, *120*, 12131.

(19) P. Mourgues; J. Chamot-Rooke; G. van der Rest; H. Nedev; H. E. Audier; McMahon, T. B. *Int. J. Mass Spectrom.* **2001**, *210/211*, 429.

(20) Wang, X.; Holmes, J. L. *Int. J. Mass Spectrom.* **2005**, *242*, 75.

(21) Haranczyk, M.; Burgers, P. C.; Ruttink, P. J. A. *Int. J. Mass Spectrom.* **2002**, *220*, 53.

(22) Tu, Y.-P.; Holmes, J. L. *J. Am. Chem. Soc.* **2000**, *122*, 3695.

(23) Holmes, J. L.; Mayer, P. M. *J. Phys. Chem.* **1995**, *99*, 1366.

(24) Rennie, E.; Mayer, P. M. *J. Chem. Phys.* **2004**, *120*, 10561.

(25) Scott, A. P.; Radom, L. *J. Phys. Chem.* **1996**, *100*, 16502.

(26) Hunter, E. P. L.; Lias, S. G. *J. Phys. Chem. Ref. Data* **1998**, *27*, 413

(27) Holmes, J. L. In *The Encyclopedia of Mass Spectrometry*; Armentrout, P. B., Ed.; Elsevier: Amsterdam, 2003; Vol. 1, p 91.

(28) Lias, S. G.; Bartmess, J. E.; Liebman, J. G.; Holmes, J. L.; Levin, R. D.; Mallard, W. G. *J. Phys. Chem. Ref. Data* **1988**, *17, Suppl. 1.*, 1.

(29) McLafferty, F. W.; Proctor, C. J. *Org. Mass Spectrom.* **1983**, *18*, 272.

(30) Larson, J. W.; McMahon, T. B. *J. Am. Chem. Soc.* **1982**, *104*, 6255.

(31) Holmes, J. L.; Lossing, F. P. *J. Am. Chem. Soc.* **1980**, *102*, 1591.

(32) G. van der Rest; H. Nedev; J. Chamot-Rooke; P. Mourgues; T.B. McMahon; H.E. Audier *Int. J. Mass Spectrom.* **2000**, *202*, 161.

(33) Fridgen, T. D.; McMahon, T. B. *J. Phys. Chem. A.* **2002**, *106*, 1576.

CHAPTER 6

THE WATER-ASSISTED INTERCONVERSIONS AND DISSOCIATIONS OF THE ACETALDEHYDE ION AND ITS ISOMERS

6.1 Introduction

In this chapter, the gas-phase reactions of the ion $[CH_3CHO/H_2O]^{+\bullet}$ have been investigated by mass spectrometry. The structures of stable complexes and transition states involved in the potential energy surface (PES) have been studied by the G3//B3-LYP/6-31+G(d) computational method. Calculations have also been used to aid mass spectrometry by assigning product ion structures and reaction mechanisms. The interconversions among water-solvated $CH_3CHO^{+\bullet}$, $CH_3COH^{+\bullet}$ and $CH_2CHOH^{+\bullet}$ have been discovered and the reaction pathway between each isomer is illustrated by the PES.

In earlier studies, the water-assisted isomerization of the methanol ions, $CH_3OH^{+\bullet}/H_2O \rightleftharpoons {}^{\bullet}CH_2OH_2^{+}/H_2O$, has been investigated in detail.[1-4] In this system the PTC mechanism can operate because the PA of the catalyst, H_2O, meets the PA criterion for PTC, i.e. it lies between the PA value of the C and O sites of the ${}^{\bullet}CH_2OH$ radical (PA[H_2O] = 691 kJ/mol[5]; PA[${}^{\bullet}CH_2OH$]at O = 695 kJ/mol[5] and at C = 663 kJ/mol[5]). The catalyzed reaction is calculated to proceed with less than half the activation energy of the unimolecular rearrangement of $CH_3OH^{+\bullet}$ to ${}^{\bullet}CH_2OH_2^{+}$. Note that the uncatalyzed

activation energy (108 kJ/mol) exceeds the dissociation limit (66.2 kJ/mol) for $CH_3OH^{+\bullet} \rightarrow {}^{+}CH_2OH + H^{\bullet}$.[3,4]

Nedev et al.[6] studied the isomerization of $CH_3COH^{+\bullet}$ and $CH_3CHO^{+\bullet}$ with water under Fourier transform ion cyclotron resonance (FT-ICR) conditions and observed that the bimolecular reaction proceeded via a catalyzed 1,2-H transfer. The potential energy surface was also calculated by them and it showed that the reactions for H_2O loss and for $^{\bullet}CH_3$ loss shared the same transition state (TS1/4), an unusual situation for a reaction pathway. As will be described below, our calculations at the B3-LYP/6-31+G(d) and G3 level of theories showed that the above two reactions take place via different pathways, i.e. a distinguishable transition state leads to each product corresponding to the loss of H_2O or $^{\bullet}CH_3$. In addition to the isomerization between water-solvated $CH_3COH^{+\bullet}$ and $CH_3CHO^{+\bullet}$ that was discussed in Nedev et al.'s paper[6], we have also investigated the potential energy surface that includes the interconversion paths involving acetaldehyde's enol ion ($CH_2CHOH^{+\bullet}$) and the above two species.

The acetaldehyde/H_2O system was first studied by Cao et al.[7] in this laboratory and a new $CH_6O^{+\bullet}$ ion was found to be produced by the loss of CO from the metastable $[CH_3CHO/H_2O]^{+\bullet}$ ion. However, a detailed mechanism for this and other reactions was not provided. In the present work we have explored in greater detail the isomerization and decomposition chemistry of water-solvated acetaldehyde ions and other isomers including the carbene and vinyl alcohol ions. We also describe the structures of new

fragment ions produced by H_2O and $^{\bullet}CH_3$ loss and complete potential energy surfaces have been established to delineate the reaction mechanism.

6.2 Experimental and Theoretical Approaches

As also described in Chapters 4 and 5, the experiments were performed on a modified VG ZAB research mass spectrometer[8] (VG Analytical, Manchester, U.K.), which incorporates a magnetic analyzer followed by two electrostatic analyzers (i.e. BEE geometry). Metastable ion (MI) and collision-induced dissociation (CID) mass spectra of selected proton-bound pairs were acquired in the usual manner in the mass spectrometer.[9] The desired ion-molecule complex was produced by CID of the appropriate proton-bound pair in the second field-free region (2FFR) of the instrument. MI and CID dissociations of the ion-molecule complex were observed in the third field-free region (3FFR). The ion accelerating voltage of the proton-bound pairs was 8 kV. In the 2FFR and 3FFR helium was used as the collision gas. All spectra were recorded with the ZABCAT program developed by Mommers Technologies[8].

The proton-bound dimer of acetaldehyde and ethanol was generated by admitting the mixed reagents into a high pressure ion source via the liquid septum inlet. The pressure in this high pressure source is approximately one order of magnitude higher than that achievable in a standard lower pressure source. The pressure in the ion source chamber, read with an ionization gauge located above the ion source diffusion pump, was ca. 8×10^{-5} mbar, indicating an in-source pressure of ca. 0.3 mbar.[10] The proton-bound

dimer $CH_3CHO\cdots H^+\cdots O(H)CH_2CH_3$ (m/z = 91) was mass-selected by the magnet and dissociated by collision in the second field-free region. The fragment ion $[CH_3CHO/HO(H)]^{+\bullet}$ (m/z 62) resulting from the loss of $CH_3CH_2^\bullet$ from the precursor ion (m/z 91) was transmitted into the third field-free region in order to observe its MI and CID characteristics.

The molecules CH_3CHO, CH_3CH_2OH and the isotopically labelled compounds, CD_3CHO, CD_3CDO were used to generate various isotopomeric ion-molecule pairs. The unlabeled chemicals were purchased from Aldrich and all the labelled samples, of 99.5%-99.9% isotopic purity, were obtained from CDN Isotopes (Montreal, QC, Canada) and were used without further purification.

Standard *ab initio* molecular orbital calculations[11] were performed using the GAUSSIAN 98 programs[12] to investigate the potential energy surface. Optimized geometries and the energies of all minima and transition states were calculated using Becke 3 parameter exchange[13] with the functional of Lee-Yang-Parr correlation[14] (B3-LYP) and the 6-31+G(d) basis set. Vibrational frequency analysis was performed to confirm that the equilibrium and transition state structures were obtained. Intrinsic Reaction Coordinate (IRC) calculations have been used to follow the reaction paths from all transition states in order to identify intermediates. IRCs were also used to test whether a transition state is the correct structure that connects two minimum wells. G3[15] single-point energy calculations were carried out on the optimized B3-LYP/6-31+G(d) geometries of all the stable and transition states. A scaling factor of 0.96[16] (rather than

0.9806[17]) was used in G3 calculations for the zero-point vibrational energies (ZPE) obtained from B3-LYP/6-31+G(d). The heats of formation of new products, those resulting from the losses of H_2O and $^{\bullet}CH_3$, were obtained by converting their G3 total energies into enthalpies of the ions, based on the atomization method reported by Nicolaides et al.[18] 298K heats of formation were evaluated with the aid of standard thermodynamic formulas in conjunction with the B3-LYP/6-31+G(d) frequencies and experimental thermo-corrections for the elements[17]. Binding energies of the electrostatically bound species were calculated from the difference in energy between the intact cluster and the dissociation products.

6.3 Results and Discussion

6.3.1 Dissociation Reactions of $[CH_3CHO/H_2O]^{+\bullet}$

The MI mass spectrum of the proton-bound dimer $CH_3CHO\cdots H^+\cdots O(H)CH_2CH_3$ (m/z 91), shows two peaks, i.e. protonated ethanol (m/z 47) and protonated acetaldehyde (m/z 45) (PA[CH_3CHO] = 768.5 kJ/mol[5], PA[CH_3CH_2OH] = 777 kJ/mol)[5]. These are the only MI processes, showing that no rearrangement of the proton bound dimer occurs at internal energies up to those for MI dissociations. This proton-bound dimer readily lost a $CH_3CH_2^{\bullet}$ radical by collisional excitation showing a signal at m/z 62, the reaction is shown in Equation 6.1. The m/z 62 peak intensified with additional collision gas and when the main beam had been reduced by ca. 20% it was intense enough to be

transmitted (by the electrostatic sector) into the third free-field region in order that its dissociation characteristics could be studied.

$$CH_3CHO\cdots H^+\cdots O(H)CH_2CH_3 \rightarrow [CH_3CHO/HOH]^{+\bullet} + CH_3CH_2^{\bullet} \text{ (CID)} \qquad 6.1$$

m/z 91 m/z 62, (Ion **1**)

The MI mass spectrum of ion **1,** Figure 6.1-A, shows three competing dissociation processes: the losses of $^{\bullet}CH_3$ (m/z 47, 44%), H_2O (m/z 44, 100%) and CO (m/z 34, 56%). The observation that a metastable ion peak is insensitive to collision gas signifies that the mass selected ion has undergone a rearrangement to an isomeric species over an energy barrier close to the lowest energy fragmentation for that ion.[19] In cases where this energy barrier is lower or non-existent, the collision sensitivity of the peak is correspondingly greater. If the MI peak arises from a simple bond cleavage in the mass selected ion, the collision sensitivity is great and often produces the base peak in a CID mass spectrum.[19]

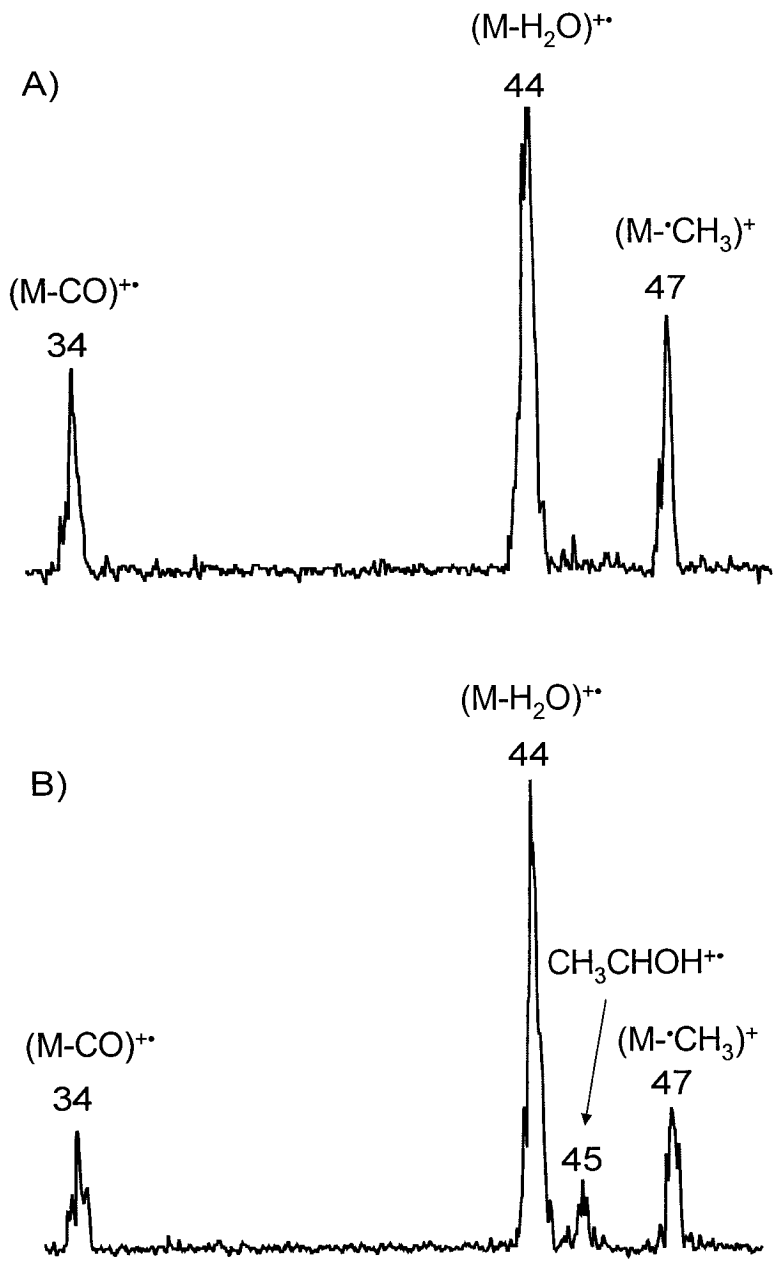

Figure 6.1. A) MI mass spectrum of $[CH_3CHO/H_2O]^{+\bullet}$, ion **1**, B) CID mass spectrum of $[CH_3CHO/H_2O]^{+\bullet}$, ion **1**.

In the CID mass spectrum of ion **1,** Figure 6.1-B, the peak at m/z 45, CH_3CHOH^+, intensifies, from having been barely visible in the MI mass spectrum. The formation of CH_3CHOH^+, m/z 45, being a simple-bond cleavage in ion **1**, is thus collision sensitive. This indicates that ion **1** has kept the proton bridged form of the precursor proton-bound pair, m/z 91, and so its structure is better represented as $[CH_3C(H)OH^+\cdots{}^{\bullet}O(H)]$. The proton is more strongly attached to acetaldehyde because the PA of CH_3CHO at O, 768.5 kJ/mol[20] is significantly higher than that of $^{\bullet}OH$, 593 kJ/mol[5]. However, note that the peak at m/z 44 is also slightly *sensitive* to the collision gas, indicating that at least some of ion **1** can be represented as $CH_3CHO^{+\bullet}/H_2O$, an acetaldehyde ion electrostatically bound to a water molecule, in keeping with acetaldehyde having a lower ionization energy (IE) than water, (IE[CH_3CHO] = 10.2 eV, IE[H_2O] = 12.6 eV).[21]

What is the product ion resulting from H_2O loss from the $[CH_3CHO/H_2O]^{+\bullet}$ complex: $CH_3CHO^{+\bullet}$, $CH_2CHOH^{+\bullet}$, $CH_3COH^{+\bullet}$ or a mixture of these ions? Isotopic labelling experiments indicate that vinyl alcohol ions (m/z 44) are produced, but there remain some keto (acetaldehyde) ions. The MI mass spectra of three isotopic labelled samples, $[CH_3CHO/D_2O]^{+\bullet}$ (m/z 64, ion **1**-d_2), $[CD_3CHO/H_2O]^{+\bullet}$ (m/z 65, ion **1**-d_3) and $[CD_3CDO/H_2O]^{+\bullet}$ (m/z 66, ion **1**-d_4), provided consistent results showing that the enol ion was produced (Figure 6.2). The fully deuterated acetaldehyde was used to form $[CD_3CDO/H_2O]^{+\bullet}$. Its MI mass spectrum is shown in Figure 6.2-A, in which the most intense peak is due to the loss of –HDO rather than the direct loss of H_2O. This m/z 47 ion produced by ion **1**-d_4 is proposed to have the enol structure $CD_2CDOH^{+\bullet}$. In the MI mass spectrum of $[CD_3CHO/D_2O]^{+\bullet}$, Figure 6.2-B, the enol ion appears at m/z 46,

$CD_2CHOH^{+\bullet}$. Note that the loss of H_2O or a methyl radical ($-^{\bullet}CD_3$) from ion **1**-d_4 and ion **1**-d_3 produces only an (M-18) ion. Figure 6.2-C shows that the dissociation of metastable $[CH_3CHO/D_2O]^{+\bullet}$ ions produces $CH_3CHO^{+\bullet}$ (m/z 44) and $CH_2CHOD^{+\bullet}$ (m/z 45) in a ratio of ca. 1.9:1. The above three experiments show that the mechanism for generating the enol (vinyl alcohol ion) involves moving the proton to the carbonyl oxygen and shifting a methyl H to the $^{\bullet}OH$ group. The reaction path and transition state of such a rearrangement is shown on the PES (Figure 6.3).

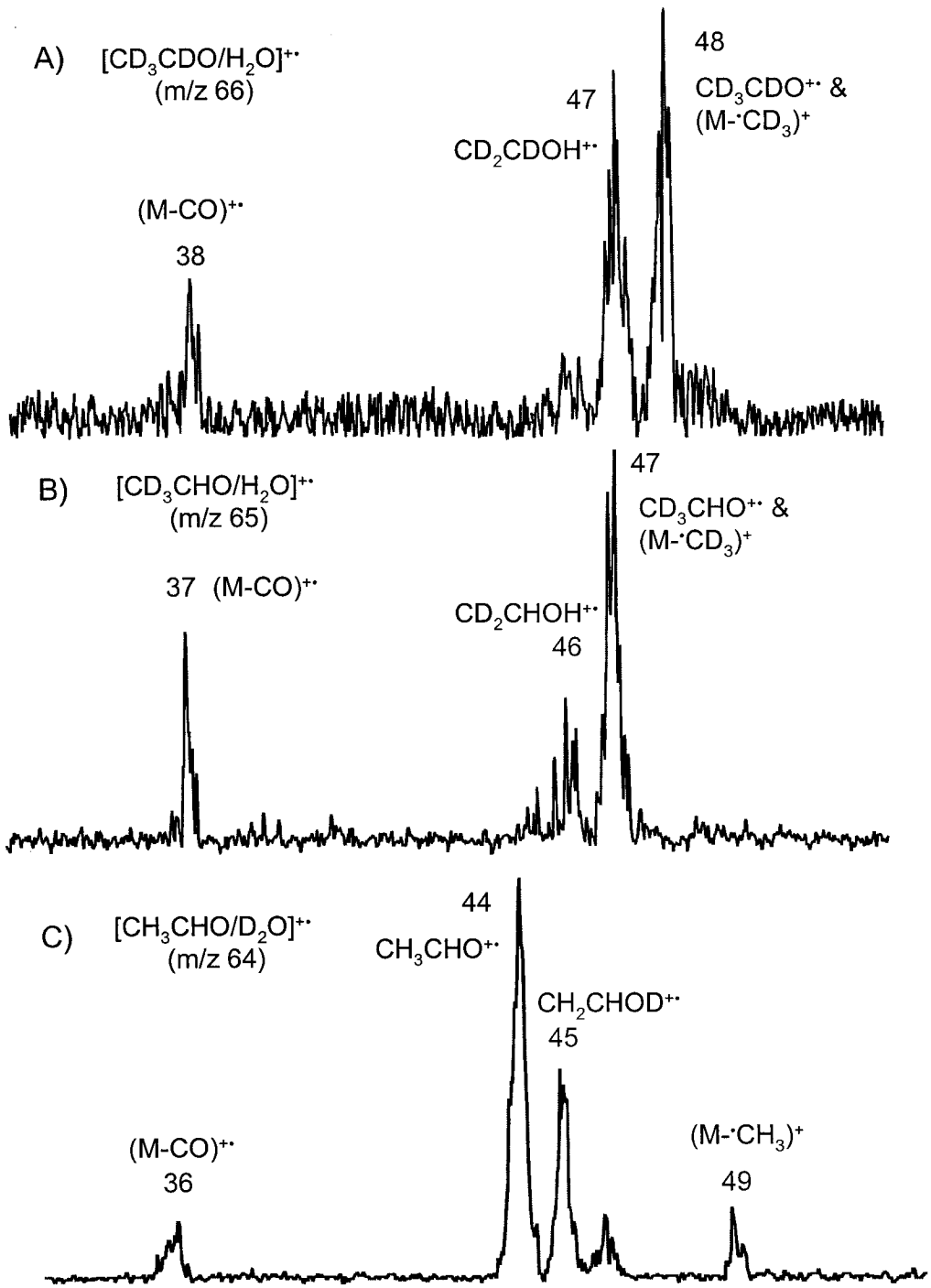

Figure 6.2. A) MI mass spectrum of $[CD_3CDO/H_2O]^{+\bullet}$ (m/z 66, ion **1**-d_4), B) MI mass spectrum of $[CD_3CHO/H_2O]^{+\bullet}$ (m/z 65, ion **1**-d_3), C) MI mass spectrum of $[CH_3CHO/D_2O]^{+\bullet}$ (m/z 64, ion **1**-d_2).

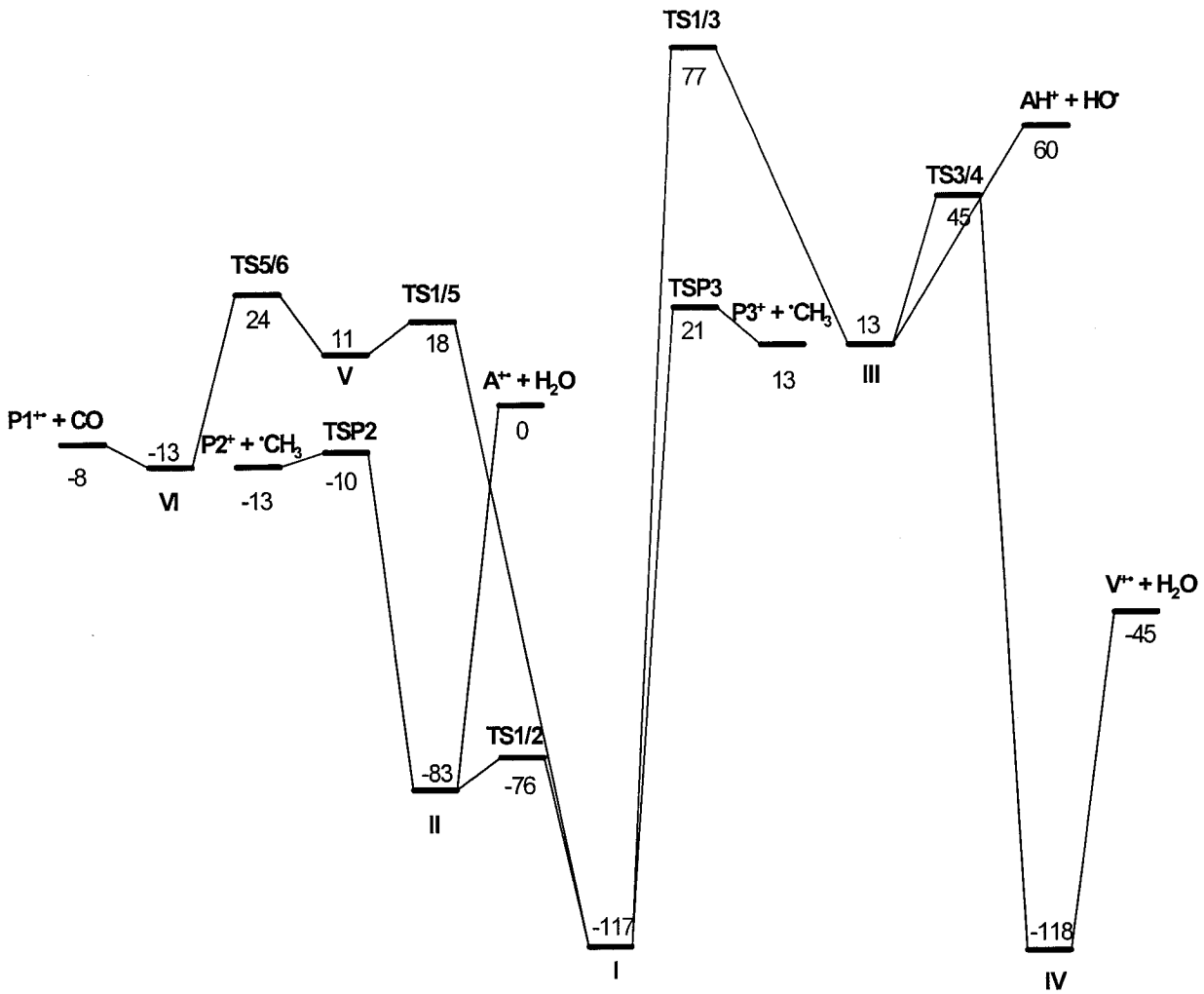

Figure 6.3. Potential energy surface of $[CH_3CHO/H_2O]^{+\bullet}$ based on calculations at the G3 level of theory. Relative energies are given in kJ/mol. $A^{+\bullet}$, AH^+ and $V^{+\bullet}$ refer to the acetaldehyde ion, protonated acetaldehyde and the vinyl alcohol ion, respectively. $P1^{+\bullet}$, $P2^+$ and $P3^+$ represent the products from the loss of CO and CH_3, respectively.

The dissociation channel that leads to $CH_2CHOH^{+\bullet}$ is enthalpically more favourable than that for producing other isomers of $C_2H_4O^{+\bullet}$. The dissociation limit for

the generation of $CH_2CHOH^{+\bullet}$ is 529 kJ/mol (from $\Delta_fH[^{\bullet}CH_2CHOH^+]$ = 771 kJ/mol[22], $\Delta_fH[H_2O]$ = -242 kJ/mol[22]). This is lower than the dissociation limit, 579 kJ/mol, for the formation of the acetaldehyde ion, (from $\Delta_fH[CH_3CHO^{+\bullet}]$ = 821 kJ/mol[22]). Although the dissociation leading to $CH_2CHOH^{+\bullet}$ is lower in energy, whether the $CH_3CHO^{+\bullet}$ isomerized to $CH_2CHOH^{+\bullet}$ within the complex $[CH_3CHO/H_2O]^{+\bullet}$ depends on whether there is a barrier for the tautomerization. The reaction path is shown in the potential energy surface (Figure 6.4 and 6.5 and also see the discussion below). In addition, the threshold energy (623 kJ/mol) for dissociation to the carbene ion ($CH_3COH^{+\bullet}$) and water is much higher, from ($\Delta_fH[(CH_3COH^{+\bullet}]$ = 865 kJ/mol[22]), and is energetically the least favourable process and so this dissociation channel can be ruled out.

The $(M-28)^{+\bullet}$ peak is common to the mass spectra of all the deuterated samples and there are no $(M- 29 \text{ or } 30)^{+\bullet}$ peaks (see Figure 6.2). Therefore this $(M-28)^{+\bullet}$ ion arises from the loss of a CO molecule and not from C_2H_4, as shown by the labelled samples. This product ion resulting from the loss of CO has been found to be the ion $CH_6O^{+\bullet}$ [a missing member of the remarkable series of ions CH_nO^+, n=0-7]. The structure of $CH_6O^{+\bullet}$ was found by computation to be a methyl radical electrostatically bound to protonated water, $[^{\bullet}CH_3\cdots H^+OH_2]$, as described by Cao et al.[7].

The mass spectra of the isotopically labelled samples also show that no isotopic mixing precedes the elimination of a methyl radical and that all the methyl-H atoms of acetaldehyde retain their position prior to the fragmentation. The loss of $^{\bullet}CH_3$ produces a

$CH_3O_2^+$ ion which has been characterized by theory and is discussed in the following section.

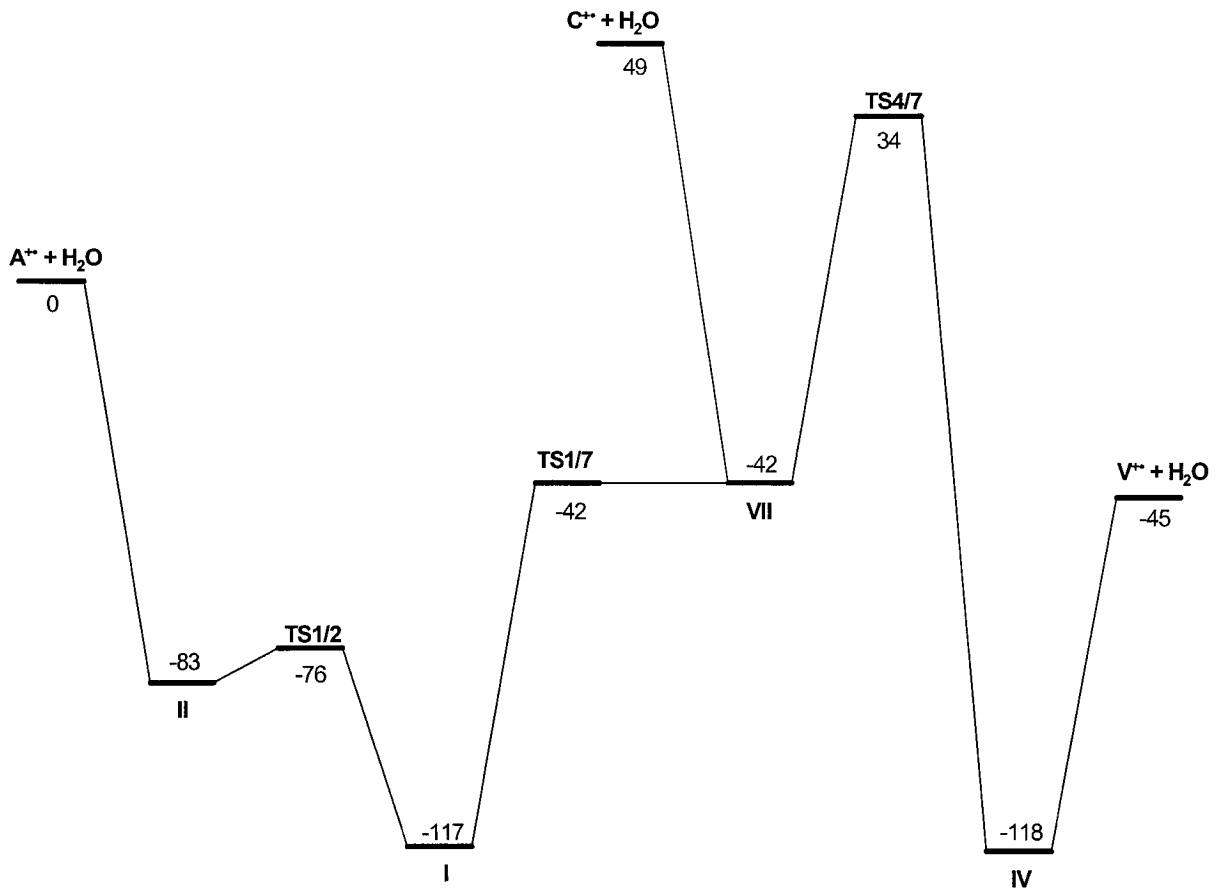

Figure 6.4. Energy diagram for the water catalyzed 1,2-H transfer and PTC isomerizations of the acetaldehyde ion, ($CH_3CHO^{+\bullet}$, shown as $A^{+\bullet}$), its carbene ($CH_3COH^{+\bullet}$, shown as $C^{+\bullet}$) and enol isomers ($CH_2CHOH^{+\bullet}$, shown as $V^{+\bullet}$). The relative energies are calculated at the G3 level of theory and are given in kJ/mol.

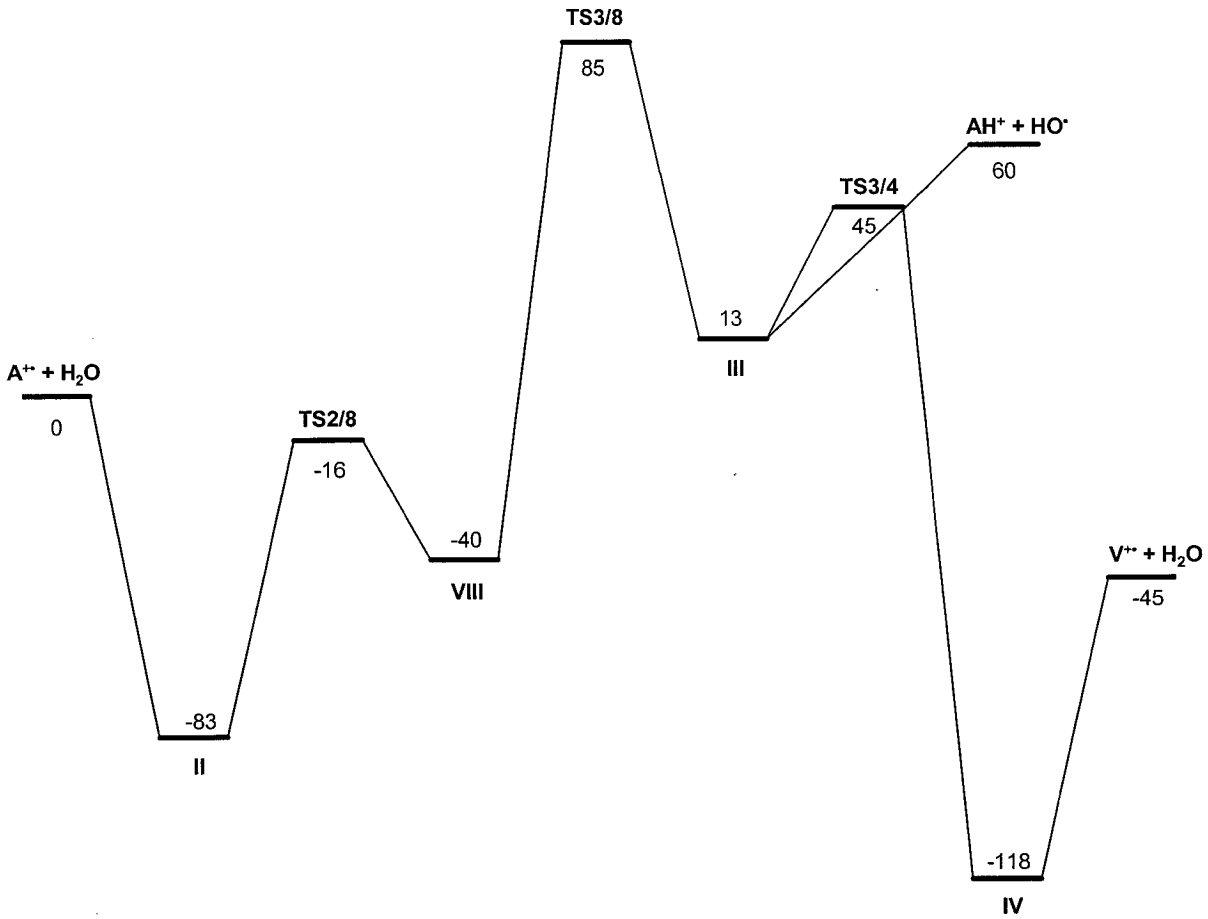

Figure 6.5. Energy diagram for the H-atom transfer mechanism of keto-enol isomerization of the acetaldehyde ion with water. $A^{+\bullet}$, AH^{+} and $V^{+\bullet}$ refer to the acetaldehyde ion, protonated acetaldehyde and the vinyl alcohol ion, respectively. The relative energies are calculated at the G3 level of theory and are given in kJ/mol.

6.3.2 Computational Analysis of the Chemistry of $[CH_3CHO/H_2O]^{+\bullet}$

With the above mass spectrometric experiments as a guide, the theoretical calculations revealed the reaction paths for each dissociation process, i.e. the losses of

H_2O, $^{\bullet}OH$, $^{\bullet}CH_3$ and CO, respectively. The potential energy profile for the dissociation reactions of the $[C_2H_4O/H_2O]^{+\bullet}$ complex (ion **1**) is shown in Figure 6.3. Eight significant isomers of ion **1** have been found by density functional theory (DFT) calculations at the B3-LYP/6-31+G(d) level to be stable and their optimized geometries are shown in Figure 6.6. All relative energies that are indicated on the PESs in this Chapter refer to G3 results at 0 K and are relative to the sum of the G3 energies of $CH_3CHO^{+\bullet}$ and H_2O.

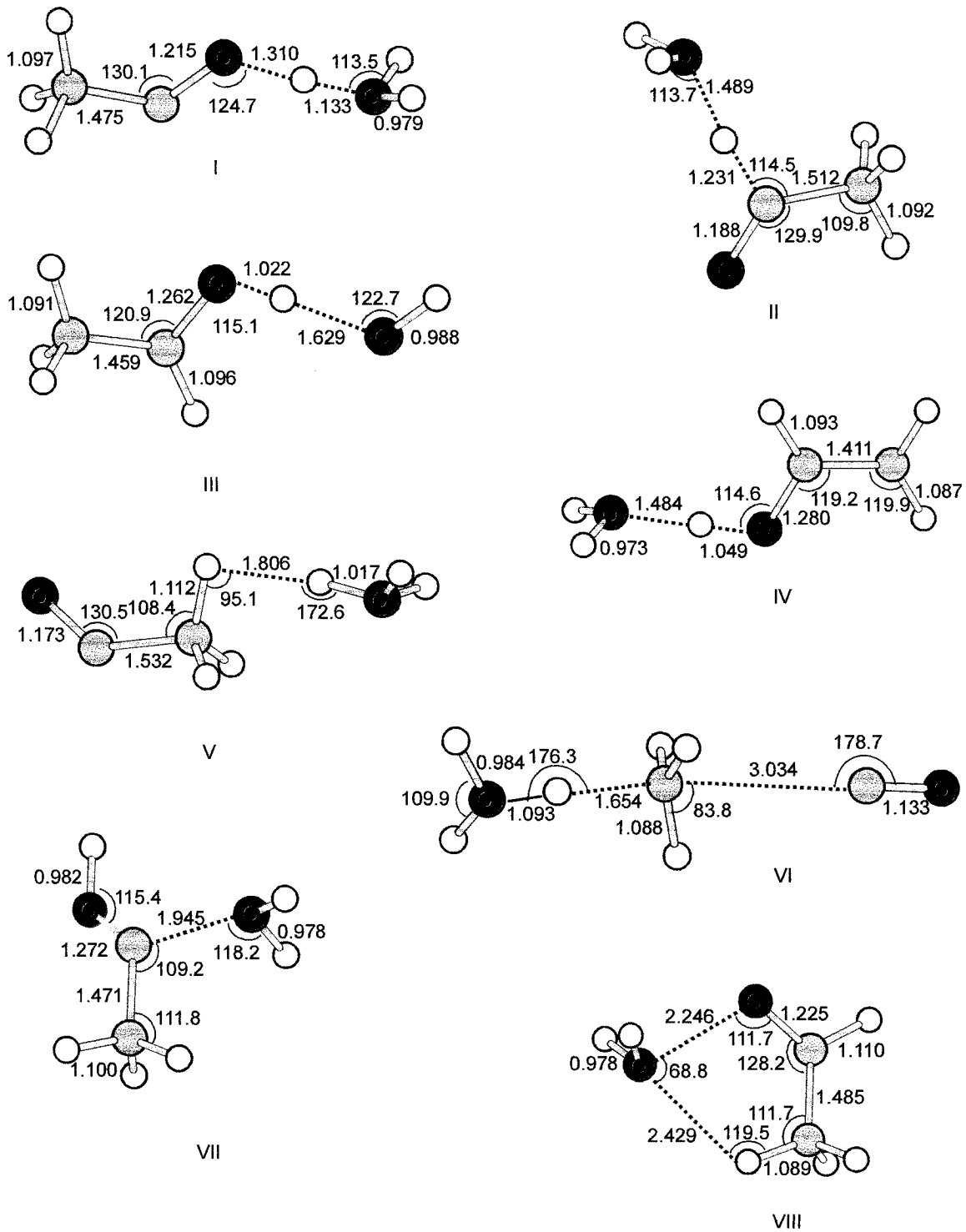

Figure 6.6. Optimized structures of the intermediate (structure V) and stable states at B3-LYP/6-31+G(d).

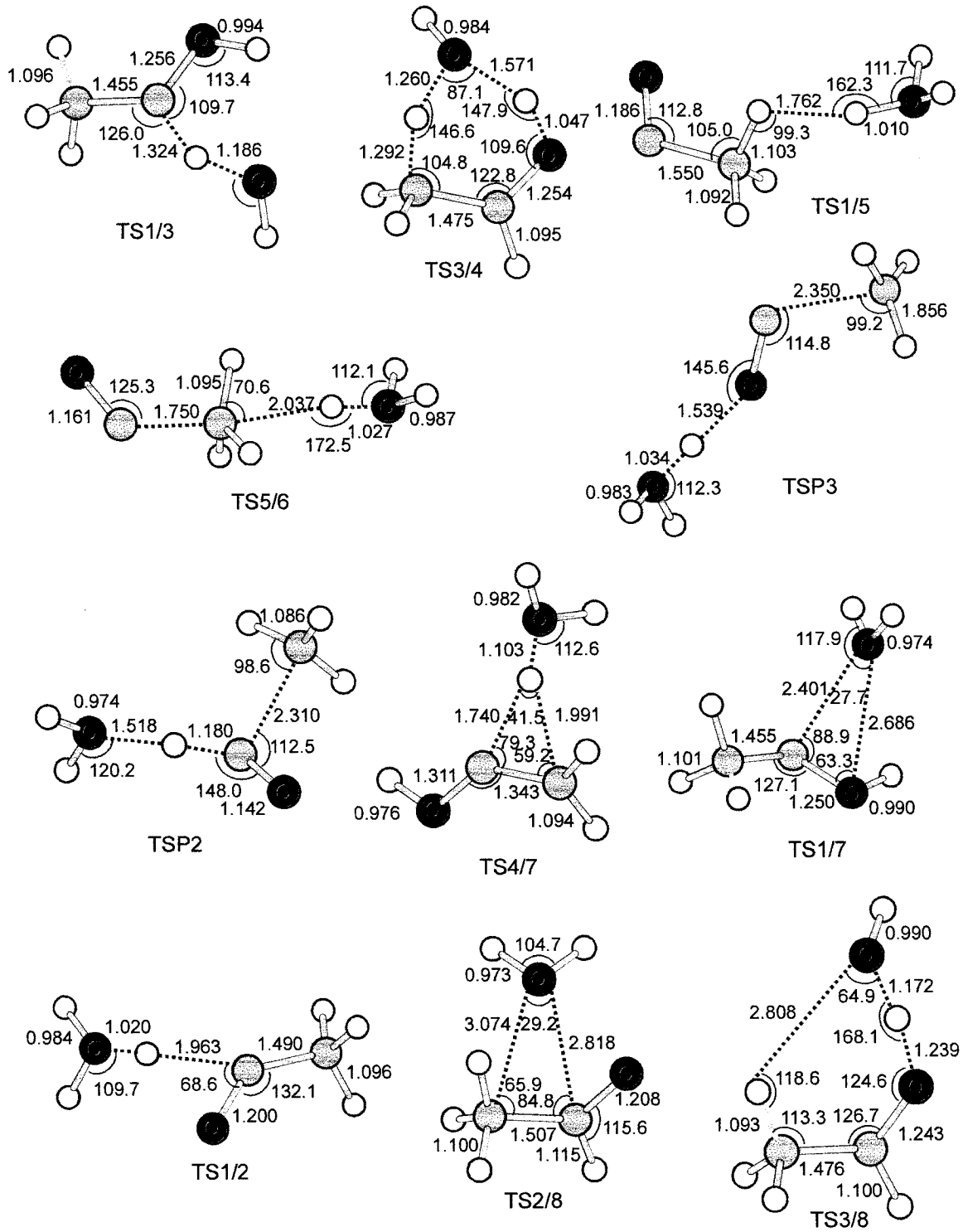

Figure 6.7. Optimized structures of the transition states at B3-LYP/6-31+G(d).

The acetaldehyde ion/water complex ($[CH_3CHO^{+\bullet}\cdots OH_2]$, stable state II) can readily convert into a more stable structure I, via a low energy barrier (TS1/2, -76 kJ/mol). A relatively high energy barrier (TS 1/3, 77 kJ/mol), that lies above all the dissociation limits, prevents the isomerization of isomer I to III and therefore it divides the PES (Figure 6.3) into two parts: the left-hand energy profile incorporates the reaction paths that produce the acetaldehyde ion and the CO and $^{\bullet}CH_3$ loss ions; the right-hand surface involves the generation of the vinyl alcohol ion and protonated acetaldehyde. From the experiments discussed above, ion **1** consists of a mixture of $[CH_3CHO^{+\bullet}\cdots OH_2]$ (complex II) and $[CH_3CHOH^{+}\cdots{}^{\bullet}OH]$ (complex III) and the calculations show that complexes II and III cannot freely interconvert at any energy below their dissociation limits. Therefore the dissociation reactions of ion **1** involve the chemistry of both II and III.

Complex III rearranges to the vinyl alcohol ion/ water complex, $[CH_2CHOH^{+\bullet}\cdots OH_2]$ (ion IV) via a six-membered transition state TS3/4. This transition state is ca. 15 kJ/mol lower that the dissociation threshold of III (to produce protonated acetaldehyde) and ion IV is the global minimum of ion **1**, and so the vinyl alcohol ion is produced in the metastable ion time frame (see Figure 6.1).

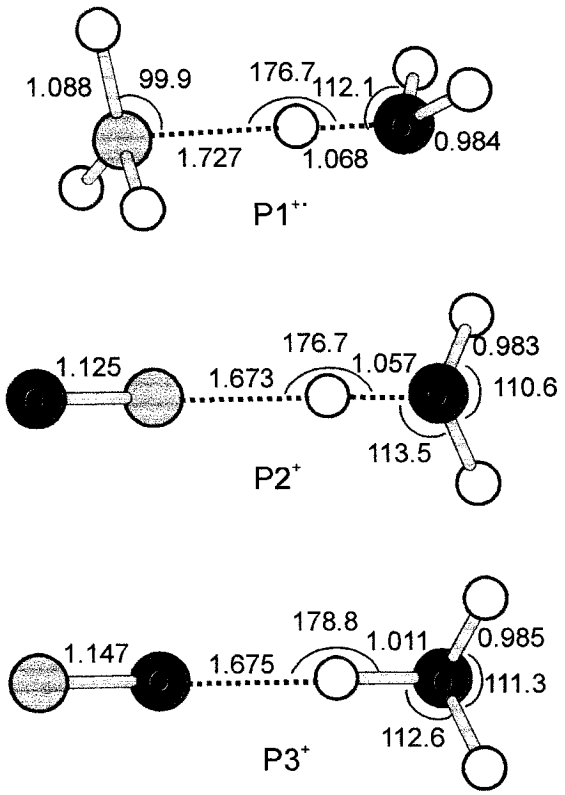

Figure 6.8. Optimized structures of CO and $^{\bullet}CH_3$ loss products at the B3-LYP/6-31+G(d) level of theory.

The earlier study found the CO loss product to be protonated water electrostatically bound to a methyl radical, [$^{\bullet}CH_3\cdots H^+OH_2$]. The calculated 298 K $\Delta_f H$ was 690 kJ/mol and the binding energy was only 58 kJ/mol based on G3 results.[7] The optimized structure of this ion, $P1^{+\bullet}$, is given in Figure 6.8, and the reaction mechanism has been explored and is shown in the PES (Figure 6.3). This ion, $P1^{+\bullet}$ is generated from ion **1** by the loss of CO via a backside displacement mechanism, as shown in Scheme 6.1.

Backside Displacement Mechanism

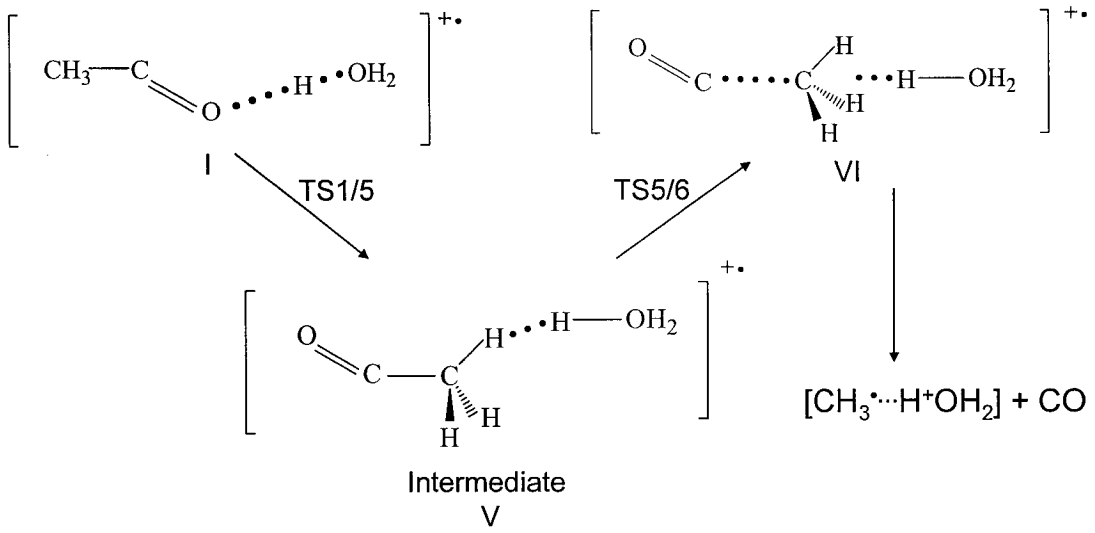

Scheme 6.1. The backside displacement mechanism for the reaction involving CO loss from $[CH_3CHO/H_2O]^{+\bullet}$.

The first step of this process involves the H_3O^+ back-attacking the acetyl radical through a methyl hydrogen atom to form an intermediate complex, Structure V in Figure 6.6. The second step consists of stretching the C-C bond in the acetyl group and shortening the electrostatic bond between the proton (in H_3O^+) and the methyl radical in the centre, followed by the formation of the stable state VI, $[H_2OH^+\cdots{}^\bullet CH_3\cdots CO]$. Transition states TS1/5 and TS5/6 correspond to this backside displacement reaction and their optimized structures are shown in Figure 6.7.

Methyl loss from ion **1** produces $[C,H_3,O_2]^+$ ions, the most stable isomer of which is protonated formic acid, $\Delta_fH[HC^+(OH)_2] = 403$ kJ/mol[22]. However, the transition states involved in this reaction channel leading to protonated formic acid and a methyl radical were calculated to be too high (relative energy is ca. 90 kJ/mol) to compete with other

dissociation processes in the metastable ion time frame. This transition state involved a 1,3-hydroxyl group migration with a large energy requirement. Possible structures for the $^{\bullet}CH_3$ loss ions have been proposed by calculations to be $[OC\cdots H^{+}OH_2]$, $P2^{+}$, and $[CO\cdots H^{+}OH_2]$, $P3^{+}$. They are both hydrogen-bridged complex (HBC) ions and represent CO attached to protonated water, similar in type to the CO loss product from ion **1** where the $^{\bullet}CH_3$ radical was the ligand. In $P2^{+}$ the protonated water and CO are bound via a $C\cdots H^{+}\cdots O$ bridge and in $P3^{+}$ via an $O\cdots H^{+}\cdots O$ bridge. The optimized structures of $P2^{+}$ and $P3^{+}$ are shown in Figure 6.8. 298 K heats of formation of these two stable $[C,H_3,O_2]^{+}$ ions were obtained from G3 calculations as $\Delta_fH[OC\cdots H^{+}OH_2]$ = 420 kJ/mol and $\Delta_fH[CO\cdots H^{+}OH_2]$ = 448 kJ/mol. Using these enthalpy values, the binding energies at 298 K have been determined as $[OC\cdots{}^{+}H_3O]$ = 66 kJ/mol and $[CO\cdots{}^{+}H_3O]$ = 38 kJ/mol, respectively, from ($\Delta_fH[CO]$ = -111 kJ/mol[21] and $\Delta_fH[H_3O^{+}]$ = 597 kJ/mol[30]). Note that these results show that the in the above HBC ions the $C\cdots H^{+}\cdots O$ bond is stronger than the $O\cdots H^{+}\cdots O$ bond, in contrast with the observation that the latter bond is usually the stronger in such HBC ions, e.g. the ion $CH_3CO^{\bullet}\cdots H^{+}\cdots OH_2$ is more stable than the $CH_3C^{\bullet}(O)\cdots H^{+}\cdots OH_2$. This reflects to the greater PA of CO at C (594 kJ/mol)[5] than at O (426 kJ/mol)[5].

It remains to consider whether or not the isomeric complexes $[OC\cdots{}^{+}H_3O]$ and $[CO\cdots{}^{+}H_3O]$ can freely interconvert. A computational study by Chalk and Radom investigated the catalyzed rearrangement of the formyl cation (HCO^{+}) to the isoformyl cation (HOC^{+}) by a wide variety of catalysts.[23] The energy difference between the two $[H,C,O]^{+}$ isomers is 164 kJ/mol ($\Delta_fH[HCO^{+}]$ = 826 kJ/mol[22], $\Delta_fH[HOC^{+}]$ = 990 kJ/mol[22])

and there is a significant energy barrier separating them (ca. 147 kJ/mol above HCO^+). The water-assisted interconversion of the isoformyl and formyl cation was calculated[23] to test whether or not water molecule can catalyze the isomerization. However, the optimized ground state IMCs were found to have the configurations $[OC\cdots{}^+H_3O]$ and $[CO\cdots{}^+H_3O]$, rather than $[OCH^+\cdots OH_2]$ and $[COH^+\cdots OH_2]$. Because the PA of H_2O (697 kJ/mol) is much greater than that of CO at either the O or C site, the water molecule readily captures the proton from either HCO^+ or HOC^+. Their G2 calculations showed that energy difference between $[OC\cdots{}^+H_3O]$ and $[CO\cdots{}^+H_3O]$ is 25 kJ/mol, which is in excellent agreement with the result obtained in this study ($\Delta\Delta_fH$ = 448 kJ/mol - 420 kJ/mol = 28 kJ/mol). The barrier for this rearrangement was determined to be 52 kJ/mol.[23] The potential energy diagram (Figure 6.9) gives the energy for each species and dissociation reaction. The ions $[OC\cdots{}^+H_3O]$ and $[CO\cdots{}^+H_3O]$ reside in separate potential energy wells and so they are both stable species. In the study presented in this chapter, the two ions are made by different reaction channels and thus both isomers can be obtained in our experiments. The dissociation limit to produce H_3O^+ and CO lies only 9 kJ/mol higher than the transition state, well below that to generate H_2O and OCH^+ or COH^+. Water therefore cannot catalyze the rearrangement from COH^+ to HCO^+; the dissociation reaction to H_3O^+ and CO is preferred to the proton migration (from the H_2O to CO) to produce the HCO^+ ion.

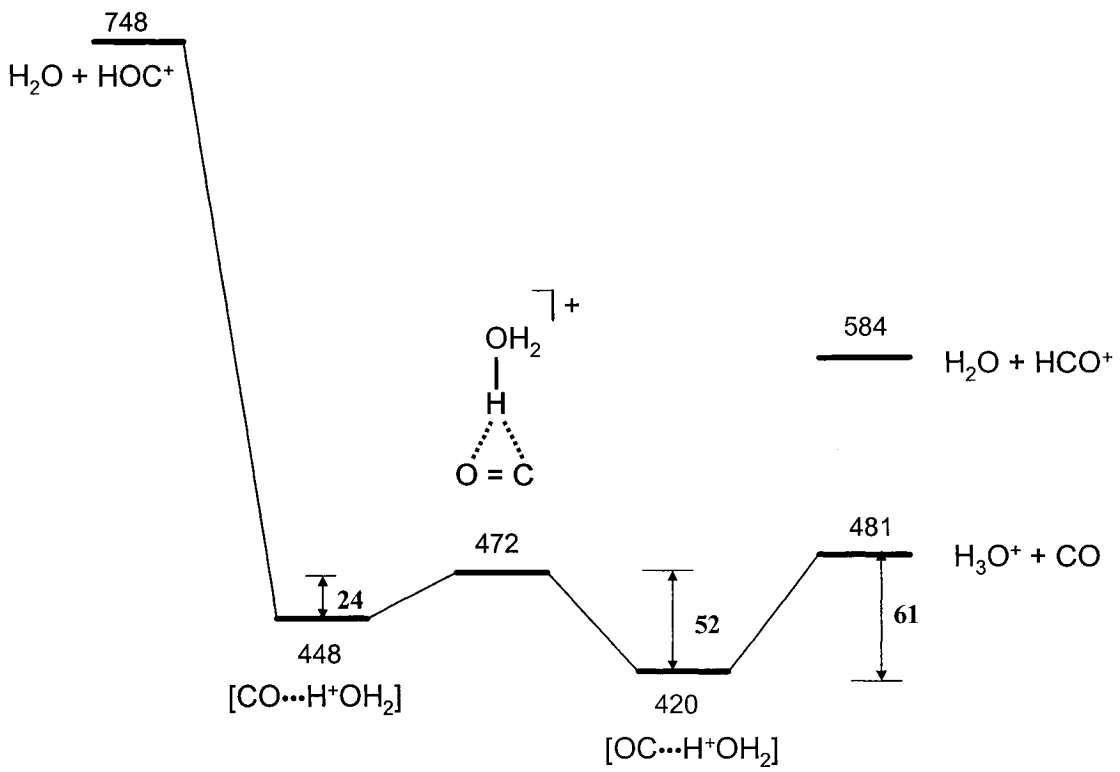

Figure 6.9. Potential energy diagram for the interconversion between $[OC\cdots{}^+H_3O]$ and $[CO\cdots{}^+H_3O]$. All energies are given in kJ/mol.

The $^{\bullet}CH_3$ loss ions are thus produced by the following processes: cleavage of the C-C bond in $[CH_3(O{=})C^{+\bullet}H\cdots OH_2]$, complex II, leads to the production of the $[OC\cdots H^+OH_2]$ ion; also, $[CO\cdots H^+OH_2]$ is generated from the C-C bond dissociation of complex I, $[CH_3CO^{\bullet}\cdots H^+OH_2]$. TSP2 and TSP3 are the corresponding transition states for these two dissociations and their respective configurations are shown in Figure 6.7.

6.3.3 Mechanisms of Keto-Enol-Carbene isomerization in $C_2H_4O^{+\bullet}/H_2O$ ions

For the water-solvated interconversions among the isomers $CH_3CHO^{+\bullet}$ ($A^{+\bullet}$), $CH_3COH^{+\bullet}$ ($C^{+\bullet}$) and $CH_2CHOH^{+\bullet}$ ($V^{+\bullet}$), a proton-transport catalysis mechanism was first considered, because the proton affinity of H_2O (PA = 691 kJ/mol[5]) meets the PA criterion for PTC of $CH_3COH^{+\bullet}$ to $CH_3CHO^{+\bullet}$, lying between the PA value of the C and O sites of the $CH_3CO^{\bullet}$ radical (PA [$CH_3CO^{\bullet}$]at O = 679 kJ/mol[6] and at C = 694 kJ/mol[6]). For the tautomerization from $CH_3COH^{+\bullet}$ to $CH_2CHOH^{+\bullet}$, PA of H_2O does not fall in the range of the PA values of the two C atoms in the $CH_2C^{\bullet}OH$ radical. These PA values are estimated to be 882 ± 15 kJ/mol and 788 ± 15 kJ/mol, respectively, by the following method. The effect of -OH substitution at an olefinic carbon or at a hydrocarbon radical site can readily be estimated from available data in NIST Chemistry WebBook and Handbook of Bond Dissociation Energies in Organic Compounds by Luo[24], and it lies in the range -177 ± 12 kJ/mol. Δ_fH [$CH_2C^{\bullet}OH$] can thus be given a value of (300 ± 3 - 177 ± 12= 123 ± 15) kJ/mol. Even with this uncertainty, the PA of this radical at methylene (788 ± 15 kJ/mol) and at the radical site (882 ± 15 kJ/mol) are both high above that of H_2O, PA = 691 kJ/mol.

The energy barrier of the rearrangement between isolated $CH_3COH^{+\bullet}$ and $CH_3CHO^{+\bullet}$ was calculated by Bouchoux et al.[25] as 143 kJ/mol which is above the dissociation limit (121 kJ/mol) for the loss of the hydroxyl-$H^{\bullet}$ from $CH_3COH^{+\bullet}$. In the present study, the PES (Figure 6.4) obtained from the G3 calculations shows that a water molecule catalyzes two-step H-shifts in converting $CH_3COH^{+\bullet}$ to $CH_3CHO^{+\bullet}$. Starting

from the $[CH_3COH^{+\bullet}\cdots OH_2]$ complex (Structure VII), the water molecule abstracts a proton from $CH_3CHO^{+\bullet}$ to form stable state I, $[CH_3CO^{\bullet}\cdots H^+OH_2]$, via a very flat transition state (TS1/7). Next, the water "transports" the H^+ between the C and O site of the $CH_3CO^{\bullet}$ radical via TS1/2, followed by the production of the ion $[CH_3CHO^{+\bullet}/OH_2]$ (complex II), as shown in Equation 6.3.

$$CH_3COH^{+\bullet} + H_2O \rightarrow [CH_3COH^{+\bullet}/OH_2] \rightarrow [CH_3CO^{\bullet}/H^+OH_2]$$
$$\rightarrow [CH_3CHO^{+\bullet}/OH_2] \rightarrow CH_3CHO^{+\bullet} + H_2O \qquad 6.3$$

The energy barriers, TS1/2 (-76 kJ/mol) and TS1/7 (-42 kJ/mol), involved in the above process are lower than the dissociation thresholds to $CH_3COH^{+\bullet} + H_2O$ (49 kJ/mol) or to $CH_3CHO^{+\bullet} + H_2O$ (0 kJ/mol), and so water can indeed catalyze the isomerization from $CH_3COH^{+\bullet}$ to $CH_3CHO^{+\bullet}$. However, the reverse reaction in Equation 6.2 does not occur, i.e. starting from the $CH_3CHO^{+\bullet} + H_2O$ bimolecular reactant pair cannot produce $CH_3COH^{+\bullet} + H_2O$ because the dissociation energy for the latter is too high and so only $CH_3CHO^{+\bullet}$ would be the observed product. Therefore, in bimolecular reactions, whether or not a PTC process can be observed depends on the starting point and on the initial internal energy carried in the bimolecular reactants. For the unimolecular reactions of a given ion's structure, interconversions among all the stable structures that lie below or close above its lowest dissociation limit will be observed in the MI time frame.

We have also observed that a water molecule catalyzes the 1,2 H-shift between C and C sites in a $CH_2{}^{\bullet}COH$ radical (TS4/7, 34 kJ/mol), resulting in the generation of $CH_2CHOH^{+\bullet}$ and water. The reaction is represented by Equation 6.4.

$$CH_3COH^{+\bullet} + H_2O \rightarrow [CH_3COH^{+\bullet}/OH_2] \rightarrow$$
$$[CH_2CHOH^{+\bullet}/OH_2] \rightarrow CH_2CHOH^{+\bullet} + H_2O \qquad 6.4$$

G2 calculations by Bouchoux et al.[25] showed that the energy barrier of the 1,2 H-shift for isolated $CH_3COH^{+\bullet}$ and $CH_2CHOH^{+\bullet}$ ions is 7 kJ/mol lower than the energy barrier to the dissociation of $CH_3COH^{+\bullet}$ to CH_3CO^+ and $H^{\bullet}$. As shown in the PES (Figure 6.4), the water-assisted transition state (TS4/7) for such a 1,2-H shift is 15 kJ/mol lower than the dissociation limit of $[CH_3COH^{+\bullet}/H_2O]$ to $CH_3COH^{+\bullet}$ and H_2O. Therefore, the 1,2 H-shift energy barrier is lowered by the water-catalyst by ca. 8 kJ/mol.

In previous studies[26,27] as described in Chapter 4 and 5, we found that the keto-enol isomerization of acetaldehyde and acetone occurred in the presence of a distonic methanol, $^{\bullet}CH_2OH_2^+$, via a H-atom transfer mechanism. Calculations have been performed to examine whether or not H_2O catalyzed the H-atom transfer process for the rearrangement of $CH_3CHO^{+\bullet}$ to $CH_2CHOH^{+\bullet}$. The reaction path is given by the PES shown in Figure 6.5. The reaction is shown in Equation 6.5.

$$CH_3CHO^{+\bullet} + H_2O \rightarrow [CH_3CHO^{+\bullet}/H_2O] \rightarrow [CH_3CHOH^+/{}^{\bullet}OH]$$
$$[CH_2CHOH^{+\bullet}/OH_2] \rightarrow CH_2CHOH^{+\bullet} + H_2O \qquad 6.5$$

A H-atom is transferred from the H_2O to $CH_3CHO^{+\bullet}$ in the $[CH_3CHO^{+\bullet}/H_2O]$ complex (structure VIII) to form the $[CH_3CHOH^{+}/^{\bullet}OH]$ complex (Structure III), and this is followed by a methyl-H migration to the $^{\bullet}OH$ group to form $[CH_2CHOH^{+\bullet}/H_2O]$ (complex IV) via TS3/4 (45 kJ/mol). Note that complexes VIII and II (see Figure 6) are isomers of $[CH_3CHO^{+\bullet}/H_2O]$; the latter is more stable and can be reached by the former via TS2/8 (-11 kJ/mol). A high energy barrier (TS3/8, 85 kJ/mol) is involved in the rearrangement from III to VIII and thus makes a H-atom transfer mechanism energetically unfavourable.

6.4 Conclusions

The $[CH_3CHO/H_2O]^{+\bullet}$, ion **1**, made by the CID of an appropriate proton-bound dimer, carries sufficient internal energy to undergo metastable ion dissociations in the 3FFR of the mass spectrometer. The product ion from the loss of H_2O has been shown to have the $CH_2CHOH^{+\bullet}$ structure by isotopic labelling experiments, indicating that rearrangement occurs prior to the dissociation. Theoretical calculations were used to analyze the rearrangement and dissociation reactions of this complex ion and were found to involve no less than eight stable isomers of $[CH_3CHO/H_2O]^{+\bullet}$. The interconversions among these stable isomers can be observed so long as transition state energy barriers lie below the dissociation limit of the initial ion structure. These methods provide us with an insight into the chemistry of these ion-molecule complexes, rather than only to focus on the production of keto, enol or carbene ions. As the PA rule predicts, water is able to catalyze the proton transfer processes for the isomerization of $CH_3COH^{+\bullet}$ to $CH_3CHO^{+\bullet}$.

The rearrangement of $CH_3COH^{+\bullet}$ to $CH_2CHOH^{+\bullet}$ involves a water-catalyzed 1,2 H-shift mechanism. $CH_3CHO^{+\bullet}$ cannot be enolized by water to $CH_2CHOH^{+\bullet}$ via either PTC or a H-atom transfer mechanism.

Hydrogen-bridged water complexes ($[X\cdots H^+OH_2]$ shown in detail in Fig. 8) have been found to be the major products of the losses of CO and $^{\bullet}CH_3$. An unexpected CO loss produced the $[^{\bullet}CH_3\cdots H_3O^+]$ ion via a backside displacement mechanism. The metastable ion of $[CH_3CHO/H_2O]^{+\bullet}$ can lose the $^{\bullet}CH_3$ via two reaction channels and the products have been shown by computations to be $[OC\cdots H_3O^+]$ and $[CO\ldots H_3O^+]$. The 298 K enthalpies of this two fragments are $\Delta_fH[OC\cdots H_3O^+]$ = 420 kJ/mol and $\Delta_fH[CO\cdots H_3O^+]$ = 448 kJ/mol (from G3 results).

References

(1) Mourgues, P.; Audier, H. E.; Leblanc, D.; Hammerum, S. *Org. Mass Spectrom.* **1993**, *27*, 1098.

(2) Audier, H. E.; Leblanc, D.; Mourgues, P.; McMahon, T. B. *J. Chem. Soc., Chem. Commun.* **1994**, *20*, 2329.

(3) Gauld, J. W.; Audier, H.; Fossey, J.; Radom, L. *J. Am. Chem. Soc.* **1996**, *118*, 6299.

(4) Gauld, J. W.; Radom, L. *J. Am. Chem. Soc.* **1997**, *119*, 9831.

(5) Hunter, E. P. L.; Lias, S. G. *J. Phys. Chem. Ref. Data* **1998**, *27*, 413.

(6) Nedev, H.; van der Rest, G.; Mourgues, P.; Audier, H. E. *Eur. J. Mass Spectrom.* **2003**, *9*, 319.

(7) Cao, J.; Sun, W.; Holmes, J. L. *Int. J. Mass Spectrom.* **2002**, *217*, 179.

(8) Holmes, J. L.; Mayer, P. M. *J. Phys. Chem.* **1995**, *99*, 1366.

(9) Busch, K. L.; Glish, G. L.; McLuckey, S. A. *Mass Spectrometry/Mass Spectrometry Techniques and Applications of Tandem Mass Spectrometry*; VCH Publishers: New York, 1988.

(10) Rennie, E.; Mayer, P. M. *J. Chem. Phys.* **2004**, *120*, 10561.

(11) Hehre, W. J.; Radom, L.; Schleyer, P. v. R.; Pople, J. A. *Ab Initio Molecular Orbital Theory*; John Wiley & Sons: New York, 1986.

(12) Frisch, M. J.; Trucks, G. W.; Schlegel, H. B.; Scuseria, G. E.; Robb, M. A.; Cheeseman, J. R.; Zakrzewski, V. G.; Montgomery, J. A.; Stratmann, R. E.; Burant, J. C.; Dapprich, S.; Millam, J. M.; Daniels, A. D.; Kudin, K. N.; Strain, M. C.; Farkas, O.; Tomasi, J.; Barone, V.; Cossi, M.; Cammi,

R.; Mennucci, B.; Pomelli, C.; Adamo, C.; Clifford, S.; Ochterski, J.; Petersson, G. A.; Ayala, P. Y.; Cui, Q.; Morokuma, K.; Malick, D. K.; Rabuck, A. D.; Raghavachari, K.; Foresman, J. B.; Cioslowski, J.; Ortiz, J. V.; Stefanov, B. B.; Liu, G.; Al-Laham, A.; Peng, C. Y.; Nanayakkara, A.; Gonzalez, C.; Challacombe, M.; Gill, P. M. W.; Johnson, B.; Chen, W.; Wong, W. W.; Andres, J. L.; Gonzalez, C.; Head-Gordon, M.; Replogle, E. S.; Pople, J. A. *"GAUSSIAN 98 Rev. A. 7"*; Gaussian Inc.: Pittsburgh, PA, 1998.

(13) Becke, A. D. *Phys. Rev. A* **1988**, *38*, 3098.

(14) Lee, C.; Yang, W.; Parr, R. G. *Phys. Rev. B* **1988**, *37*, 785.

(15) Curtiss, L. A.; Raghavachari, K.; Redfern, P. C.; Rassolov, V.; Pople, J. A. *J. Chem. Phys.* **1998**, *109*, 7764.

(16) Baboul, A. G.; Curtiss, L. A.; Redfern, P. C.; Raghavachari, K. *J. Chem. Phys.* **1999**, *110*, 7650.

(17) Scott, A. P.; Radom, L. *J. Phys. Chem.* **1996**, *100*, 16502.

(18) Nicolaides, A.; Rauk, A.; Gluckhovtsev, M. N.; Radom, L. *J. Phys. Chem.* **1996**, *100*, 17460.

(19) Holmes, J. L. In *The Encyclopedia of Mass Spectrometry*; Armentrout, P. B., Ed.; Elsevier: Amsterdam, 2003; Vol. 1, pp 91.

(20) van der Rest, G.; Nedev, H.; Chamot-Rooke, J.; Mourgues, P.; McMahon, T. B.; Audier, H. E. *Int. J. Mass Spectrom.* **2000**, *202*, 161.

(21) *NIST Chemistry Webbook; NIST Standard Reference Database Number*; National Institute of Standards and Technology: Gaithersburg MD, 1998.

(22) Lias, S. G.; Bartmess, J. E.; Liebman, J. G.; Holmes, J. L.; Levin, R. D.; Mallard, W. G. *J. Phys. Chem. Ref. Data* **1988**, *17, Suppl. 1.*, 1.

(23) Chalk, A. J.; Radom, L. *J. Am. Chem. Soc.* **1997**, *119*, 7573.

(24) Luo, Y.-R. *Handbook of Bond Dissociation energies in Organic Compounds*; CRC Press: Boca Raton, 2003.

(25) Bertrand, W.; Bouchoux, G. *Rapid Commun. Mass Spectrom.* **1998**, *22*, 1697.

(26) Wang, X.; Holmes, J. L. *Int. J. Mass Spectrom.* **2005**, *242*, 75.

(27) Wang, X.; Holmes, J. L. *Can. J. Chem.* **2005**, *83*, 1903.

CHAPTER 7

THE UNEXPECTED DISSOCIATION OF IONIZED 2,3-PENTANEDIONE AND RELATED DIKETONES

7.1 Introduction

The McLafferty rearrangement takes place among a wide variety of organic radical cations.[1-3] Carbonyl groups are particularly typical hydrogen acceptors and therefore this rearrangement is common to almost all aliphatic aldehydes, ketones, carboxylic acids, esters and amides, giving rise to odd-electron enol ions as the primary fragments by the loss of an alkene molecule.[4] Diketone cations contain two carbonyl groups functioning as efficient hydrogen atom acceptors and so they would be expected to undergo McLafferty rearrangement if there is a H-atom γ- to one (or both) of the C=O groups. 2,3-Pentanedione is the smallest diketone that could display a McLafferty rearrangement and the reaction would involve the loss of an ethene molecule, $(M-28)^{+\bullet}$ as shown in Scheme 7.1.

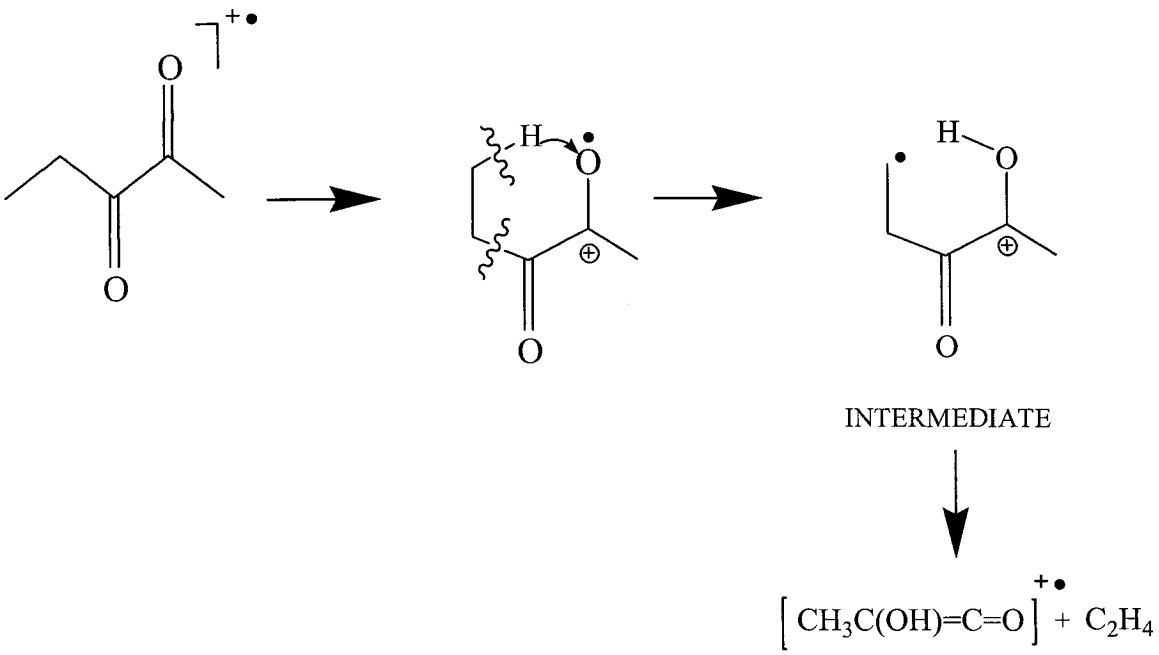

Scheme 7.1. The McLafferty rearrangement of ionized 2,3-pentanedione leading to the loss of C_2H_4.

Very recently, Kercher et al.[5] determined the 298 K heats of formation (Δ_fH^o) of the propanoyl ion and radical and of ionized 2,3-pentanedione itself by the use of threshold photoelectron photoion coincidence (TPEPICO) spectroscopy. This chapter describes the investigation of the unimolecular dissociations of ionized 2,3-pentanedione and its homologues 2,3-butanedione and 3,4-hexanedione. These three compounds are pale yellow liquids and are used as flavouring agents to give a pleasant taste and a sweet odour to a variety of foods, such as margarine, candies and some beers.[6]

Low internal energy (metastable ion dissociation) and relatively higher internal energy processes (collision-induced dissociation) for such ionized diketones have been examined. The typical flight-time of a MI in a sector mass spectrometer is 10^{-4}-10^{-6} s

during which time they decompose in a field-free region of the instrument[7,8]. In this study, the 2,3-pentanedione radical cation was observed to apparently undergo a McLafferty rearrangement in the MI time-frame, but unexpectedly giving a composite peak. As will be described below, this arises because CO loss competes with the ethene loss. The energy barriers for fragmentation channels of 2,3-pentanedione were determined by G3//B3-LYP6-31+G(d) calculations. By combining the interpretation of the mass spectra with computational analysis, the fragmentation for each reaction has been identified. The 298 K heats of formation of new products are determined from the G3 energies and are compared with the experimentally estimated values. A PES for the gas-phase reactions of ionized 2,3-pentanedione will be also given in Section 7.3. In addition, the behaviours of the homologues, 2,3-butanedione and 3,4-hexanedione have been also investigated for a serial study of the decarbonylation process in ionized diketones.

7.2 Experimental and Theoretical Section

All experiments were carried out on a modified VG-ZAB tandem mass spectrometer [9] with BEE geometry (VG Analytical, Manchester, U.K.). Metastable ion (MI) and collision-induced dissociation (CID) mass spectra of the ionized diketone molecules were observed in the second field-free region (2FFR) of the mass spectrometer. The ion accelerating voltage was 8 kV. Helium was used as the collision gas for the CID experiments. The fragment ions generated in the 2FFR from the mass selected ionized diketones were energy selected by the first electrostatic analyzer and transmitted into the 3FFR to study their MI and CID characteristics to aid their structure identification. All

spectra were recorded with the ZABCAT program developed by Mommers Technologies[9].

The ionized molecules were generated in a low pressure ion source[10] by 70 eV electron impact ionization. Liquid samples were introduced into the source via a liquid septum inlet. The compounds $CH_3CH_2COCOCH_2CH_3$, $CH_3CH_2COCOCH_3$, $CH_3COCOCH_3$, $CH_3CH_2COCH_3$ and CH_3COCH_3 were of research grade and were purchased from Aldrich and were used without further purification.

The GAUSSIAN 98 programs[11] were used to perform standard ab initio molecular orbital calculations to investigate the potential energy surface (PES). Optimized geometries and the energies of all minima and transition states were calculated at the B3-LYP/6-31+G(d) level of theory. Zero point energies obtained from calculations of vibrational frequencies at the same level of theory were scaled by a factor of 0.9806.[12] A single point energy calculation at the G3 level of theory on the optimized ion structures at the B3-LYP/6-31+G(d) level of theory was applied to obtain accurate relative energies and also the heat of formation of the new ion, $CH_3C(OH)=C=O^{+\bullet}$, resulting from the loss of ethene from ionized 2,3-pentanedione.

7.3 Results and Discussion

7.3.1 The 2,3-Pentanedione Radical Cation

7.3.1.1 The MI and CID Mass Spectra of Ionized 2,3-pentanedione

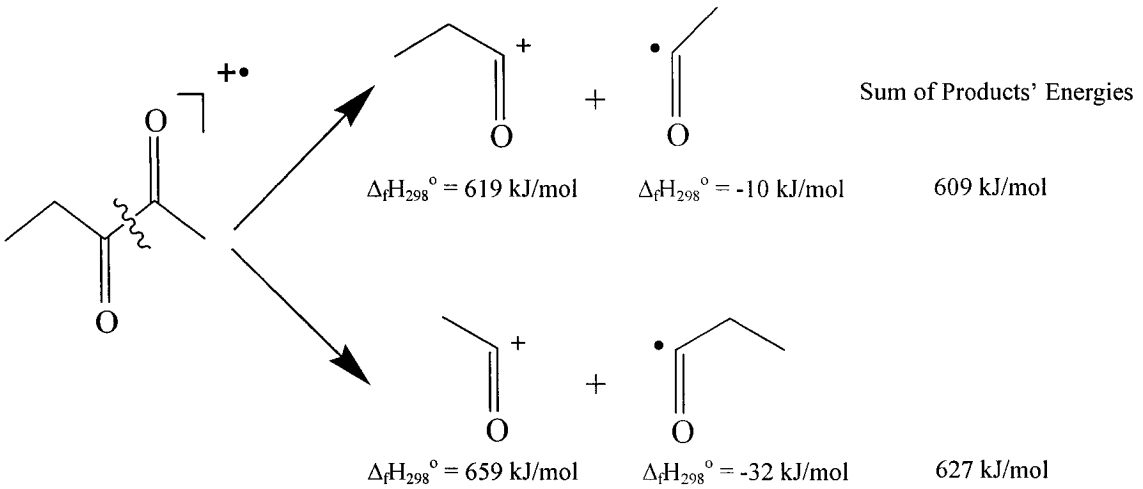

Scheme 7.2. The simple bond dissociation paths of ionized 2,3-pentanedione.

There are two competing dissociations, as shown in Scheme 7.2, arising from the cleavage of the 2,3 C-C bond, the weakest bond in the radical cation, leading to the formation of the propanoyl ion (m/z 57) and an acetyl radical and the generation of the acetyl cation (m/z 43) and a propanoyl radical. The enthalpy values for CH_3CO^+ and $CH_3CO^\bullet$ have been determined by Fogleman et al.[13] as $\Delta_fH^\circ[CH_3CO^+]$ = 659 kJ/mol (very close to the earlier result of Traeger et al., 656 kJ/mol[14]) and $\Delta_fH^\circ[CH_3CO^\bullet]$ = -10 kJ/mol[15]. The heat of formation of the $C_2H_5CO^+$ ion has been recently measured as 619 kJ/mol by Kercher[5], in very good agreement with Harvey and Traeger's value of 617.8 ± 0.9 kJ/mol[16]. The product energies given in Scheme 7.2 show that the first dissociation channel (to produce the $C_2H_5CO^+$ ion) is energetically more favourable than the second, (to yield the CH_3CO^+ ion) by ca. 18 kJ/mol. Thus in the metastable ion mass spectrum of ionized 2,3-pentanedione (Figure 7.1-A) the base peak is m/z 57, i.e. the propanoyl ion, with a very much weaker signal corresponding to the acetyl ion (m/z 43), only ca 3% of

m/z 57. Kercher et al. could not measure a threshold for m/z 43. Because these ions arise from a simple 2,3 C-C bond cleavage, the collision-induced dissociation (CID) mass spectrum of ionized 2,3-pentanedione (Figure 7.1-B) showed that the peaks for $C_2H_5CO^+$ and CH_3CO^+ are both strongly sensitive to collision gas.

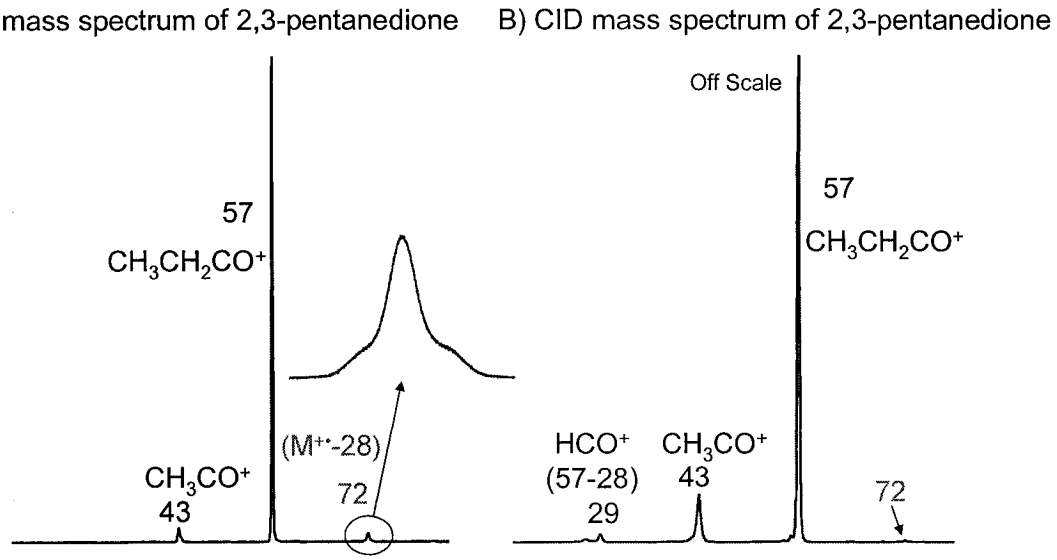

Figure 7.1. (A) Metastable ion (MI) and (B) collision-induced dissociation (CID) mass spectra of ionized 2,3-pentanedione.

The MI mass spectrum however also shows a small composite peak corresponding to m/z 72 (ca. 1.6% of m/z 57), the loss of 28 mass units from the ionized diketone. It is expected to arise from the McLafferty rearrangement of the molecular ion, leading to C_2H_4 loss. This MI peak was wholly insensitive to collision gas signifying that the mass selected precursor ion has undergone rearrangement prior to this fragmentation.[17] The composite peak consists of a large kinetic energy release (KER) component, giving rise to the broad base and a small KER component at the peak's center

(Figure 7.1). This could result from the metastable ion undergoing two competing dissociations to give fragment ions of different structures[7] or less likely, from two transition states leading to a single product ion. The structure of each component of the composite peak was identified as follows. Slices of this peak (from the edge or at the centre) were transmitted by the electrostatic analyzer into the third field-free region (3FFR), where the CID characteristics of the ions in these slices were recorded. The CID mass spectrum of each component of the $(M-28)^{+\bullet}$ peak is shown in Figure 7.2. That of the large kinetic energy release (KER) component produced two major fragment ions (m/z 43 and m/z 57), as shown in Figure 7.2-B. This CID mass spectrum is identical to that of ionized 2-butanone (Figure 7.2-C), showing that the large KER component arises from the loss of CO from a rearranged ionized 2,3-pentanedione. The large kinetic energy release indicates that the reaction has a significant reverse energy barrier[7]. This dissociation thus requires a rearrangement of the 2,3-pentanedione ion to an isomeric species, over an energy barrier that is higher than that of the thermochemical dissociation limit for the decarbonylation reaction. The reaction path includes the stable state and transition state structures that are shown in the potential energy surface for ionized 2,3-pentanedione (see Figure 7.3). The loss of a CO molecule is commonly observed in the (MI) mass spectra of ionized organic ions that contain one or more than one carbonyl groups, such as esters, phenols, acetamides and diketones[18-22]. In all the above systems, the low-energy (metastable) ion undergoes decarbonylation via a rearrangement process and so in the present example the hidden mechanism of the decarbonylation is worth discovering. Although such rearrangements involve an energy barrier, the production of the low energy CO molecule ($\Delta_f H°(CO)$ = -110.53 kJ/mol[23]) makes the decarbonylation reaction able to compete with other fragmentation processes.

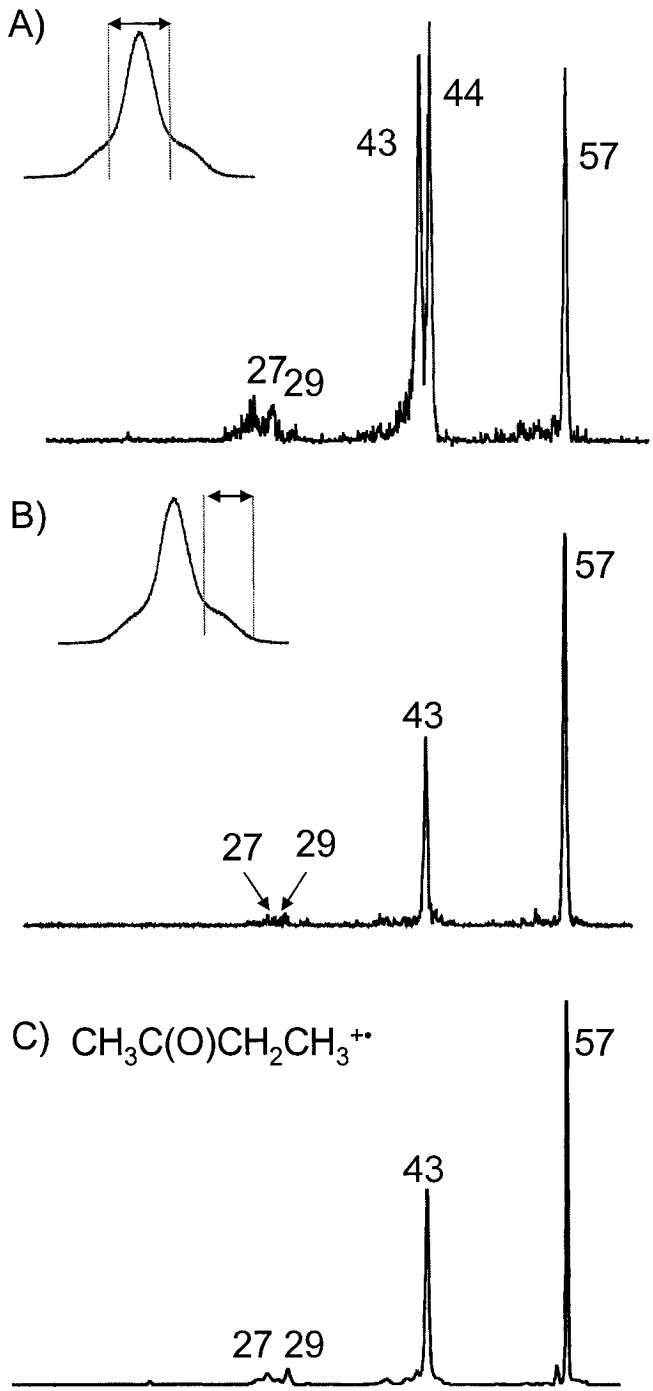

Figure 7.2. CID mass spectra of (A) the middle and (B) the edge component of the composite $(M-28)^{+\bullet}$ peak and (C) ionized 2-butanone.

The centre of the $(M-28)^{+\bullet}$ ion peak contains fragments resulting from both components, i.e. it is contaminated by some ionized 2-butanone (the broad component). However the CID mass spectrum contains an intense signal at m/z 44 which does not appear in the CID mass spectrum of the 2-butanone ion and so must arise from the dissociation of the centre ion structure. The 2,3-pentanedione ion contains a carbonyl group (at atom 2) that can accept a γ-hydrogen from the ethyl group via a McLafferty rearrangement. The product ion is a hydroxyl-substituted methylketene. The computations showed that this 1,5-H transfer process leads to an intermediate (structure III in Figure 7.4) which can lose ethene by cleavage of the α-β bond in ion (III) and the detailed mechanism is described in the section below.

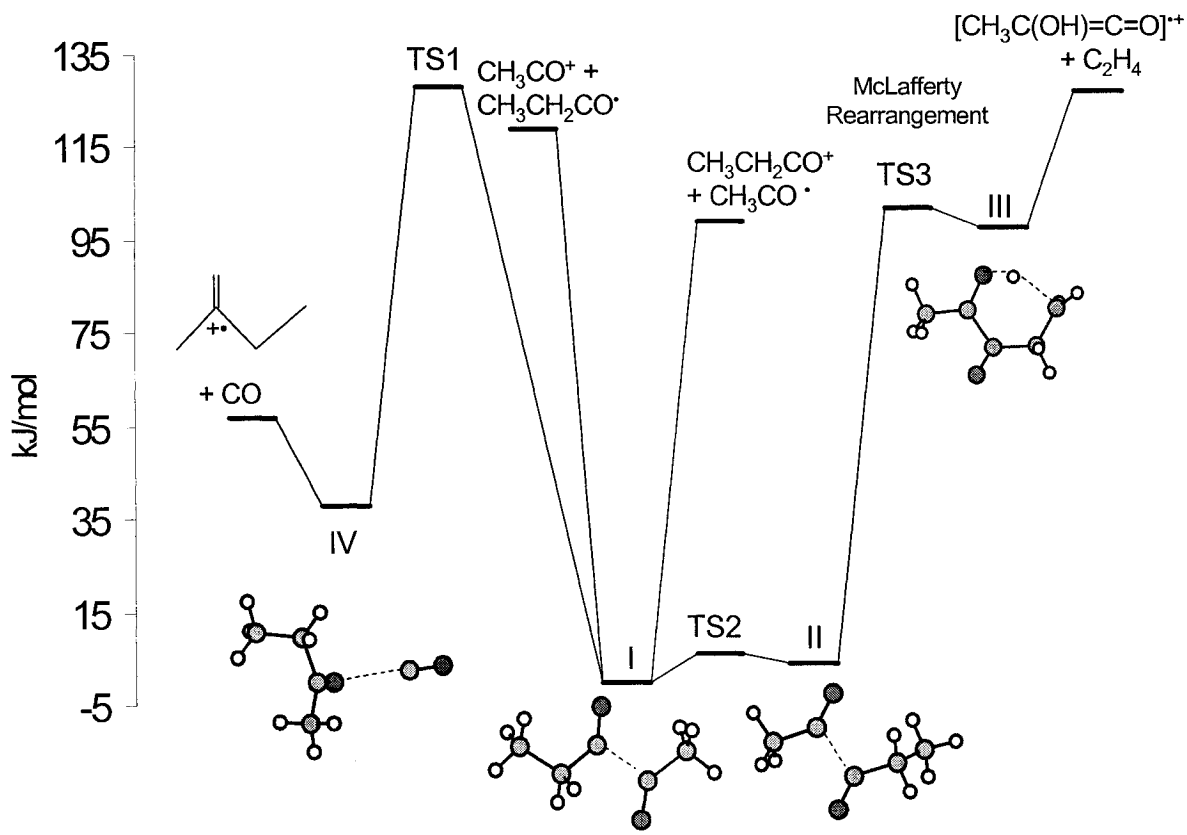

Figure 7.3. Potential energy surface of the 2,3-pentanedione radical cation.

7.3.1.2 The Potential Energy Surface of Ionized 2,3-Pentanedione

Calculations at the G3//B3-LYP level of theory were performed to produce a PES for ionized 2,3-pentanedione. Also investigated were the mechanisms of the isomerizations for the losses of CO and C_2H_4. The energies (in kJ/mol) shown on the PES are relative to the calculated energy of the global minimum I of ionized 2,3-pentanedione, obtained at the B3-LYP/6-31+G(d) and G3 level of theories, and are given in Table 7.1. The 0 K potential energy profile is shown in Figure 7.3.

Table 7.1. Calculated relative energies, E_{rel} (in kJ mol^{-1}) at 0 K for the different structures obtained from B3-LYP/6-31+G(d) and G3 levels of theory.

Structures	B3-LYP/6-31+G(d) E_{rel} (0 K)	G3 E_{rel} (0 K)
I	0	0
II	5	4
III	114	98
IV	50	38
TS1	142	128
TS2	5	6
TS3	108	102
$CH_3CH_2CO^+ + CH_3CO^{\bullet}$	106	99
$CH_3CH_2CO^{\bullet} + CH_3CO^+$	129	119
$CH_3CH_2C^{+\bullet}(=O)CH_3 + CO$	62	57
$CH_3C^{+\bullet}(OH)CO + C_2H_4$	163	127

The ground state of ionized 2,3-pentanedione is a loosely C_2-C_3 bonded species (see in Figure 7.4, the geometry of ion I). This is similar to that described by Meurer et al.[24], who regarded it as a loosely electron-bonded acylium ion dimer: R_1-C=O^+···e^- ···$^+$O=C-R_2. In their paper, they observed m/z 43 ion as the base peak in the 70 eV EI mass spectrum of 2,3-pentanedione ion, contrary to their expectation based on the ionization energies of the two keto-radicals, (IE ($CH_3CO^•$) =7.0 eV[25] and IE ($CH_3CH_2CO^•$) = 6.75 eV[15], not 5.7 eV as quoted in [24]). However when all the fragment ions arising from further dissociation of the m/z 57 and m/z 43 ions are summed, the apparent discrepancy disappears.

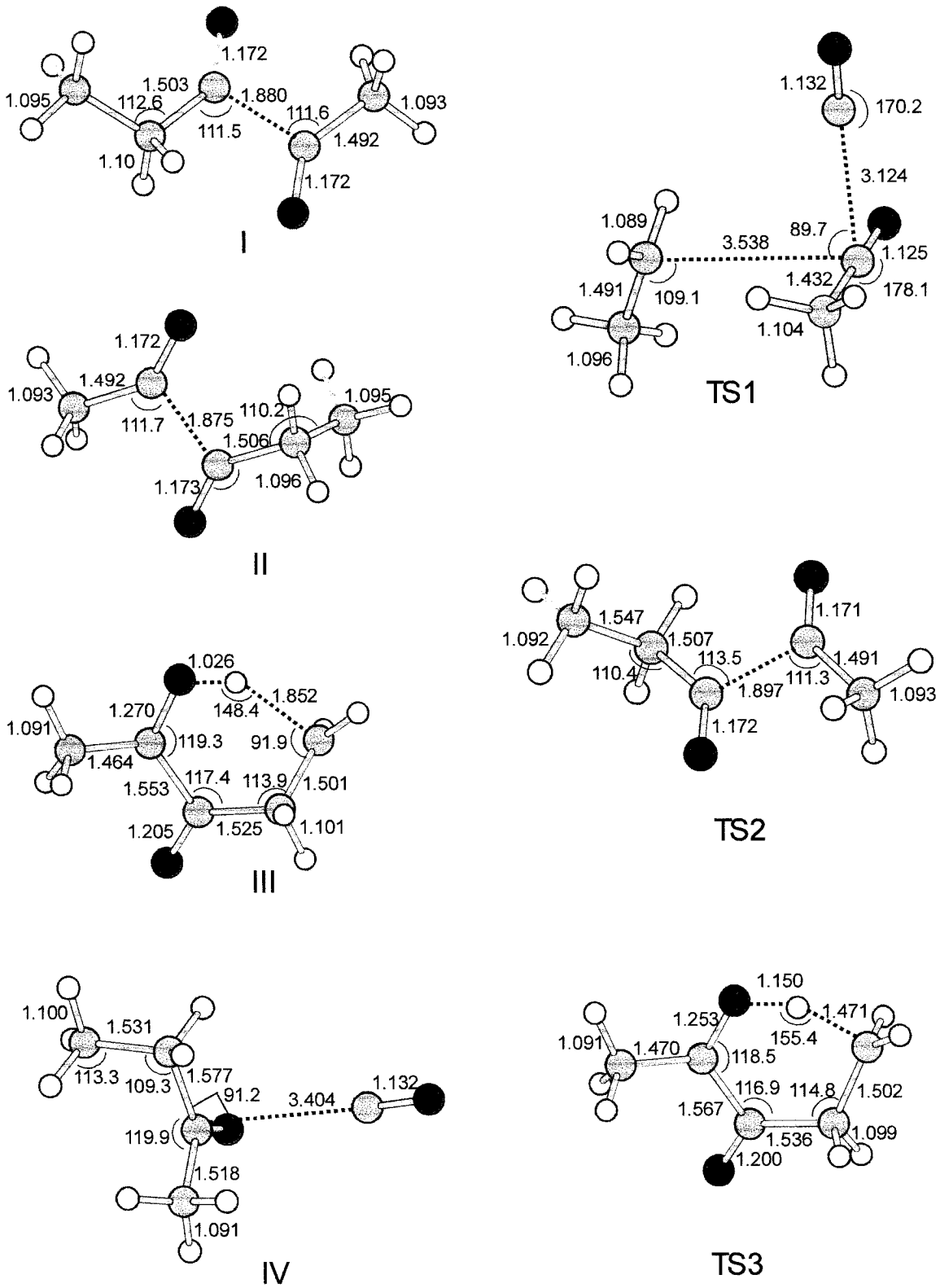

Figure 7.4. Optimized geometries of the stable and transition states at the B3-LYP/6-31+G(d) level of theory.

The calculated dissociation limits are 99 kJ/mol and 119 kJ/mol respectively, corresponding to the two simple bond fragmentations in the 2,3-pentanedione ion. The PES also shows that the energy barriers for the two competing 28 amu loss channels are very close, i.e. 128 kJ/mol and 127 kJ/mol resulting from the loss of CO and C_2H_4, respectively. For the CO loss, the 2,3-pentanedione ion, I, rearranges to the stable state IV (38 kJ/mol) via TS1 (128 kJ/mol), an energy at which the three other dissociation processes can all kinetically compete within the MI time-frame. Stable state IV is represented as a 2-butanone ion electrostatically bound to CO by a long bond (3.404 Å), as shown in Figure 7.4. The reverse activation energy barrier for this CO loss reaction is ca. 90 kJ/mol (128 kJ/mol - 38 kJ/mol) and this is in keeping with the significant KER peak observed in the MI mass spectrum (Figure 7.1). In contrast, the loss of C_2H_4 does not involve a reverse energy barrier. TS3 is a 6-membered cyclic transition state for the 1,5-H transfer, corresponding to the McLafferty rearrangement and it lies at ca. 102 kJ/mol on the PES, which is ca. 25 kJ/mol below the dissociation threshold (127 kJ/mol) for the C_2H_4 loss. Structure III, having a distonic ion structure, is the intermediate for this McLafferty rearrangement process and it loses ethene by cleavage of the α-β bond to produce a new ion, $CH_3C^{+\bullet}(OH)C=O$, 2-hydroxymethyl ketene. Stable structure II is an isomer of ground state I, in which the ethyl group rotates and approaches the acetyl carbonyl group ($CH_3\underline{C=O}$), followed by the McLafferty rearrangement.

The PES also summarizes the dissociation and rearrangement energy barriers for all the processes in the MI mass spectrum of 2,3-pentanedione. The energy difference between the highest and the lowest barrier is 29 kJ/mol and so the internal energy of the

metastable ions lies in a 29 kJ energy band above the lowest dissociation limit. This energy range is typical for MI processes, giving relative peak abundances of from 1-2 % to 100%.

The calculated product energies at the B3LYP/6-31+G(d) and G3 level of theory are shown in Table 7.1. 298 K G3 results are further compared with experimental data in Table 7.2, which shows that the accuracy of G3 calculations for the products is quite good, with the differences falling in the range of ± 4 kJ/mol. Note that there is no direct experimental value for Δ_fH^o of the 2-hydroxymethyl ketene ion, $CH_3C^{+\bullet}(OH)CO$. This can however usefully be estimated using the empirical relationship between Δ_fH^o and ln (n) (n = the number of atoms in the ion) from the effect of –OH substitution in homologous ions.[26] $\Delta_fH^o[CH_3CH=C=O^{+\bullet}]$ = 783.5 ± 0.3 kJ/mol was determined by Traeger[27]; the substitution of –OH at C-2 lowered the enthalpy value by ca 185 kJ/mol (obtained from the slope of the Δ_fH^o vs ln (n) plot[26]), and thus $\Delta_fH^o[CH_3C^{+\bullet}(OH)C=O]$ was estimated to be 599 kJ/mol (784 – 185 kJ/mol). The calculated $\Delta_fH^o[CH_3C^{+\bullet}(OH)C=O]$ value 604 kJ/mol obtained from the G3 total energies (according to the atomization method reported by Nicolaides et al.[28]) is in good agreement with the estimated value.

Table 7.2. Comparison of the calculated product energies from the G3 level of theory (at 298 K) with experimental values.

Products	G3 Product Energies (298 K)	Experimental Product Energies (298 K)	E_{rel} (G3 – Exp. Value)
$CH_3CH_2CO^+ + CH_3CO^{\bullet}$	606	609	-3
$CH_3CH_2CO^{\bullet} + CH_3CO^+$	625	627	-2
$CH_3CH_2C^{+\bullet}(=O)CH_3 + CO$	570	566	4
$CH_3C^{+\bullet}(OH)=C=O + C_2H_4$	656	652*	4

*Experimental data uses the estimated $\Delta_fH°[CH_3C^{+\bullet}(OH)=C=O]$ = 599 kJ/mol, see the text.

Some additional comments deserve to be made concerning 2,3-pentanedione and its energetics. There is no experimental value for its $\Delta_fH°$ but it can most readily be estimated by additivity or an equivalent method. For example the known $\Delta_fH°$ for 2,3-butanedione is -327.2 kJ/mol[29]; addition of the difference between $\Delta_fH°[CH_3COCH_3]$ = -217.3 ± 0.7 kJ/mol[29], and $\Delta_fH°[CH_3COCH_2CH_3]$ = -238.7 ± 0.8 kJ/mol[29], namely -21.4 ± 1.5 kJ/mol, gives an estimated $\Delta_fH°[CH_3COCOCH_2CH_3]$ = -349 ± 2 kJ/mol, close to those reported by Kercher et al[5], -348 and -344 kJ/mol. The ground state of ionized 2,3-pentanedione was found to have a very long OC—CO bond (see Figure 7.4) and its $\Delta_fH°$ was computed to be 513.7 kJ/mol at the G3 level. The adiabatic Ionization Energy (IE) is thus only 8.94 eV, slightly below the previously reported value of 9.1 eV[5] estimated from the molecule's photoelectron spectrum. From ref 15, the vertical IE was ca 9.4 eV, leading to an ion $\Delta_fH°$ of 558 kJ/mol, an energy well on the way to the lowest

dissociation limit at 609 kJ/mol (to produce $C_2H_5CO^+$ + $CH_3CO^{\bullet}$). Note that the McLafferty intermediate, ion III, lies in only a shallow potential well, unlike the analogous distonic ions from simple ketones. (Δ_fH^o values for the latter can reliably be estimated using Proton Affinity (PA) data and alkyl C-H bond strengths; e.g. for $CH_3COCH_2CH_3^{+\bullet}$, Δ_fH^o = 677 kJ/mol[25], and $\Delta_fH^o[CH_3C^+(OH)CH_2CH_2^{\bullet}]$ = ca 667 kJ/mol, using PA[$CH_3COCH_2CH_3$] = 827 kJ/mol[30] and D[RCH_2-H] = 420 kJ/mol[15]). A computational exploration of alternative geometries for ion III did not disclose another minimum. The ion III is still less stable than its vertically ionized keto-analog, presumably as a result of a destabilizing influence by the (additional) CO group adjacent to the principal charge site (i.e. at $CH_3C^+(OH)$-); for example, the PA of $CH_3COCOCH_3$ is some 25 kJ/mol lower than that of $CH_3CH_2COCH_3$[30].

7.3.2 The Dissociation Characteristics of the 2,3-Butanedione and 3,4-Hexanedione Radical Cations

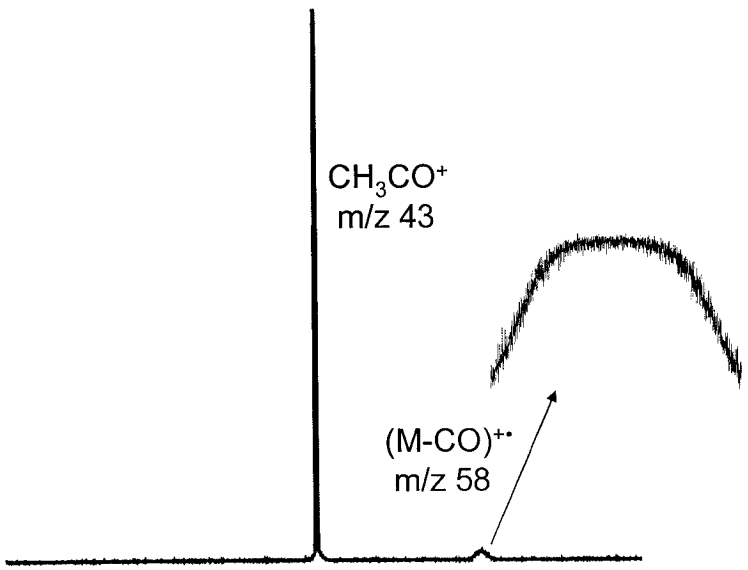

Figure 7.5. MI mass spectrum of ionized 2,3-butanedione (m/z 86).

We also investigated the dissociations of the homologous diketones, 2,3-butanedione and 3,4-hexanedione. The MI mass spectrum of ionized 2,3-butanedione (the biacetyl ion) is straightforward (Figure 7.5), producing the acetyl ion (m/z 43, 100%) and a weak m/z 58 ion (ca. 1.9%) resulting from the loss of 28 amu. The CID mass spectrum of this m/z 58 ion is the same as that of the acetone radical cation and so m/z 58 arises from the loss of CO from the ionized 2,3-butanedione, a reaction analogous to that described for 2,3-pentanedione. The MI signal at m/z 58 is a flat-topped peak with a significant KER showing that this reaction similarly has a reverse energy barrier. The calculated dissociation threshold for this CO loss channel is 40.5 kJ/mol lower than that for the generation of the acetyl ion, using the following established experimental data: $\Delta_f H^o[CH_3COCH_3^{+\bullet}]$= 719 kJ/mol[25] and $\Delta_f H^o(CO)$ = -110.5 kJ/mol[23], sum = 608.5 kJ/mol and $\Delta_f H^o[CH_3CO^+]$= 659 kJ/mol[13], $\Delta_f H^o[CH_3CO^\bullet]$= -10 kJ/mol[13], sum = 649 kJ/mol. The MI mass spectrum of 2,3-butanedione, with the acetyl ion as the base peak, indicates that the transition state for the CO loss reaction must lie above 649 kJ/mol, resulting in a significant KER. This result parallels the observations for the decarbonylation of ionized 2,3-pentanedione where the large KER component of the composite $(M-28)^{+\bullet}$ peak corresponded to CO loss with a remarkable energy difference between the transition state and the dissociation limit on the PES of 2,3-pentanedione.

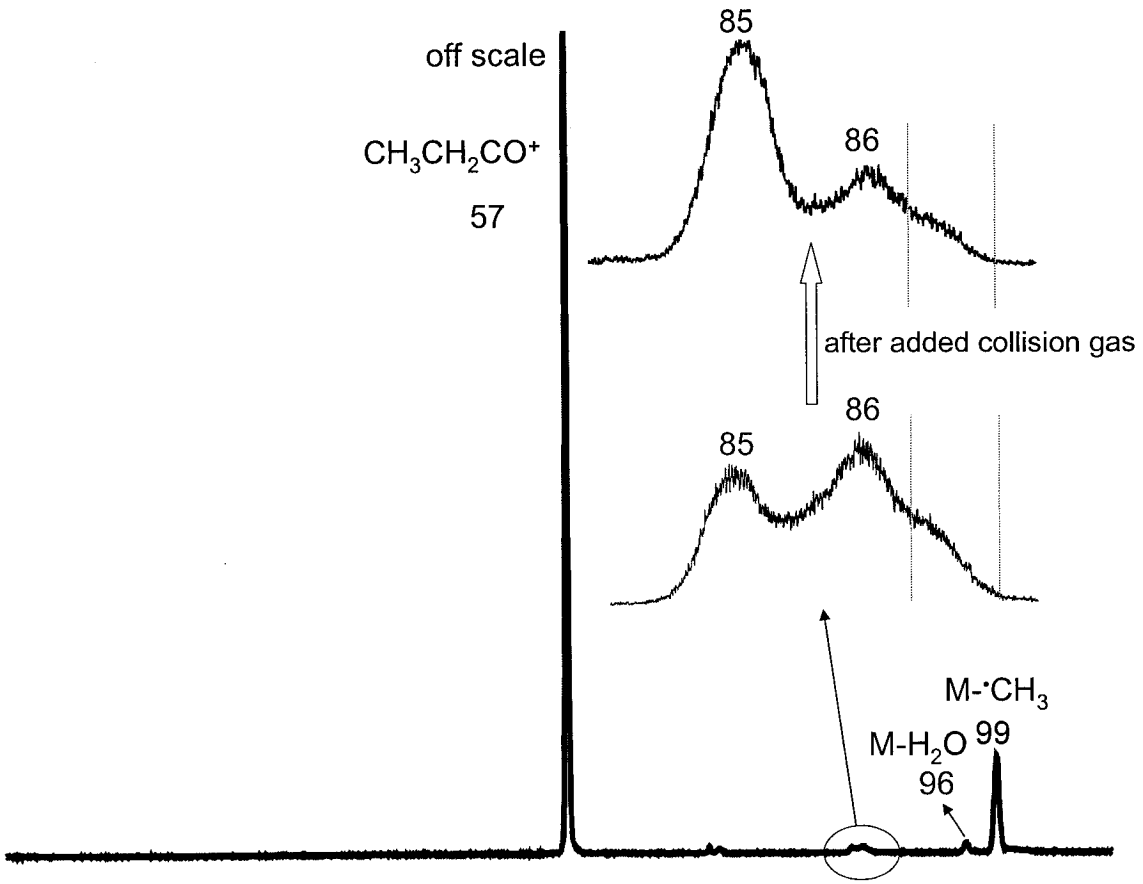

Figure 7.6. MI mass spectrum of ionized 3,4-hexanedione (m/z = 114).

Ionized 3,4-hexanedione is a symmetrical diketone and so the peak for the propanoyl ion (m/z 57 = 100%) dominates the MI mass spectrum (see Figure 7.6). There are however some minor MI peaks: m/z 99 (ca. 10%), m/z 96 (ca. 1%), resulting from the loss of a methyl radical $(M-15)^{+\bullet}$ and the loss of H_2O $(M-18)^{+\bullet}$, respectively and two very weak peaks at m/z 85 and m/z 86 (both < 1%). The m/z 86 peak (the loss of 28 amu) is composite, similar to the $(M-28)^{+\bullet}$ peak in the MI mass spectrum of ionized 2,3-pentanedione and thus can be expected to result from the loss of CO and C_2H_4. Because the large KER component of this composite peak was partially overlapped by the m/z 85 ion and because the signal was too weak, it was not transmitted to the next FFR in order

to investigate each component's structure. When collision gas was added (to single collision conditions), m/z 85 $(M-29)^{+\bullet}$ increased three fold, indicating that this ion arises from a simple bond cleavage, very likely the loss of an ethyl radical from the 3,4-hexanedione ion. We were asked (by T. Baer, private communication) whether the m/z 57 product ion consisted of more than one component. The CID mass spectra (Figure 7.7) of the m/z 57 ions from ionized 2,3-pentanedione, 3,4-hexanedione and 2-butanone generated in the ion source or as metastable ions, are identical and so there is no evidence for a second ion structure being present.

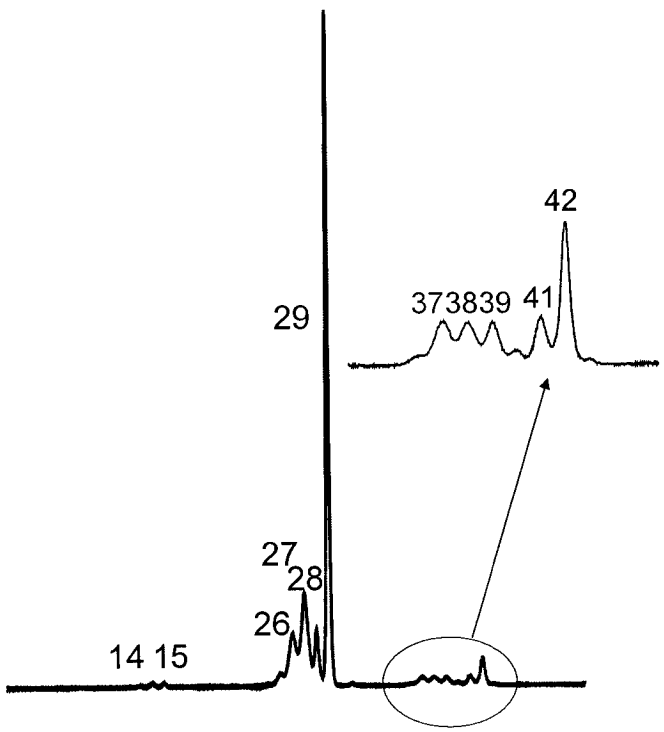

Figure 7.7. CID mass spectrum of the m/z 57 ion generated from the metastable ionized diketones.

The mass spectra do however contain very weak peaks at m/z 37, 38 and 39, indicating that a minor, high energy rearrangement can occur following collisional excitation. To check the hydrocarbon ion content of the m/z 42 ion in the above spectra, the m/z 42 fragment ion from a source-generated m/z 57 ion was transmitted into the 3FFR and its CID mass spectrum was recorded (Figure 7.8). This CID mass spectrum was identical with that of ionized ketene (which can directly be produced from ionized acetone) and shows no 37, 38 or 39 ions. We conclude that the hydrocarbon contamination in the m/z 57 ions is very minor indeed.

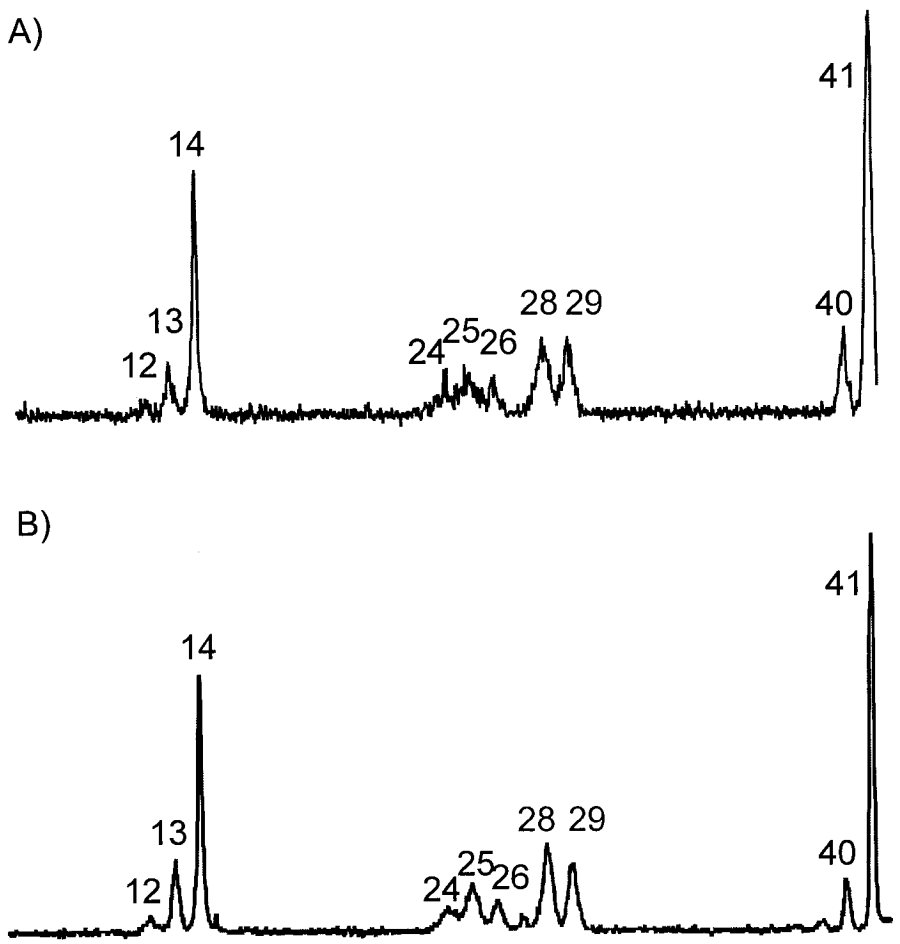

Figure 7.8. A) CID mass spectrum of the collision-generated m/z 42 ion produced from ionized 3,4- hexanedione; B) CID mass spectrum of ketene ion produced from ionized acetone.

7.4 Conclusions

The four competing processes for metastable 2,3-pentanedione cation are the simple bond cleavages to the losses of $CH_3CO^{\bullet}$, $CH_3CH_2CO^{\bullet}$, and the rearrangement dissociations to lose C_2H_4 and CO molecules. The energy barriers for these processes were placed on a potential energy surface computed at the G3 level of theory. Metastable dissociation of the 2,3-pentanedione radical cation gives rise to a composite metastable ion peak, m/z 72, resulting from the isobaric losses of CO and C_2H_4. These two fragmentation channels are energetically competitive (i.e. the transition states have similar energies.) and they yield $[CH_3C(O)CH_2CH_3]^{+\bullet}$ and $[CH_3C(OH)=C=O]^{+\bullet}$ respectively. The latter is a new ion, produced by a McLafferty rearrangement, and has Δ_fH^o = 604 kJ/mol, obtained from G3 calculations. The homologous ionized diketone 2,3-butanedione also displays the decarbonylation channel yielding $CH_3COCH_3^{+\bullet}$ and 3,4-hexanedione gives rise to a composite metastable ion peak from the losses of both CO and C_2H_4.

References

(1) Nicholson, A. J. C. *Trans. Faraday Soc.* **1954**, *50*, 1067.

(2) McLafferty, F. W. *Anal. Chem.* **1956**, *28*, 306.

(3) McLafferty, F. W.; Hamming, M. C. *Chem. Ind. (London)* **1958**, 1366.

(4) Turecek, F. In *Encyclopedia of Mass Spectrometry*; Elsevier: Amsterdam, 2005; Vol. 4, p 396.

(5) Kercher, J. P.; Fogleman, E. A.; Koizumi, H.; Sztaray, B.; Baer, T. *J. Phys. Chem. A* **2005**, *109*, 939.

(6) Coghe, S.; D'Hollander, H.; Verachtert, H.; Delvaux, F. R. *J. Inst. Brew.* **2005**, *111*, 51.

(7) Holmes, J. L.; Terlouw, J. K. *Org. Mass Spectrom.* **1980**, *15*, 383.

(8) Cooks, R. G.; Beynon, J. H.; Caprioli, R. M.; Lester, G. R. *Metastable Ions*; Elsevier: Amsterdam, 1973.

(9) Holmes, J. L.; Mayer, P. M. *J. Phys. Chem.* **1995**, *99*, 1366.

(10) Rennie, E.; Mayer, P. M. *J. Chem. Phys.* **2004**, *120*, 10561.

(11) Frisch, M. J.; Trucks, G. W.; Schlegel, H. B.; Scuseria, G. E.; Robb, M. A.; Cheeseman, J. R.; Zakrzewski, V. G.; Montgomery, J. A.; Stratmann, R. E.; Burant, J. C.; Dapprich, S.; Millam, J. M.; Daniels, A. D.; Kudin, K. N.; Strain, M. C.; Farkas, O.; Tomasi, J.; Barone, V.; Cossi, M.; Cammi, R.; Mennucci, B.; Pomelli, C.; Adamo, C.; Clifford, S.; Ochterski, J.; Petersson, G. A.; Ayala, P. Y.; Cui, Q.; Morokuma, K.; Malick, D. K.; Rabuck, A. D.; Raghavachari, K.; Foresman, J. B.; Cioslowski, J.; Ortiz, J. V.; Stefanov, B. B.; Liu, G.; Al-Laham, A.; Peng, C. Y.; Nanayakkara, A.; Gonzalez, C.; Challacombe, M.; Gill, P. M. W.; Johnson, B.; Chen, W.;

Wong, W. W.; Andres, J. L.; Gonzalez, C.; Head-Gordon, M.; Replogle, E. S.; Pople, J. A. *in "GAUSSIAN 98 Rev. A. 7"*; Gaussian Inc.: Pittsburgh, PA, 1998.

(12) Scott, A. P.; Radom, L. *J. Phys. Chem.* **1996**, *100*, 16502.

(13) Fogleman, E. A.; Kiozumi, H.; Kercher, J. P.; Sztaray, B.; Baer, T. *J. Phys. Chem. A* **2004**, *108*, 5288.

(14) Traeger, J. C.; McLoughlin, R. G.; Nicholson, A. J. C. *J. Am. Chem. Soc.* **1982**, *104*, 5318.

(15) Luo, Y.-R. *Handbook of Bond Dissociation energies in Organic Compounds*; CRC Press: Boca Raton, 2003.

(16) Harvey, Z. A.; Traeger, J. C. *J. Mass Spectrom.* **2004**, *39*, 802.

(17) Holmes, J. L. In *The Encyclopedia of Mass Spectrometry*; Armentrout, P. B., Ed.; Elsevier: Amsterdam, 2003; Vol. 1, pp 91.

(18) Burgers, P. C.; Holmes, J. L.; Hop, C. E. C. A.; Postma, R.; Ruttink, P. J. A.; Terlouw, J. K. *J. Am. Chem. Soc.* **1987**, *109*, 7315.

(19) Russell, D. H.; Gross, M. L.; Nibbering, N. M. M. *J. Am. Chem. Soc.* **1977**, *100*, 6133.

(20) Drewello, T.; Heinrich, N.; Maas, W. P. M.; Nibbering, N. M. M.; Weiske, T.; Schwarz, H. *J. Am. Chem. Soc.* **1986**, *109*, 4810.

(21) Heydorn, L. N.; Burgers, P. C.; Ruttink, P. J. A.; Terlouw, J. K. *Int. J. Mass Spectrom.* **2003**, *228*, 759.

(22) Goge, P. H.; Hughes, G. K. *J. Am. Chem. Soc.* **1950**, *72*, 5570.

(23) Cox, J. D.; Wagman, D. D.; Medvedev, V. A. In *CODARA Key Values For Thermodynamics*; Hemisphere Publishing Corp.: New York, 1984, p 1.

(24) Meurer, E. C.; Gozzo, F. C.; Augusti, R.; Eberlin, M. N. *Eur. J. Mass Spectrom.* **2003**, *9*, 295.

(25) Lias, S. G.; Bartmess, J. E.; Liebman, J. G.; Holmes, J. L.; Levin, R. D.; Mallard, W. G. *J. Phys. Chem. Ref. Data* **1988**, *17, Suppl. 1.*, 1.

(26) Aubry, C.; Holmes, J. L. *Int. J. Mass Spectrom.* **2000**, *200*, 277.

(27) Traeger, J. C. *Int. J. Mass Spectrom.* **2000**, *194*, 261.

(28) Nicolaides, A.; Rauk, A.; Gluckhovtsev, M. N.; Radom, L. *J. Phys. Chem.* **1996**, *100*, 17460.

(29) Pedley, J. B.; Naylor, R. D.; Kirby, S. P. *Thermochemical Data of Organic Compounds*; 2nd ed.; Chapman and Hall: London, 1986.

(30) Hunter, E. P. L.; Lias, S. G. *J. Phys. Chem. Ref. Data* **1998**, *27*, 413.

Claims to Original Research

1. A unimolecular reaction method combined with theoretical calculations was used to investigate the isomerization and dissociation reactions of gas-phase ion-molecule complexes (IMC) in this thesis. This approach allows one to study the metastable ion (MI) and collision-induced dissociation (CID) characteristics of each stable isomer of an IMC provided that it can be generated in the mass spectrometer. The energy barriers separating the isomers can be approximately estimated by such experiments, but theoretical calculations are required to obtain accurate energies of the barriers for the important reactions which have been observed in the mass spectra and to create a potential energy surface (PES) for the entire system.

2. The stable and metastable adduct ions $[CH_3CHO/H^+O(H)CH_2^\bullet]$, $[CH_3CHO/^{+\bullet}HOCH_3]$, $[(CH_3)_2C{=}O/H^+O(H)CH_2^\bullet]$, $[(CH_3)_2C{=}O/^{+\bullet}HOCH_3]$ and $[CH_3CHO/H_2O]^{+\bullet}$ were directly made in the second field-free region of a sector instrument (the VG ZAB mass spectrometer). These desired IMCs were generated from an appropriate proton-bound dimer by collisional removal of a selected radical species, according to an experimental method first used by Tu et. al.[1]

3. The isomerization and dissociation chemistry of the IMCs, $[CH_3CHO/H^+O(H)CH_2^\bullet]$, $[CH_3CHO/^{+\bullet}HOCH_3]$, $[(CH_3)_2C{=}O/H^+O(H)CH_2^\bullet]$ and $[(CH_3)_2C{=}O/^{+\bullet}HOCH_3]$ were investigated in detail.[2,3] Such IMCs were formed by acetaldehyde/acetone association with the distonic and conventional form of

methanol, respectively. A $H^+/H^\bullet$ transfer mechanism was assigned for the rearrangement of the keto-isomer (i.e. ionized acetaldehyde or acetone) to its enol-form ion ($CH_2CHOH^{+\bullet}$ or $CH_2C(CH_3)=OH^{+\bullet}$), by using isotopic labelled samples together with computational analysis. A PES was obtained to illustrate the detailed reaction paths (including structures and energies for minima, transition states and products) for each system.

4. The unimolecular reactions of the acetaldehyde and water IMC, $[CH_3CHO/H_2O]^{+\bullet}$, were studied.[4] Reaction mechanisms for the inverconversions among water-solvated three $C_2H_4O^{+\bullet}$ isomers, i.e. $CH_3CHO^{+\bullet}$, $CH_3COH^{+\bullet}$ and $CH_2CHOH^{+\bullet}$, were explored by calculations and were found to involve proton-transport catalysis (PTC), a catalyzed-1,2-H transfer and an uncatalyzed H-atom transfer mechanism, respectively.

5. The fragmentation processes of ionized 2,3-pentanedione, 2,3-butanedione and 3,4-hexanedione were investigated for both MI and CID reactions.[5] The energy barriers for the isobaric losses of CO and C_2H_4 from the 2,3-pentanedione radical cation were determined by G3 calculations and a complete PES was obtained for the four dissociation channels of $[CH_3COCOCH_2CH_3]^{+\bullet}$, resulting in the productions of CH_3CO^+, $CH_3CH_2CO^+$, $[CH_3C(O)CH_2CH_3]^{+\bullet}$ and $[CH_3C(OH)=C=O]^{+\bullet}$, respectively.

6. In this thesis, a few new gas-phase ions were produced by experiment and their heats of formation values (Δ_fH^o) were also determined by theoretical calculations, which complement literature values for gas-phase ion thermochemistry.[6,7] A new $[C_3H_7O_2]^+$ isomer, namely $[CH_3C^+(O)\cdots(H)OCH_3]$, was produced from the MI

dissociation of acetone and methanol complex, $[(CH_3)_2C{=}O/^{+\bullet}HOCH_3]$, by the loss of a methyl radical. Its 298 K Δ_fH^o was estimated to be 322 kJ/mol. Hydrogen-bridged Water Complexes were found to be the major products of the losses of CO and $^{\bullet}CH_3$ from acetaldehyde and water complex, $[CH_3CHO/H_2O]^{+\bullet}$. The two new ions arising from $^{\bullet}CH_3$ loss were assigned by theory to be the isomers, $[OC\cdots H_3O^+]$ and $[CO\ldots H_3O^+]$, and their 298 K enthalpy values, calculated at the G3 level of theory are $\Delta_fH[OC\cdots H_3O^+]$ = 420 kJ/mol and $\Delta_fH[CO\cdots H_3O^+]$ = 448 kJ/mol. The new ion, $[CH_3C(OH){=}C{=}O]^{+\bullet}$, was produced by a McLafferty rearrangement of ionized 2,3-pentanedione (it lost an ethene C_2H_4), and has Δ_fH^o = 604 kJ/mol, obtained from G3 calculations.

References

(1) Tu, Y.-P.; Holmes, J. L. *J. Am. Chem. Soc.* **2000**, *122*, 3695.

(2) Wang, X.; Holmes, J. L. *Int. J. Mass Spectrom.* **2005**, *242*, 75.

(3) Wang, X.; Holmes, J. L. *Can. J. Chem.* **2005**, *83*, 1903.

(4) Wang, X.; Sun, W.; Holmes, J. L. *J. Phys. Chem. A.* **2006**, in press.

(5) Wang, X.; Holmes, J. L. *Int. J. Mass Spectrom.* **2006**, *249-250*, 222.

(6) *NIST Chemistry Webbook; NIST Standard Reference Database Number*; National Institute of Standards and Technology: Gaithersburg MD, 1998.

(7) Lias, S. G.; Bartmess, J. E.; Liebman, J. G.; Holmes, J. L.; Levin, R. D.; Mallard, W. G. *J. Phys. Chem. Ref. Data* **1988**, *17, Suppl. 1.*, 1.

SUPPORTING INFORMATION

Appendix A:

Archive entries for MP2/6-31+G(d) optimized geometries of the stable states, transition states and some of the products on the potential energy surfaces of the $[CH_3CHO\cdots H^+\cdots O(H)CH_2^{\bullet}]$ and $[CH_3CHO\cdots H^+\cdots {}^{\bullet}OCH_3]$ complexes (in Chapter 4).

$[CH_3CHOH\cdots OCH_3]^{+\bullet}$, Stable State I

Frequencies --	48.0985	61.2248	80.0372
Frequencies --	132.2889	140.8401	142.5405
Frequencies --	292.3347	530.8970	789.3779
Frequencies --	938.2099	951.5288	1026.0634
Frequencies --	1126.4912	1173.9027	1192.9051
Frequencies --	1251.8274	1415.9572	1426.8188
Frequencies --	1432.2398	1461.9651	1482.2233
Frequencies --	1485.5046	1537.7745	1552.2241
Frequencies --	1719.6340	2506.1096	3029.6138
Frequencies --	3083.0995	3151.1459	3157.6206
Frequencies --	3190.3803	3228.5185	3246.9935

Zero-point correction=	0.109321 (Hartree/Particle)
Thermal correction to Energy=	0.117525
Thermal correction to Enthalpy=	0.118469
Thermal correction to Gibbs Free Energy=	0.075199
Sum of electronic and zero-point Energies=	-268.273482
Sum of electronic and thermal Energies=	-268.265278
Sum of electronic and thermal Enthalpies=	-268.264334
Sum of electronic and thermal Free Energies=	-268.307604

1\1\GINC-MS8\Freq\UMP2-FC\6-31+G(d)\C3H8O2(1+,2)\CWANG\23-Aug-2004\0\\
#N GEOM=ALLCHECK GUESS=TCHECK UMP2(FC)/6-31+G(D) FREQ\\confI
protonated aldehyde.....och3. geom=aldehch3o.log on ms7/B3LYP\\1,2\C,1.3464396265
,2.5598050206,-0.25647364\H,1.9352727696,2.5428737994,0.6601843241\H,1
.9937815848,2.6570770948,-1.138733607\H,0.6789744464,3.4320983553,-0.2
796708482\C,0.5367417748,1.3527935818,-0.4064388467\O,0.5683590977,0.4
408576202,0.4663325942\H,-0.1135402366,1.2125062529,-1.2761789243\C,-1
.3301101979,-2.6518157208,0.4062791643\H,-0.7140374982,-3.4066962508,-
0.1124349217\H,-2.37768044,-2.8990954417,0.2151320858\H,-1.0767435759,
-2.6291357096,1.4673600572\O,-1.0171753463,-1.4537291038,-0.2467503264
\H,-0.0539242809,-0.3713535218,0.2474836261\\Version=x86-Linux-G98RevA
.7\HF=-267.6792964\MP2=-268.3828029\PUHF=-267.6828659\PMP2-0=-268.3850
312\S2=0.760042\S2-1=0.75246\S2A=0.75008\RMSD=2.279e-10\RMSF=6.634e-08

$[CH_3CHO\cdots O(H)CH_3]^{+\bullet}$, Stable State II

Frequencies --	16.0497	61.1059	84.6940
Frequencies --	97.6931	117.5276	190.3738
Frequencies --	245.8392	395.7267	468.3036
Frequencies --	910.1907	945.1568	1109.4437
Frequencies --	1178.5938	1182.4071	1279.5170
Frequencies --	1282.2623	1393.9665	1489.7581
Frequencies --	1502.9879	1579.4929	1580.1875
Frequencies --	1626.5442	1638.6017	1652.4276
Frequencies --	1694.9355	2948.7950	3212.0410
Frequencies --	3242.5707	3285.9161	3325.2235
Frequencies --	3335.3667	3357.9781	4087.5333

Zero-point correction=	0.110745 (Hartree/Particle)
Thermal correction to Energy=	0.116556
Thermal correction to Enthalpy=	0.117500
Thermal correction to Gibbs Free Energy=	0.080190
Sum of electronic and zero-point Energies=	-268.251701
Sum of electronic and thermal Energies=	-268.245889
Sum of electronic and thermal Enthalpies=	-268.244945
Sum of electronic and thermal Free Energies=	-268.282256

\1\GINC-MS8\Freq\UMP2-FC\6-31+G(d)\C3H8O2(1+,2)\CWANG\23-Aug-2004\0\\
#N GEOM=ALLCHECK GUESS=TCHECK UMP2(FC)/6-31+G(D) FREQ\\confI
protonated aldehyde.....och3. geom=aldehch3o.log on ms7/B3LYP\\1,2\C,-
1.4947664446,0.337488984,-1.4062639018\C,-1.5090053407,0.3733982746,0.0760
709574\O,-0.5288997273,0.3308833673,0.8206205185\O,1.3550253796,0.1015008755,-
0.0974301242\C,1.8410967756,-1.037974804,0.6740851888\H,-1.9806591247,
1.2432363421,-1.7738309978\H,-0.4864791338,0.2549931853,-1.7964432956\H,-
2.1104135363,-0.5015112607,-1.7350106637\H,-2.4836414205,0.4457131403,0.578093
2342\H,1.542028802,0.9311519845,0.3932400752\H,2.9265768176,-
1.0125014424,0.5767522588\H,1.5330075628,-0.9411349496,1.7102813672\H,1.
4266248725,-1.9164956699,0.1980414004\\\\Version=x86-Linux-G98RevA.7\HF==-
267.6493192\MP2=-268.3729005\PUHF=-267.6460589\PMP2-0=-
268.3749574\S2=0.791\S2-1=0.766\S2A=0.751\RMSD=4.681e-10\RMSF=1.237e-08

$[CH_3C(O)\cdots HO(H)CH_3]^{+\bullet}$, Stable State III

Frequencies --	20.8940	60.6509	76.4102
Frequencies --	116.4336	136.1395	215.4142
Frequencies --	252.4421	514.4347	516.2669
Frequencies --	882.7707	915.3428	949.0336
Frequencies --	1024.7785	1082.0110	1141.2470
Frequencies --	1210.9150	1349.7196	1420.8497
Frequencies --	1485.3047	1498.7986	1507.4497

Frequencies --	1529.3695	1533.0004	1728.0658
Frequencies --	1979.1098	2798.8323	3105.5040
Frequencies --	3168.6862	3214.5883	3218.3809
Frequencies --	3304.8935	3314.0311	3638.8910

Zero-point correction= 0.111427 (Hartree/Particle)
Thermal correction to Energy= 0.119861
Thermal correction to Enthalpy= 0.120805
Thermal correction to Gibbs Free Energy= 0.076283
Sum of electronic and zero-point Energies= -268.291474
Sum of electronic and thermal Energies= -268.283041
Sum of electronic and thermal Enthalpies= -268.282096
Sum of electronic and thermal Free Energies= -268.326618

1\1\GINC-MS8\Freq\UMP2-FC\6-31+G(d)\C3H8O2(1+,2)\CWANG\12-Feb-2004\0\\
#N GEOM=ALLCHECK GUESS=TCHECK UMP2(FC)/6-31+G(D) FREQ\\confII
mp2\\1,2\C,1.043821723,1.4514195972,1.7965752841\H,0.8087264427,1.3309989122,2
.8581392844\H,2.1213643498,1.37594954,1.6286765721\H,0.7091349704,2.42
68256474,1.4339011053\C,0.3496025308,0.376233322,1.0183838353\O,-0.365
3524799,-0.5271760379,1.3405008852\H,0.3298619852,0.0909967864,-0.7954
438522\C,-1.1701475615,-0.9897477595,-1.8389985146\H,-1.9232457374,-0.
270064091,-1.5328924866\H,-1.1191439911,-1.8499684888,-1.1758868454\H,
-1.2747051707,-1.2576492935,-2.8866228032\O,0.1298317072,-0.2356510288
,-1.7545761606\H,0.8925131786,-0.7719034375,-2.0730324003\\Version=x86
-Linux-G98RevA.7\HF=-267.6577676\MP2=-268.4029011\PUHF=-267.661711\PMP
2-0=-268.4052304\S2=0.762933\S2-1=0.752304\S2A=0.750085\RMSD=1.147e-09
\RMSF=1.491e-05

$[CH_3CHOH\cdots OHCH_2]^{+\bullet}$, Stable State IV

Frequencies --	41.8742	106.5270	111.1821
Frequencies --	145.4268	159.6627	250.9347
Frequencies --	314.9370	496.1263	548.1446
Frequencies --	745.4961	807.8140	940.2550
Frequencies --	1090.7769	1107.5428	1167.9526
Frequencies --	1184.1590	1356.1490	1385.3167
Frequencies --	1427.2965	1441.2356	1485.7322
Frequencies --	1489.3549	1498.8723	1525.9767
Frequencies --	1711.9755	2339.5146	3084.4101
Frequencies --	3153.3124	3230.6635	3243.1060
Frequencies --	3250.2447	3407.7009	3715.6753

Zero-point correction= 0.109273 (Hartree/Particle)
Thermal correction to Energy= 0.117333
Thermal correction to Enthalpy= 0.118277
Thermal correction to Gibbs Free Energy= 0.075926

Sum of electronic and zero-point Energies= -268.288460
Sum of electronic and thermal Energies= -268.280400
Sum of electronic and thermal Enthalpies= -268.279456
Sum of electronic and thermal Free Energies= -268.321808

1\1\GINC-MS8\Freq\UMP2-FC\6-31+G(d)\C3H8O2(1+,2)\CWANG\15-Jan-2004\0\\
#N GEOM=ALLCHECK GUESS=TCHECK UMP2(FC)/6-31+G(D) FREQ\\conf V by
mp2 (by using ms7/B3LYP-min./vanlch3oh.chk)\\1,2\C,1.0410161333,1.676927264
3,-0.6214001157\H,0.9373067355,1.3964017331,0.4267899572\H,2.090097042
9,1.6078844424,-0.9394937609\H,0.756315874,2.7275108726,-0.7695045111\
C,0.2333675621,0.8531504038,-1.5297689664\O,-0.5226248039,-0.096379249
2,-1.1897049328\H,0.2511647056,1.0351185716,-2.6057602999\O,-0.6589191
643,-0.6317655526,1.2943051913\H,-1.5369190769,-0.5021865848,1.7059644
765\H,-0.5732675214,-0.3073940971,-0.1547067875\C,-0.1006917968,-1.854
1678203,1.7227810144\H,-0.4288070293,-2.2046986366,2.6908970462\H,0.91
43096234,-1.982936973,1.3793402181\\Version=x86-Linux-G98RevA.7\HF=-26
7.6713477\MP2=-268.3977333\PUHF=-267.6740259\PMP2-0=-268.3994199\S2=0.
759752\S2-1=0.752502\S2A=0.750065\RMSD=2.553e-09\RMSF=1.729e-05

$[CH_2CHOH\cdots O(H)CH_3]^{+\bullet}$, Stable State V

Frequencies --	56.0120	99.6712	112.5103
Frequencies --	138.1536	224.6195	333.1290
Frequencies --	425.8829	502.2244	555.6564
Frequencies --	872.9589	980.8103	1004.9233
Frequencies --	1024.8814	1094.7355	1196.4157
Frequencies --	1245.0203	1350.4976	1389.1700
Frequencies --	1459.8442	1488.9310	1521.6281
Frequencies --	1527.2805	1543.3734	1555.7852
Frequencies --	1622.6921	2091.6689	3142.7336
Frequencies --	3240.0965	3253.2980	3255.5656
Frequencies --	3270.5608	3367.9914	3723.6480

Zero-point correction= 0.110884 (Hartree/Particle)
Thermal correction to Energy= 0.118520
Thermal correction to Enthalpy= 0.119464
Thermal correction to Gibbs Free Energy= 0.078188
Sum of electronic and zero-point Energies= -268.301233
Sum of electronic and thermal Energies= -268.293597
Sum of electronic and thermal Enthalpies= -268.292653
Sum of electronic and thermal Free Energies= -268.333929

1\1\GINC-MS8\Freq\UMP2-FC\6-31+G(d)\C3H8O2(1+,2)\CWANG\15-Jan-2004\0\\
#N GEOM=ALLCHECK GUESS=TCHECK UMP2(FC)/6-31+G(D) FREQ\\conf V by
mp2 (by using ms7/B3LYP-min./vanlch3oh.chk)\\1,2\C,0.6031504608,0.159939948
,-2.0369247463\H,0.3918045392,-1.8182903974,1.5970934267\H,1.376928656

5,0.0917020582,-1.2800702788\H,0.8738790939,0.1174671055,-3.0847222801
\C,-0.7634656589,0.3037735074,-1.67721384\O,-1.1863139023,0.3656233547
,-0.4738218406\H,-1.5423087288,0.3699647365,-2.4360579197\O,0.58956037
49,0.200046672,1.2830321911\H,0.751734393,1.0230378927,1.785245286\H,-
0.4348338448,0.3057076307,0.2935648888\C,0.5268096833,-0.9326975423,2.
214207112\H,-0.3133477941,-0.8084500096,2.8976105021\H,1.4712049927,-0
.992594709,2.7532424172\\Version=x86-Linux-G98RevA.7\HF=-267.6845831\M
P2=-268.4121169\PUHF=-267.6894215\PMP2-0=-268.4157559\S2=0.782706\S2-1
=0.766364\S2A=0.750426\RMSD=1.488e-09\RMSF=3.425e-05

$[CH_3CO\cdots HO(H)CH_3]^{+\bullet}$, Stable State VI

Frequencies --	22.7457	64.9534	82.2762
Frequencies --	95.2421	131.7701	140.3692
Frequencies --	274.8026	512.7649	523.2223
Frequencies --	907.7780	938.4170	974.0183
Frequencies --	997.3212	1106.1735	1134.9722
Frequencies --	1214.9014	1364.5724	1424.6632
Frequencies --	1480.9668	1494.3271	1508.7036
Frequencies --	1533.1349	1537.7589	1770.5331
Frequencies --	1846.5485	2743.6921	3101.2070
Frequencies --	3166.7458	3203.2000	3214.2235
Frequencies --	3299.6978	3311.8162	3661.3436

Zero-point correction=	0.111140 (Hartree/Particle)
Thermal correction to Energy=	0.119674
Thermal correction to Enthalpy=	0.120618
Thermal correction to Gibbs Free Energy=	0.075938
Sum of electronic and zero-point Energies=	-268.300739
Sum of electronic and thermal Energies=	-268.292205
Sum of electronic and thermal Enthalpies=	-268.291261
Sum of electronic and thermal Free Energies=	-268.335942

1\1\GINC-MS8\Freq\UMP2-FC\6-31+G(d)\C3H8O2(1+,2)\CWANG\29-Jan-2004\0\\
#N GEOM=ALLCHECK GUESS=TCHECK UMP2(FC)/6-31+G(D) FREQ\\ground
states VI geom=ch3comethanol.log at b3lyp\\1,2\C,1.0298015471,0.8770787657,2.7
144356174\H,0.373499347,0.1972777092,3.2653515973\H,2.0780594793,0.705
7575315,2.9762308231\H,0.8029241694,1.9197788367,2.955877887\C,0.87504
1779,0.6917975099,1.2485924275\O,0.1519625907,-0.0703265373,0.63909158
92\H,0.0086948008,-0.1935610409,-0.9013665943\C,-1.5607793717,-0.86617
56811,-2.1593818127\H,-2.2323888707,-0.1508094212,-1.6941518883\H,-1.6
314589811,-1.855947766,-1.7137298482\H,-1.6772083703,-0.8772774165,-3.
2393664227\O,-0.1896359518,-0.3164891059,-1.9082150977\H,0.514881588,-
0.8668968534,-2.3177348797\\Version=x86-Linux-G98RevA.7\HF=-267.679688
4\MP2=-268.4118795\PUHF=-267.682289\PMP2-0=-268.4136056\S2=0.760859\S2
-1=0.753522\S2A=0.750085\RMSD=6.634e-10\RMSF=2.210e-06

$[CH_3COH\cdots O(H)CH_3]^{+\bullet}$, Stable State VII

Frequencies --	66.4180	183.4856	206.4786
Frequencies --	230.4480	313.9393	388.0312
Frequencies --	458.8635	482.6843	584.7023
Frequencies --	704.7211	920.1158	980.4938
Frequencies --	1059.1199	1090.0903	1156.7866
Frequencies --	1196.5312	1261.0546	1382.2895
Frequencies --	1445.5984	1483.1791	1502.3476
Frequencies --	1510.1608	1523.9410	1534.5399
Frequencies --	1544.1823	3098.0944	3154.0225
Frequencies --	3197.1954	3225.2015	3280.7160
Frequencies --	3305.5960	3617.8990	3670.1170

Zero-point correction=	0.113359 (Hartree/Particle)
Thermal correction to Energy=	0.120379
Thermal correction to Enthalpy=	0.121323
Thermal correction to Gibbs Free Energy=	0.082496
Sum of electronic and zero-point Energies=	-268.272572
Sum of electronic and thermal Energies=	-268.265552
Sum of electronic and thermal Enthalpies=	-268.264608
Sum of electronic and thermal Free Energies=	-268.303436

1\1\GINC-MS8\Freq\UMP2-FC\6-31+G(d)\C3H8O2(1+,2)\CWANG\17-Feb-2004\0\\
#MP2/6-31+G(D) FREQ\\carbene...methanol mp2 freq geom=carbenemethanol-
mp2.log\\1,2\C,-1.8027860595,-0.6654528055,0.0448843477\H,-1.879298693
7,-0.7347675132,1.1368995883\H,-2.6853127399,-0.1472171091,-0.33781423
3\H,-1.7725527067,-1.6680516955,-0.3869082201\C,-0.6119036883,0.133434
2359,-0.3275902499\O,-0.4951657599,1.3558729222,0.1639967377\O,0.66496
8783,-0.7015806087,0.0636829824\H,-0.0542983074,1.9823498872,-0.447582
1491\C,1.9999153487,-0.0368712056,0.0370845732\H,0.6755818412,-1.53489
12381,-0.4630707525\H,2.1954683667,0.3333681242,-0.9686912191\H,2.7086
672941,-0.804629947,0.33950499\H,1.9419671556,0.7528396347,0.779952209
2\\Version=x86-Linux-G98RevA.7\HF=-267.6560793\MP2=-268.3859316\PUHF=-
267.6579637\PMP2-0=-268.3870226\S2=0.755804\S2-1=0.750904\S2A=0.750025
\RMSD=4.887e-09\RMSF=1.585e-05

$[CH_2CHOCH_3\cdots OH_2]^{+\bullet}$, Stable State VIII (minimum for H_2O loss from $CH_3CHO/^{\bullet}CH_2OH_2^{+}$)

Frequencies --	41.0194	51.3228	101.4960
Frequencies --	145.5569	152.0804	286.1900
Frequencies --	294.8853	314.5184	337.5920
Frequencies --	451.2906	585.7922	826.9092
Frequencies --	880.6051	998.5424	1023.2345
Frequencies --	1177.6012	1218.4724	1268.4340

Frequencies --	1414.6998	1462.5733	1497.9006
Frequencies --	1529.8478	1543.7438	1623.7828
Frequencies --	1719.6550	3171.8891	3248.0503
Frequencies --	3256.4635	3300.3599	3331.4587
Frequencies --	3371.4186	3726.4630	3852.4616

Zero-point correction=	0.109822 (Hartree/Particle)
Thermal correction to Energy=	0.118713
Thermal correction to Enthalpy=	0.119657
Thermal correction to Gibbs Free Energy=	0.075208
Sum of electronic and zero-point Energies=	-268.290662
Sum of electronic and thermal Energies=	-268.281771
Sum of electronic and thermal Enthalpies=	-268.280827
Sum of electronic and thermal Free Energies=	-268.325276

1\1\GINC-MS8\Freq\UMP2-FC\6-31+G(d)\C3H8O2(1+,2)\CWANG\23-Apr-2004\0\\
#N GEOM=ALLCHECK GUESS=TCHECK UMP2(FC)/6-31+G(D) FREQ\\methoxy
l ethene\\1,2\C,2.0375080449,0.0138704561,-0.8012658777\H,1.9147583914,-0.0191
393896,0.2744147618\H,3.0393191295,0.0210701587,-1.2138294703\C,0.9389
672545,0.0481318516,-1.6973505822\O,-0.2990378242,0.0451397794,-1.3686
379965\H,1.0926928217,0.0807044511,-2.7750488614\C,-0.740828029,0.0035
536243,0.055114167\H,-1.82232589,0.0114641041,-0.0113088876\H,-0.37073
10685,-0.9166880096,0.4996247148\H,-0.3610164152,0.8907143812,0.555254
7078\O,-1.400868582,-0.0790579608,2.7200144796\H,-1.6628160831,-0.8638
662589,3.233409391\H,-1.6445132585,0.6737504223,3.2874855359\\Version=
x86-Linux-G98RevA.7\HF=-267.676632\MP2=-268.4004839\PUHF=-267.6815616\
PMP2-0=-268.4042347\S2=0.784608\S2-1=0.767925\S2A=0.750461\RMSD=2.328e
-09\RMSF=4.120e-06

$[CH_2CHO\cdots CH_3\cdots OH_2]^{+\bullet}$, Intermediate for H_2O loss reaction in $CH_3CHO/^{\bullet}CH_2OH_2^{+}$

Frequencies --	10.5402	56.3743	69.6950
Frequencies --	117.8752	122.1645	151.9986
Frequencies --	265.4116	355.0053	522.4735
Frequencies --	736.8435	736.8799	784.5259
Frequencies --	941.0668	998.5687	1064.9230
Frequencies --	1181.2579	1198.8519	1293.2869
Frequencies --	1453.8465	1459.8787	1505.2969
Frequencies --	1507.5078	1516.0529	1731.9927
Frequencies --	1992.0591	3059.9414	3199.1826
Frequencies --	3241.6280	3354.8897	3359.2689
Frequencies --	3371.4806	3588.6873	3689.6636

Zero-point correction=	0.110808 (Hartree/Particle)
Thermal correction to Energy=	0.119707
Thermal correction to Enthalpy=	0.120651

Thermal correction to Gibbs Free Energy= 0.074643
Sum of electronic and zero-point Energies= -268.264948
Sum of electronic and thermal Energies= -268.256049
Sum of electronic and thermal Enthalpies= -268.255105
Sum of electronic and thermal Free Energies= -268.301112

1\1\GINC-MS8\Freq\UMP2-FC\6-31+G(d)\C3H8O2(1+,2)\CWANG\29-Apr-2004\1\\
#MP2/6-31+G(D) OPT=(EF,CALCALL)\\intermediate ion-dipole complex CH2CH
O_CH3_OH2\\1,2\C\H,1,R2\H,1,R3,2,A3\H,1,R4,2,A4,3,D4,0\O,1,R5,2,A5,3,D
5,0\H,5,R6,1,A6,2,D6,0\H,5,R7,1,A7,6,D7,0\O,1,R8,2,A8,3,D8,0\C,8,R9,1,
A9,2,D9,0\C,9,R10,8,A10,1,D10,0\H,9,R11,8,A11,10,D11,0\H,10,R12,9,A12,
8,D12,0\H,10,R13,9,A13,12,D13,0\\R2=1.08379656\R3=1.08312509\R4=1.0831
2508\R5=1.55052496\R6=0.98537146\R7=0.98537145\R8=2.56835479\R9=1.2206
9761\R10=1.44919489\R11=1.10484894\R12=1.0829272\R13=1.08298931\A3=114
.07922426\A4=114.07912274\A5=107.68477094\A6=112.97864628\A7=112.97868
171\A8=69.25407884\A9=163.81434088\A10=123.59863642\A11=120.34798274\A
12=120.66121302\A13=119.3419429\D4=131.43374364\D5=-114.28313229\D6=-6
1.69134488\D7=123.38239731\D8=65.71785191\D9=-179.9884539\D10=179.9968
192\D11=-180.00003575\D12=-180.00016852\D13=180.0000548\\Version=x86-L
inux-G98RevA.7\HF=-267.6631029\MP2=-268.3757558\PUHF=-267.6736971\PMP2
-0=-268.3843671\S2=0.848605\S2-1=0.811219\S2A=0.752124\RMSD=5.808e-09\
RMSF=3.331e-08

$[CH_3C(OH)_2\cdots CH_3]^{+\bullet}$, Stable State IX (minimum for $^{\bullet}CH_3$ loss from $CH_3CHO/^{\bullet}CH_2OH_2^{+}$)

Frequencies -- 45.8477 49.8982 64.7513
Frequencies -- 72.9978 174.8528 277.2575
Frequencies -- 283.1750 442.0020 565.1816
Frequencies -- 594.0789 657.2582 872.0717
Frequencies -- 923.8030 954.2167 1074.2258
Frequencies -- 1101.2759 1176.6836 1255.8256
Frequencies -- 1447.4924 1462.1243 1465.1617
Frequencies -- 1483.7275 1502.2475 1605.7633
Frequencies -- 1651.3690 3107.0890 3148.5885
Frequencies -- 3172.5635 3206.7595 3258.1615
Frequencies -- 3346.1571 3353.9711 3604.3902

Zero-point correction= 0.107987 (Hartree/Particle)
Thermal correction to Energy= 0.116599
Thermal correction to Enthalpy= 0.117543
Thermal correction to Gibbs Free Energy= 0.073232
Sum of electronic and zero-point Energies= -268.304967
Sum of electronic and thermal Energies= -268.296356
Sum of electronic and thermal Enthalpies= -268.295411
Sum of electronic and thermal Free Energies= -268.339723

1\1\GINC-MS8\Freq\UMP2-FC\6-31+G(d)\C3H8O2(1+,2)\CWANG\20-May-2004\0\\
#N GEOM=ALLCHECK GUESS=TCHECK UMP2(FC)/6-31+G(D) FREQ\\ch3loss
minimum geom=ch3loss at b3lyp\\1,2\C,2.2220495121,0.1990997977,0.1688971585\H
,2.5378481297,-0.6514528573,0.7733605254\H,2.7611937863,0.246260029,-0
.7779310435\H,2.4214923415,1.1217157098,0.7291877573\C,0.7706094513,0.
1271928115,-0.0795752482\O,0.029070728,-0.4720870485,0.781953915\H,-0.
9611122116,-0.4743737549,0.5936709933\O,0.3195678341,0.7047061834,-1.1
496772421\H,-0.6578363406,0.6685863706,-1.2718443476\C,-2.9345799933,-
0.517975634,0.2599611516\H,-3.2324500684,0.5244727126,0.2689964347\H,-
3.024858987,-1.0785329864,-0.6637213936\H,-2.9818589666,-1.0675301536,
1.1943693196\\Version=x86-Linux-G98RevA.7\HF=-267.6892637\MP2=-268.412
9544\PUHF=-267.6917173\PMP2-0=-268.4144933\S2=0.758998\S2-1=0.752267\S
2A=0.750049\RMSD=3.233e-09\RMSF=1.015e-05

TS0 (for the rearrangement from I to IV)

Frequencies --	-2052.8286	49.7014	68.9025
Frequencies --	113.3472	142.6111	157.7650
Frequencies --	255.2888	327.5683	533.0766
Frequencies --	816.7524	888.1419	948.2271
Frequencies --	1028.7900	1138.5243	1169.5964
Frequencies --	1174.1543	1198.6118	1325.0637
Frequencies --	1421.2075	1440.2859	1485.1798
Frequencies --	1487.6469	1505.5411	1570.2520
Frequencies --	1724.1643	1964.4310	2463.6052
Frequencies --	3086.2261	3156.0816	3180.8345
Frequencies --	3200.3914	3246.2088	3348.7323

Zero-point correction=	0.103923 (Hartree/Particle)
Thermal correction to Energy=	0.111778
Thermal correction to Enthalpy=	0.112722
Thermal correction to Gibbs Free Energy=	0.070707
Sum of electronic and zero-point Energies=	-268.228890
Sum of electronic and thermal Energies=	-268.221035
Sum of electronic and thermal Enthalpies=	-268.220091
Sum of electronic and thermal Free Energies=	-268.262106

1\1\GINC-MS8\Freq\UMP2-FC\6-31+G(d)\C3H8O2(1+,2)\CWANG\20-Feb-2004\1\\
#N GEOM=ALLCHECK GUESS=TCHECK UMP2(FC)/6-31+G(D) FREQ\\ts0
geom=ms9/ts0-g3.log\\1,2\C\H,1,R2\H,1,R3,2,A3\H,1,R4,2,A4,3,D4,0\C,1,R5,2,A5,4,D5
,0\O,5,R6,1,A6,2,D6,0\H,5,R7,1,A7,6,D7,0\H,6,R8,5,A8,1,D8,0\O,8,R9,5,A
9,1,D9,0\C,9,R10,6,A10,5,D10,0\H,10,R11,9,A11,6,D11,0\H,10,R12,9,A12,6
,D12,0\H,10,R13,9,A13,6,D13,0\\R2=1.08965984\R3=1.09838038\R4=1.097909
64\R5=1.4639704\R6=1.25984828\R7=1.09564576\R8=1.07966547\R9=1.42283\R
10=1.40715706\R11=1.08530069\R12=1.08583769\A3=110.86648572\A4=111.012

98331\A5=111.67997225\A6=121.05261512\A7=120.80704242\A8=113.91019504\
A9=137.07929797\A10=124.84687841\A11=115.32814698\A12=117.82834256\D4=
-117.41074996\D5=-121.51712027\D6=-0.67538949\D7=180.14879047\D8=180.4
9869499\D9=180.98918617\D10=206.45690364\D11=154.24511685\D12=-1.42178
587\A13=54.06050604\R13=1.27945916\D13=-106.1735149\\Version=x86-Linux
-G98RevA.7\HF=-267.5936359\MP2=-268.3328129\PUHF=-267.6012534\PMP2-0=-
268.3383092\S2=0.790494\S2-1=0.767793\S2A=0.750448\RMSD=9.942e-10\RMSF
=6.090e-05

TS1 (for the rearrangement from III to VI)

Frequencies --	-129.7733	31.0060	53.6820
Frequencies --	95.2972	118.7727	187.9172
Frequencies --	213.9568	421.5634	482.8455
Frequencies --	865.1253	888.1817	917.4736
Frequencies --	978.1887	1006.3641	1116.2401
Frequencies --	1205.2921	1315.7543	1422.1012
Frequencies --	1484.9440	1496.6977	1508.0705
Frequencies --	1527.3877	1531.3085	1702.6353
Frequencies --	1876.4988	3104.1218	3171.4259
Frequencies --	3209.9907	3217.6038	3257.3582
Frequencies --	3308.5040	3321.6991	3646.3032

Zero-point correction=	0.110911 (Hartree/Particle)
Thermal correction to Energy=	0.118863
Thermal correction to Enthalpy=	0.119807
Thermal correction to Gibbs Free Energy=	0.076713
Sum of electronic and zero-point Energies=	-268.290761
Sum of electronic and thermal Energies=	-268.282809
Sum of electronic and thermal Enthalpies=	-268.281865
Sum of electronic and thermal Free Energies=	-268.324959

1\1\GINC-MS8\Freq\UMP2-FC\6-31+G(d)\C3H8O2(1+,2)\CWANG\19-Mar-2004\1\\
#MP2/6-31+G(D) OPT=(TS,EF,CALCALL)\\ts9 geom=ts9-rcfc.log on b3lyp\\1,
2\C\C,1,cc2\O,2,oc3,1,occ3\H,1,hc4,2,hcc4,3,dih4,0\H,1,hc5,2,hcc5,3,di
h5,0\H,1,hc6,2,hcc6,3,dih6,0\H,3,ho7,2,hoc7,1,dih7,0\O,2,oh8,3,oho8,1,
dih8,0\C,8,co9,7,coh9,3,dih9,0\H,8,ho10,7,hoh10,3,dih10,0\H,9,hc11,8,h
co11,7,dih11,0\H,9,hc12,8,hco12,7,dih12,0\H,9,hc13,8,hco13,7,dih13,0\\
hc4=1.09386023\hcc4=109.91154575\dih4=-2.72234152\hc5=1.09371645\hcc5=
108.54215318\dih5=118.41462606\hc6=1.09296706\hcc6=109.04459389\dih6=-
124.43207042\co9=1.50795005\coh9=112.65015233\dih9=12.51219546\ho10=0.
98486522\hoh10=108.98002554\dih10=138.56678753\hc11=1.08702688\hco11=1
08.62726664\dih11=62.2421532\hc12=1.08509067\hco12=104.43149574\dih12=
-58.17929331\hc13=1.08623352\hco13=104.74116537\dih13=183.79654946\cc2
=1.49360205\oc3=1.20639466\occ3=131.34806433\ho7=2.05396477\hoc7=70.56
571412\dih7=183.60064242\oh8=3.00799854\oho8=72.83740556\dih8=-184.333

33247\\Version=x86-Linux-G98RevA.7\HF=-267.6618664\MP2=-268.4016716\PU
HF=-267.6654072\PMP2-0=-268.4038104\S2=0.762387\S2-1=0.752543\S2A=0.75
0073\RMSD=8.066e-09\RMSF=5.051e-08

TS2 (for the rearrangement from II to III)

Frequencies --	-107.1368	48.1551	102.2793
Frequencies --	108.4006	131.2434	150.2900
Frequencies --	178.5606	410.9416	424.7599
Frequencies --	762.5084	931.1958	1025.3263
Frequencies --	1069.2136	1104.7838	1116.5232
Frequencies --	1193.4977	1248.8257	1362.5048
Frequencies --	1401.4115	1470.5268	1490.9867
Frequencies --	1524.7395	1545.5603	1562.0935
Frequencies --	1590.2233	3004.3731	3096.6057
Frequencies --	3118.9992	3191.9784	3216.3946
Frequencies --	3237.2276	3278.0450	3742.8620

Zero-point correction=	0.108990 (Hartree/Particle)
Thermal correction to Energy=	0.116930
Thermal correction to Enthalpy=	0.117874
Thermal correction to Gibbs Free Energy=	0.075647
Sum of electronic and zero-point Energies=	-268.248713
Sum of electronic and thermal Energies=	-268.240773
Sum of electronic and thermal Enthalpies=	-268.239829
Sum of electronic and thermal Free Energies=	-268.282056

1\1\GINC-MS8\Freq\UMP2-FC\6-31+G(d)\C3H8O2(1+,2)\CWANG\17-Jan-2004\1\\
#N GEOM=ALLCHECK GUESS=TCHECK UMP2(FC)/6-31+G(D) FREQ\\TS2
geom=ms5/AHM/ts2-opt.log\\1,2\C\H,1,B1\H,1,B2,2,A1\H,1,B3,2,A2,3
,D1,0\C,1,B4,2,A3,4,D2,0\O,5,B5,1,A4,2,D3,0\H,5,B6,6,A5,1,D4,0\O,6,B7,
5,A6,1,D5,0\C,8,B8,6,A7,5,D6,0\H,8,B9,6,A8,5,D7,0\H,9,B10,8,A9,6,D8,0\
H,9,B11,8,A10,6,D9,0\H,9,B12,8,A11,6,D10,0\\B1=1.08718491\B2=1.0939873
\B3=1.09846978\B4=1.48704478\B5=1.21871123\B8=1.45103153\B10=1.0895106
\B11=1.09205921\B12=1.09203291\A1=112.99164167\A2=110.25798946\A3=110.
98378072\A4=125.38255543\A7=103.02919875\A9=106.43977848\A10=110.74662
242\A11=110.52710805\D1=122.27458275\D2=116.36723113\D3=-13.76474019\D
6=-138.02797738\D8=23.53828146\D9=-95.30749784\D10=142.07177806\B9=0.9
7493839\A8=141.61946446\D7=80.51903603\B7=2.58648853\A6=91.51311899\D5
=-47.87988061\B6=1.10924626\A5=112.88236052\D4=-179.7593633\\Version=x
86-Linux-G98RevA.7\HF=-267.6537575\MP2=-268.357703\PUHF=-267.6592297\P
MP2-0=-268.3618452\S2=0.777339\S2-1=0.763909\S2A=0.750484\RMSD=1.208e-
09\RMSF=3.120e-06

TS3 (for the rearrangement from IV to V)

Frequencies --	-836.2787	96.7566	137.6684
Frequencies --	219.2628	250.2312	455.6604
Frequencies --	510.7081	584.2507	660.4524
Frequencies --	771.3971	782.0747	1011.3625
Frequencies --	1036.4240	1105.3408	1130.8978
Frequencies --	1163.1915	1177.4937	1219.5036
Frequencies --	1335.9188	1388.1486	1404.9199
Frequencies --	1445.0718	1479.6045	1532.5594
Frequencies --	1536.1166	1639.5644	3165.5375
Frequencies --	3173.9177	3266.1947	3283.2749
Frequencies --	3306.2921	3504.7771	3703.4983

Zero-point correction=	0.108163 (Hartree/Particle)
Thermal correction to Energy=	0.114578
Thermal correction to Enthalpy=	0.115522
Thermal correction to Gibbs Free Energy=	0.077626
Sum of electronic and zero-point Energies=	-268.257451
Sum of electronic and thermal Energies=	-268.251036
Sum of electronic and thermal Enthalpies=	-268.250092
Sum of electronic and thermal Free Energies=	-268.287988

1\1\GINC-MS8\Freq\UMP2-FC\6-31+G(d)\C3H8O2(1+,2)\CWANG\06-Oct-2003\1\\
#N GEOM=ALLCHECK GUESS=TCHECK UMP2(FC)/6-31+G(D)
FREQ\\ts3\\1,2\C\H,1,b1\H,1,b2,2,a2\H,1,b3,2,a3,3,h3,0\C,1,b4,2,a4,4,h4,0\O,5,b5,1,a5,2
,h5,0\H,5,b6,1,a6,2,h6,0\O,6,b7,5,a7,1,h7,0\H,8,b8,6,a8,5,h8,0\H,6,b9,5,a9
,1,h9,0\C,8,b10,6,a10,5,h10,0\H,11,b11,8,a11,6,h11,0\H,11,b12,8,a12,6,
h12,0\\b6=1.0877553\b8=0.97843664\a8=134.72235591\h8=93.42709798\b9=0.
99112002\a9=112.52966093\a11=112.05044489\h11=-65.82237167\a12=117.443
93\h12=153.04170789\b1=1.29929256\b2=1.08757407\a2=107.97136576\a4=103
.63692315\b3=1.09273396\b4=1.41342616\b5=1.30101572\h3=-118.46614027\a
3=96.39149159\a5=124.13411148\a6=123.22525904\h4=-118.76011291\b10=1.3
6776842\a10=94.29369445\h10=-33.32694227\b11=1.08841938\b12=1.0887164\
h5=64.64636149\h6=250.48706999\h7=-26.85985158\h9=-1.48826645\b7=2.895
5556\a7=93.55448568\\Version=x86-Linux-G98RevA.7\HF=-267.6212895\MP2=-
268.3656141\PUHF=-267.6270674\PMP2-0=-268.3697174\S2=0.787497\S2-1=0.7
65594\S2A=0.750483\RMSD=1.486e-09\RMSF=1.548e-05

TS4 (for the rearrangement from IV to VI)

Frequencies --	-2037.7366	89.7621	127.5418
Frequencies --	159.0670	238.6942	299.7578
Frequencies --	444.5258	492.3738	535.1732
Frequencies --	594.6258	931.5328	979.5119
Frequencies --	1062.9078	1101.6491	1156.4719

Frequencies --	1191.7379	1238.9233	1354.0696
Frequencies --	1399.3092	1419.7112	1466.3672
Frequencies --	1475.5349	1494.1214	1516.7830
Frequencies --	1607.1373	1707.6649	2630.0664
Frequencies --	3082.6525	3163.5334	3168.1877
Frequencies --	3214.0141	3288.0460	3706.8835

Zero-point correction=	0.105567 (Hartree/Particle)
Thermal correction to Energy=	0.112490
Thermal correction to Enthalpy=	0.113435
Thermal correction to Gibbs Free Energy=	0.074427
Sum of electronic and zero-point Energies=	-268.246232
Sum of electronic and thermal Energies=	-268.239308
Sum of electronic and thermal Enthalpies=	-268.238363
Sum of electronic and thermal Free Energies=	-268.277371

1\1\GINC-MS8\Freq\UMP2-FC\6-31+G(d)\C3H8O2(1+,2)\CWANG\27-Feb-2004\1\\
#MP2/6-31+G(D) OPT=(TS,EF,CALCALL)\\ts4 mp2 geom=ms6/G3/ts4-g3.log rew
rite z-matrix by molden\\1,2\C\H,1,hc2\H,1,hc3,2,hch3\H,1,hc4,2,hch4,3
,dih4,0\C,1,cc5,2,cch5,3,dih5,0\O,5,oc6,1,occ6,2,dih6,0\H,6,ho7,5,hoc7
,1,dih7,0\H,5,hc8,1,hcc8,6,dih8,0\C,8,ch9,5,chc9,1,dih9,0\O,9,oc10,5,o
cc10,1,dih10,0\H,9,hc11,10,hco11,5,dih11,0\H,9,hc12,10,hco12,5,dih12,0
\H,10,ho13,9,hoc13,11,dih13,0\\hc2=1.09808587\hc3=1.09308854\hch3=110.
85422505\hc4=1.0970741\hch4=106.21259968\dih4=-120.91298292\cc5=1.4646
6144\cch5=108.15594846\dih5=122.67326147\oc6=1.25943544\occ6=122.70473
223\dih6=-120.15138192\ho7=1.04198123\hoc7=108.65072377\dih7=178.80286
071\hc8=1.41559671\hcc8=129.03685143\dih8=175.88339331\ch9=1.30966552\
chc9=147.40712982\dih9=-170.04778556\oc10=1.41631561\occ10=84.64461922
\dih10=-179.15932547\hc11=1.0893828\hco11=114.48968569\dih11=119.78790
308\hc12=1.08935655\hco12=110.4930749\dih12=-107.1892775\ho13=0.978998
72\hoc13=111.72474691\dih13=0.40141442\\Version=x86-Linux-G98RevA.7\HF
=-267.6088083\MP2=-268.351798\PUHF=-267.6166312\PMP2-0=-268.3571699\S2
=0.789915\S2-1=0.764681\S2A=0.750595\RMSD=5.538e-09\RMSF=8.389e-07

TS5 (for the rearrangement from V to VI)

Frequencies --	-1672.8442	40.4042	68.4174
Frequencies --	84.5892	133.1291	143.1970
Frequencies --	298.6225	499.5059	554.9516
Frequencies --	669.7645	931.8878	959.7995
Frequencies --	1019.9497	1057.5381	1161.4731
Frequencies --	1194.0202	1237.5241	1282.5268
Frequencies --	1367.5963	1494.0656	1504.9084
Frequencies --	1535.8342	1540.3180	1734.7274
Frequencies --	1772.5876	2191.4480	2262.5906
Frequencies --	3159.4479	3164.0605	3293.2063

Frequencies -- 3306.9220 3315.8815 3674.2726

Zero-point correction= 0.106288 (Hartree/Particle)
Thermal correction to Energy= 0.114072
Thermal correction to Enthalpy= 0.115016
Thermal correction to Gibbs Free Energy= 0.072662
Sum of electronic and zero-point Energies= -268.227966
Sum of electronic and thermal Energies= -268.220182
Sum of electronic and thermal Enthalpies= -268.219238
Sum of electronic and thermal Free Energies= -268.261592

1\1\GINC-MS8\Freq\UMP2-FC\6-31+G(d)\C3H8O2(1+,2)\CWANG\23-Feb-2004\1\\
#N GEOM=ALLCHECK GUESS=TCHECK UMP2(FC)/6-31+G(D) FREQ\\ts5 mp2
geom=ms6/g3/ts5-g3.log\\1,2\C\C,1,b2\O,2,b3,1,a3\O,3,b4,2,a4,1,h4,0\C,4,b5,3,
a5,2,h5,0\H,3,b6,2,a6,4,h6,0\H,4,b7,5,a7,2,h7,0\H,5,b8,4,a8,3,h8,0\H,5
,b9,4,a9,3,h9,0\H,5,b10,4,a10,3,h10,0\H,1,b11,2,a11,3,h11,0\H,1,b12,2,
a12,3,h12,0\H,2,b13,1,a13,12,h13,0\\b8=1.08601245\a8=104.81646546\h8=-
60.60571527\b9=1.08657215\a9=106.14174673\h9=-178.47543969\b10=1.08814
032\a10=109.13302412\h10=59.71742412\b12=1.08499203\a12=118.51439119\h
12=169.61484168\b11=1.09312227\a11=121.49783315\h11=-11.22411863\a3=13
5.93219036\b4=2.48949\a4=131.42074693\h4=164.16078647\a5=109.30910626\
b5=1.49106909\h5=111.93273311\b7=0.98221955\a7=111.72577026\h7=-137.57
475244\b2=1.38435265\b6=1.42551283\a6=129.32083614\h6=-2.07709283\b3=1
.24635059\b13=1.23897111\a13=68.82699613\h13=-67.86137264\\Version=x86
-Linux-G98RevA.7\HF=-267.5883594\MP2=-268.3342546\PUHF=-267.5927163\PM
P2-0=-268.3372683\S2=0.772545\S2-1=0.758537\S2A=0.750291\RMSD=1.862e-0
9\RMSF=2.546e-06

TS6a (step 1 of the S_N2 mechanism for H_2O loss reaction in $CH_3CHO/^{\bullet}CH_2OH_2^{+}$)

Frequencies -- -95.9572 15.2420 27.9302
Frequencies -- 57.4554 71.8036 145.0643
Frequencies -- 256.1815 352.6348 520.2535
Frequencies -- 731.5816 785.8103 813.1334
Frequencies -- 950.6711 996.3701 1065.7844
Frequencies -- 1179.4630 1196.2007 1310.0088
Frequencies -- 1459.0285 1496.0125 1515.8693
Frequencies -- 1521.7987 1532.1636 1735.9665
Frequencies -- 1993.9601 3061.7489 3176.8816
Frequencies -- 3241.7629 3325.3954 3332.3996
Frequencies -- 3371.3934 3581.6284 3679.0736

Zero-point correction= 0.110493 (Hartree/Particle)
Thermal correction to Energy= 0.118865
Thermal correction to Enthalpy= 0.119809
Thermal correction to Gibbs Free Energy= 0.073978

Sum of electronic and zero-point Energies= -268.263119
Sum of electronic and thermal Energies= -268.254746
Sum of electronic and thermal Enthalpies= -268.253802
Sum of electronic and thermal Free Energies= -268.299633

1\1\GINC-MS8\Freq\UMP2-FC\6-31+G(d)\C3H8O2(1+,2)\CWANG\12-May-2004\1\\
#MP2/6-31+G(D) OPT=(TS,EF,CALCALL)\\Sn2 ts1 for CH2CHO_OH2CH3
geom=h2oloss_ts1_calcall2.log\\1,2\O\C,1,R2\H,1,R3,2,A3\H,1,R4,2,A4,3,D4,0\H,2
,R5,1,A5,3,D5,0\H,2,R6,1,A6,5,D6,0\H,2,R7,1,A7,5,D7,0\O,1,R8,2,A8,3,D8
,0\C,8,R9,1,A9,2,D9,0\C,9,R10,8,A10,1,D10,0\H,9,R11,8,A11,10,D11,0\H,1
0,R12,9,A12,8,D12,0\H,10,R13,9,A13,12,D13,0\\R2=1.53690006\R3=0.986011
37\R4=0.98601162\R5=1.08554555\R6=1.08554435\R7=1.08538433\R8=4.204766
57\R9=1.2197585\R10=1.45007026\R11=1.10469409\R12=1.0829127\R13=1.0829
4507\A3=112.40069785\A4=112.39996214\A5=103.58979275\A6=103.58990217\A
7=108.98312211\A8=27.57019884\A9=177.38999255\A10=123.77866942\A11=120
.21271079\A12=120.65667088\A13=119.39191401\D4=122.26997497\D5=60.2740
7963\D6=117.18299211\D7=-121.41031926\D8=61.17565949\D9=0.30735836\D10
=179.7489876\D11=179.99996232\D12=180.0001735\D13=-179.99974453\\Versi
on=x86-Linux-G98RevA.7\HF=-267.6612806\MP2=-268.3736116\PUHF=-267.6720
037\PMP2-0=-268.3823366\S2=0.850212\S2-1=0.812379\S2A=0.752183\RMSD=5.
108e-09\RMSF=1.958e-07

TS6b (step 2 of the S_N2 mechanism for H_2O loss reaction in $CH_3CHO/^{\bullet}CH_2OH_2^{+}$)

Frequencies --	-484.1471	40.9835	83.7517
Frequencies --	91.1077	179.4493	263.1277
Frequencies --	287.7918	312.3834	371.4697
Frequencies --	560.4403	569.7982	752.9326
Frequencies --	789.6339	1016.9940	1064.2991
Frequencies --	1150.4534	1190.1779	1227.5364
Frequencies --	1331.7290	1446.9902	1447.5717
Frequencies --	1458.4218	1518.3667	1705.5635
Frequencies --	1943.1412	3075.6125	3221.2673
Frequencies --	3243.3274	3375.5475	3426.5984
Frequencies --	3437.1997	3652.8940	3778.6356

Zero-point correction= 0.109387 (Hartree/Particle)
Thermal correction to Energy= 0.117518
Thermal correction to Enthalpy= 0.118462
Thermal correction to Gibbs Free Energy= 0.076292
Sum of electronic and zero-point Energies= -268.255815
Sum of electronic and thermal Energies= -268.247683
Sum of electronic and thermal Enthalpies= -268.246739
Sum of electronic and thermal Free Energies= -268.288909

1\1\GINC-MS8\Freq\UMP2-FC\6-31+G(d)\C3H8O2(1+,2)\CWANG\03-May-2004\1\\

#N GEOM=ALLCHECK GUESS=TCHECK UMP2(FC)/6-31+G(D) FREQ\\Sn2_TS2
CH2CHO_OH2CH3geom=ms5/ts/h2oloss_ts2_z1.log\\1,2\C\H,1,R2\H,1,R3,2,A3\H,1,R
4,2,A4,3,D4,0\O,1,R5,2,A5,4,D5,0\H,5,R6,1,A6,2,D6,0\H,5,R7,1,A7,2,D7,0\
O,1,R8,2,A8,5,D8,0\C,8,R9,5,A9,1,D9,0\C,9,R10,8,A10,5,D10,0\H,10,R11,9
,A11,8,D11,0\H,10,R12,9,A12,8,D12,0\H,9,R13,8,A13,10,D13,0\\R9=1.23378
466\R10=1.43879162\R11=1.08288062\R12=1.08309917\A9=133.23507972\A10=1
22.27356176\A11=120.50424508\A12=119.10220668\D9=0.01382788\D10=-180.0
0350957\D11=-180.00207929\D12=-0.00171672\R13=1.10360885\A13=120.64025
688\D13=-180.00014058\R5=1.84657974\R6=0.97983107\R7=0.97982889\A5=96.
24816282\A6=116.00532721\A7=116.01333608\D5=96.44824078\D6=-63.6030315
8\D7=63.51784603\R2=1.07904212\R3=1.07777715\R4=1.07777356\R8=2.050084
89\A3=120.18874912\A4=120.18496301\A8=90.26251167\D4=167.09749404\D8=1
80.02321191\\Version=x86-Linux-G98RevA.7\HF=-267.6481104\MP2=-268.3652
015\PUHF=-267.6576955\PMP2-0=-268.3729289\S2=0.836164\S2-1=0.802358\S2
A=0.751751\RMSD=7.491e-10\RMSF=6.120e-06

TS7 (for the rearrangement from VI to VII)

Frequencies --	-140.1616	66.2129	91.9757
Frequencies --	114.4722	124.6843	215.7434
Frequencies --	287.6237	420.2871	477.3293
Frequencies --	667.2483	942.6116	1009.7171
Frequencies --	1017.5301	1065.6382	1100.0027
Frequencies --	1194.4139	1296.3293	1393.5152
Frequencies --	1420.0944	1453.5150	1471.5709
Frequencies --	1519.8517	1544.1685	1558.7169
Frequencies --	1701.2560	3083.8948	3128.9850
Frequencies --	3176.8534	3205.8005	3232.0805
Frequencies --	3253.0188	3454.9914	3717.8886

Zero-point correction=	0.110282 (Hartree/Particle)
Thermal correction to Energy=	0.117930
Thermal correction to Enthalpy=	0.118874
Thermal correction to Gibbs Free Energy=	0.077546
Sum of electronic and zero-point Energies=	-268.260517
Sum of electronic and thermal Energies=	-268.252868
Sum of electronic and thermal Enthalpies=	-268.251924
Sum of electronic and thermal Free Energies=	-268.293252

1\1\GINC-MS8\Freq\UMP2-FC\6-31+G(d)\C3H8O2(1+,2)\CWANG\04-Feb-2004\1\\
#N GEOM=ALLCHECK GUESS=TCHECK UMP2(FC)/6-31+G(D) FREQ\\ts7
geom=ts7-opt2.log\\1,2\C\H,1,R2\H,1,R3,2,A3\H,1,R4,2,A4,3,D4,0\C
,1,R5,2,A5,3,D5,0\O,5,R6,1,A6,2,D6,0\O,5,R7,1,A7,2,D7,0\H,6,R8,5,A8,1,
D8,0\C,7,R9,5,A9,1,D9,0\H,7,R10,5,A10,1,D10,0\H,9,R11,7,A11,5,D11,0\H,
9,R12,7,A12,5,D12,0\H,9,R13,7,A13,5,D13,0\\R2=1.09526312\R3=1.09476581
\R4=1.0978169\R5=1.45579155\R9=1.45867446\R10=0.97734891\R11=1.0911456

2\R12=1.09097176\R13=1.088591\A3=111.46896188\A4=106.94293988\A5=108.3
4627804\A9=121.42478567\A10=123.95235285\A11=110.3549857\A12=109.84914
584\A13=106.10108897\D4=-121.32544771\D5=122.63546239\D9=88.06546298\D
10=-60.53006821\D11=-92.48569857\D12=-214.73199326\D13=26.66052149\R6=
1.25193964\A6=127.0228023\D6=-131.39985023\D8=172.08601692\R8=0.997392
11\A8=110.88166202\R7=2.37579153\A7=126.33249792\D7=-12.7530066\\Versi
on=x86-Linux-G98RevA.7\HF=-267.647138\MP2=-268.3707986\PUHF=-267.64900
01\PMP2-0=-268.3719886\S2=0.756853\S2-1=0.751891\S2A=0.750035\RMSD=1.1
55e-09\RMSF=5.718e-08\

TS8 (for the rearrangement from VII to IX)

Frequencies --	-1743.2487	98.1007	134.8925
Frequencies --	161.9919	206.0535	391.6014
Frequencies --	404.7449	478.1036	538.2648
Frequencies --	688.3320	747.4471	846.8754
Frequencies --	908.9769	1009.3837	1060.3242
Frequencies --	1132.5336	1209.5562	1219.2474
Frequencies --	1433.6834	1453.0654	1475.4227
Frequencies --	1483.1108	1502.7691	1518.7153
Frequencies --	1540.8004	3073.6250	3157.5300
Frequencies --	3181.8130	3239.0203	3331.5458
Frequencies --	3342.8257	3556.3003	3681.1746

Zero-point correction=	0.109826 (Hartree/Particle)
Thermal correction to Energy=	0.116786
Thermal correction to Enthalpy=	0.117731
Thermal correction to Gibbs Free Energy=	0.078913
Sum of electronic and zero-point Energies=	-268.249466
Sum of electronic and thermal Energies=	-268.242505
Sum of electronic and thermal Enthalpies=	-268.241560
Sum of electronic and thermal Free Energies=	-268.280378

1\1\GINC-MS8\Freq\UMP2-FC\6-31+G(d)\C3H8O2(1+,2)\CWANG\02-Mar-2004\1\\
#N GEOM=ALLCHECK GUESS=TCHECK UMP2(FC)/6-31+G(D) FREQ\\ts8
geom=ts5/ts/ts8-opt.log\\1,2\C\H,1,R2\H,1,R3,2,A3\H,1,R4,2,A4,3,D4,0\C,1,R5,2,A5,
3,D5,0\O,5,R6,1,A6,2,D6,0\O,5,R7,1,A7,6,D7,0\H,6,R8,5,A8,1,D8,0\C,7,R9
,5,A9,1,D9,0\H,7,R10,5,A10,6,D10,0\H,9,R11,7,A11,5,D11,0\H,9,R12,7,A12
,5,D12,0\H,9,R13,7,A13,5,D13,0\\R2=1.10039589\R3=1.09330098\R4=1.09043
863\R6=1.32786776\R8=0.9800879\R10=0.99074886\R11=1.08650054\R12=1.086
10511\R13=1.08456858\A3=108.21295422\A4=109.47582501\A6=124.71529576\A
8=113.1690622\A10=109.7476322\A11=103.18303665\A12=99.50534727\A13=98.
92251893\D4=-118.51275167\D6=-66.60221695\D8=-17.68673031\D10=-30.9631
8288\D11=-52.77831068\D12=186.23604634\D13=67.94189939\R5=1.47693662\R
7=1.33707381\R9=1.91481533\A5=110.07891202\A7=117.58750031\A9=120.6660
8703\D5=120.33619734\D7=152.34268009\D9=-75.27842158\\Version=x86-Linu

x-G98RevA.7\HF=-267.6243293\MP2=-268.3592911\PUHF=-267.6315127\PMP2-0=
-268.3647836\S2=0.803495\S2-1=0.778045\S2A=0.75095\RMSD=6.207e-10\RMSF
=3.270e-05

CH_2=C(H)$OCH_3^{+\bullet}$ (H_2O loss product from $CH_3CHO/^{\bullet}CH_2OH_2^+$)

Frequencies --	135.0377	278.1077	297.7913
Frequencies --	449.7536	582.9449	853.6165
Frequencies --	884.6412	994.8646	1025.8561
Frequencies --	1183.9351	1223.3839	1269.9933
Frequencies --	1428.5036	1481.7319	1512.5854
Frequencies --	1539.4268	1547.5172	1613.4453
Frequencies --	3147.0349	3248.2599	3259.7715
Frequencies --	3269.5171	3303.2919	3370.5613

Zero-point correction=	0.086346 (Hartree/Particle)
Thermal correction to Energy=	0.091419
Thermal correction to Enthalpy=	0.092363
Thermal correction to Gibbs Free Energy=	0.058523
Sum of electronic and zero-point Energies=	-192.087071
Sum of electronic and thermal Energies=	-192.081998
Sum of electronic and thermal Enthalpies=	-192.081054
Sum of electronic and thermal Free Energies=	-192.114894

1\1\GINC-MS7\Freq\UMP2-FC\6-31+G(d)\C3H6O1(1+,2)\CWANG\23-Apr-2004\0\\
#N GEOM=ALLCHECK GUESS=TCHECK UMP2(FC)/6-31+G(D)
FREQ\\CH2CHOCH3, water loss product\\1,2\C,1.5751331237,-0.185751367,-
0.1511226868\H,1.5680083413,-0.5708756678,0.8612372265\H,2.519245919,-
0.1297691532,-0.6801808125\C,0.4036485551,0.2497575514,-0.8182498326\O,-
0.7859253844,0.2494
169784,-0.3355355106\H,0.4418725454,0.6324576377,-1.8369278245\C,-1.09
46173445,-0.2248080712,1.0327892588\H,-2.1686781701,-0.0892437739,1.11
32373089\H,-0.8190376105,-1.2765202932,1.1027416219\H,-0.5589939559,0.
4034267443,1.743676128\\Version=x86-Linux-G98RevA.7\HF=-191.6452529\MP
2=-192.173417\PUHF=-191.6496405\PMP2-0=-192.1767023\S2=0.778901\S2-1=0
.764273\S2A=0.750358\RMSD=5.734e-10\RMSF=5.541e-05

$CH_3C^+(OH)_2$ ($^{\bullet}CH_3$ loss product from $CH_3CHO/^{\bullet}CH_2OH_2^+$)

Frequencies --	63.1632	441.8402	554.6840
Frequencies --	566.3590	582.3299	712.4630
Frequencies --	918.7631	1071.0367	1098.5246
Frequencies --	1134.6967	1191.5738	1445.5078
Frequencies --	1479.8564	1499.5571	1602.6051
Frequencies --	1642.5264	3104.2499	3205.2865
Frequencies --	3258.5874	3590.1456	3609.1274

Zero-point correction= 0.074662 (Hartree/Particle)
Thermal correction to Energy= 0.079382
Thermal correction to Enthalpy= 0.080326
Thermal correction to Gibbs Free Energy= 0.047244
Sum of electronic and zero-point Energies= -228.649074
Sum of electronic and thermal Energies= -228.644355
Sum of electronic and thermal Enthalpies= -228.643411
Sum of electronic and thermal Free Energies= -228.676492

1\1\GINC-MS8\Freq\RMP2-FC\6-31+G(d)\C2H5O2(1+)\CWANG\05-Mar-2004\0\\#N GEOM=ALLCHECK GUESS=TCHECK RMP2(FC)/6-31+G(D) FREQ\\protonated acetic acid cation MP2\\1,1\C,0.590956231,1.1928002334,0.5097122682\H,0.5793718418,1.1829364329,1.6001674973\H,1.6359630664,1.2062399291,0.1723959444\H,0.0831873964,2.0687033708,0.1049559579\C,-0.0314507726,-0.0366767459,-0.0113434871\O,0.0570719598,-1.104803168,0.7099359099\H,-0.3321593438,-1.9330109159,0.3426288125\O,-0.5992894245,0.023348255,-1.1701220024\H,-0.9856559926,-0.8099704383,-1.5288721581\\Version=x86-Linux-G98RevA.7\HF=-228.1175749\MP2=-228.7237365\RMSD=4.831e-10\RMSF=5.540e-05

Appendix B:

Archive entries for MP2/6-31+G(d) optimized geometries of the stable states, transition states and some products on the potential energy surfaces of the $[(CH_3)_2C{=}O\cdots H^+\cdots O(H)CH_2^{\bullet}]$ and $[(CH_3)_2C{=}O\cdots H^+\cdots {}^{\bullet}OCH_3]$ complexes (in Chapter 5).

$[(CH_3)_2C{=}OH\cdots OCH_3]^{+\bullet}$, Stable State I

Frequencies --	47.9664	68.7367	71.1905
Frequencies --	99.4855	115.9432	130.8921
Frequencies --	141.0438	262.0559	403.0539
Frequencies --	495.1284	562.1331	832.3959
Frequencies --	880.4577	941.3807	978.5978
Frequencies --	1015.5999	1112.7879	1123.6197
Frequencies --	1140.8701	1204.3227	1289.2224
Frequencies --	1430.0369	1433.3689	1442.2401
Frequencies --	1462.3435	1473.5364	1490.5035
Frequencies --	1501.2168	1518.0293	1539.9682
Frequencies --	1549.6166	1678.8054	2809.9479
Frequencies --	3033.1311	3086.8055	3092.8455
Frequencies --	3155.9862	3176.9673	3181.3480
Frequencies --	3223.2466	3237.2162	3244.4185

Zero-point correction=	0.138236 (Hartree/Particle)
Thermal correction to Energy=	0.147857
Thermal correction to Enthalpy=	0.148801
Thermal correction to Gibbs Free Energy=	0.101816
Sum of electronic and zero-point Energies=	-307.434779
Sum of electronic and thermal Energies=	-307.425157
Sum of electronic and thermal Enthalpies=	-307.424213
Sum of electronic and thermal Free Energies=	-307.471198

1\1\GINC-MS8\Freq\UMP2-FC\6-31+G(d)\C4H10O2(1+,2)\CWANG\11-Mar-2004\0\
\#N GEOM=ALLCHECK GUESS=TCHECK UMP2(FC)/6-31+G(D)
FREQ\\Protonated acetone with CH3O radical\\1,2\C,1.49192395,2.2160736606,
0.7409720272\H,1.6755731604,1.9981534784,1.793192831\H,2.4232460354,2.4303607
711,0.2090579415\H,0.8672573656,3.1174963335,0.6632912744\C,0.7661429379,1.112
0293282,0.0837333141\O,0.2090338724,0.2644272675,0.8541517446\C,-1.8396
50035,-2.6947961052,0.1768268743\H,-1.1584644442,-3.5505071869,0.03083
17308\H,-2.7438039941,-2.894469626,-0.4045431004\H,-2.0351423148,-2.55
50419347,1.2415454556\O,-1.1549896238,-1.6136306439,-0.3885733971\H,-0
.3179517761,-0.4812758812,0.3812839212\C,0.6980621583,0.9988627007,-1.
3909773831\H,0.5700320278,1.9911484643,-1.8329780282\H,1.6724251716,0.
6245447306,-1.7368022781\H,-0.0843992876,0.3202003553,-1.7328355234\\V
ersion=x86-Linux-G98RevA.7\HF=-306.7381687\MP2=-307.5730142\PUHF=-306.
7416962\PMP2-0=-307.575211\S2=0.759851\S2-1=0.752384\S2A=0.750077\RMSD

=4.869e-10\RMSF=1.016e-05

$[(CH_3)_2C{=}O\cdots(H)OCH_3]^{+\bullet}$, Stable State II

Frequencies --	29.3898	48.7557	69.0318
Frequencies --	91.3111	100.9100	147.6813
Frequencies --	149.7413	176.8542	357.3679
Frequencies --	365.9249	456.7940	488.8788
Frequencies --	780.2877	914.5157	1008.4265
Frequencies --	1021.7214	1094.4366	1102.1546
Frequencies --	1123.1808	1166.1554	1192.4732
Frequencies --	1360.5161	1392.0564	1415.3800
Frequencies --	1481.6791	1484.8749	1494.6134
Frequencies --	1505.8991	1523.2377	1545.9118
Frequencies --	1560.0448	1590.5341	3099.8484
Frequencies --	3102.7060	3119.1373	3193.5467
Frequencies --	3203.6644	3214.7107	3243.7592
Frequencies --	3252.5352	3255.8017	3736.4870

Zero-point correction=	0.138200 (Hartree/Particle)
Thermal correction to Energy=	0.148480
Thermal correction to Enthalpy=	0.149424
Thermal correction to Gibbs Free Energy=	0.100628
Sum of electronic and zero-point Energies=	-307.415241
Sum of electronic and thermal Energies=	-307.404961
Sum of electronic and thermal Enthalpies=	-307.404017
Sum of electronic and thermal Free Energies=	-307.452814

1\1\GINC-MS8\Freq\UMP2-FC\6-31+G(d)\C4H10O2(1+,2)\CWANG\11-Mar-2004\0\
\#N GEOM=ALLCHECK GUESS=TCHECK UMP2(FC)/6-31+G(D) FREQ\\acetone
ion with methanol\\1,2\C,1.7029252649,1.9384325429,0.7504848135\H,1.76286795
19,1.8016995213,1.8296327719\H,2.6697225577,1.7325634833,0.2772201894\
H,1.4031044418,2.9616903948,0.4989321053\C,0.6992305655,1.0147570326,0
.1086046639\O,0.1430383639,0.2199904546,0.8645469118\C,-1.3800407887,-
2.5620490969,0.277168547\H,-0.6222037075,-2.5525071006,1.0591094039\H,
-1.2073750229,-3.4079471005,-0.3917880853\H,-2.3700657302,-2.635461966
3,0.7323170682\O,-1.2391360318,-1.3123157274,-0.4490313284\H,-2.021855
8343,-1.2162691564,-1.0229403357\C,0.3697719233,1.0698263245,-1.347856
621\H,1.1712142961,1.5838635628,-1.8789557018\H,0.1922047177,0.0590188
114,-1.7179524295\H,-0.5601541172,1.6461509143,-1.4401080748\\Version=
x86-Linux-G98RevA.7\HF=-306.7160994\MP2=-307.5534412\PUHF=-306.7211834
\PMP2-0=-307.5571761\S2=0.772824\S2-1=0.760595\S2A=0.750366\RMSD=9.865
e-10\RMSF=1.195e-04

$[(CH_3)_2C{=}OH\cdots(H)OCH_2]^{+\bullet}$, Stable State III

Frequencies --	25.2224	66.5186	87.8498
Frequencies --	102.2684	116.0390	128.8934
Frequencies --	176.1240	262.5111	360.1464
Frequencies --	401.7420	496.6544	549.2488
Frequencies --	757.8713	836.9109	905.2212
Frequencies --	976.4708	1089.7760	1112.6557
Frequencies --	1136.4879	1142.3935	1228.9583
Frequencies --	1289.1142	1401.6960	1427.0795
Frequencies --	1442.3266	1474.5687	1488.1361
Frequencies --	1497.1359	1511.8508	1520.3654
Frequencies --	1530.9132	1682.8621	2771.1078
Frequencies --	3088.1403	3094.1003	3176.7428
Frequencies --	3182.1208	3237.9298	3244.0189
Frequencies --	3244.2092	3397.7860	3741.8869

Zero-point correction=	0.137611 (Hartree/Particle)
Thermal correction to Energy=	0.147572
Thermal correction to Enthalpy=	0.148516
Thermal correction to Gibbs Free Energy=	0.100776
Sum of electronic and zero-point Energies=	-307.450706
Sum of electronic and thermal Energies=	-307.440744
Sum of electronic and thermal Enthalpies=	-307.439800
Sum of electronic and thermal Free Energies=	-307.487541

1\1\GINC-MS8\Freq\UMP2-FC\6-31+G(d)\C4H10O2(1+,2)\CWANG\05-Mar-2004\0\
\#N GEOM=ALLCHECK GUESS=TCHECK UMP2(FC)/6-31+G(D) FREQ\\
protonated acetone...OHCH2. geom=ahohch2.log at HF\\1,2\C,1.5322476697,
0.2896105259,0.516294011\H,1.5461377521,0.3061768126,1.6152404167\H,2.576833
7285,0.2532440844,0.1927441586\H,1.0465660694,1.1945916752,0.1499101388\C,0.8
354790652,-0.9486671002,0.0970831026\O,-0.3459682375,-0.9326262342,-0.
3756810823\O,-1.4912071904,1.37344483,-0.6953164247\H,-1.6527222211,1.
7400549421,-1.5857589047\H,-0.7725415781,-0.0001755798,-0.4818901297\C
,-1.9205364458,2.2564928567,0.3046210672\H,-1.9980989085,1.7805649494,
1.2707710612\H,-2.6130329469,3.0263831691,-0.0055317619\C,1.4801423769
,-2.2720320822,0.2087518677\H,0.7470574077,-3.0754784244,0.1333999945\
H,2.1988801677,-2.3631262875,-0.6182024393\H,2.0543279566,-2.341209309
,1.1367972309\\Version=x86-Linux-G98RevA.7\HF=-306.7311776\MP2=-307.58
83163\PUHF=-306.7338729\PMP2-0=-307.5900127\S2=0.759858\S2-1=0.752521\
S2A=0.750067\RMSD=8.961e-10\RMSF=2.421e-05

$[CH_2C(CH_3)=OH\cdots O(H)CH_3]^{+\bullet}$, Stable State IV

Frequencies --	35.7618	53.9947	73.0299
Frequencies --	102.1857	135.2743	165.3705
Frequencies --	290.5614	355.6250	402.7390
Frequencies --	482.9981	532.7587	559.4958
Frequencies --	841.4699	883.8276	993.0090
Frequencies --	1002.1007	1041.4274	1091.9465
Frequencies --	1092.6513	1196.1911	1321.2984
Frequencies --	1339.1195	1420.0008	1444.0344
Frequencies --	1492.7281	1495.5262	1513.5478
Frequencies --	1520.3093	1543.8733	1555.1963
Frequencies --	1564.3441	1612.5662	2353.9791
Frequencies --	3099.0954	3138.9359	3175.8138
Frequencies --	3239.0085	3244.0119	3249.1539
Frequencies --	3265.1496	3364.7748	3729.0158

Zero-point correction=	0.139000 (Hartree/Particle)
Thermal correction to Energy=	0.148410
Thermal correction to Enthalpy=	0.149354
Thermal correction to Gibbs Free Energy=	0.102944
Sum of electronic and zero-point Energies=	-307.460981
Sum of electronic and thermal Energies=	-307.451572
Sum of electronic and thermal Enthalpies=	-307.450627
Sum of electronic and thermal Free Energies=	-307.497037

1\1\GINC-MS8\Freq\UMP2-FC\6-31+G(d)\C4H10O2(1+,2)\CWANG\05-Mar-2004\0\
\#N GEOM=ALLCHECK GUESS=TCHECK UMP2(FC)/6-31+G(D) FREQ\\distonic
acetone with methanol geom=disaohch2.log HF\\1,2\C,0.3557245512,-0.14727378
92,1.729211551\H,0.33652634,-0.1151017041,2.8115755152\H,1.3088184388,
-0.1337906036,1.2127943324\H,0.0684073252,-0.2381012746,-0.7424798109\
C,-0.8758385747,-0.2065047669,1.0012957514\C,-2.1922466575,-0.22934106
86,1.6825074818\H,-2.2859117506,0.6451149677,2.3362229978\H,-3.0006909
589,-0.2407847736,0.95188927\H,-2.2555511898,-1.1168724118,2.323382036
3\O,1.4180765584,-0.2000064499,-1.3586672585\H,1.692695851,-1.02622355
03,-1.8022413689\O,-0.8814323603,-0.2477838806,-0.2838598258\C,1.76409
13189,0.9412259192,-2.2086002842\H,1.4816489411,1.8287317471,-1.646043
6844\H,2.8393513798,0.9384434637,-2.3841638156\H,1.2111682117,0.892269
0166,-3.1472057972\\Version=x86-Linux-G98RevA.7\HF=-306.7411309\MP2=-3
07.5999814\PUHF=-306.7446687\PMP2-0=-307.602499\S2=0.769302\S2-1=0.758
092\S2A=0.750227\RMSD=2.558e-09\RMSF=1.513e-05

$[CH_3\cdots(CH_3)C(=O)\cdots O(H)CH_3]^{+\bullet}$, Stable State V

Frequencies --	17.4396	47.1725	51.3650

Frequencies --	69.7907	88.0152	91.6213
Frequencies --	123.0646	166.8731	181.5830
Frequencies --	193.0332	207.1210	243.8662
Frequencies --	309.6682	396.6645	406.4414
Frequencies --	766.7635	914.4065	1010.4791
Frequencies --	1067.0875	1071.7241	1106.0644
Frequencies --	1190.7534	1390.7696	1427.3897
Frequencies --	1461.3170	1468.8927	1471.1001
Frequencies --	1483.1684	1521.5661	1541.9835
Frequencies --	1558.4063	2261.3091	3107.3995
Frequencies --	3129.4364	3185.4992	3211.5901
Frequencies --	3236.0936	3237.5508	3245.4841
Frequencies --	3367.8691	3371.6184	3734.6713

Zero-point correction=	0.132439 (Hartree/Particle)
Thermal correction to Energy=	0.145011
Thermal correction to Enthalpy=	0.145955
Thermal correction to Gibbs Free Energy=	0.091377
Sum of electronic and zero-point Energies=	-307.419559
Sum of electronic and thermal Energies=	-307.406987
Sum of electronic and thermal Enthalpies=	-307.406043
Sum of electronic and thermal Free Energies=	-307.460622

1\1\GINC-MS7\Freq\UMP2-FC\6-31+G(d)\C4H10O2(1+,2)\CWANG\14-Oct-2004\0\
\#N GEOM=ALLCHECK GUESS=TCHECK UMP2(FC)/6-31+G(D) FREQ\\trans
minimum geom for ch3 loss CH3C(CH3)O...OCH3\\1,2\C,-0.2960604172,1.78996324
56,0.5848855951\H,-0.2912871991,1.8465158492,1.6777290065\H,0.7147563976,
1.8983288497,0.1880589972\H,-0.9678083264,2.5404488047,0.1551413885\C,
-0.8038031932,0.4870525264,0.205772115\O,-1.4688329258,-0.3687599855,-
0.1567759894\C,0.8841503791,-2.1064500033,1.0681445643\H,1.7834507705,
-2.49178093,0.5861456962\H,0.0070828468,-2.4017261288,0.4930384916\H,0
.7970128904,-2.4774569057,2.0902489444\O,0.906611493,-0.6501690722,1.0
644710198\H,1.6842636533,-0.3460119025,1.5702766846\C,0.216374417,0.95
37070296,-2.7603078973\H,-0.6428113806,0.4284873856,-3.1566541373\H,0.
2993504166,2.0185551724,-2.9339227049\H,1.1097942798,0.3904354777,-2.5
225888723\\Version=x86-Linux-G98RevA.7\HF=-306.6876042\MP2=-307.551998
4\PUHF=-306.6902525\PMP2-0=-307.5536982\S2=0.760031\S2-1=0.75282\S2A=0
.75006\RMSD=9.131e-10\RMSF=1.880e-05

$[(CH_3)_2C{=}OH\cdots CH_2OH]^{+\bullet}$, Stable State VI

Frequencies --	26.1336	45.0210	82.2136
Frequencies --	112.3577	115.1274	143.7207
Frequencies --	186.3286	318.6910	401.5765
Frequencies --	502.8738	542.2238	597.0192
Frequencies --	835.5596	874.9630	980.0532

Frequencies --	997.2391	1070.6895	1093.5920
Frequencies --	1104.1019	1143.6059	1238.5195
Frequencies --	1254.1541	1379.0454	1418.2566
Frequencies --	1440.9608	1465.1137	1488.8337
Frequencies --	1495.9326	1503.9667	1531.6918
Frequencies --	1537.8294	1665.3001	2797.2569
Frequencies --	3083.5114	3092.0102	3163.8329
Frequencies --	3175.7881	3193.6317	3233.4586
Frequencies --	3245.6496	3329.7337	3716.4304

Zero-point correction=	0.138112 (Hartree/Particle)
Thermal correction to Energy=	0.147767
Thermal correction to Enthalpy=	0.148711
Thermal correction to Gibbs Free Energy=	0.101298
Sum of electronic and zero-point Energies=	-307.439868
Sum of electronic and thermal Energies=	-307.430213
Sum of electronic and thermal Enthalpies=	-307.429269
Sum of electronic and thermal Free Energies=	-307.476682

1\1\GINC-MS8\Freq\UMP2-FC\6-31+G(d)\C4H10O2(1+,2)\CWANG\07-May-2004\0\
\#N GEOM=ALLCHECK GUESS=TCHECK UMP2(FC)/6-31+G(D) FREQ\\
protonated acetone/ch2oh confVI isomer of III\\1,2\C,-0.8604910246,1.4038940
13,0.1501117319\C,-1.2605802475,-0.0138639162,-0.0109198094\C,-2.6575438221,-
0.4161191168,-0.2514443042\O,-0.413153912,-0.9617876186,0.0869836681\H,
-1.6192056843,2.0705776188,-0.2619230682\H,-0.7785914633,1.6112293769,
1.2272292467\H,0.1124827211,1.6003681973,-0.3104886452\H,-2.760962524,
-1.5002409131,-0.2865170823\H,-3.2869038057,0.0072285264,0.5421282331\
H,-3.0024931698,0.0350416126,-1.1902858009\H,0.5533415029,-0.677364793
,0.2899233932\C,2.3643203938,-0.3259571,0.6242354494\H,2.8548665368,-1
.2698765284,0.845388206\H,2.2587942687,0.4145409644,1.4106499454\O,2.5
584461483,0.2379409869,-0.6023894518\H,2.99210193,-0.388454288,-1.2147
565638\\Version=x86-Linux-G98RevA.7\HF=-306.7159801\MP2=-307.5779801\P
UHF=-306.7187503\PMP2-0=-307.5796779\S2=0.759982\S2-1=0.752219\S2A=0.7
50074\RMSD=1.500e-09\RMSF=1.705e-04

$[(CH_3)_2C(=O)\cdots O(H)CH_3]^{+\bullet}$, Stable State VII

Frequencies --	8.6653	74.9341	108.2421
Frequencies --	122.4354	150.3478	163.8036
Frequencies --	194.8420	217.9901	340.1232
Frequencies --	360.0329	399.1605	462.8272
Frequencies --	769.0770	915.2090	1005.9239
Frequencies --	1018.5608	1085.6396	1100.6252
Frequencies --	1129.3878	1158.2746	1191.1623
Frequencies --	1336.7492	1397.6541	1411.4412
Frequencies --	1473.1238	1482.0216	1490.6701

Frequencies -- 1516.1628 1521.3825 1544.6423
Frequencies -- 1560.9520 1570.7401 3107.5479
Frequencies -- 3110.7525 3123.3725 3219.9815
Frequencies -- 3222.2960 3224.5927 3241.5615
Frequencies -- 3267.7923 3269.7142 3743.6623

Zero-point correction= 0.138545 (Hartree/Particle)
Thermal correction to Energy= 0.148528
Thermal correction to Enthalpy= 0.149472
Thermal correction to Gibbs Free Energy= 0.101456
Sum of electronic and zero-point Energies= -307.421559
Sum of electronic and thermal Energies= -307.411576
Sum of electronic and thermal Enthalpies= -307.410632
Sum of electronic and thermal Free Energies= -307.458648

1\1\GINC-MS7\Freq\UMP2-FC\6-31+G(d)\C4H10O2(1+,2)\CWANG\03-Oct-2004\0\\#N GEOM=ALLCHECK GUESS=TCHECK UMP2(FC)/6-31+G(D) FREQ\\CH3...(CH3)CO...OHCH3\\1,2\C,0.0665893413,1.6729017339,0.887648168\H,0.5137629426,2.0684909119,1.8082155361\H,0.5238856076,2.1503200856,0.0217429334\H,-1.0116183126,1.8267307888,0.8988539527\C,0.4083623493,0.2065122676,0.8522118366\O,-0.399647495,-0.5791050154,1.3461859354\C,-1.4514813028,-0.9641815276,-1.7013828703\H,-1.7771639226,-1.4101302443,-0.7621226214\H,-1.1104581385,-1.7491376773,-2.3789013651\H,-2.2771787145,-0.4050056396,-2.1452645211\O,-0.3545593224,-0.0693426895,-1.3717935822\H,-0.0410059217,0.3463351914,-2.196597028\C,1.7877237349,-0.313669425,0.543710299\H,2.1780488144,0.2407145736,-0.309014812\H,2.3979990475,-0.10601379,1.4315963568\H,1.7702184013,-1.3841008548,0.3432281427\\Version=x86-Linux-G98RevA.7\HF=-306.723881\MP2=-307.5601041\PUHF=-306.7284916\PMP2-0=-307.5633222\S2=0.767579\S2-1=0.756874\S2A=0.75024\RMSD=4.229e-09\RMSF=8.626e-07

TS0 (for the rearrangement from VII to IV)

Frequencies -- -1960.4765 50.1598 96.7315
Frequencies -- 115.3125 132.2742 174.0431
Frequencies -- 180.6107 199.3506 375.4768
Frequencies -- 385.9411 409.4535 492.7596
Frequencies -- 696.7624 918.9071 945.5593
Frequencies -- 1018.7453 1021.2254 1072.4927
Frequencies -- 1091.4794 1102.6365 1146.2660
Frequencies -- 1192.5894 1371.2991 1389.3079
Frequencies -- 1396.5640 1443.7085 1486.2910
Frequencies -- 1502.8730 1521.4673 1546.5145
Frequencies -- 1560.9634 1607.6048 2016.4209
Frequencies -- 3083.2001 3120.7668 3170.9222
Frequencies -- 3192.0623 3220.8810 3239.6189

Frequencies -- 3249.2719 3309.5365 3738.5725

Zero-point correction= 0.134381 (Hartree/Particle)
Thermal correction to Energy= 0.143563
Thermal correction to Enthalpy= 0.144507
Thermal correction to Gibbs Free Energy= 0.099791
Sum of electronic and zero-point Energies= -307.365558
Sum of electronic and thermal Energies= -307.356376
Sum of electronic and thermal Enthalpies= -307.355432
Sum of electronic and thermal Free Energies= -307.400148

1\1\GINC-MS8\Freq\UMP2-FC\6-31+G(d)\C4H10O2(1+,2)\CWANG\27-Mar-2004\1\
\#MP2/6-31+G(D) OPT=(TS,EF,CALCALL)\\enol_keto 1,3-H shift assisted wi
th methanol continue ts0_ace.log\\1,2\C\H,1,hc2\H,1,hc3,2,hch3\H,1,hc4
,2,hch4,3,dih4,0\C,1,cc5,2,cch5,3,dih5,0\O,5,oc6,1,occ6,2,dih6,0\C,5,c
c7,1,ccc7,2,dih7,0\H,7,hc8,5,hcc8,1,dih8,0\H,7,hc9,5,hcc9,1,dih9,0\H,7
,hc10,5,hcc10,1,dih10,0\O,6,oo11,5,ooc11,1,dih11,0\C,11,co12,6,coo12,5
,dih12,0\H,12,hc13,11,hco13,6,dih13,0\H,12,hc14,11,hco14,6,dih14,0\H,1
2,hc15,11,hco15,6,dih15,0\H,11,ho16,12,hoc16,13,dih16,0\\hc2=1.1005910
9\hc3=1.09115105\hch3=108.81515991\hc4=1.09044337\hch4=108.26659228\di
h4=-121.27743155\cc5=1.46298107\cch5=106.85994228\dih5=119.52381565\oc
6=1.27078498\occ6=125.76252043\dih6=271.91787157\cc7=1.47394497\ccc7=1
37.00955531\dih7=77.04256205\hc8=1.08860326\hcc8=116.90984658\dih8=90.
53713889\hc9=1.09077167\hcc9=117.47315633\dih9=-67.88693011\oo11=2.842
56366\ooc11=58.663597\dih11=-99.85432719\co12=1.45317045\coo12=93.7760
359\dih12=158.71098714\hc13=1.09162348\hco13=110.20394212\dih13=128.45
198889\hc14=1.08970138\hco14=106.26758312\dih14=9.90738756\hc15=1.0919
8986\hco15=110.67858789\dih15=-109.07480094\ho16=0.97575524\hoc16=108.
11718733\dih16=-63.04087506\hc10=1.35534449\hcc10=78.32648123\dih10=-1
69.6660773\\Version=x86-Linux-G98RevA.7\HF=-306.6310549\MP2=-307.49993
94\PUHF=-306.6406706\PMP2-0=-307.507055\S2=0.802982\S2-1=0.775046\S2A=
0.751245\RMSD=6.943e-09\RMSF=1.019e-06

TS1 (for the rearrangement from III to IV)

Frequencies -- -1319.6658 59.2972 96.5846
Frequencies -- 136.0053 157.9081 225.7228
Frequencies -- 408.4499 418.4574 503.1083
Frequencies -- 525.9125 555.1235 640.3504
Frequencies -- 768.8133 831.6856 898.1819
Frequencies -- 1021.7726 1037.1563 1072.5963
Frequencies -- 1104.4679 1132.6195 1159.0264
Frequencies -- 1225.6864 1262.4896 1384.0068
Frequencies -- 1423.3248 1436.5859 1467.7943
Frequencies -- 1485.5878 1498.5399 1516.6891
Frequencies -- 1532.7283 1564.9318 1587.7578

Frequencies -- 3092.3033 3167.9132 3171.7585
Frequencies -- 3180.4403 3234.5131 3283.9071
Frequencies -- 3293.8981 3419.6225 3716.9874

Zero-point correction= 0.136008 (Hartree/Particle)
Thermal correction to Energy= 0.144015
Thermal correction to Enthalpy= 0.144960
Thermal correction to Gibbs Free Energy= 0.102900
Sum of electronic and zero-point Energies= -307.418114
Sum of electronic and thermal Energies= -307.410106
Sum of electronic and thermal Enthalpies= -307.409162
Sum of electronic and thermal Free Energies= -307.451222

1\1\GINC-MS8\Freq\UMP2-FC\6-31+G(d)\C4H10O2(1+,2)\CWANG\04-Mar-2004\1\
\#MP2/6-31+G(D) FREQ GUESS=CHECK GEOM=CHECK\\ts3 continue ts3acetone-r
cfc.log\\1,2\C\H,1,hc2\H,1,hc3,2,hch3\H,1,hc4,2,hch4,3,dih4,0\C,1,cc5,
2,cch5,4,dih5,0\O,5,oc6,1,occ6,2,dih6,0\O,6,oo7,5,ooc7,1,dih7,0\H,7,ho
8,6,hoo8,5,dih8,0\H,6,ho9,5,hoc9,1,dih9,0\C,7,co10,6,coo10,5,dih10,0\H
,10,hc11,7,hco11,6,dih11,0\H,10,hc12,7,hco12,6,dih12,0\C,5,cc13,1,ccc1
3,6,dih13,0\H,13,hc14,5,hcc14,1,dih14,0\H,13,hc15,5,hcc15,1,dih15,0\H,
13,hc16,5,hcc16,1,dih16,0\\hc3=1.08724678\hch3=107.95149286\hc4=1.0919
4324\hch4=95.64105481\dih4=-118.11559646\ho8=0.9775259\hoo8=134.436312
91\dih8=93.85730295\ho9=0.99500052\hoc9=112.46636284\dih9=-4.35214077\
hc11=1.08906435\hco11=111.29910856\dih11=-69.38418464\hc12=1.08923651\
hco12=116.46314136\dih12=153.59023633\cc13=1.47927615\ccc13=124.198240
51\dih13=-177.6357889\hc14=1.09328232\hcc14=110.54402005\dih14=34.6779
9956\hc15=1.09102306\hcc15=110.929641\dih15=-201.83393931\hc16=1.09868
142\hcc16=108.44687376\dih16=-82.52856586\hc2=1.34021398\cc5=1.4260173
3\cch5=103.70822158\dih5=-118.2176647\oc6=1.30512891\occ6=120.66460108
\dih6=61.69062479\oo7=2.80008515\ooc7=97.60145475\dih7=-25.37542677\co
10=1.38299313\coo10=94.31484557\dih10=-32.51294816\\Version=x86-Linux-
G98RevA.7\HF=-306.6777025\MP2=-307.5541218\PUHF=-306.6841349\PMP2-0=-3
07.5585506\S2=0.786163\S2-1=0.763456\S2A=0.750482\RMSD=1.811e-09\RMSF=
2.338e-05

TS3 (for the rearrangement from II to VI)

Frequencies -- -1136.9871 34.4292 110.9712
Frequencies -- 136.3986 153.5720 173.9049
Frequencies -- 203.9638 299.4538 363.8358
Frequencies -- 371.2042 504.2035 507.9725
Frequencies -- 775.9834 816.7936 914.2951
Frequencies -- 1017.7904 1099.0053 1104.7937
Frequencies -- 1122.9011 1143.7501 1194.2348
Frequencies -- 1364.3912 1371.2768 1416.9714
Frequencies -- 1434.6220 1456.0585 1485.0398

Frequencies -- 1491.5374 1498.2378 1503.5730
Frequencies -- 1524.8398 1587.2491 1810.8951
Frequencies -- 3088.8218 3095.6875 3146.1668
Frequencies -- 3175.7582 3185.4047 3238.1913
Frequencies -- 3247.6430 3252.4521 3757.4465

Zero-point correction= 0.134826 (Hartree/Particle)
Thermal correction to Energy= 0.143668
Thermal correction to Enthalpy= 0.144612
Thermal correction to Gibbs Free Energy= 0.100441
Sum of electronic and zero-point Energies= -307.401041
Sum of electronic and thermal Energies= -307.392199
Sum of electronic and thermal Enthalpies= -307.391255
Sum of electronic and thermal Free Energies= -307.435426

\#MP2/6-31+G(D) OPT=(TS,EF,CALCALL)\\new ts4 geom start pacetone_ch2oh
-2.log, geom=nts4.log\\1,2\C\C,1,R2\H,1,R3,2,A3\H,1,R4,2,A4,3,D4,0\H,1
,R5,2,A5,3,D5,0\C,2,R6,1,A6,3,D6,0\O,2,R7,1,A7,6,D7,0\H,6,R8,2,A8,1,D8
,0\H,6,R9,2,A9,8,D9,0\H,6,R10,2,A10,8,D10,0\H,1,R11,2,A11,3,D11,0\C,11
,R12,1,A12,2,D12,0\H,12,R13,11,A13,1,D13,0\H,12,R14,11,A14,13,D14,0\O,
12,R15,11,A15,13,D15,0\H,15,R16,12,A16,11,D16,0\\R2=1.4923006\R3=1.089
23176\R4=1.09638229\R5=1.09708456\R6=1.50640823\R7=1.23541105\R8=1.089
29158\R9=1.09609115\R10=1.09664631\R11=2.73361523\R12=1.15311319\R13=1
.09245585\R14=1.09142693\R15=1.40146646\R16=0.97429086\A3=110.04424222
\A4=108.32504476\A5=108.58840928\A6=121.80134645\A7=123.37215021\A8=11
2.21837237\A9=107.1348624\A10=106.8333249\A11=62.02575473\A12=107.6671
9426\A13=105.60546584\A14=105.91287003\A15=108.93480501\A16=110.844455
78\D4=120.57037967\D5=-122.11561788\D6=-2.29884902\D7=-180.01140209\D8
=-179.08820728\D9=122.17932165\D10=-121.84023223\D11=-174.80884644\D12
=153.6750128\D13=189.54054997\D14=-118.83353938\D15=123.41685321\D16=-
101.11158078\\Version=x86-Linux-G98RevA.7\HF=-306.6877647\MP2=-307.535
8669\PUHF=-306.693779\PMP2-0=-307.5401529\S2=0.777188\S2-1=0.761361\S2
A=0.750586\RMSD=4.289e-09\RMSF=4.607e-08

TS4 (for the rearrangement from II to VII)

Frequencies -- -61.5244 10.7204 67.3388
Frequencies -- 86.6572 108.3975 140.8959
Frequencies -- 167.0654 201.8415 357.1035
Frequencies -- 401.3599 417.3038 486.2411
Frequencies -- 757.8143 919.8869 1022.8201
Frequencies -- 1055.8710 1085.4668 1109.6179
Frequencies -- 1126.5679 1144.9454 1199.8424
Frequencies -- 1344.5617 1409.4776 1421.9244
Frequencies -- 1488.7947 1496.3572 1505.0918
Frequencies -- 1518.6310 1538.1066 1558.7284

Frequencies --	1575.1825	1589.9317	3086.4136
Frequencies --	3109.4031	3113.9988	3193.1111
Frequencies --	3204.3128	3204.5738	3234.9582
Frequencies --	3260.7174	3262.8752	3774.5887

Zero-point correction= 0.138420 (Hartree/Particle)
Thermal correction to Energy= 0.147845
Thermal correction to Enthalpy= 0.148789
Thermal correction to Gibbs Free Energy= 0.101494
Sum of electronic and zero-point Energies= -307.398326
Sum of electronic and thermal Energies= -307.388902
Sum of electronic and thermal Enthalpies= -307.387958
Sum of electronic and thermal Free Energies= -307.435253

1\1\GINC-MS7\Freq\UMP2-FC\6-31G(d)\C4H10O2(1+,2)\CWANG\27-Oct-2004\1\\
#MP2/6-31G(D) OPT=(TS,EF,CALCALL)\\ts for confVII to confII\\1,2\C\C,1
,cc2\C,2,cc3,1,ccc3\O,2,oc4,3,occ4,1,dih4,0\O,1,oc5,2,occ5,3,dih5,0\C,
5,co6,1,coc6,2,dih6,0\H,1,hc7,2,hcc7,3,dih7,0\H,1,hc8,2,hcc8,3,dih8,0\
H,1,hc9,2,hcc9,3,dih9,0\H,3,hc10,2,hcc10,1,dih10,0\H,3,hc11,2,hcc11,1,
dih11,0\H,3,hc12,2,hcc12,1,dih12,0\H,6,hc13,5,hco13,1,dih13,0\H,6,hc14
,5,hco14,1,dih14,0\H,6,hc15,5,hco15,1,dih15,0\H,5,ho16,1,hoc16,2,dih16
,0\\hc7=1.09338464\hcc7=109.27854396\dih7=231.01174536\hc8=1.0982905\h
cc8=105.62971404\dih8=115.03139249\hc9=1.08875175\hcc9=109.41992037\di
h9=-6.83201228\hc10=1.0887997\hcc10=112.2451237\dih10=182.07283021\hc1
1=1.09482411\hcc11=106.80289791\dih11=60.06983951\hc12=1.09512585\hcc1
2=106.50423474\dih12=-56.10141722\hc13=1.09302353\hco13=111.13770572\d
ih13=-132.15285419\hc14=1.0896694\hco14=106.55309715\dih14=-13.4980797
2\hc15=1.09297296\hco15=111.2581393\dih15=105.19230829\ho16=0.97258788
\hoc16=133.24055279\dih16=-75.65986217\cc2=1.49747378\cc3=1.50871965\c
cc3=123.36083072\co6=1.44238533\coc6=117.63177042\dih6=123.76644637\oc
4=1.22476193\occ4=116.45788593\dih4=-180.94118104\oc5=2.98682251\occ5=
79.77273549\dih5=135.26476696\\Version=x86-Linux-G98RevA.7\HF=-306.711
0836\MP2=-307.5367467\PUHF=-306.7160072\PMP2-0=-307.5403229\S2=0.77111
3\S2-1=0.759453\S2A=0.750318\RMSD=9.559e-09\RMSF=4.136e-08

TS5 (for the rearrangement from V to VII)

Frequencies --	-219.5357	40.3415	92.6667
Frequencies --	104.0452	110.5776	131.1252
Frequencies --	143.0183	202.5347	214.7987
Frequencies --	251.0917	378.2125	401.6081
Frequencies --	418.8118	506.5164	538.1613
Frequencies --	913.3805	1019.3360	1064.9507
Frequencies --	1076.9505	1087.6634	1103.7069
Frequencies --	1192.5999	1395.7853	1425.1205
Frequencies --	1462.2293	1466.4875	1476.0496

Frequencies -- 1492.8229 1523.5551 1545.1626
Frequencies -- 1561.6304 2338.2762 3102.3887
Frequencies -- 3121.6563 3163.2831 3200.8143
Frequencies -- 3222.0157 3238.8944 3263.0365
Frequencies -- 3349.2834 3357.3842 3737.6969

Zero-point correction= 0.135404 (Hartree/Particle)
Thermal correction to Energy= 0.145800
Thermal correction to Enthalpy= 0.146744
Thermal correction to Gibbs Free Energy= 0.099183
Sum of electronic and zero-point Energies= -307.412254
Sum of electronic and thermal Energies= -307.401859
Sum of electronic and thermal Enthalpies= -307.400915
Sum of electronic and thermal Free Energies= -307.448476

1\1\GINC-MS7\Freq\UMP2-FC\6-31+G(d)\C4H10O2(1+,2)\CWANG\28-Oct-2004\1\
\#MP2/6-31+G(D) OPT=(TS,EF,CALCALL)\\ts for min ch3 loss CH3C(CH3)O...
OCH3 and confVII\\1,2\C\H,1,R2\H,1,R3,2,A3\H,1,R4,2,A4,3,D4,0\C,1,R5,2
,A5,3,D5,0\O,5,R6,1,A6,2,D6,0\C,1,R7,2,A7,3,D7,0\H,7,R8,1,A8,2,D8,0\H,
7,R9,1,A9,8,D9,0\H,7,R10,1,A10,8,D10,0\O,7,R11,1,A11,8,D11,0\H,11,R12,
7,A12,1,D12,0\C,1,R13,2,A13,3,D13,0\H,13,R14,1,A14,2,D14,0\H,13,R15,1,
A15,14,D15,0\H,13,R16,1,A16,14,D16,0\\R2=1.09653863\R3=1.08794322\R4=1
.09484545\R6=1.14785359\R7=4.17640611\R8=1.09170967\R9=1.08967847\R10=
1.09174954\R12=0.9756378\R14=1.08469624\R15=1.08516271\R16=1.08461882\
A3=110.93508191\A4=110.50522987\A6=152.27308907\A7=87.48367565\A8=130.
71167112\A9=85.74477466\A10=107.32294693\A12=107.71042042\A14=122.7811
9404\A15=77.89475924\A16=90.93800258\D4=-123.51624279\D6=31.69177751\D
7=75.42665019\D8=-134.3362459\D9=-112.13232357\D10=138.80041466\D12=-2
13.54531901\D14=63.02231391\D15=115.21182019\D16=-125.35883615\R11=1.4
5338692\A11=24.16933845\D11=36.86858749\R5=1.46677641\A5=105.63577824\
D5=119.75002054\R13=2.89762822\A13=151.64651794\D13=95.44705631\\Versi
on=x86-Linux-G98RevA.7\HF=-306.6786107\MP2=-307.5476585\PUHF=-306.6846
208\PMP2-0=-307.5523243\S2=0.794171\S2-1=0.774149\S2A=0.750986\RMSD=3.
397e-09\RMSF=9.740e-08

$[CH_3C(=O)\cdots O(H)CH_3]^{+\bullet}$, the $^{\bullet}CH_3$ loss product from $[(CH_3)_2C=O\cdots H^{+}\cdots {}^{\bullet}OCH_3]$ ion.

Frequencies -- 61.2567 114.4588 136.5706
Frequencies -- 194.3873 248.1418 338.0215
Frequencies -- 458.6580 501.0641 586.1999
Frequencies -- 939.0604 953.9209 1076.9307
Frequencies -- 1102.2766 1127.4447 1190.7689
Frequencies -- 1373.0001 1442.1878 1493.2167
Frequencies -- 1502.5198 1507.2590 1534.7847
Frequencies -- 1538.1122 2107.0544 3112.4545
Frequencies -- 3151.7110 3212.5603 3231.3705

Frequencies -- 3275.0664 3291.3011 3646.0107

Zero-point correction= 0.101259 (Hartree/Particle)
Thermal correction to Energy= 0.108579
Thermal correction to Enthalpy= 0.109523
Thermal correction to Gibbs Free Energy= 0.070230
Sum of electronic and zero-point Energies= -267.772616
Sum of electronic and thermal Energies= -267.765297
Sum of electronic and thermal Enthalpies= -267.764353
Sum of electronic and thermal Free Energies= -267.803646

1\1\GINC-MS7\Freq\RMP2-FC\6-31+G(d)\C3H7O2(1+)\CWANG\08-Oct-2004\0\\#N GEOM=ALLCHECK GUESS=TCHECK RMP2(FC)/6-31+G(D) FREQ\\CH3CO-OHCH3 ch3 loss product from CH3C(CH3)O...OCH3\\1,1\C,0.7255635331,0.2956622687,0.0529089985\O,0.4623674083,1.4237730162,0.1627808933\C,-2.0159921913,0.0043015752,-0.0106334784\H,-2.7774026681,-0.6552913642,-0.4226081556\H,-1.9506625742,0.9232554627,-0.5870179309\H,-2.1694734266,0.2053510588,1.0487851875\O,-0.7180518924,-0.6836267685,-0.2050487649\H,-0.713988774,-1.5626443747,0.2364414396\C,1.8423468339,-0.6612187952,-0.0165131227\H,1.8053457779,-1.3364493502,0.8439318572\H,1.7675456494,-1.2392342301,-0.9412188114\H,2.7726028334,-0.0886274763,0.0052550021\\Version=x86-Linux-G98RevA.7\HF=-267.1185777\MP2=-267.8738759\RMSD=2.792e-09\RMSF=1.018e-07

Appendix C:

Archive entries for B3-LYP/6-31+G(d) optimized geometries of the stable states, transition states and some products on the potential energy surfaces in Chapter 6 ($[CH_3CHO/H_2O]^{+\bullet}$).

$[CH_3CO^{\bullet}\cdots H^{+}OH_2]$, Stable State I

Frequencies --	70.2023	104.7129	110.1096
Frequencies --	127.1383	335.8762	528.9339
Frequencies --	536.5651	571.3840	923.2357
Frequencies --	966.1605	1092.3077	1245.0794
Frequencies --	1263.7878	1385.3001	1436.3419
Frequencies --	1458.5069	1671.7746	1752.3476
Frequencies --	1846.0263	3039.1288	3115.9476
Frequencies --	3135.1198	3645.0554	3732.6794

Zero-point correction=	0.077671 (Hartree/Particle)
Thermal correction to Energy=	0.084547
Thermal correction to Enthalpy=	0.085491
Thermal correction to Gibbs Free Energy=	0.046882
Sum of electronic and zero-point Energies=	-229.855960
Sum of electronic and thermal Energies=	-229.849084
Sum of electronic and thermal Enthalpies=	-229.848139
Sum of electronic and thermal Free Energies=	-229.886749

1\1\GINC-MS9\Freq\UB3LYP\6-31+G(d)\C2H6O2(1+,2)\CWANG\25-Nov-2005\0\\#
B3LYP/6-31+G(D) FREQ\\conf1 on PES\\1,2\C,2.3181014706,-0.0514214706,0
.0035494118\H,2.7655014706,-0.5767214706,-0.8502205882\H,2.7605214706,
-0.4953614706,0.9048994118\H,2.5242814706,1.0247485294,-0.0454905882\C
,0.8684814706,-0.3237914706,0.0128794118\O,-0.0724185294,0.4440885294,
-0.0216405882\O,-2.4298785294,-0.1934014706,0.0139694118\H,-1.33131852
94,0.0824585294,-0.0043805882\H,-2.9034385294,0.0229085294,-0.81539058
82\H,-2.9166685294,0.1877485294,0.7733794118\\Version=x86-Linux-G98Rev
A.7\HF=-229.9336308\S2=0.752458\S2-1=0.\S2A=0.750004\RMSD=8.481e-09\RM
SF=9.695e-06

$[CH_3CHO^{+\bullet}\cdots OH_2]$, Stable State II

Frequencies --	58.7428	85.8178	114.7935
Frequencies --	238.6993	263.9360	475.8431
Frequencies --	521.5213	567.1398	848.4094
Frequencies --	963.9854	1035.8727	1229.0259
Frequencies --	1237.7325	1357.3008	1445.2862
Frequencies --	1459.8917	1557.3624	1686.7946
Frequencies --	1833.9129	3058.1218	3133.2576

Frequencies -- 3187.5703 3654.4728 3763.1480

Zero-point correction= 0.076953 (Hartree/Particle)
Thermal correction to Energy= 0.083869
Thermal correction to Enthalpy= 0.084813
Thermal correction to Gibbs Free Energy= 0.045617
Sum of electronic and zero-point Energies= -229.851150
Sum of electronic and thermal Energies= -229.844234
Sum of electronic and thermal Enthalpies= -229.843290
Sum of electronic and thermal Free Energies= -229.882486

1\1\GINC-MS5\Freq\UB3LYP\6-31+G(d)\C2H6O2(1+,2)\CWANG\01-Oct-2004\0\\#
N GEOM=ALLCHECK GUESS=TCHECK UB3LYP/6-31+G(D)
FREQ\\H2O...CH3CHO geom= a_disa_h2otscalcallircrev.log\\1,2\C,1.2961191707,-
1.0860226971,-0.0054907666\C,0.5429523013,0.2254353524,-
0.0094649138\O,0.9527907492,1.3404832142,-0.0301208826\H,2.3701417896,-
0.8956003143,-0.057855601\H,1.0219757368,-1.6213040677,0.9122722077\H,-
0.6821855643,0.1108127315,0.0118972084\O,-2.1356228273,-
0.2144169648,0.0304677855\H,-2.6233740515,0.1242426609,-
0.7456734075\H,0.9422294815,-1.6778073385,-0.8581932464\H,-
2.6005595996,0.1146504014,0.8245116978\\Version=x86-Linux-G98RevA.7\HF
=-229.9281031\S2=0.755142\S2-1=0.\S2A=0.75002\RMSD=1.281e-09\RMSF=3.27
9e-05

[$CH_3CHOH^+\cdots{}^{\bullet}OH$], Stable State III

Frequencies -- 90.3399 111.8957 152.3689
Frequencies -- 195.1765 263.8726 432.7354
Frequencies -- 536.3623 755.7337 931.9972
Frequencies -- 1050.1408 1156.5851 1161.4808
Frequencies -- 1373.9517 1379.0026 1447.9558
Frequencies -- 1456.6012 1491.0421 1682.7552
Frequencies -- 2890.6844 3021.9505 3060.8510
Frequencies -- 3138.7466 3187.8018 3604.9852

Zero-point correction= 0.078768 (Hartree/Particle)
Thermal correction to Energy= 0.085464
Thermal correction to Enthalpy= 0.086408
Thermal correction to Gibbs Free Energy= 0.048439
Sum of electronic and zero-point Energies= -229.822783
Sum of electronic and thermal Energies= -229.816087
Sum of electronic and thermal Enthalpies= -229.815143
Sum of electronic and thermal Free Energies= -229.853112

1\1\GINC-MS9\Freq\UB3LYP\6-31+G(d)\C2H6O2(1+,2)\CWANG\25-Nov-2005\0\\#
B3LYP/6-31+G(D) FREQ\\confIII on PES\\1,2\C,-0.1140491176,-0.238321764

7,-0.7599994118\O,-0.5078191176,0.0213882353,0.4106005882\H,0.94803088
24,-0.0972317647,-0.9929894118\C,-1.0468491176,-0.7143217647,-1.775429
4118\H,-1.0003291176,-0.0319717647,-2.6401394118\H,-0.6786591176,-1.67
91217647,-2.1619394118\H,-2.0675691176,-0.8052517647,-1.4006494118\O,1
.5180508824,0.8382182353,1.9026905882\H,1.4625608824,1.1047582353,2.85
23005882\H,0.2195008824,0.3478282353,1.0496605882\\Version=x86-Linux-G
98RevA.7\HF=-229.901551\S2=0.752582\S2-1=0.\S2A=0.750004\RMSD=9.853e-0
9\RMSF=4.875e-05

[$CH_2CHOH^{+\bullet}\cdots OH_2$], Stable State IV

Frequencies --	108.0591	124.7239	137.4316
Frequencies --	299.7060	400.8667	450.0941
Frequencies --	478.7840	525.8374	891.7459
Frequencies --	1002.2827	1011.4609	1221.3843
Frequencies --	1295.5211	1349.6326	1441.2444
Frequencies --	1493.7506	1612.1968	1690.2306
Frequencies --	2432.3162	3171.7180	3188.1234
Frequencies --	3304.7786	3711.7439	3809.3877

Zero-point correction=	0.080084 (Hartree/Particle)
Thermal correction to Energy=	0.086609
Thermal correction to Enthalpy=	0.087553
Thermal correction to Gibbs Free Energy=	0.050272
Sum of electronic and zero-point Energies=	-229.871719
Sum of electronic and thermal Energies=	-229.865194
Sum of electronic and thermal Enthalpies=	-229.864250
Sum of electronic and thermal Free Energies=	-229.901532

1\1\GINC-MS12\Freq\UB3LYP\6-31+G(d)\C2H6O2(1+,2)\CWANG\25-Nov-2005\1\\
#B3LYP/6-31+G(D) FREQ\\conflV on PES\\1,2\C\O,1,B1\H,2,B2,1,A1\C,1,B3,
2,A2,3,D1,0\H,4,B4,1,A3,2,D2,0\H,4,B5,1,A4,2,D3,0\O,2,B6,1,A5,4,D4,0\H
,7,B7,2,A6,1,D5,0\H,7,B8,2,A7,1,D6,0\H,1,B9,2,A8,4,D7,0\\B1=1.28054\B2
=1.04875\B3=1.41103\B4=1.08686\B5=1.08541\B6=2.53117\B7=0.97338\B8=0.9
7338\B9=1.09264\A1=114.6584\A2=119.20358\A3=119.93211\A4=120.13968\A5=
112.45213\A6=119.77121\A7=119.78567\A8=119.06832\D1=179.98508\D2=0.004
58\D3=179.99987\D4=-180.01409\D5=-112.24152\D6=-247.91961\D7=180.00576
\\Version=x86-Linux-G98RevA.7\HF=-229.9518035\S2=0.756089\S2-1=0.\S2A=
0.750019\RMSD=6.809e-09\RMSF=2.137e-05\Dipole=0.3279236,0.0005258,-0.2
588748

[$^{\bullet}OCCH_3\cdots H^{+}OH_2$], Stable State V

Frequencies --	51.2827	56.2804	86.6817
Frequencies --	120.3288	162.5252	293.4213
Frequencies --	337.3302	455.8823	784.9121

Frequencies -- 927.0283 993.6656 1089.3476
Frequencies -- 1348.1553 1471.4089 1475.7727
Frequencies -- 1669.9831 1698.7629 1957.9559
Frequencies -- 2848.7173 2972.8725 3108.9907
Frequencies -- 3154.5515 3513.3666 3592.7898

Zero-point correction= 0.077675 (Hartree/Particle)
Thermal correction to Energy= 0.084661
Thermal correction to Enthalpy= 0.085605
Thermal correction to Gibbs Free Energy= 0.046484
Sum of electronic and zero-point Energies= -229.805123
Sum of electronic and thermal Energies= -229.798137
Sum of electronic and thermal Enthalpies= -229.797193
Sum of electronic and thermal Free Energies= -229.836314

1\1\GINC-MS12\Freq\UB3LYP\6-31+G(d)\C2H6O2(1+,2)\CWANG\29-Oct-2004\0\\
#N GEOM=ALLCHECK GUESS=TCHECK UB3LYP/6-31+G(D) FREQ\\intermediate
complex for CO loss H2OH...CH3..C=O\\1,2\C,-0.120613903,-0.1018304458,-1.7
656028012\C,-0.2909038172,-0.1007902213,-0.2426521207\O,0.8402806396,0
.0300889615,-2.4257349898\H,0.7137323442,0.0029895527,0.2234663555\H,-
0.7768509275,-1.04001338,0.0389382514\H,-0.9499547589,0.7374098971,0.0
062353062\H,0.0960311376,0.0739718346,1.9193499409\O,-0.3705915025,0.1
260837897,2.8220100369\H,-0.0813260641,0.9055805691,3.3554209664\H,-0.
2900385068,-0.7135964806,3.3359183333\\Version=x86-Linux-G98RevA.7\HF=
-229.8827978\S2=0.753146\S2-1=0.\S2A=0.750006\RMSD=5.495e-09\RMSF=4.11
8e-04\Dipole=-0.3377895,0.0506839,5.0630199

[$H_2OH^+\cdots{}^{\bullet}CH_3\cdots CO$], Stable State VI

Frequencies -- 42.0866 47.8444 52.7428
Frequencies -- 66.1904 87.1796 88.1589
Frequencies -- 302.8784 381.8043 401.4334
Frequencies -- 545.0904 576.3091 1034.7229
Frequencies -- 1047.5963 1416.6878 1418.0376
Frequencies -- 1604.1862 1662.9532 1923.5221
Frequencies -- 2236.2357 3099.2391 3267.2634
Frequencies -- 3271.7930 3579.5205 3671.1347

Zero-point correction= 0.072502 (Hartree/Particle)
Thermal correction to Energy= 0.081675
Thermal correction to Enthalpy= 0.082619
Thermal correction to Gibbs Free Energy= 0.036831
Sum of electronic and zero-point Energies= -229.809345
Sum of electronic and thermal Energies= -229.800173
Sum of electronic and thermal Enthalpies= -229.799228
Sum of electronic and thermal Free Energies= -229.845016

1\1\GINC-MS8\Freq\UB3LYP\6-31+G(d)\C2H6O2(1+,2)\CWANG\14-Oct-2004\0\\#
N GEOM=ALLCHECK GUESS=TCHECK UB3LYP/6-31+G(D) FREQ\\ch3...h+oh2
ground state\\1,2\C,0.6516625857,0.0678569972,0.0802971906\H,0.4688740324,-0
.9553206184,-0.2431403421\H,2.302323532,-0.0107174418,0.0001399855\H,0
.5217859428,0.8633109802,-0.6514312197\H,0.5051460544,0.3078626467,1.1
313839289\O,3.3861004491,-0.0865035329,-0.1191033412\H,3.7527922652,-0
.8690418515,0.3511426128\H,3.8482817298,0.7301746002,0.1765763686\C,-2
.3816372039,0.0326488554,0.0059969832\O,-3.51351993,0.002840604,-0.041
201206\\Version=x86-Linux-G98RevA.7\HF=-229.8818472\S2=0.752642\S2-1=0
.\S2A=0.750005\RMSD=4.112e-09\RMSF=4.239e-05\Dipole=4.6527911,-0.01482
34,0.5742763

$[CH_3C(OH)^{+\bullet}\cdots OH_2]$, Stable State VII

Frequencies --	128.8470	152.5760	173.5935
Frequencies --	263.5312	392.6536	439.7794
Frequencies --	535.0858	575.8445	680.8520
Frequencies --	929.8047	1018.6074	1031.5165
Frequencies --	1256.4489	1398.4563	1457.6286
Frequencies --	1469.0743	1561.3343	1660.2389
Frequencies --	3032.3819	3096.5585	3176.6333
Frequencies --	3598.2037	3639.9383	3758.3884

Zero-point correction=	0.080711 (Hartree/Particle)
Thermal correction to Energy=	0.087171
Thermal correction to Enthalpy=	0.088115
Thermal correction to Gibbs Free Energy=	0.051234
Sum of electronic and zero-point Energies=	-229.829143
Sum of electronic and thermal Energies=	-229.822683
Sum of electronic and thermal Enthalpies=	-229.821739
Sum of electronic and thermal Free Energies=	-229.858620

1\1\GINC-MS5\Freq\UB3LYP\6-31+G(d)\C2H6O2(1+,2)\CWANG\07-Jan-2005\0\\#
N GEOM=ALLCHECK GUESS=TCHECK UB3LYP/6-31+G(D) FREQ\\ts for
CH3CO..HOH2 to CH3C(OH)...OH2 geom=tscarbene-z1.log\\1,2\C,1.1639799689,-
0.9630043755,0.0459556663\C,0.2936953967,0.1559082882,-
0.3464563341\O,0.4186465955,1.3203193959,0.1496726853\H,0.8094439314,-
1.912947822,-0.3572510321\H,2.1561815135,-0.7520106308,-
0.3795443575\H,1.2697103367,-1.0163002622,1.139399393\H,-
0.1505306744,2.0129141771,-0.2522598682\O,-1.5556417633,-
0.3078256587,0.0399094743\H,-1.9929752094,-0.7571480839,-0.7089
982807\H,-1.7419207486,-0.8318807525,0.845000875\\Version=x86-Linux-G9
8RevA.7\HF=-229.909854\S2=0.752037\S2-1=0.\S2A=0.750003\RMSD=4.554e-09
\RMSF=8.664e-05

[$CH_3CHO^{+\bullet}/OH_2$], Stable State VIII (an isomer of I)

Frequencies --	124.7341	158.6650	169.7512
Frequencies --	219.0178	261.5404	475.1108
Frequencies --	494.1790	581.3941	791.0717
Frequencies --	899.7534	1098.8643	1109.2242
Frequencies --	1295.9213	1360.8468	1458.2248
Frequencies --	1458.3823	1638.2811	1663.6772
Frequencies --	2965.1072	3040.8240	3093.8730
Frequencies --	3208.5746	3639.0293	3755.1484

Zero-point correction=	0.079647 (Hartree/Particle)
Thermal correction to Energy=	0.086272
Thermal correction to Enthalpy=	0.087216
Thermal correction to Gibbs Free Energy=	0.049817
Sum of electronic and zero-point Energies=	-229.842757
Sum of electronic and thermal Energies=	-229.836133
Sum of electronic and thermal Enthalpies=	-229.835188
Sum of electronic and thermal Free Energies=	-229.872588

1\1\GINC-MS12\Freq\UB3LYP\6-31+G(d)\C2H6O2(1+,2)\CWANG\25-Nov-2005\0\\
#B3LYP/6-31+G(D) FREQ\\confVIII on PES\\1,2\C,-1.3681397059,0.7603702941,0.2708491176\H,-0.5337297059,1.4606202941,0.2593191176\H,-2.1158497059,1.0057902941,-0.4977008824\H,-1.9017097059,0.7786202941,1.2325191176\C,-0.9187997059,-0.6348197059,0.0317291176\O,0.2207002941,-1.0405397059,-0.1641608824\H,-1.6785097059,-1.4441197059,0.0207191176\O,1.7171302941,0.6342402941,-0.1315208824\H,2.1286202941,0.4487902941,-0.9995208824\H,2.3201702941,0.2473902941,0.5346491176\\Version=x86-Linux-G98RevA.7\HF=-229.9224045\S2=0.756845\S2-1=0.\S2A=0.750036\RMSD=2.008e-09\RMSF=1.505e-05\

TS1/3

Frequencies --	-1818.1120	99.9523	113.4962
Frequencies --	193.9156	229.1305	340.2067
Frequencies --	545.4452	709.4334	811.0686
Frequencies --	955.7460	986.3005	1044.0364
Frequencies --	1128.2537	1338.2693	1385.8363
Frequencies --	1411.6187	1438.0790	1515.4888
Frequencies --	1641.0606	3018.0897	3071.3113
Frequencies --	3139.4902	3440.7330	3651.0625

Zero-point correction=	0.073375 (Hartree/Particle)
Thermal correction to Energy=	0.079662
Thermal correction to Enthalpy=	0.080606
Thermal correction to Gibbs Free Energy=	0.043439
Sum of electronic and zero-point Energies=	-229.791492

Sum of electronic and thermal Energies= -229.785206
Sum of electronic and thermal Enthalpies= -229.784262
Sum of electronic and thermal Free Energies= -229.821429

1\1\GINC-MS8\Freq\UB3LYP\6-31+G(d)\C2H6O2(1+,2)\CWANG\02-Nov-2004\1\\#
B3LYP/6-31+G(D) OPT=(EF,TS,CALCALL)\\1,4-H shift for confl and III geo
m=ms4/PTC/ts1_3z2.log\\1,2\C\H,1,R2\H,1,R3,2,A3\H,1,R4,2,A4,3,D4,0\C,1
,R5,2,A5,3,D5,0\O,5,R6,1,A6,2,D6,0\H,6,R7,5,A7,1,D7,0\H,5,R8,6,A8,1,D8
,0\O,8,R9,5,A9,1,D9,0\H,9,R10,8,A10,5,D10,0\\R2=1.10242961\R3=1.095871
97\R4=1.10159224\R5=1.4554638\R6=1.25608431\R10=0.98263506\A3=111.1466
9592\A4=105.4034227\A5=108.28702526\A6=124.23618856\A7=113.35156552\A1
0=107.74703625\D4=-120.63405765\D5=123.12070502\D6=-121.44662033\D7=18
0.91821686\D10=233.05515343\R9=1.18650619\A9=145.56648973\D9=-193.4302
0092\R7=0.99375989\R8=1.32452605\A8=109.72205295\D8=-177.97711753\\Ver
sion=x86-Linux-G98RevA.7\HF=-229.8648676\S2=0.757909\S2-1=0.\S2A=0.750
026\RMSD=7.548e-09\RMSF=6.887e-06

TS3/4

Frequencies --	-1690.1920	160.6460	290.0691
Frequencies --	361.9549	476.5213	505.8968
Frequencies --	701.0841	745.5949	861.4926
Frequencies --	934.6169	1123.2663	1154.9379
Frequencies --	1250.6898	1296.3527	1331.8993
Frequencies --	1381.6185	1468.7908	1571.5187
Frequencies --	1655.7365	2492.9915	3071.3836
Frequencies --	3141.8751	3161.1751	3638.6453

Zero-point correction= 0.074676 (Hartree/Particle)
Thermal correction to Energy= 0.079791
Thermal correction to Enthalpy= 0.080735
Thermal correction to Gibbs Free Energy= 0.046550
Sum of electronic and zero-point Energies= -229.801430
Sum of electronic and thermal Energies= -229.796314
Sum of electronic and thermal Enthalpies= -229.795370
Sum of electronic and thermal Free Energies= -229.829555

1\1\GINC-MS8\Freq\UB3LYP\6-31+G(d)\C2H6O2(1+,2)\CWANG\25-Aug-2004\1\\#
N GEOM=ALLCHECK GUESS=TCHECK UB3LYP/6-31+G(D) FREQ\\ts for water-
catalyzed a_disa geom=nts2-z2.log\\1,2\C\O,1,R2\H,1,R3,2,A3\C,1,R4,2,A4,3,D
4,0\H,4,R5,1,A5,2,D5,0\H,4,R6,1,A6,2,D6,0\H,4,R7,1,A7,2,D7,0\H,2,R8,1,
A8,4,D8,0\O,8,R9,2,A9,1,D9,0\H,9,R10,8,A10,1,D10,0\\R2=1.25366419\R3=1
.09513034\R6=1.09807382\R7=1.09779079\R10=0.98381814\A3=115.49969025\A
6=112.90665666\A7=113.73692462\A10=118.80252966\D6=109.07367629\D7=-12
2.42022697\D10=-107.58559074\R4=1.47553668\A4=122.82199606\D4=-179.825
81629\R9=1.57157693\A9=147.91972731\D9=9.56739183\R5=1.29252484\R8=1.0

472672\A5=104.8241994\A8=109.63813418\D5=-7.98302198\D8=1.54847949\\Ve
rsion=x86-Linux-G98RevA.7\HF=-229.8761052\S2=0.757534\S2-1=0.\S2A=0.75
0024\RMSD=2.226e-09\RMSF=3.812e-05\Dipole=0.0974316,0.6064547,-1.07758
78

TS1/5

Frequencies --	-72.5015	57.1497	101.1603
Frequencies --	149.7935	268.0771	286.8664
Frequencies --	336.1493	508.8467	820.9589
Frequencies --	928.6913	982.7945	1043.6549
Frequencies --	1334.7899	1471.2508	1510.1383
Frequencies --	1700.3136	1708.5415	1889.3218
Frequencies --	2963.5353	3082.5253	3137.6393
Frequencies --	3167.9619	3540.8505	3612.6986

Zero-point correction=	0.078833 (Hartree/Particle)
Thermal correction to Energy=	0.085571
Thermal correction to Enthalpy=	0.086515
Thermal correction to Gibbs Free Energy=	0.047647
Sum of electronic and zero-point Energies=	-229.797855
Sum of electronic and thermal Energies=	-229.791116
Sum of electronic and thermal Enthalpies=	-229.790172
Sum of electronic and thermal Free Energies=	-229.829040

1\1\GINC-MS8\Freq\UB3LYP\6-31+G(d)\C2H6O2(1+,2)\CWANG\17-Sep-2004\1\\#
N GEOM=ALLCHECK GUESS=TCHECK UB3LYP/6-31+G(D) FREQ\\Sn2 ts1
H3O_CH3_CO for CO loss geom=coloss_tsz5.log\\1,2\C\C,1,R2\O,1,R3,2,A3
\H,2,R4,1,A4,3,D4,0\H,2,R5,1,A5,4,D5,0\H,2,R6,1,A6,4,D6,0\O,2,R7,1,A7,3,D7,0\H,7,
R8,2,A8,1,D8,0\H,7,R9,8,A9,2,D9,0\H,7,R10,9,A10,8,D10,0\\R7=3.21892433
\D7=-8.1357775\R8=0.98714537\R9=0.98766722\R10=1.00990282\A8=115.58143
995\A9=111.18018866\A10=111.73091808\D8=124.47635111\D9=134.32017475\D
10=126.06289862\R4=1.09221127\R5=1.09865979\R6=1.10338172\A4=113.95281
105\A5=105.25434931\D4=165.44318922\D5=119.11311878\R3=1.18568216\A6=1
05.0286851\D6=-120.01552435\A3=112.835737\A7=138.98\R2=1.55\\Version=x
86-Linux-G98RevA.7\HF=-229.8766876\S2=0.753234\S2-1=0.\S2A=0.750007\RM
SD=6.170e-09\RMSF=8.701e-03

TS5/6

Frequencies --	-199.6238	38.6319	56.0975
Frequencies --	116.4277	152.0139	188.2201
Frequencies --	308.8823	364.1106	441.6553
Frequencies --	912.2463	952.0722	993.3870
Frequencies --	1144.0994	1456.0078	1468.0074
Frequencies --	1659.4374	1696.9111	1987.5857

Frequencies -- 2807.0060 3045.2966 3180.3802
Frequencies -- 3208.4143 3530.7049 3613.6643

Zero-point correction= 0.075911 (Hartree/Particle)
Thermal correction to Energy= 0.083546
Thermal correction to Enthalpy= 0.084490
Thermal correction to Gibbs Free Energy= 0.043174
Sum of electronic and zero-point Energies= -229.800744
Sum of electronic and thermal Energies= -229.793110
Sum of electronic and thermal Enthalpies= -229.792166
Sum of electronic and thermal Free Energies= -229.833482

1\1\GINC-MS8\Freq\UB3LYP\6-31+G(d)\C2H6O2(1+,2)\CWANG\31-Oct-2004\1\\#
N GEOM=ALLCHECK GUESS=TCHECK UB3LYP/6-31+G(D) FREQ\\coloss_ts2 for
confVI and CH6O_CO geom=coloss_ts2z4.log\\1,2\C\H,1,R2\H,1,R3,2,A3\H,1,R4
,2,A4,3,D4,0\C,1,R5,2,A5,3,D5,0\O,5,R6,1,A6,2,D6,0\H,1,R7,2,A7,3,D7,0\
X,7,R11,1,A11,2,D11,0\O,7,R8,8,A8,1,D8,0\H,9,R9,7,A9,1,D9,0\H,9,R10,7,
A10,10,D10,0\\R2=1.09525605\R3=1.0903234\R4=1.09292291\R6=1.16067608\A
3=115.76231684\A4=115.72062127\A6=125.3502068\D4=223.15070698\D6=17.65
318636\R8=1.02754377\R9=0.98694542\R10=0.98700911\A8=74.04945805\A9=11
2.08125137\A10=112.10808418\D8=183.02478112\D9=-101.3187154\D10=-125.3
7162013\R7=2.03709468\A7=70.5801716\D7=-71.47586507\D5=112.87578021\R1
1=1.60295226\A11=99.09899335\D11=157.23217123\A5=102.27070168\R5=1.75\
\Version=x86-Linux-G98RevA.7\HF=-229.8766555\S2=0.75505\S2-1=0.\S2A=0.
750016\RMSD=9.124e-10\RMSF=5.748e-03\Dipole=1.855509,3.994402,1.285543
1

TSP2 (for the production of $[OC\cdots H^{+}OH_2]$ ion)

Frequencies -- -214.1734 23.8743 86.8203
Frequencies -- 100.1274 222.1904 234.1187
Frequencies -- 323.6050 387.4239 487.3559
Frequencies -- 559.7935 564.9673 1054.3439
Frequencies -- 1057.3933 1204.6437 1429.4258
Frequencies -- 1429.9679 1641.5926 1843.0069
Frequencies -- 2269.4395 3117.7404 3293.7852
Frequencies -- 3298.2545 3696.4626 3798.7442

Zero-point correction= 0.073186 (Hartree/Particle)
Thermal correction to Energy= 0.080844
Thermal correction to Enthalpy= 0.081788
Thermal correction to Gibbs Free Energy= 0.040253
Sum of electronic and zero-point Energies= -229.818020
Sum of electronic and thermal Energies= -229.810362
Sum of electronic and thermal Enthalpies= -229.809418
Sum of electronic and thermal Free Energies= -229.850953

1\1\GINC-MS8\Freq\UB3LYP\6-31+G(d)\C2H6O2(1+,2)\CWANG\13-Dec-2004\0\\#
B3LYP/6-31+G(D) FREQ\\CH3...OC...H3O geom=ch3_oc_h3otsz2calcall.log 2
yes with predicted energy 0\\1,2\C,0.5942191472,0.0049256726,-1.947897
7016\C,0.5942191472,0.0049256726,0.3621022984\O,1.649232081,0.00492567
26,0.7998581996\H,1.1208875623,0.9487184769,-2.0630392086\H,-0.4797234
577,-0.0161263493,-2.1098680785\H,1.1575935597,-0.9173057333,-2.063581
4452\H,-0.5701956969,0.0038777597,0.5560804057\O,-2.0683443265,-0.0111
300087,0.8030450951\H,-2.5121449561,0.7688861235,1.1822809269\H,-2.494
1488141,-0.7975236599,1.1896734614\\Version=x86-Linux-G98RevA.7\HF=-22
9.891206\S2=0.755386\S2-1=0.\S2A=0.750018\RMSD=4.880e-09\RMSF=3.330e-0
3

TSP3 (for the production of $[CO\cdots H^{+}OH_2]$ ion)

Frequencies --	-270.0259	32.0872	55.0430
Frequencies --	79.9438	93.0255	222.4707
Frequencies --	331.7597	413.1549	492.6521
Frequencies --	523.0577	525.4853	945.2994
Frequencies --	1041.7884	1426.8601	1437.1682
Frequencies --	1703.5099	1740.2108	1910.1033
Frequencies --	2723.6450	3127.2949	3298.7746
Frequencies --	3303.5117	3601.7912	3678.4373

Zero-point correction=	0.074512 (Hartree/Particle)
Thermal correction to Energy=	0.082507
Thermal correction to Enthalpy=	0.083451
Thermal correction to Gibbs Free Energy=	0.041107
Sum of electronic and zero-point Energies=	-229.802561
Sum of electronic and thermal Energies=	-229.794566
Sum of electronic and thermal Enthalpies=	-229.793622
Sum of electronic and thermal Free Energies=	-229.835966

1\1\GINC-MS7\Freq\UB3LYP\6-31+G(d)\C2H6O2(1+,2)\CWANG\08-Dec-2004\1\\#
B3LYP/6-31+G(D) FREQ GUESS=CHECK GEOM=CHECK\\CH3...CO...H3O
geom=ch3_co_h3otscalcall4.log\\1,2\C\H,1,B1\H,1,B2,2,A1\H,1,B3,2,A2,3,D1,0\C,1,2
.35,2,A3,3,D2,0\O,5,B5,1,A4,2,D3,0\H,6,B6,5,A5,1,D4,0\X,7,B7,6,A6,5,D5
,0\O,7,B8,8,A7,6,D6,0\H,9,B9,6,A8,5,D7,0\H,9,B10,6,A9,5,D8,0\\B1=1.085
74658\B2=1.08502402\B3=1.08498155\B5=1.17058773\A1=118.54303197\A2=118
.55342769\A4=114.77245322\D1=154.28431699\D3=0.81494381\B6=1.53907484\
A5=145.56511201\D4=-179.34795534\B8=1.03452522\A7=134.19521552\D6=-181
.38782163\B9=0.98309199\A8=112.20321459\D7=-112.69934789\B10=0.9830967
1\A9=111.95709151\D8=122.13741908\B7=1.63171685\A6=45.55449936\D5=-111
.17724533\A3=99.18493083\D2=-102.85825431\\Version=x86-Linux-G98RevA.7
\HF=-229.8770728\S2=0.762415\S2-1=0.\S2A=0.750052\RMSD=2.287e-09\RMSF=
2.774e-03

TS4/7

Frequencies --	-400.1475	112.7473	137.8306
Frequencies --	276.9569	342.9995	436.2312
Frequencies --	510.9947	564.8121	692.4022
Frequencies --	859.1982	984.3875	1066.5246
Frequencies --	1139.9785	1236.7995	1439.2460
Frequencies --	1529.8171	1572.8344	1677.7607
Frequencies --	1854.2440	3118.0990	3244.7783
Frequencies --	3598.4034	3686.8657	3691.1553

Zero-point correction=	0.076945 (Hartree/Particle)
Thermal correction to Energy=	0.082944
Thermal correction to Enthalpy=	0.083888
Thermal correction to Gibbs Free Energy=	0.047444
Sum of electronic and zero-point Energies=	-229.788595
Sum of electronic and thermal Energies=	-229.782597
Sum of electronic and thermal Enthalpies=	-229.781652
Sum of electronic and thermal Free Energies=	-229.818096

1\1\GINC-MS5\Freq\UB3LYP\6-31+G(d)\C2H6O2(1+,2)\CWANG\26-Nov-2004\1\\#
B3LYP/6-31+G(D) OPT=(TS,EF,CALCALL)\\ts 1_2-H with H2O between ch3coh/
ch2choh\\1,2\C\C,1,B1\O,2,B2,1,A1\H,1,B3,2,A2,3,D1,0\H,1,B4,2,A3,3,D2,
0\H,3,B5,2,A4,1,D3,0\H,2,B6,1,A5,3,D4,0\O,7,B7,2,A6,1,D5,0\H,8,B8,7,A7
,2,D6,0\H,8,B9,7,A8,2,D7,0\\B1=1.34334042\B2=1.31112802\B3=1.08645275\
B4=1.09356107\B5=0.97556959\B8=0.98213891\B9=0.98236357\A1=129.1135567
7\A2=120.31358145\A3=121.21088692\A4=114.27840978\A7=112.73705216\A8=1
12.60434987\D1=-161.28611466\D2=16.54911389\D3=-157.66390675\D6=83.546
89379\D7=-151.40149874\B6=1.74033387\B7=1.10315459\A5=79.30002392\A6=1
61.25881473\D4=-125.84619688\D5=-180.8673492\\Version=x86-Linux-G98Rev
A.7\HF=-229.8655405\S2=0.753706\S2-1=0.\S2A=0.750008\RMSD=3.937e-09\RM
SF=1.391e-05

TS1/7

Frequencies --	-110.7223	83.6054	212.0374
Frequencies --	247.1686	260.5819	370.6724
Frequencies --	424.7624	438.6620	645.6823
Frequencies --	918.1932	989.3227	1038.1746
Frequencies --	1272.5407	1380.9411	1414.8880
Frequencies --	1441.8832	1659.1876	1681.9942
Frequencies --	3024.8758	3096.0296	3128.2868
Frequencies --	3499.6007	3696.8977	3802.5963

Zero-point correction=	0.079118 (Hartree/Particle)

Thermal correction to Energy= 0.085415
Thermal correction to Enthalpy= 0.086360
Thermal correction to Gibbs Free Energy= 0.049480
Sum of electronic and zero-point Energies= -229.828778
Sum of electronic and thermal Energies= -229.822480
Sum of electronic and thermal Enthalpies= -229.821536
Sum of electronic and thermal Free Energies= -229.858415

1\1\GINC-MS5\Freq\UB3LYP\6-31+G(d)\C2H6O2(1+,2)\CWANG\04-Jan-2005\1\\#
UB3LYP/6-31+G(D) OPT=(TS,EF,CALCALL)\\ts for CH3CO..HOH2 to CH3C(OH).
..OH2 geom=tscarbene-z1.log\\1,2\C\C,1,R2\O,2,R3,1,A3\H,1,R4,2,A4,3,D4
,0\H,1,R5,2,A5,3,D5,0\H,1,R6,2,A6,3,D6,0\H,3,R7,2,A7,1,D7,0\O,2,R8,3,A
8,7,D8,0\H,8,R9,2,A9,1,D9,0\H,8,R10,2,A10,1,D10,0\\R2=1.45471595\R3=1.
24961098\A3=127.14020756\R4=1.09784362\A4=108.93440177\D4=132.00666334
\R5=1.10135954\A5=107.84692408\D5=-113.18661494\R6=1.09811353\A6=111.7
1887886\D6=8.53619704\R7=0.98985294\A7=113.37337543\D7=185.99625521\R9
=0.97331571\A9=117.9171775\D9=-87.9370932\R10=0.97405391\A10=127.49310
3\D10=54.22548604\R8=2.40116728\A8=88.94798715\D8=-39.32493956\\Versio
n=x86-Linux-G98RevA.7\HF=-229.9078953\S2=0.752517\S2-1=0.\S2A=0.750005
\RMSD=6.050e-09\RMSF=9.867e-06

TS1/2

Frequencies -- -390.6826 73.8834 108.2970
Frequencies -- 130.4420 186.5604 244.5527
Frequencies -- 423.6768 470.0461 890.4028
Frequencies -- 974.8962 1020.2425 1077.9036
Frequencies -- 1385.2591 1448.9960 1465.3762
Frequencies -- 1602.0782 1709.7382 1882.1022
Frequencies -- 2982.8803 3048.6706 3130.7348
Frequencies -- 3144.7626 3580.8517 3659.8605

Zero-point correction= 0.078921 (Hartree/Particle)
Thermal correction to Energy= 0.085730
Thermal correction to Enthalpy= 0.086675
Thermal correction to Gibbs Free Energy= 0.048030
Sum of electronic and zero-point Energies= -229.837094
Sum of electronic and thermal Energies= -229.830285
Sum of electronic and thermal Enthalpies= -229.829340
Sum of electronic and thermal Free Energies= -229.867985

1\1\GINC-MS8\Freq\UB3LYP\6-31+G(d)\C2H6O2(1+,2)\CWANG\26-Nov-2004\1\\#
B3LYP/6-31+G(D) OPT=(TS,EF,CALCALL)\\ts CH3CO..H3O to CH3COH...H2O
\\1,2\C\H,1,B1\H,1,B2,2,A1\H,1,B3,2,A2,3,D1,
0\C,1,B4,2,A3,3,D2,0\O,5,B5,1,A4,2,D3,0\H,6,B6,5,A5,1,D4,0\O,6,B7,5,A6

,1,D5,0\H,8,B8,6,A7,5,D6,0\H,8,B9,6,A8,5,D7,0\\B1=1.0966906\B2=1.09604
384\B3=1.09615316\B4=1.48981961\B5=1.19939941\B7=2.7588358\B8=0.985281
55\B9=0.98376789\A1=107.05125994\A2=110.7154844\A3=108.57034014\A4=132
.12231504\A6=88.61956839\A7=84.33385588\A8=127.46391722\D1=120.9847974
5\D2=-117.55189985\D3=-119.85204173\D5=-183.86801727\D6=-184.40064201\
D7=63.6094524\B6=1.89092497\A5=75.17820004\D4=-183.00030597\\Version=x
86-Linux-G98RevA.7\HF=-229.9160148\S2=0.753276\S2-1=0.\S2A=0.750005\RM
SD=3.754e-09\RMSF=1.907e-05

TS2/8

Frequencies --	-154.1805	99.9088	131.3745
Frequencies --	136.9357	154.1988	320.7398
Frequencies --	383.3344	411.0084	765.4605
Frequencies --	859.4231	1021.5567	1054.6710
Frequencies --	1191.2691	1329.6544	1438.0699
Frequencies --	1456.8770	1653.2456	1695.1639
Frequencies --	2904.3123	3045.5937	3124.1827
Frequencies --	3214.0780	3688.9701	3800.8166

Zero-point correction=	0.077186 (Hartree/Particle)
Thermal correction to Energy=	0.084012
Thermal correction to Enthalpy=	0.084956
Thermal correction to Gibbs Free Energy=	0.046628
Sum of electronic and zero-point Energies=	-229.833827
Sum of electronic and thermal Energies=	-229.827001
Sum of electronic and thermal Enthalpies=	-229.826057
Sum of electronic and thermal Free Energies=	-229.864385

1\1\GINC-MS5\Freq\UB3LYP\6-31+G(d)\C2H6O2(1+,2)\CWANG\24-Oct-2004\1\\#
B3LYP/6-31+G(D) OPT=(TS,EF,CALCALL)\\TS for VI and isoIII geom=isoIIt
s2 similar to ts2 of CH3CHO/CH3OH pair\\1,2\C\H,1,R2\H,1,R3,2,A3\H,1,R
4,2,A4,3,D4,0\C,1,R5,2,A5,4,D5,0\O,5,R6,1,A6,2,D6,0\H,5,R7,1,A7,2,D7,0
\O,6,R8,5,A8,1,D8,0\H,8,R9,6,A9,5,D9,0\H,8,R10,6,A10,5,D10,0\\R2=1.089
42956\R3=1.10025195\A3=112.17746593\R4=1.09655112\A4=112.31281501\D4=1
22.42279312\R5=1.50661897\A5=110.62491329\D5=119.19900467\R6=1.2082771
2\A6=125.48622841\D6=6.43941964\R7=1.11460238\A7=118.86217475\D7=183.7
9823684\R8=2.77246056\A8=79.63617224\D8=-72.57897175\R9=0.97347386\A9=
153.84754709\D9=70.32594744\R10=0.97364264\A10=95.36834382\D10=-149.51
885938\\Version=x86-Linux-G98RevA.7\HF=-229.9110133\S2=0.756685\S2-1=0
.\S2A=0.750034\RMSD=8.584e-09\RMSF=1.554e-05

TS3/8

Frequencies --	-1890.1713	99.0944	140.7487
Frequencies --	191.8065	236.6162	450.0784

Frequencies -- 555.6818 673.6255 801.8384
Frequencies -- 912.7346 1124.0280 1142.3865
Frequencies -- 1217.6028 1380.1589 1396.2588
Frequencies -- 1446.4927 1469.5382 1495.1289
Frequencies -- 1693.2580 3031.2861 3081.5263
Frequencies -- 3084.9904 3164.9921 3558.8579

Zero-point correction= 0.073696 (Hartree/Particle)
Thermal correction to Energy= 0.079800
Thermal correction to Enthalpy= 0.080745
Thermal correction to Gibbs Free Energy= 0.043992
Sum of electronic and zero-point Energies= -229.814418
Sum of electronic and thermal Energies= -229.808313
Sum of electronic and thermal Enthalpies= -229.807369
Sum of electronic and thermal Free Energies= -229.844121

1\1\GINC-MS5\Freq\UB3LYP\6-31+G(d)\C2H6O2(1+,2)\CWANG\04-Aug-2004\1\\#
B3LYP/6-31+G(D) OPT=(TS,EF,CALCALL)\\TS for proton transfer of acetade
hyde with water\\1,2\C\C,1,cc2\O,2,oc3,1,occ3\H,1,hc4,2,hcc4,3,dih4,0\
H,1,hc5,2,hcc5,3,dih5,0\H,1,hc6,2,hcc6,3,dih6,0\H,2,hc7,1,hcc7,3,dih7,
0\H,3,ho8,2,hoc8,1,dih8,0\O,8,oh9,3,oho9,2,dih9,0\H,9,ho10,8,hoh10,3,d
ih10,0\\cc2=1.47637515\oc3=1.24278915\occ3=126.67516935\hc4=1.09271591
\hcc4=113.29521768\dih4=-0.48789183\hc5=1.10090633\hcc5=108.2051682\di
h5=-123.68474513\hc6=1.100888\hcc6=108.29471354\dih6=122.65020679\hc7=
1.10031011\hcc7=118.83345657\dih7=-179.80419825\ho10=0.99034826\hoh10=
111.61435737\dih10=-89.77986537\ho8=1.23940793\hoc8=124.5849111\dih8=7
.74717976\oh9=1.17206439\oho9=168.13111178\dih9=-50.50599564\\Version=
x86-Linux-G98RevA.7\HF=-229.8881134\S2=0.754196\S2-1=0.\S2A=0.750013\R
MSD=9.300e-09\RMSF=8.913e-06

$^{\bullet}CH_3\cdots H^+OH_2$ ($P1^{+\bullet}$, the CO loss products of $[CH_3CHO/H_2O]^{+\bullet}$ ion)

Frequencies -- 24.0107 263.2994 312.2439
Frequencies -- 321.9380 478.1968 536.3946
Frequencies -- 1001.2515 1028.8322 1419.6032
Frequencies -- 1421.6055 1631.6374 1685.3692
Frequencies -- 2232.0590 3095.2531 3263.7080
Frequencies -- 3267.6219 3574.1655 3661.0022

Zero-point correction= 0.066564 (Hartree/Particle)
Thermal correction to Energy= 0.072082
Thermal correction to Enthalpy= 0.073026
Thermal correction to Gibbs Free Energy= 0.038994
Sum of electronic and zero-point Energies= -116.494716
Sum of electronic and thermal Energies= -116.489198
Sum of electronic and thermal Enthalpies= -116.488254

Sum of electronic and thermal Free Energies= -116.522285

1\1\GINC-MS8\Freq\UB3LYP\6-31+G(d)\C1H6O1(1+,2)\CWANG\24-Nov-2005\1\\#
B3LYP/6-31+G(D) FREQ\\ch6o b3lyp/6-31+g(d)geom\\1,2\C\H,1,B1\H,1,B2,2,
A1\H,1,B3,2,A2,3,D1,0\H,1,B4,2,A3,4,D2,0\O,1,B5,2,A4,4,D3,0\H,6,B6,1,A
5,2,D4,0\H,6,B7,1,A6,2,D5,0\\B1=1.088995\B2=1.726845\B3=1.089037\B4=1.
088535\B5=2.794004\B6=0.984599\B7=0.984514\A1=96.64573\A2=117.979239\A
3=118.358052\A4=96.07611\A5=113.167491\A6=112.945798\D1=101.015448\D2=
153.901907\D3=-99.90873\D4=-56.269037\D5=177.317999\\Version=x86-Linux
-G98RevA.7\HF=-116.5612795\S2=0.752545\S2-1=0.\S2A=0.750004\RMSD=5.446
e-09\RMSF=5.178e-05

$OC\cdots H^+OH_2$ ($P2^+$, one of the $^{\bullet}CH_3$ loss products of $[CH_3CHO/H_2O]^{+\bullet}$ ion)

Frequencies --	196.1779	197.8281	265.3796
Frequencies --	525.9209	570.6962	1089.6784
Frequencies --	1690.2858	1749.6501	2313.7094
Frequencies --	2361.8498	3600.8762	3681.3248

Zero-point correction= 0.041561 (Hartree/Particle)
Thermal correction to Energy= 0.046403
Thermal correction to Enthalpy= 0.047347
Thermal correction to Gibbs Free Energy= 0.015779
Sum of electronic and zero-point Energies= -189.993406
Sum of electronic and thermal Energies= -189.988565
Sum of electronic and thermal Enthalpies= -189.987621
Sum of electronic and thermal Free Energies= -190.019188

1\1\GINC-MS8\Freq\RB3LYP\6-31+G(d)\C1H3O2(1+)\CWANG\08-Nov-2004\0\\#N
GEOM=ALLCHECK GUESS=TCHECK RB3LYP/6-31+G(D) FREQ\\OC...HOH2 CH3
loss product\\1,1\O,-0.0939404106,0.0046359684,-1.9545047119\C,-0.0309279177
,0.0027403268,-0.8307913984\H,0.0328528646,-0.0017212171,0.840596127\O
,0.0123380752,-0.0062394292,1.897921526\H,0.3885524627,0.8072250446,2.
301587978\H,0.416980862,-0.8091181017,2.2952297724\\Version=x86-Linux-
G98RevA.7\HF=-190.0349676\RMSD=8.295e-10\RMSF=6.164e-05

$CO\cdots H^+OH_2$ ($P3^+$, one of the $^{\bullet}CH_3$ loss products of $[CH_3CHO/H_2O]^{+\bullet}$ ion)

Frequencies --	114.3389	117.1539	240.8073
Frequencies --	356.4563	450.2569	979.0224
Frequencies --	1715.0788	1746.6021	2123.6264
Frequencies --	3151.1586	3583.5347	3654.0871

Zero-point correction= 0.041536 (Hartree/Particle)
Thermal correction to Energy= 0.046940

Thermal correction to Enthalpy= 0.047884
Thermal correction to Gibbs Free Energy= 0.014951
Sum of electronic and zero-point Energies= -189.983690
Sum of electronic and thermal Energies= -189.978286
Sum of electronic and thermal Enthalpies= -189.977342
Sum of electronic and thermal Free Energies= -190.010275

1\1\GINC-MS8\Freq\RB3LYP\6-31+G(d)\C1H3O2(1+)\CWANG\08-Nov-2004\0\\#N GEOM=ALLCHECK GUESS=TCHECK RB3LYP/6-31+G(D) FREQ\\CO...HOH2 CH3 loss p roduct\\1,1\C,0.0780190935,0.0331207787,-2.041852409\O,0.0268145785,0.0146997091,-0.8962101481\H,0.0005240776,0.0193778965,0.7784092079\O,0.0008896794,0.0101502376,1.7891697923\H,0.0837517471,-0.8994346491,2.1574773605\H,-0.7740244486,0.4825325064,2.1715507322\\Version=x86-Linux-G98RevA.7\HF=-190.0252254\RMSD=5.565e-10\RMSF=1.801e-04

Appendix D:

Archive entries for B3-LYP/6-31+G(d) optimized geometries of the stable states, transition states and the new product (arising from the C_2H_4 loss of ionized 2,3-pentanedione) on the potential energy surface of ionized 2,3-pentanedione (Chapter 7).

$[CH_3C(=O)\cdots C(=O)CH_2CH_3]^{+\bullet}$, Stable State I

Frequencies --	17.2455	56.6595	101.3262
Frequencies --	156.8963	206.0157	211.6268
Frequencies --	264.8017	311.3246	371.2982
Frequencies --	475.3783	514.5111	592.3222
Frequencies --	775.8046	818.0289	900.1583
Frequencies --	972.8382	1027.1658	1047.4311
Frequencies --	1081.6492	1099.6138	1263.2686
Frequencies --	1319.8333	1384.3464	1434.1667
Frequencies --	1440.4599	1448.1713	1461.0065
Frequencies --	1498.9375	1515.6914	1957.3703
Frequencies --	1979.2709	3049.0809	3062.1644
Frequencies --	3074.3536	3082.5221	3137.5258
Frequencies --	3148.1492	3164.7822	3177.2336

Zero-point correction=	0.119833 (Hartree/Particle)
Thermal correction to Energy=	0.129117
Thermal correction to Enthalpy=	0.130061
Thermal correction to Gibbs Free Energy=	0.083701
Sum of electronic and zero-point Energies=	-345.359853
Sum of electronic and thermal Energies=	-345.350568
Sum of electronic and thermal Enthalpies=	-345.349624
Sum of electronic and thermal Free Energies=	-345.395984

1\1\GINC-MS7\Freq\UB3LYP\6-31+G(d)\C5H8O2(1+,2)\CWANG\19-Dec-2004\0\\#
N GEOM=ALLCHECK GUESS=TCHECK UB3LYP/6-31+G(D) FREQ\\trans
pentanedione radical cation\\1,2\C,-1.3107021574,0.0421103968,0.5711060409\O,
-1.1271420348,0.2010186986,1.7179850978\C,0.280816919,0.0406451157,-0.42935
41815\O,0.0872440357,0.1860244661,-1.5758830126\C,1.4860167341,-0.1348
535372,0.4518575409\H,1.3346282669,-1.0811550249,0.9915035385\H,1.4152
025838,0.6542917088,1.214190098\C,2.8003605614,-0.1002048978,-0.335350
6366\H,2.8559865523,-0.9103354589,-1.0670920014\H,2.9377085683,0.85507
09479,-0.8485935892\H,3.6188948394,-0.2275609029,0.3808678591\C,-2.506
3022356,-0.1478465594,-0.3005337297\H,-3.4032034299,-0.1004083865,0.32
2481114\H,-2.4297400051,-1.1178490511,-0.8063701744\H,-2.5114323113,0.
6324977408,-1.0701537304\\Version=x86-Linux-G98RevA.7\HF=-345.4796852\
S2=0.755249\S2-1=0.\S2A=0.750017\RMSD=6.697e-09\RMSF=1.785e-06

$[CH_3C(=O)\cdots C(=O)CH_2CH_3]^{+\bullet}$, Stable State II (an isomer of I)

Frequencies --	14.0402	50.7182	102.3488
Frequencies --	180.4891	198.5538	233.4440
Frequencies --	240.4672	330.9594	399.9790
Frequencies --	464.8234	495.0529	632.4676
Frequencies --	807.3053	822.6595	902.8838
Frequencies --	945.8886	1024.3923	1045.7086
Frequencies --	1063.3339	1110.2488	1267.9904
Frequencies --	1298.2416	1383.6674	1429.0726
Frequencies --	1448.7806	1460.3205	1475.1956
Frequencies --	1502.8859	1516.3689	1949.4296
Frequencies --	1977.8344	3062.5162	3073.6180
Frequencies --	3083.6515	3137.5291	3149.0152
Frequencies --	3149.8688	3169.9604	3178.4101

Zero-point correction=	0.120242 (Hartree/Particle)
Thermal correction to Energy=	0.129461
Thermal correction to Enthalpy=	0.130405
Thermal correction to Gibbs Free Energy=	0.083988
Sum of electronic and zero-point Energies=	-345.358091
Sum of electronic and thermal Energies=	-345.348871
Sum of electronic and thermal Enthalpies=	-345.347927
Sum of electronic and thermal Free Energies=	-345.394344

1\1\GINC-MS8\Freq\UB3LYP\6-31+G(d)\C5H8O2(1+,2)\CWANG\05-Apr-2005\0\\#
N GEOM=ALLCHECK GUESS=TCHECK UB3LYP/6-31+G(D) FREQ\\1,4-H transfer
pentanedione radical cation\\1,2\C,-1.2217821757,-0.2630536273,0.00060079
62\O,-1.2566649155,-0.8902632787,0.9905612718\C,0.5267018044,0.0984130
933,-0.5711942696\O,0.5532160162,0.8251325454,-1.4912193225\C,1.567437
4581,-0.5606262079,0.2948970978\H,2.4340425428,-0.7120082906,-0.359061
3515\H,1.1800652432,-1.5249231909,0.6329633053\C,1.920041589,0.3509360
561,1.4955425743\H,1.06750938,0.500477693,2.1635356505\H,2.7051465089,
-0.1597940325,2.0626777753\H,2.3056770758,1.318944297,1.1659998302\C,-
2.2365096275,0.3238592671,-0.921901099\H,-3.2330158821,0.0979990161,-0
.5340029433\H,-2.0960687395,-0.1019897846,-1.9225443887\H,-2.071099224
,1.4051686709,-0.9919740697\\Version=x86-Linux-G98RevA.7\HF=-345.47833
27\S2=0.755371\S2-1=0.\S2A=0.750018\RMSD=1.360e-09\RMSF=3.065e-06

$[CH_3C(=OH)C(=O)CH_2CH_2]^{+\bullet}$, Stable State III

Frequencies --	65.3467	98.8866	114.8751
Frequencies --	225.1551	283.0284	303.8491
Frequencies --	331.3925	391.0035	506.8426
Frequencies --	557.5908	653.6969	684.4123

Frequencies --	772.3485	810.8531	931.8819
Frequencies --	972.1518	1028.4867	1039.0469
Frequencies --	1073.6534	1101.5263	1187.3745
Frequencies --	1247.2111	1322.8862	1371.1141
Frequencies --	1435.0071	1443.8729	1449.4822
Frequencies --	1459.6692	1484.2727	1604.3327
Frequencies --	1813.6184	2714.2840	3020.5284
Frequencies --	3026.6174	3070.6290	3077.6729
Frequencies --	3151.2691	3189.7689	3259.7402

Zero-point correction=	0.119092 (Hartree/Particle)
Thermal correction to Energy=	0.127359
Thermal correction to Enthalpy=	0.128304
Thermal correction to Gibbs Free Energy=	0.085678
Sum of electronic and zero-point Energies=	-345.319456
Sum of electronic and thermal Energies=	-345.311188
Sum of electronic and thermal Enthalpies=	-345.310244
Sum of electronic and thermal Free Energies=	-345.352870

1\1\GINC-MS7\Freq\UB3LYP\6-31+G(d)\C5H8O2(1+,2)\CWANG\05-Apr-2005\0\\#
N GEOM=ALLCHECK GUESS=TCHECK UB3LYP/6-31+G(D) FREQ\\ENOL ion of
CH2CH2COCHOCH3\\1,2\C,-0.9550221549,-0.0070155947,0.0197028109\O,-
1.0345342905,-0.0519225769,1.2860119848\C,0.4420169173,0.0939430547,-
0.6521549515\O,0.4758072702,0.6454120107,-1.7236426535\C,1.6272252724,-
0.5063217723,0.096422827\H,2.52105844,-0.2154987518,-
0.4773894576\H,1.5447495977,-1.6014325543,0.0331683987\C,1.733390807,-
0.05912759,1.52508937\H,-0.1074506896,-
0.052104204,1.7254023695\H,2.0061933961,-0.7757255326,2.29
57932308\H,1.9040074395,0.9946405427,1.7412782405\C,-2.1804746909,-0.0
211835795,-0.781159266\H,-3.0758016577,0.010832558,-0.1588766982\H,-2.
1808092071,-0.9259054981,-1.4116554312\H,-2.1449480623,0.8155108617,-1
.4940800458\\Version=x86-Linux-G98RevA.7\HF=-345.4385478\S2=0.755195\S
2-1=0.\S2A=0.75002\RMSD=8.474e-10\RMSF=1.527e-05

$[CH_3C(=O)(CH_2CH_3)\cdots CO]^{+\bullet}$, Stable State IV

Frequencies --	27.9840	43.2329	63.1900
Frequencies --	81.1267	94.4577	105.0860
Frequencies --	110.6225	207.5627	236.4611
Frequencies --	332.0679	381.4201	534.1917
Frequencies --	614.8567	802.4852	878.6309
Frequencies --	929.4568	979.6565	1027.0252
Frequencies --	1050.5288	1091.4530	1243.3143
Frequencies --	1286.4442	1352.6057	1411.2325
Frequencies --	1447.9700	1463.2803	1471.6199
Frequencies --	1481.3543	1510.3706	1685.6545

Frequencies --	2242.5403	3036.3862	3059.7161
Frequencies --	3077.5736	3122.4318	3148.8463
Frequencies --	3159.5739	3177.5268	3202.0740

Zero-point correction=	0.116578 (Hartree/Particle)
Thermal correction to Energy=	0.127407
Thermal correction to Enthalpy=	0.128352
Thermal correction to Gibbs Free Energy=	0.077214
Sum of electronic and zero-point Energies=	-345.342021
Sum of electronic and thermal Energies=	-345.331192
Sum of electronic and thermal Enthalpies=	-345.330248
Sum of electronic and thermal Free Energies=	-345.381385

1\1\GINC-MS11\Freq\UB3LYP\6-31+G(d)\C5H8O2(1+,2)\CWANG\15-Sep-2005\0\\
#N GEOM=ALLCHECK GUESS=TCHECK UB3LYP/6-31+G(D)
FREQ\\geom=ms8/dione/ts3_1bz3.log\\1,2\C,0.7970556749,0.0483425874,-
0.3762279344\C,0.8541018237,-0.2906796083,1.1633042034\C,2.2896214428,-
0.1166089051,1.666093976\H,0.1474767666,0.4208344279,1.6075163944\H,0.4894847
765,-1.3116879726,1.2892643965\H,2.9804466204,-0.8281188055,1.2053460412\
H,2.6697533214,0.901018782,1.5457930012\H,2.2601025509,-
0.3371412714,2.7435160459\O,0.815923355,-0.8797708429,-1.1403663417\
C,0.7290635108,1.4949061986,-0.8317039285\H,1.3810236361,2.096434989,-
0.1925633182\H,0.9977230372,1.5790264889,-1.8855274406\H,-
0.3148619087,1.8005705663,-0.6769610202\C,-2.6014446615,-0.1424051593,-
0.3637262315\O,-3.6936152981,-0.4055126426,-0.5074867346\\Version=x86-Linux-
G98RevA.7\HF=-345.4585991\S2=0.755722\S2-1=0.\S2A=0.750025\RMSD=5.275e-
09\RMSF=3.551e-05\Dipole=1.5393552,0.8046161,0.4910848

TS1 (for the rearrangement from I to IV)

Frequencies --	-263.0295	7.9962	14.4874
Frequencies --	49.4952	69.8526	72.7911
Frequencies --	90.2496	116.4942	124.8778
Frequencies --	130.4327	135.8761	251.7889
Frequencies --	331.0998	381.6395	695.7321
Frequencies --	816.1293	891.5189	1005.5216
Frequencies --	1038.0105	1040.5536	1064.0066
Frequencies --	1213.9654	1370.9848	1403.3170
Frequencies --	1415.7845	1420.5616	1481.1075
Frequencies --	1498.1640	1504.6012	2250.9292
Frequencies --	2352.8246	2952.4384	2981.1409
Frequencies --	3067.1385	3077.1436	3112.1348
Frequencies --	3127.1048	3131.2299	3222.4138

Zero-point correction=	0.111429 (Hartree/Particle)
Thermal correction to Energy=	0.123635

Thermal correction to Enthalpy= 0.124580
Thermal correction to Gibbs Free Energy= 0.067394
Sum of electronic and zero-point Energies= -345.309735
Sum of electronic and thermal Energies= -345.297528
Sum of electronic and thermal Enthalpies= -345.296584
Sum of electronic and thermal Free Energies= -345.353770

1\1\GINC-MS12\Freq\UB3LYP\6-31+G(d)\C5H8O2(1+,2)\CWANG\12-Jan-2006\1\\
#B3LYP/6-31+G(D) OPT=(TS,EF,CALCALL) GUESS=CHECK
GEOM=CHECK\\coloss ts for 2,3-pentanedione\\1,2\C\C,1,R2\H,1,R3,2,A3\H,1,R4,2
,A4,3,D4,0\H,2,R5,1,A5,4,D5,0\H,2,R6,1,A6,4,D6,0\H,2,R7,1,A7,4,D7,0\C,1,R8,2,A8,3,
D8,0\C,8,R9,1,A9,2,D9,0\O,8,R10,9,A10,1,D10,0\H,9,R11,8,A11,10,D11,0\H,9
,R12,8,A12,10,D12,0\H,9,R13,8,A13,10,D13,0\C,1,R14,8,A14,2,D14,0\O,14,
R15,1,A15,2,D15,0\\R2=1.49092653\R3=1.08961039\R4=1.08925769\R5=1.0963
4748\R6=1.09660146\R7=1.10492484\R9=1.43157408\R10=1.12516579\R11=1.09
955677\R12=1.09818543\R13=1.10470915\R15=1.13165566\A3=119.51991726\A4
=119.70297456\A5=112.62840201\A6=112.57270239\A7=110.14430797\A9=75.84
631005\A10=178.11428754\A11=108.47827986\A12=109.08315071\A13=106.1999
3292\A15=131.26640604\D4=-154.23366598\D5=39.99804074\D6=163.77576636\
D7=-78.20762199\D9=-87.54796387\D10=-90.45940361\D11=11.97357209\D12=1
33.23959037\D13=253.86596491\D15=-188.32265553\R8=3.53798334\R14=4.707
96205\A8=109.11180783\A14=41.57696591\D8=120.0885434\D14=177.58858121\
\Version=x86-Linux-G98RevA.7\HF=-345.4211635\S2=0.753482\S2-1=0.\S2A=0
.750009\RMSD=4.078e-09\RMSF=1.378e-05\Dipole=0.1482742,-1.9113162,0.80
12956

TS2 (for the rearrangement from I to II)

Frequencies --	-43.6380	23.4461	101.2456
Frequencies --	186.0260	195.8589	221.1585
Frequencies --	247.5063	325.5996	380.9670
Frequencies --	469.6800	501.1751	628.9538
Frequencies --	800.1247	817.1624	901.1081
Frequencies --	947.2767	1022.2207	1046.4234
Frequencies --	1060.2349	1113.5699	1254.3396
Frequencies --	1317.1944	1383.9695	1429.7959
Frequencies --	1448.6129	1460.6116	1473.8922
Frequencies --	1500.1073	1516.4401	1957.7291
Frequencies --	1984.4389	3058.6385	3063.1988
Frequencies --	3073.7790	3139.0143	3148.6827
Frequencies --	3160.2499	3175.5547	3177.1500

Zero-point correction= 0.120089 (Hartree/Particle)
Thermal correction to Energy= 0.128482
Thermal correction to Enthalpy= 0.129426
Thermal correction to Gibbs Free Energy= 0.085677

Sum of electronic and zero-point Energies= -345.357948
Sum of electronic and thermal Energies= -345.349555
Sum of electronic and thermal Enthalpies= -345.348611
Sum of electronic and thermal Free Energies= -345.392360

1\1\GINC-MS12\Freq\UB3LYP\6-31+G(d)\C5H8O2(1+,2)\CWANG\04-May-2005\1\\
#B3LYP/6-31+G(D) OPT=(TS,EF,CALCALL)\\ts between transch3co_coch2ch3.l
og and its isomer\\1,2\C\O,1,R2\C,1,R3,2,A3\O,3,R4,1,A4,2,D4,0\C,3,R5,
1,A5,2,D5,0\H,5,R6,3,A6,1,D6,0\H,5,R7,3,A7,1,D7,0\C,5,R8,3,A8,1,D8,0\H
,8,R9,5,A9,3,D9,0\H,8,R10,5,A10,3,D10,0\H,8,R11,5,A11,3,D11,0\C,1,R12,
2,A12,3,D12,0\H,12,R13,1,A13,2,D13,0\H,12,R14,1,A14,2,D14,0\H,12,R15,1
,A15,2,D15,0\\R2=1.17105262\R3=1.89662761\A3=112.82244804\R4=1.1721794
6\A4=111.74833318\D4=-172.15106707\R5=1.50665287\A5=113.48630422\D5=6.
46368326\R6=1.0994552\A6=104.54554315\D6=124.02807222\R7=1.09075364\A7
=109.28112287\D7=7.22628534\R8=1.54668401\A8=110.41668074\R9=1.0933961
7\A9=111.80974154\D9=64.3568595\R10=1.09501306\A10=106.97904362\D10=-1
77.55038594\R11=1.09252227\A11=111.63258533\D11=-58.78700749\R12=1.491
04128\A12=135.89366067\D12=-179.57672661\R13=1.09311191\A13=108.532366
81\D13=0.71534146\R14=1.09637548\A14=109.01382034\D14=-120.41194369\R1
5=1.09596476\A15=109.00397038\D15=122.11237721\D8=-116.68726877\\Versi
on=x86-Linux-G98RevA.7\HF=-345.4780375\S2=0.755259\S2-1=0.\S2A=0.75001
7\RMSD=9.390e-09\RMSF=8.628e-06

TS3 (for the rearrangement from II to III)

Frequencies --	-952.2153	59.5847	93.1564
Frequencies --	117.0461	288.3846	318.9234
Frequencies --	415.4059	453.6181	464.4871
Frequencies --	544.6356	607.9213	643.2113
Frequencies --	724.7410	804.9885	931.4154
Frequencies --	978.0265	1007.6830	1059.2019
Frequencies --	1087.4883	1115.7623	1136.3093
Frequencies --	1225.9479	1267.5616	1304.7231
Frequencies --	1380.4095	1438.8957	1442.0579
Frequencies --	1456.6650	1480.2611	1502.9144
Frequencies --	1664.3193	1837.7105	3032.6470
Frequencies --	3036.3747	3085.7891	3088.9692
Frequencies --	3129.7912	3191.4753	3229.9346

Zero-point correction= 0.115386 (Hartree/Particle)
Thermal correction to Energy= 0.123093
Thermal correction to Enthalpy= 0.124037
Thermal correction to Gibbs Free Energy= 0.082361
Sum of electronic and zero-point Energies= -345.321740
Sum of electronic and thermal Energies= -345.314033
Sum of electronic and thermal Enthalpies= -345.313089

Sum of electronic and thermal Free Energies= -345.354765

1\1\GINC-MS8\Freq\UB3LYP\6-31+G(d)\C5H8O2(1+,2)\CWANG\23-Dec-2004\1\\#
B3LYP/6-31+G(D) OPT=(TS,EF,CALCALL)\\1,5-H shift MacLafferty rearrange
ment pentanedione radical cation\\1,2\C\O,1,R2\C,1,R3,2,A3\O,3,R4,1,A4
,2,D4,0\C,3,R5,1,A5,2,D5,0\H,5,R6,3,A6,1,D6,0\H,5,R7,3,A7,1,D7,0\C,5,R
8,3,A8,1,D8,0\H,8,R9,2,A9,5,D9,0\H,8,R10,5,A10,3,D10,0\H,8,R11,5,A11,3
,D11,0\C,1,R12,2,A12,3,D12,0\H,12,R13,1,A13,2,D13,0\H,12,R14,1,A14,2,D
14,0\H,12,R15,1,A15,2,D15,0\\R2=1.25353256\R3=1.56698461\A3=118.479633
74\R4=1.20032722\A4=117.18242244\D4=-162.85841322\R5=1.53647155\A5=116
.85995392\D5=18.32696934\R6=1.09926862\A6=105.38565535\D6=-154.5582727
8\R7=1.09966267\A7=105.9700927\D7=91.65600791\R8=1.50162949\A8=114.828
76488\D8=-31.445291\R10=1.08984707\A10=118.84589177\D10=129.92626291\R
11=1.09120534\A11=118.12283349\D11=-81.08095128\R12=1.47052124\A12=121
.16442496\D12=180.84991251\R13=1.0906989\A13=111.72373476\D13=5.766133
37\R14=1.10203162\A14=108.4557079\D14=-116.13461508\R15=1.09871311\A15
=108.94300963\D15=129.9268165\R9=1.47148868\A9=10.74678021\D9=-167.700
84994\\Version=x86-Linux-G98RevA.7\HF=-345.437126\S2=0.754835\S2-1=0.\
S2A=0.750018\RMSD=4.159e-09\RMSF=1.860e-05

$[CH_3C(OH)=C=O]^{+\bullet}$, the product of the C_2H_4 loss from 2,3-pentanedione ion

Frequencies --	89.3133	184.4969	282.7843
Frequencies --	396.1718	399.1411	498.7036
Frequencies --	650.4448	763.0332	1008.1183
Frequencies --	1022.9930	1129.0088	1348.5664
Frequencies --	1413.7222	1447.6566	1461.3071
Frequencies --	1494.9982	2246.5589	3040.2138
Frequencies --	3104.8785	3162.7110	3640.7334

Zero-point correction=	0.065578 (Hartree/Particle)
Thermal correction to Energy=	0.071391
Thermal correction to Enthalpy=	0.072335
Thermal correction to Gibbs Free Energy=	0.035908
Sum of electronic and zero-point Energies=	-266.759551
Sum of electronic and thermal Energies=	-266.753738
Sum of electronic and thermal Enthalpies=	-266.752794
Sum of electronic and thermal Free Energies=	-266.789221

1\1\GINC-MS8\Freq\UB3LYP\6-31+G(d)\C3H4O2(1+,2)\CWANG\16-Dec-2004\0\\#
N GEOM=ALLCHECK GUESS=TCHECK UB3LYP/6-31+G(D)
FREQ\\CH3C(OH)CO\\1,2\C,0.7855109131,1.2312498718,0.8566777417\H,0.21108231
7,1.6578695989,1.6904576109\H,1.7877646153,0.9745691724,1.2264903078\H,0.87328
893,1.9745014732,0.0603980979\C,0.1104615769,-0.0139269037,0.396675377\O,-
0.0571120057,-0.9898295428,1.2677615617\C,-0.324018567,-0.1260725761,-0.91755
86767\O,-0.6680256761,-0.1793363824,-2.010192867\H,-0.502757946,-1.801

1151951,0.9473377733\\Version=x86-Linux-G98RevA.7\HF=-266.8251291\S2=0
.753022\S2-1=0.\S2A=0.750007\RMSD=2.200e-09\RMSF=9.651e-06